Czech University of Life Sciences Prague
Faculty of Engineering

2017

Proceeding of 19th International Conference of Young Scientists 2017

Czech University of Life Sciences Prague – Faculty of Engineering

Sept. 13th – Sept. 14th 2017

CZECH UNIVERSITY OF LIFE SCIENCES PRAGUE

FACULTY OF ENGINEERING

19TH INTERNATIONAL CONFERENCE OF YOUNG SCIENTISTS 2017

PROCEEDING OF 19TH INTERNATIONAL CONFERENCE OF YOUNG SCIENTISTS 2017

September 13th 2017 – September 14th 2017

Prague

Czech Republic

Editors: Rostislav Chotěborský, Stanislav Kovář

ISBN 978-80-213-2771-9

19th International Conference of Young Scientists 2017

September 13th 2017 – September 14th 2017

Conference ICYS publishes research in engineering and physical sciences that represent advances in understanding or modelling of the performance of biological and physical systems for sustainable developments in land use and the environment, agriculture and amenity, bioproduction processes and the food chain, logistics systems in agriculture, manufacturing and material systems in design of agriculture engineering.

Conference venue:

Faculty of Engineering, Czech University of Life Sciences Prague, Kamýcká 129, Praha 6, Prague, 165 21, Czech Republic

Scientific committee:

prof. Ing. Vladimír Jurča, CSc.

prof. Ing. David Herák, Ph.D.

doc. Ing. Rostislav Chotěborský. Ph.D.

doc. Ing. Jiří Mašek, Ph.D.

doc. Ing. Marián Kučera, Ph.D.

prof. Ing. Štefan Barcík, CSc.

prof. Ing. Zdenko Tkáč, PhD.

doc. Ing. Štefan Pogran, CSc.

CONTENT

ADVANCED PRODUCT QUALITY PLANNING IN AUTOMOTIVE INDUSTRY

Martin BALÁŽ

Department of Quality and Engineering Technologies at Faculty of Engineering, Slovak agricultural University in Nitra, Slovak Republic

Abstract
The article is focused on the quality planning process for advanced products in automotive industry. This process ensures the product will be created and launched into the serial production within the three main scopes of the project quality, time and budget. The whole process consists of several elements which all of them make the process a systematic and standardized approach to reach the agreed quality of the product.

Key words: *APQP, automotive industry, approval process, quality planning.*

INTRODUCTION

In order to create and launch a new product that meets the quality requirements of the customer, systematic approach in form of advanced quality planning is required. The Advanced Product Quality Planning tool (APQP) accompanies the development process of a product during the customer's product creation and delivery and is intended to ensure that the product while launched into the serial production meets all of the quality requirements of the customer on time and within the budget.

MATERIALS AND METHODS

The APQP process monitors and manage the quality maturation of the product through the whole project. Due to the product complexity, the maturation process needs to be divided into phases and in each of them dedicated APQP elements must be shown as an evidence of the adherence to the agreed quality requirements.
To ensure the adherence to the quality planning process for timely planning, execution and documentation an appropriate organisation structure within the company needs to be established. This will specify the persons responsible for the individual workstreams and ensure the deadlines are met for each of them. In automotive industry, it is the personnel of the technical department or project manager depending on the scale of the launched product responsible for the quality maturation process of the product and if necessary for the cooperation with the suppliers and subcontractors. To be able to monitor the adherence to deadlines of the project, milestones must be set up throughout all of the launch process. The progress in the APQP process is recorded in the APQP status report.

The demands on advanced product quality planning are based on the complexity of the project and can be divided in to three project classifications:

- highest risk – project classification 1
- medium risk - project classification 2
- standard risk – project classification 3

Project classification 1 – the customer must check the progress of the quality maturation process during planned and if necessary on additional project reviews. APQP elements such as control plan, FMEA, process flow chart must by shown as evidence. The customer approves the mass production readiness after carrying out a production trial run at supplier´s and if necessary at subcontractor´s site. The date and scope of the on-site inspection are agreed within the framework of APQP.

Project classification 2 - the customer can check the progress of the quality maturation process during planned project reviews. APQP elements such as control plan, FMEA, process flow chart must be shown as evidence. The customer can approve the mass production readiness after carrying out a production trial run at supplier´s and if necessary at subcontractor´s site.

Project classification 3 – the supplier reports on an informal basis and no planned project reviews are needed. The customer can check the progress of the quality maturation process during project discussions. APQP elements such as control plan, FMEA, process flow chart must by shown as evidence.

Based on the project classification a project plan is created and the progress of the quality maturation must be monitored according to this plan. It must consist target dates for each of the APQP elements and each of the dates must be recorded in the APQP status report. A blank template of APQP status report used at the Schaeffler Grouppe automotive company is shown in Fig.1 [4]. If a date or one of the elements are at risk of not being fulfilled a suitable corrective action must be introduced and monitored. The status of the individual elements must be indicated in the APQP status report using the following colour codes (1):

- **Green:** date and quality of all elements are not at risk and start of the production is not endangered.
- **Amber:** date and quality at least one of the elements are at risk and start of the production is not endangered but an appropriate corrective action is already in place.
- **Red:** date and quality at least one of the elements are at risk and start of the production endangered and no corrective action is defined or in place.

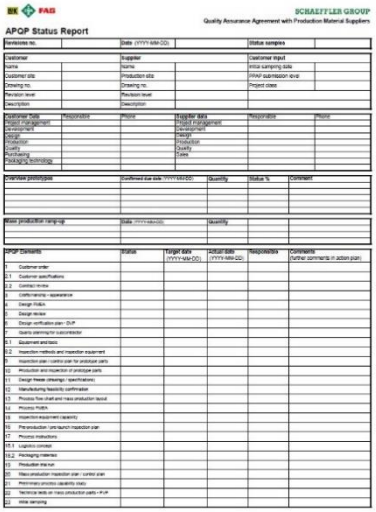

Fig. 2 A blank template of an APQP status report [4]

RESULTS AND DISCUSSION

In the below is a short description of each of the APQP elements from APQP status report.

Customer order

A formal customer order needs to be placed by the customer to start with all the necessary investment activities by the supplier. Following documents can be added to the initial customer order: nomination letter, order indicating the project classification and submission level for sampling and project plan or delivery plan.

Customer specifications

To avoid misunderstandings regarding the product the supplier must be familiar with all the requirements of the product. This includes: installation situation, ambient conditions, functional performance requirements, dimensions, weight, material, reliability, milestones, guarantee objectives, capacity data or volumes and etc. Documents such as design briefs, drawings and specifications must be provided to the supplier.

Contract review
Before entering into a delivery agreement with the customer a contract review needs to be provided to ensure the requirements of the product are set up and recorded. All deviation requirements are classified prior to submitting the quotation or closing the contract. The contract review is recorded in the form of capacity confirmation and feasibility confirmation by the supplier.

Craftsmanship – appearance
The supplier must be familiar with the requirements for appearance, texture, handling ability and acoustics. All of the requirements will be recorded in the characteristics catalogues and reference samples which are agreed with the customer.

Design FMEA
Design FMEA as an APQP element is applicable only within the own product development. It ensures problems relating to product layout are solved in good time with no effect on the launch timing plan. All potential defect modes which occur during the design review stage must be incorporated into the Design FMEA and if necessary the layout criteria must be modified in agreement with the customer. Also modifications on the product can take place on behalf of improvements regarding product reliability and manufacturing costs. Influencing defect modes are described and assessed while corrective actions are defined and monitored by responsible persons if necessary.

Design review
To prevent misunderstandings related to the product design reviews must take place and meeting reports from these reviews must be prepared by the supplier or the customer. This process ensures all problems related to the product layout are solved in advance with no effect on launch timing plan. A potential defect modes spotted during the design review stage must be incorporated in to the Design FMEA. Design reviews also involve check on potential improvements regarding product reliability and manufacturing costs.

Design Verification Plan
Design verification plan as well as Design FMEA are applicable only within the own product development. The DVP represents a systematic approach regarding planning of all required tests or calculations to meet the product requirements for application. The proven suitability of the product is recorded in the form of test reports, layout calculations and tolerance studies.

Quality planning for subcontractor
While multiple suppliers and subcontractors are involved in the process chain the APQP process must be established by all suppliers and their subcontractors. All of the suppliers and subcontractors must show an evidence of risk assessment to provide a clear illustration of the appropriate risk management within the project. The superior element in the process chain is responsible for checking the progress of the project on regular basis with the inferior element. Every subcontractor must provide their own APQP status report.

Equipment and tools
All necessary equipment and tools for the creation and delivery of the product must be planned and provisioned. Deadlines for the procurement or manufacture of equipment and tooling must be recorded, monitored and provided in the project plan. As an evidence schedules, capacity plans and proof of tools capability must be shown to the customer.

Inspection methods and equipment
Suitable inspection methods and equipment needs to be agreed between the customer and the supplier to be able to monitor and control the production process. Time plan with deadlines for procurement and manufacturing of inspection equipment and tooling must be created and provided. The proof of inspection equipment capability and where necessary inspection process suitability must be provided. With the support of this data the control plan can be created.

Inspection plan and control plan for prototype parts
To secure the required quality for prototype parts control plan must be in place in which all of the special characteristics of the product are included. In the control plan are also defined the type and scope of inspections and suitable inspection equipment.

Production and inspection of prototype parts
The production of prototype parts must be planned in advance to secure their dispatch on time. The parts must be manufactured in the agreed time and quantity. All produced prototype parts must meet agreed criteria for customer´s quality. If this is not the case an approval from the customer for dispatch of non-conforming parts must be obtained.

Design freeze of specifications and drawings
The specifications and drawings include all technical drawings, CAD data, material specifications and technical specifications from the customer or supplier. The aim of the design freeze is to ensure no major changes to the product are possible after this date. If the change is inevitable due to quality issues it is always in hand with big cost due to a tool design change.

Manufacturing feasibility confirmation
The feasibility of the launched product must be reviewed by a cross-functional team. The team will assess if the product is eligible for the intended application and can be produced, tested, packed and dispatched to the customer in requested volume, quality and date. Even in case the customer is responsible for the design and has created the drawings, the supplier is obligated to assess the feasibility in the planning phase and before prototype and serial production. In case a subcontractor is responsible for a one of the critical features of the sub-product, the supplier can demand the feasibility study from the subcontractor.

Process flow chart and mass production layout
The process flow chart for serial production is a graphical visualization of the process and shows the sequencing of all individual steps of the production process chain. It is also a baseline for the investments, Process FMEA, production plan, control plan and visual aid for the machine layout on site.

Proces FMEA
The Process FMEA is a systematic approach to prevent any defects during the process development and production. It ensures all potential production defects and their causes have been taken into account with support of a cross-functional team and have been countered by preventive measures. While assessing the potential failure modes all production and inspection stages must be reviewed and analyzed. In case of high number of potential defects a pareto analysis must be taken in account to set up the priorities and action plan for high risk priorities must be created.

Inspection equipment capability
The capability studies must be carried out in order to assess the suitability of inspection tool. The capability studies of the inspection equipment must be assessed with support of the inspection systems analysis or capability study by using the MSA method.

Pre-production inspection plan
The pre-production inspection plan sets a quality setup for product and process in pre-production and launch phases of the project. The plan enables an increased inspection frequency and additional inspection characteristics to meet the quality standards. It also defines the type and scope of the inspections and describes a matching inspection tool.

Process instructions
The process instructions describe in detail all process procedures. They include instructions for production personnel, production plans, work instructions and inspection instructions, maintenance plans, defect catalogues and process parameters. The instructions should be written in the regional language

of the associates to ensure they are clearly understood and followed. All employees must be trained along these instructions and proof of training must by shown if required.

Logistics concept
Logistic concept describes the whole transport of incoming and outgoing products. It defines the transport routes, required inventory, safety stock and customs agreements if applicable.

Packaging materials
Packaging materials ensure the quality of the product through the transport and storage. A suitable packaging material must be defined for transport from and to suppliers or subcontractors, internal transport and dispatch to the customer. Packaging specifications should also define a corrosion protection for the transport overseas or during a longer period.

Production trial run
The production trial run verifies the readiness of the mass production process for required product quality and planned nominal quantities. The verification must be run on mass production installations, machines, tooling, inspection equipment and under mass production conditions. During the production trial only mass production materials must be used. The mass production samples for PPAP process are taken from the trial. The participation of the customer during the trial must be ensured.

Mass production inspection and control plan
Mass production inspection and control plan ensures the product and process meet the mass production requirements on quality. It describes the type and scope of inspections together with inspection equipment for mass production.

Preliminary process capability study
Process capability study use statistical methods to prove that the product can be manufactured within drawing specifications. According to VDA (VDA, 1998) preliminary process capability under mass production conditions is Pp/Ppk >1,67 (for at least 25 x 5 parts) and for machine capability Cm/Cmk >1,67 (for 50 parts). If the process is not capable corrective actions must be introduced to achieve process capability. Meanwhile the process capability is not achieved a 100% inspection must be carried out.

Technical tests on mass production parts
A sample of the product is taken out from the production trial run to be tested as a proof that the product manufactured under mass production conditions meet the customer requirements. Test results must be recorded and provided to the customer.

Initial sampling
Initial samples are taken from the mass production trial run to verify in accordance with PPAP process that the product meets the customer criteria. The PPAP requirements are distinguished by various submission levels 1-5.

CONCLUSION
The APQP process is a standardized methodology to reach the agreed quality of the final product. Automotive companies acknowledge this process and make a lot of effort to embed this approach in to their workstream. This contributes to create and launch even a very complex mechatronic systems in to the serial production on time and within the budget while meeting the quality standards of the customers in automotive industry.

REFERENCES
1. VDA (1998). Quality Assurance Prior to Serial Application, 1st ed., Vol. 4, Verband der Deutschen Automobilindustrie e.V., Frankfurt a.M., part 3.

2. Gerhard Hab, Reinhard Wagner, (2015). Projektmanagement in der Automobilindustrie Effizientes Management von Fahrzeugprojekten entlang der Wertschöpfungskette Springer Fachmedien Wiesbaden (pp. 23-194) Online ISBN 978-3-8349-92529
3. Produktentstehungsprozess für Scheinwerfer und Heckleuchten ATZ - Automobiltechnische Zeitschrift, Volume 115, Issue 11 Springer Automotive Media (pp 888-893) Cover Date 2013-11 Online ISSN 2192-8800
4. Training documentation Schaeffler, APQP-Methoden , Version 2013.1

Corresponding author:
Ing. Martin Baláž, Department of Quality and Engineering Technologies at Faculty of Engineering, Slovak agricultural University in Nitra, Trieda Andreja Hlinku 2, 949 76 Nitra, Slovenská republika, phone +421 903 602 665, e-mail: xbalazm4@is.uniag.sk

DIRECTIONAL REACTIVE NAVIGATION OF A MOBILE ROBOT USING LOW COST MICROPROCESSOR

Juraj BALÁŽI, Lukáš VACHO, Dalibor VADOVIČ

Katedra Elektrotechniky, Automatizácia a Informatiky, Technická fakulta, Slovenská poľnohospodárska univerzita v Nitre, Slovenská Republika

Abstract
The paper is focused on wavefront map navigation algorithm of mobile robot in closed environment with use of small and inexpensive 8051F340 microprocessor. Used mobile robot is EN20 developed in Slovak University of Agriculture in Nitra, Faculty of Engineering, Department of Electrical Engineering, Automation and Informatics. Navigation is realized with use of HC-SR04 ultrasound sensors.

Key words: *Wavefront, microprocessor, navigation, robot.*

ÚVOD

Dôležitosť navigačných systémov rastie s myšlienkami na autonómny automobil alebo mobilného robota. Ak skombinujeme autonómnosť s lacným riešením, ako najlepšie riešenie nájdeme využitie jednočipového mikroprocesora. Samozrejme každá technológia má svoje obmedzenia, preto je nasledovné riešenie vhodné do interiéru.
Niekoľko možností navigačných algoritmov je napísaných v publikácii od *Borenstein a kol.* (1996) z Massachusetts Inštitútu Technológii (MIT) v USA. Metódy využívajúce navigačné mapy sú oblasť navigačných algoritmov. Navigačná metóda wavefront je najvhodnejšie riešenie pre realizáciu nášho projektu, pretože umožňuje v zjednodušenej forme pracovať s celými číslami, čo minimalizuje čas spracovávania a urýchli navigačný proces výpočtu trasy robota. Veľkosť navigačnej mapy sme určili poľom 100*100 bodov, pričom jeden bod vyjadruje štvorec o veľkosti strany 15 cm, z čoho vyplýva veľkosť pracovného prostredia je 15*15 metrov.
Veľkosť štvorca reprezentujúci bod v navigačnej mape nie je náhodná, ale určená na základe veľkosti chyby ultrazvukového snímača na meranie vzdialenosti. Snímanie priestoru je realizované pomocou troch ultrazvukových snímačov umiestnených na rotore servomotora v 360° okolí robota. Test algoritmu je uskutočnený na robotovi EN20 vyvinutého na Slovenskej poľnohospodárskej univerzite v Nitre, Technickej Fakulte, Katedre Elektrotechniky, Automatizácie a Informatiky. Vizualizačný program je vytvorený v programovacom prostredí Microsoft Visual Studio C#.

MATERIÁLY A METÓDY

Wavefront navigácia je zaradená pod navigačnými algoritmami využívajúcimi navigačné mapy, čo v našom prípade reprezentuje bodová 2D mapa. Body sú v navigačnej mape zobrazené ako štvorce a spolu tvoria mriežku. Wavefront navigačný algoritmus rieši spôsob navigácie v navigačnej mape pomocou určitých stanovených pravidiel. Prvé pravidlo je vyplnenie bodoch navigačnej mapy, kde sa nachádzajú prekážky, čo je reprezentované číslom jedna. Pravidlo číslo dva je určenie cieľa v navigačnej mape označením číslom dva. Tretie pravidlo je výpočet v spôsobe šírenia vĺn do šetkých smerov od určeného cieľa inkrementáciou čísla každou „vlnou“. Kalkulácia prebieha po vyplnenie všetkých bodov v navigačnej mape. Nasleduje určenie počiatočnej polohy robota v mape. Posledná udalosť je určenie trajektórie od polohy robota do cieľa bez spôsobenia kolízie z prekážkou. Príklad úplnej wavefront navigačnej mapy je na Obr. 1.

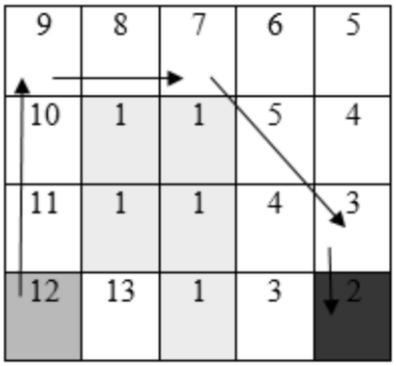

Obr. 1 Kompletná navigačná mapa s trajektóriou pohybu

Výpočet trajektórie je určený nasledovným pravidlom:

$$Np \in \max[VAp - VNxp] \quad (1)$$

Kde Np je nasledovný bod, VAp je hodnota aktuálneho bodu, VNxp je hodnota susedný bod x (bod x pre každý smer).

Po uskutočnení týchto krokov môže robot začať pohyb po vypočítanej trajektórii.

Meranie vzdialenosti zabezpečujú tri ultrazvukové snímače HC-SR04. Snímače sú umiestnené v trojuholníkovom tvare, čím znížime čas potrebný na snímanie. Otáčanie zabezpečuje servomotor HXT-900, ktorý snímače pootáča o presné uhly potrebné na zoskenovanie 360° oblasti okolia robota.

Ultrazvukový snímač bol korigovaný v reálnom čase vďaka snímaču teploty a vlhkosti HTU21D. Korekčná rovnica je (*Cviklovič, 2011*):

$$c_s = 331{,}3 + 0{,}606t + 0{,}0124RH \quad (2)$$

Kde c_s je vypočítaná rýchlosť zvuku, t je teplota vzduchu v °C, RH je relatívna vlhkosť v %.

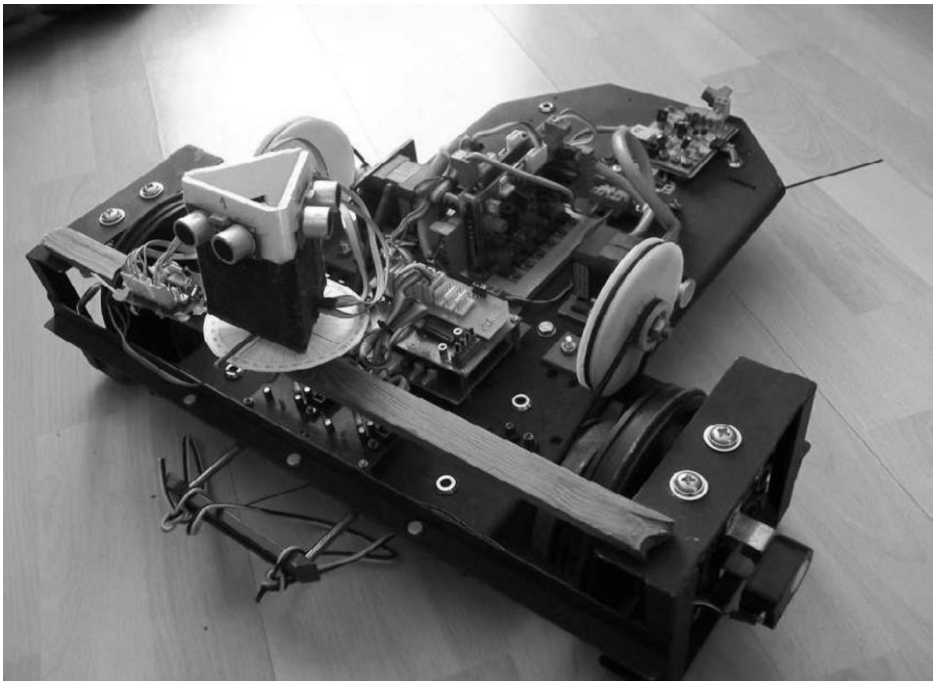

Obr. 2 Mobilný robot EN20 s ultrazvukovými símačmi

Robot EN20 je robot s diferenciálnym riadením dvoch kolies pomocou BLDC motorov a XbeeRobot 2,4GHz Wi-Fi riadiacim modulom. Tiež obsahuje pár quadratúrnych inkrementálnych snímačov pre snímanie pozície. Zdroj pohonu tvoria tri Li-Pol akumulátory. Riadiaci procesor robota EN20 je jednočipový mikroprocesor 8051F340.

VÝSLEDKY A DISKUSIA

Algoritmy výberu cieľa, sledovanie prekážok a výpočet trajektórie sú navrhnuté vo funkcii Auto_Drive_TimerTick. Táto funkcia je spúšťaná každých 300 ms, kvôli možnostiam ultrazvukového snímača. Spúšťacia podmienka závisí na prechode booleovskej premennej Start do hodnoty True a booleovskej premennej Find_New_Pos do hodnoty True. Po spustení algoritmu sú zmerané aktuálne súradnice autonómneho mobilného robota X_Pos a Y_Pos v milimetroch. Následne je potrebné vyjadriť umiestnenie pomocou súradníc zvolený cieľ v priestore a priradiť ho do navigačnej mapy. Túto konverziu dosiahneme rovnicou:

$$Point = \frac{(7500 + Distance\_mm)}{150} \quad (3)$$

Kde Point je bod X alebo Y (podľa aktuálne rátanej súradnice bodu) je súradnica objektu prepočítaná pre navigačnú mapu, distance_mm je reálna vzdialenosť súradnice X alebo Y z rozsahu od -7500 mm do 7500 mm.

Určením cieľa v navigačnej mape nasleduje skenovanie priestoru pre zistenie prekážok a rovnakým postupom ich zapísať do navigačnej mapy. Po naskenovaný celého okolia robota sa začnú počítať možné trajektórie pohybu. Výpočet zahŕňa overenie možnosti dosiahnuť cieľ. Dosiahnutie určeného cieľa funkciu Find_New_Pos nastaví na hodnotu False. V tomto momente je potrebné aktualizovať navigačnú mapu pre prípadné zmeny a určenie nového čiastkového cieľa. Nový čiastkový cieľ je určený bod v navigačnej mape a pre účely riadenia je potrebné vykonať konverziu jeho súradníc na skutočnú vzdialenosť. Na konverziu slúži nasledovná rovnica:

$$Distance\_mm = (Point * 150) - 7500 \quad (4)$$

Kde Distance_mm je vzdialenosť v mm súradnice X alebo Y pričom hodnota môže byť od -7500 mm do 7500 mm, Point je súradnica X alebo Y konvertovaných súradníc bodu navigačnej mapy.

Pokiaľ je zistená nová prekážka, tak je pridaná do navigačnej mapy a prebehne kontrola a prípadne potrebná korekcia trajektórie pohybu robota. Medzi skenovaniami prekážok, počas pohybu robota, je snímaná oblasť v smere pohybu robota vo vzdialenosti 1 m pred pohybujúcim sa robotom vďaka čomu je možné vyhnúť sa neočakávaným prekážkam. Navigačný algoritmus je zobrazený ako vývojový diagram na Obr. 3.

Princíp určenia reálnej trajektórie robota začína v prvom snímaní prekážok v okolitom priestore. Po naskenovaní okolia je nutné zadať cieľový bod. Následne robot má všetky potrebné informácie pre autonómny pohyb a začína určením čiastkového cieľa. Po dosiahnutí čiastkového cieľa nasleduje obnovenie snímania navigačnej mapy a tieto kroky sa opakujú až pokiaľ nie je dosiahnutý cieľový bod.

Pohyb robota je zobrazený v programe vytvoreného pre robota EN 20 vytvoreného v Microsoft Visual Studio C#. Program zobrazuje body navigačnej mapy, kde sú znázornené prekážky, prejdená trajektória, ciľové body, skenovacie zastavenia a bezpečnostnú vzdialenosť ktorú je možné definovať pre zlepšenie vyhnutiu sa v prekážke. Spomenutá aplikácia je zobrazená na Obr. 5, kde prekážky sú modré štvorčeky, nastavená bezpečnostná vzdialenosť je žltý štvorec, čiastkové cieľové body sú červené štvorčeky, konečný cieľový bod je má čierne orámovanie, trajektória robota je čierna čiara a čierne kružnice znázorňujú aktualizáciu navigačnej mapy.

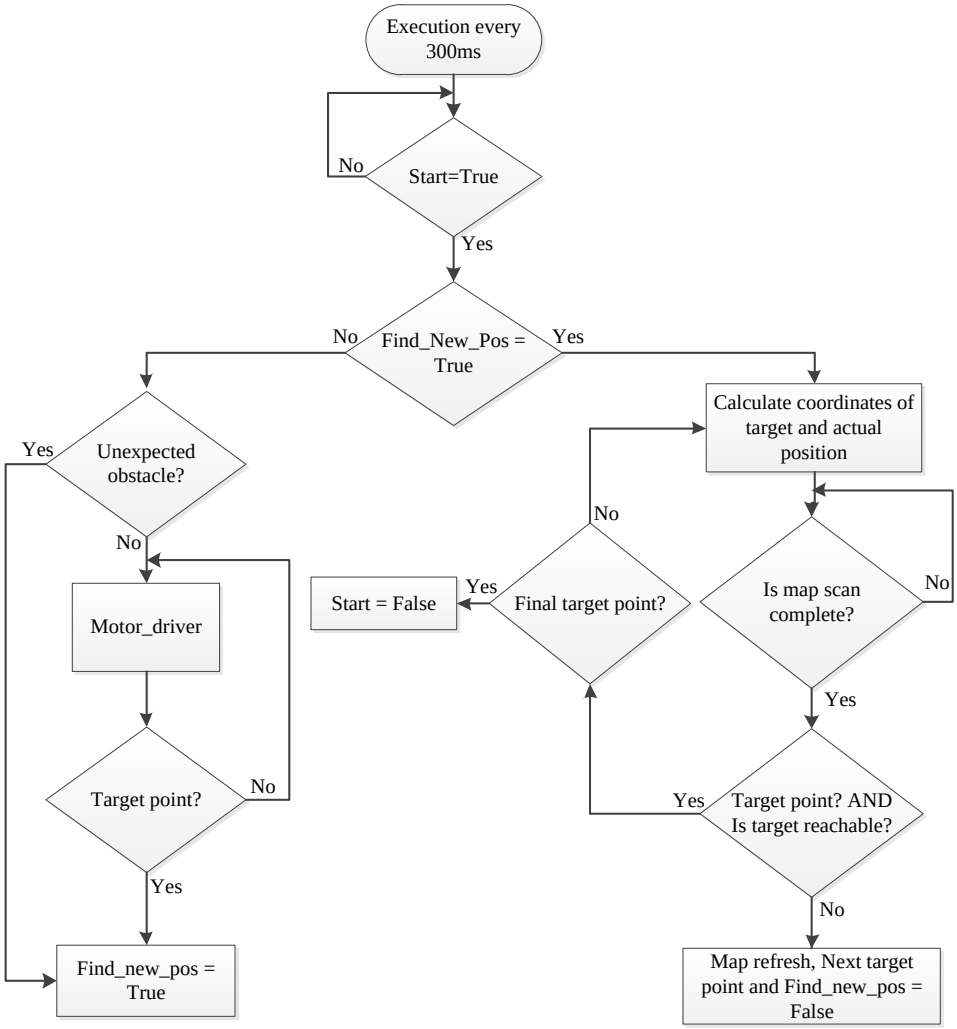

Obr. 3 Vývojový diagram navigačného algoritmu robota EN20

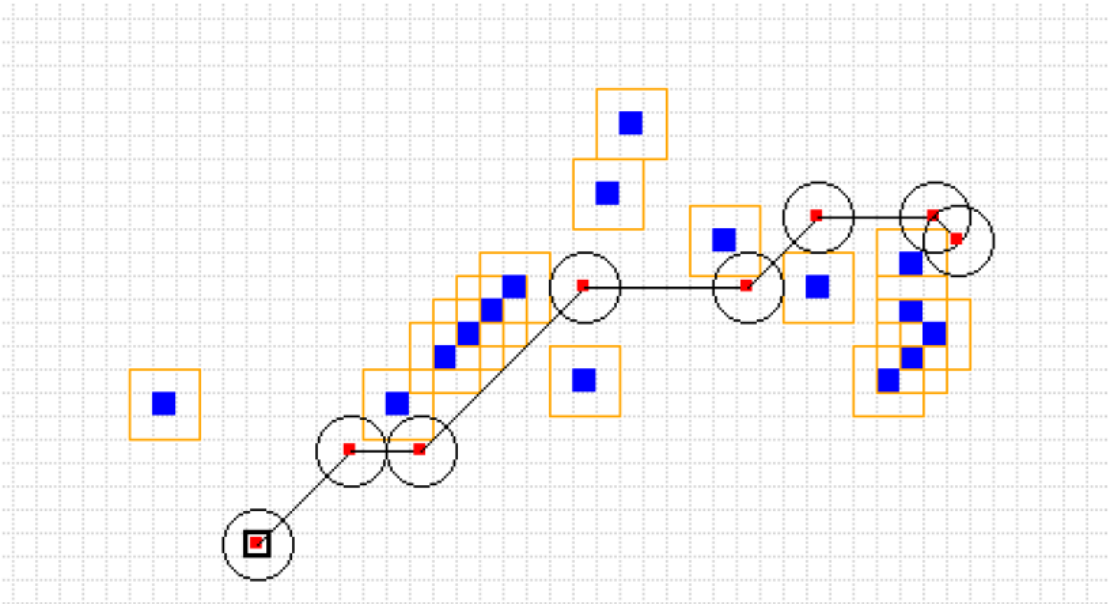

Obr. 4 Dráha prejdená robotom zobrazená v aplikácii vytvorenej v MS Visual Studio C#

ZÁVER

Wavefront navigácia je rýchly a použiteľný typ navigácie využívajúci navigačnú mapu aj pri finančne nenáročných, nízko výkonných, jednočipových mikroprocesorov pri použití v ohraničenom priestore. Túto aplikáciu je možné využiť v osobných pomôckach, ako napríklad autonómne vysávače, kosačky a iné. V prípade náhrady procesora za viac výkonný mikročip je možné aplikáciu využiť aj ako automatické zásobovanie výroby vo výrobnej hale ako finančne nenáročné riešenie. Využitie ultrazvukových snímačov má veľkú výhodu v ich cene, ale zároveň nevýhodu v presnosti snímania vzdialenosti. Vplyv na nameranú vzdialenosť má najmä veľkosť objektu, jeho povrch, umiestnenie, ale aj teplota a vlhkosť vzduchu. Merania uskutočnené s použitím ultrazvukových snímačov merajú objekty väčšie ako 20 cm^2, čo síce zaručuje presnejšie výsledky merania, no neodráža správanie snímača v reálnom prostredí. Inšpirovaný touto skutočnosťou bolo zároveň vykonané meranie vzdialenosti nôh drevených aj kovových stoličiek s použitím korekcie teploty a vlhkosti vzduchu. Obr. 5 znázorňuje spomínané meranie a porovnáva hodnoty namerané s reálnou vzdialenosťou od ultrazvukového snímača. Zároveň sú zobrazené krivky bez a s použitím korekcie teploty a vlhkosti. Je možné vidieť, že korekcia počas teplého dňa s teplotami v meranej miestnosti v priemere 29,5 °C a relatívnou vlhkosťou 34% má vplyv na namerané vzdialenosti v hodnotách niekoľko centimetrov. Zároveň je nutné spomenúť nutnosť použitia filtrovania nameraných hodnôt ultrazvukovým snímačom o viacnásobné odrazy a iné chyby vyplývajúce z funkcie ultrazvukového merania vzdialenosti, taktiež ale pri použití vhodných metód je možné eliminovať a znížiť chybu merania na dostatočne malú hodnotu. Aplikovanie týchto skutočností s pridaním bezpečnostnej vzdialenosti zaručuje predchádzaniu kolíznych situácií.

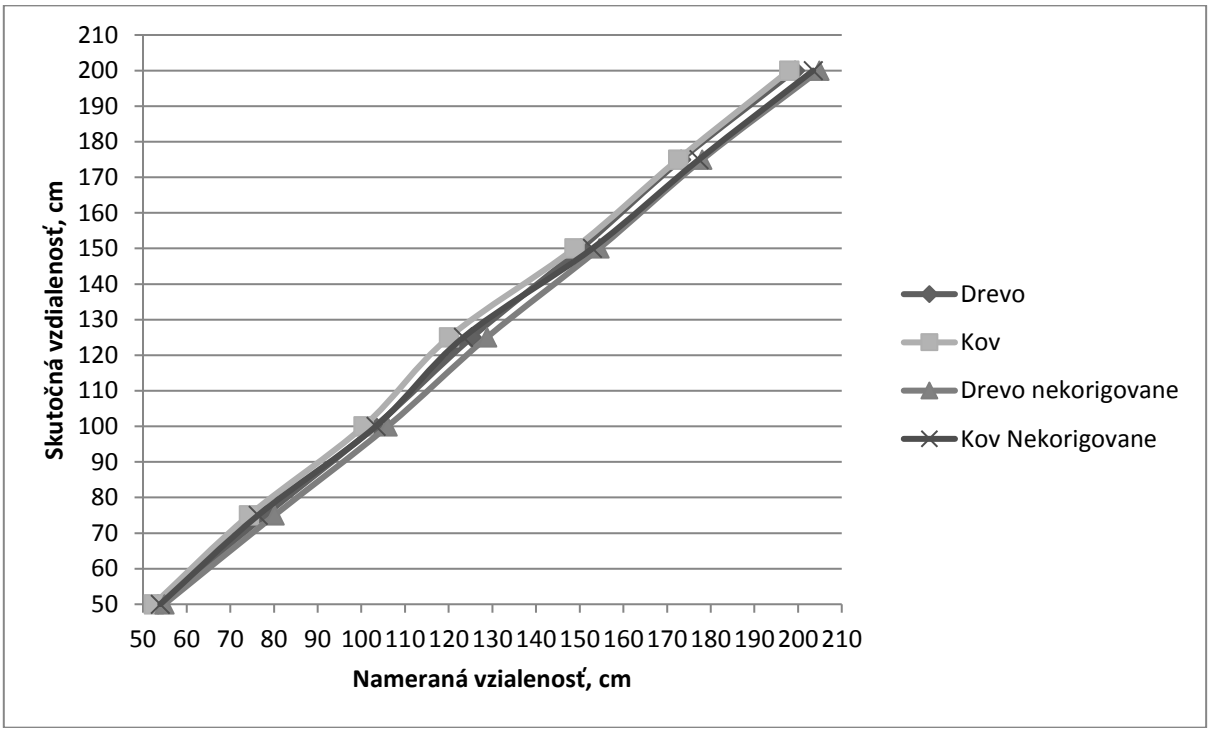

Obr. 5 Graf prirovnáva skutočnú a nameranú vzdialenosť ultrazvukovym snímačom

LITERATÚRA

1. Barrera, A. (2011). Advances in robot navigation. Rijeka: In-Tech. 250s. ISBN 978-953-307-346-0.
2. Borensrein, J., Everett, H. R., Feng, L. (1996). Where am I? Systems and Methods for Mobile Robot Positioning.[online]. Aviable from: <http://www.personal.umich.edu/~johannb/position.htm>
3. Cviklovič, V. (2011). Alternatívne spôsoby navigácie autonómnych mobilných robotov v poľnohospodárstve: Dizertačná práca. Nitra: SPU, 2011. 148s.

4. Dobeš, M. (2008). Zpracování obrazu a algoritmy v C#. Praha: BEN, 2008. 144s. ISBN 978-80-7300-233-6.
5. Duchoň, F. (2012). Lokalizácia a navigácia mobilných robotov do vnútorného prostredia. Bratislava: STU, 2008. 162s. ISBN 978 80 227-3646-6.
6. Koren,Y., Borenstein,J. (1991). Potential Field Methods and Their Inherent Limitations for Mobile Robot Navigation. [online]. Ann Arbor: University of Michigan. Dostupné na: <https://www.cs.sfu.ca/~vaughan/teaching/415/papers/PF_limitations.pdf>.
7. Lawalle, S. (2006). Planning Algorithms. [online]. Aviable from: <http://planning.cs.uiuc.edu/booka4.pdf>. ISBN-10 0-521-86205-9.
8. Topalov, A. V. (2011). Recent Advances in Mobile Robotics. Rijeka : InTech, 2011. 464s. ISBN 978-953-307-909-7.
9. Tóth, L., Hrubý, D. Cviklovič, V., Olejár, M. (2017). Algorithms of autonomous mobile robots. Nitra: SUA, 2017. 136s. ISBN 978-80-552-1681-2.

Corresponding author:
Ing. Juraj Baláži, Department of Electrical Engineering, Automatization and Informatics, Faculty of Engineering, Slovak University of Agriculture in Nitra, Tr. A. Hlinku 2, 949 76 Nitra, Slovak Republic, phone: +421 37 641 4723, e-mail: xbalazij@is.uniag.sk

IMPACT OF MULTIPLE MACHINERY PASSES ON SOIL PROPERTIES

Marek BARÁT, Vladimír RATAJ, Jana GALAMBOŠOVÁ, Marián POTOCKÝ, Tomáš GUT

Department of Machines and Production Biosystems, Slovak University of Agriculture in Nitra, Slovak Republic

Abstract
The article is focused on influence of multiple machinery passes on soil properties. Experiment area was divided into four stages of soil compaction – zero pass, 1x passed, 2x passed and 3x passed. The soil was trafficked with standard wheel tractor. Soil samples were taken from two depths and soil properties were determined. It was found, that traffic of agricultural machinery has an impact on soil properties. The bulk density was higher in all three trafficked areas, compared to non-compacted area. Similar results were found in comparison of soil porosity. The penetration resistance was higher on all three trafficked areas, but in the topsoil the first pass did not have such a great impact. Based on these results it can be concluded, that the machinery traffic has a big impact on soil compaction. The first machinery pass has the biggest influence, and next passes did not make such a damage to soil structure

Key words: *soil compaction, machinery passes, machinery traffic, soil properties, bulk density.*

INTRODUCTION

Publishes research results on the soil physical properties showed that the compaction of soil results in increasing the bulk density of soil, reducing the porosity (especially lowering the volume of non-capillary pores), and in higher level causes destruction of soil aggregates. These facts lead to further deterioration of the physical soil properties, such as a reduction in the water infiltration, changing the water content in the soil horizon and its relative movement in the soil (*Javůrek & Vach, 2008*).

Excessive soil compaction causes creation of anaerobic environment, that reduces the air exchange and microbial activity, and increases the denitrification and rate of the pores filled with water (*Torbert & Wood, 1992*). Soil compaction reduces pore size and this has a big impact on volume of water that can be absorbed into the soil. This reduces mainly the number of large pores. (*Wolkowski & Lowery, 2008*).

Heavy machinery and its multiple passes may cause significant problems. Since 1966, the mean weight and power of agricultural machinery has increased three times (Kumhála et al., 2013). Moreover, most of the field operations are conducted in so called 'random traffic' system. In conventional tillage system, 88% of field is trafficked in one year. In minimum tillage, the trafficked area can be lowered to 65% (*Kumhála et al., 2013; Rataj et al., 2014). Schjonning et al.* (2016) has shown that multiple machinery passes have big influence on yield of arable crops. They also showed, that the first machinery pass did not have impact on yield. The yield loss was significant in compacted subsoil.

Botta et al. (2016) determined the influence of heavy harvesting machines on growing soybean. Yield of soybean was influenced by weight of harvesting machines and design of wheels. Emergency of soybean was not affected by compaction of upper part of soil. *Javůrek & Vach* (2008) reported, that yield loss due to compaction in cereal was 10–20%, in corn – 10–15%, and in pulses – 15–20%. In dry conditions crop yields could be positively affected (*DeJong-Hughes, 2001*). Several measures can be taken to minimize machinery induced soil compaction. For example, *Godwin et al.* (2015) suggested that Low Ground Pressure (LGP) can avert soil compaction. In this system, special tires are used, that can operate at inflation pressure of 0.7 bar. Recently, Controlled Traffic Farming (CTF) is considered as a management method that could lower the trafficked area and optimize the growing conditions. CTF creates two zones: non-trafficked crop beds and cropped or non-cropped traffic lanes (*Chamen, 2015*). This system can be established also with normal machinery without special adjustment, with 68% non-trafficked area (*Gutu, 2015*). *Botta et al.* (2007) has shown, that with reduction of traffic intensity, yield increased by 29%, which resulted in increased income by US$134 ha^{-1}.

The aim of this work was to determine the influence of machinery traffic to soil properties, such as bulk density, porosity and penetration resistance.

MATERIALS AND METHODS

The experiment took place in a field with equal conditions. The soil type was a silk-loam. The field was shallow cultivated after the wheat harvest, and a small area was divided into four parts, that corresponds to traffic intensities. The parts were trafficked with a wheel of a standard tractor. The weight of the machine was 8200 kg.

Tractor specification:

- John Deere 6920S equipped with front loader Trima +5.0P
- Attached 4-furrow turnover plough Overum BV397F
- Tires:
  - Front: 540/65-R28 radial – pressure 1.4 bar
  - Rear: 650/65-R38 radial – pressure 1.2 bar

After the field was trafficked, the soil penetration resistance was measured with 15 measurements on each spot. The device used was a penetration resistance meter "Penetrologger" with measurement up to 80 cm and a scale of 1 cm. The cone used had an angle 30° with a surface 1 cm^2.

The soil bulk density and porosity was determined using undisturbed soil samples. The samples were taken using rustless cylinders with volume of 100 cm^3. Two cylinders were taken out of one spot and one depth, with two repetitions on each trafficked intensity area. On non-compacted are there were four repetitions. The scheme of sample is shown in Fig. 1.

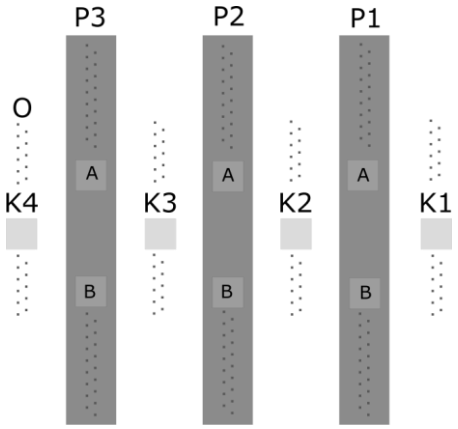

Fig. 1 scheme of sample taking (P1, P2, P3 – number of passes; K1-K4 – non compacted soil; O – measurement of penetration resistance; A, B – samples with undisturbed soil)

RESULTS AND DISCUSSION

Based on obtained data, following results were achieved. Bulk density raised after the first machinery pass. The next passes did not have influence on soil bulk density. The difference was higher in the topsoil, however, in the subsoil it did not have such an effect. The bulk density after multiple passes is shown in Fig. 2.

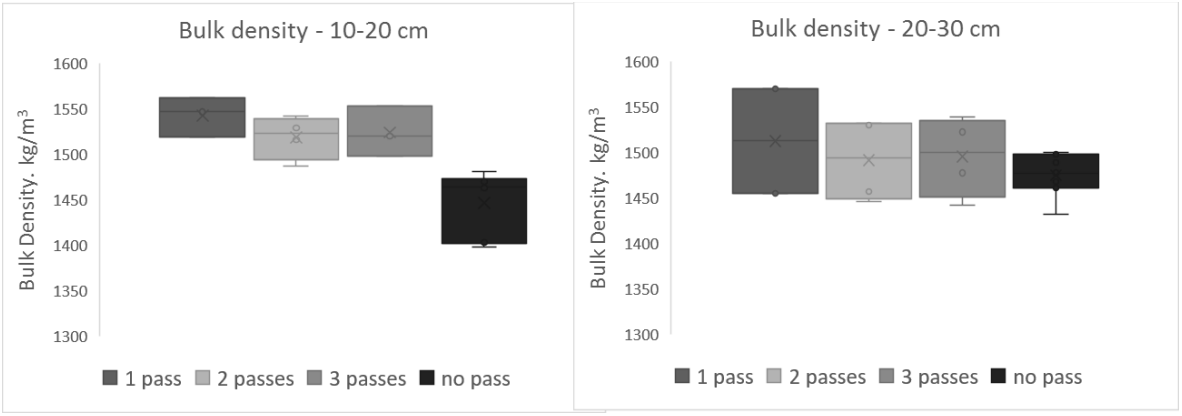

Fig. 2 Bulk density after multiple passes (left – topsoil; right – subsoil)

The porosity changed in similar way that bulk density. The first pass had the biggest influence on lowering porosity and next passes did not had any influence. The porosity was lowered after the passes mostly in Topsoil, the change was not such great in the subsoil. There is a correlation between porosity and bulk density. The porosity is shown in Fig. 3.

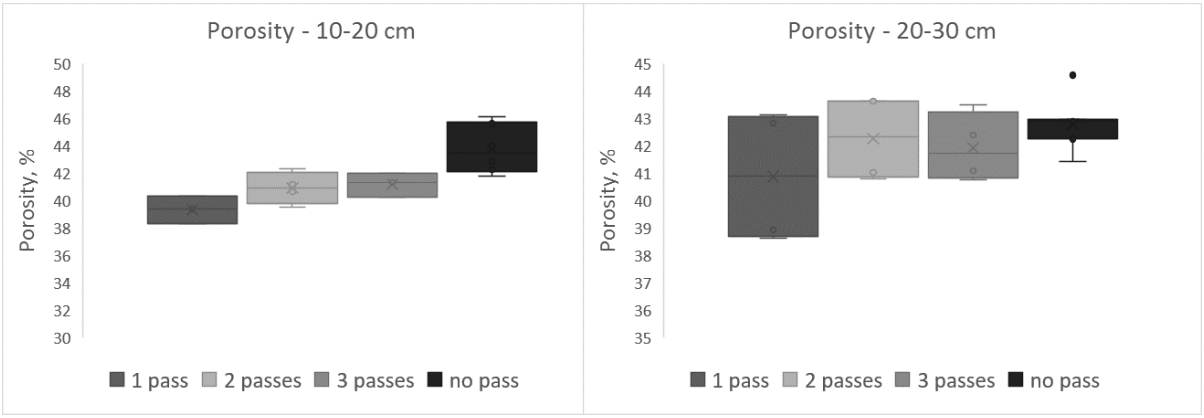

Fig. 3 Porosity after multiple passes (left – topsoil; right – subsoil)

After multiple passes, the penetration resistance changed through all profile. The first pass had the biggest influence on penetration resistance. Next passes did not raise the penetration resistance. However, the data shows, that in the topsoil, the first pass did have an influence, but also the second pass increased penetration resistance in a significant way. The penetration resistance is shown in Fig. 4.

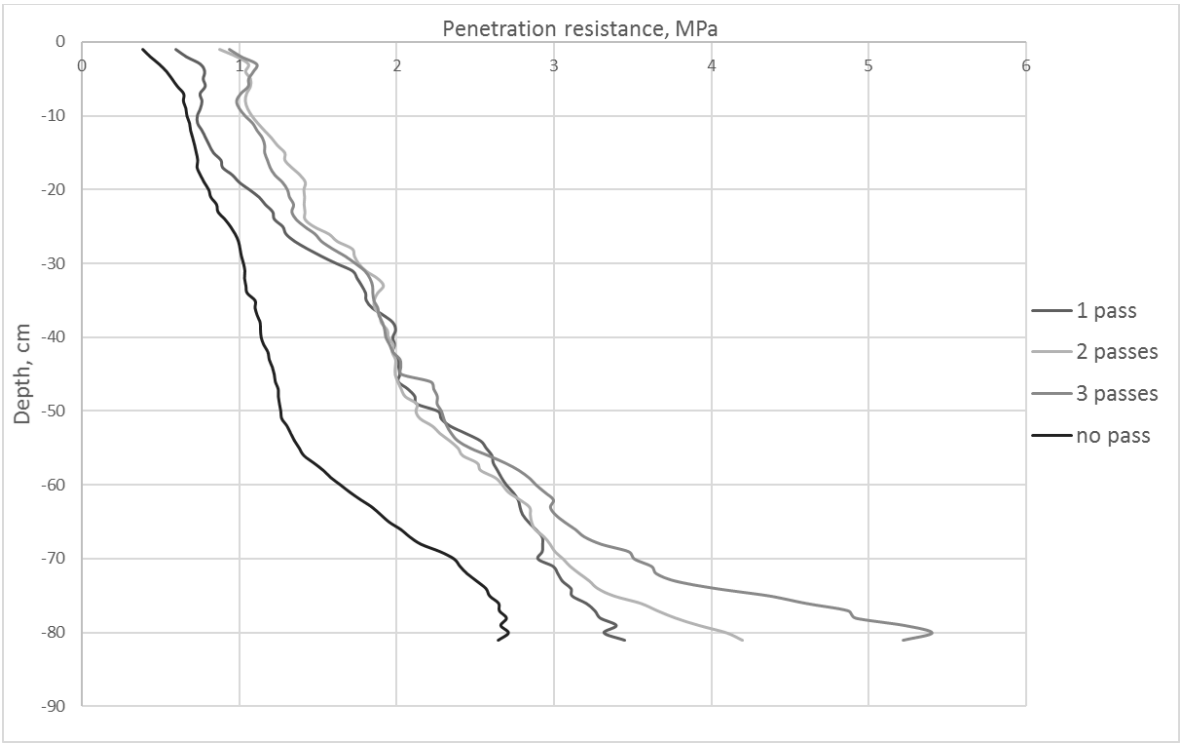

Fig. 4 Penetration resistance through all profile with multiple trafficked area

CONCLUSIONS

Based on the results it can be concluded, that first pass has the biggest influence on soil properties. The first pass influenced the topsoil the most. Next passes did not have such influence on soil. However, penetration resistance raised also with the second pass. Those results could indicate, that machinery traffic should be guided into one tracks and leave the most of the soil not trafficked. This technology is used in a system called CTF – Control Traffic System.

ACKNOWLEDGMENT

This article was prepared in the framework of a research project funded by the European Union entitled: "ITEPAg: Application of information technologies to increase the environmental and economic efficiency of production agro-system" (ITMS no. 26220220014) and „Building the Research Centre AgroBioTech" (ITMS no. 26220220180). The authors are grateful to staff at the University Farm in Kolinany (Slovakia) and also to staff at Ľuboš Barát SHR for technical and operational support to conduct this research.

REFERENCES

1. Botta, G. F., Pozzolo, O., Bomben, M., Rosatto, H., Rivero, D., Ressia, M., Tourn, M., Soza, E. & Vazquez, J. (2007). Traffic alternatives for harvesting soybean (Glycine max L.): Effect on yields and soil under a direct sowing system. *Soil & Tillage Research* 96, pp. 145–154.
2. Botta, G. F., Tolon-Becerra, A., Rivero, D., Laureda, D., Ramirez-Roman, M., Lastra-Bravo, X., Agnes, D., Flores-Parra, I. M., Pelizzari, F. & Martiren, V. (2016). Compaction produced by combine harvest traffic: Effect on soil and soybean (*Glycine max* L.) yields under direct sowing in Argentinean Pampas. *European Journal of Agronomy* 77, pp. 155–163.
3. Chamen, T. (2015). Controlled Traffic Farming – from worldwide research to adoption in Europe and its future prospects. *Acta Technologica Agriculturae* 3, pp. 64–73.
4. Dejong-Hughes, J. (2001). Soil compaction: causes, effects and control. *University of minesota*. http://www.extension.umn.edu/agriculture/tillage/soil-compaction/. Accessed 20.12.2016.

5. Godwin, R., Misiewicz, P., White, D., Smith, E., Chamen, T., Galambošová, J. & Stobart, R. (2015). Results from recent traffic systems research and the implications for future work. *Acta Technologiva Agriculturae* 3, pp. 57–63.
6. Gutu, D. (2015). Changes in traffic systems on arable land in agricultural company. *PhD Thesis*. 2015. 158 p. (in Czech).
7. Javůrek, M. & Vach, M. (2008). Negative effects of soil compaction and procedures to their elimination – Methodology for praxis. 2008. 35 p. ISBN 978-80-87011-57-7. (in Czech).
8. Kumhála, F., Gutu, D., Hůla, J., Chyba, J., Kovaříček, P., Kroulík, M., Kvíz, Z., Mašek, J. & Vlášková, M. (2013). Technology of Controlled Traffic Farming on fields. *Certificated methodology*. 2013. 40 p. ISBN 978-80-213-2425-1. (in Czech).
9. Rataj, V., Galambošová, J., Macák, M. & Nozdrovický, L. 2014. Precision Agriculture: System – machines – experiences. 160 p. ISBN 978-80-86726-64-9. (in Slovak)
10. Schjonning, P., Lamandé, M., Munkholm, L. J., Lyngvig, H. S. & Nielsen, J. A. 2016. Soil precompression stress, penetration resistance and crop yields in relation to differently-trafficked, temperare-region sandy loam soils. *Soil & Tillage Research* 163. 298–308.
11. Torbert, H. A., & Wood, C. W. (1992). Effects of soil compaction and water-filler pore space on soil microbial activity and N losses. In *Commun. SoilSci. PlantAnal.*23, pp. 1321-1331.
12. Wolkowski, R., & Lowery, B. (2008). Soil Compaction: Causes, concerns, and cures. University of Wisconsin – Extension. http://www.soils.wisc.edu/extension/pubs/A3367.pdf

Corresponding author:
Ing. Marek Barát, Department of Machines and Production Biosystems, Faculty of Engineering, Slovak University of Agriculture in Nitra, Tr. Andreja Hlinku 2, 949 76 Nitra, Slovakia, phone: +421 902209851, e-mail: baratmarek@centrum.sk

TESTING OF IRRRIGATION UNIFORMITY OF SPRAY TYPE MICRO SPRINKLER

Henrich BLEHO, Norbert MICHLIAN, František URBAN, Ivan RIGÓ

Department of Machine and Production Biosystem, Faculty of Engineering, Slovak University of Agriculture in Nitra, Slovak Republic

ABSTRACT
The irrigation machine in terms of its quality of work belongs among the most important parameters which defines the single irrigator machine regarding to its operational properties. The aim of the contribution was then to evaluate the irrigation uniformity of selected micro-irrigators Hunter 8H, 10H and 12H, respectively. Micro-irrigators was installed on specially designed and patented test console, and positioned at grassland. According to the type of used micro-irrigator a test pressure was set in range from 0.22 to 0.25 MPa when the effective irrigation range was observed at levels from 2.4 to 4 m of distance from employed irrigator. Used rain gauge containers were distributed in rectangular shape with total amount of 55 pieces (11×5) and claps 1×1 m. In order to evaluate the irrigation machines quality of work it was employed evaluation method according to Christiansen by evaluation of coefficient of irrigation uniformity Cu. It can be concluded that coefficient of irrigation uniformity did not reach the required value defined by standard in the case of considered zero overlap (8H – Cu = 42.18%; 10H – Cu = 47.30% and 12H – Cu = 7.98%). However, by applying of the overlaps from all sides in the given irrigation sector the irrigation quality of work was increased which was observed at the basis of increased coefficient of irrigation uniformity (8H – Cu = 75.00%; 10H – Cu = 73.43% and 12H – Cu = 79.62%).

Keywords: *Quality of work, Overlap, irrigation.*

ÚVOD
Nevyhnutným predpokladom úspešného hospodárenia na pôde je potrebné množstvo vody v pôde a jej správne rozdelenie v priebehu vegetačného obdobia (*Rehák a kol., 2015*). Mikrozávlaha je cielené dávkovanie vody priamo ku koreňovému systému rastlín. Mikrozávlaha je súčasťou takmer každého automatizovaného systému a navrhujeme ju takmer v každej záhrade (*Hríbik a kol., 2007*). Závlaha mikropostrekom je riešená takým spôsobom, aby sa jednotlivé plošné plochy prekrývali a tým dosiahli čo najvyššiu kvalitu práce. Systémy sú zložené s mnohých na seba nadväzujúcich prvkov – v zásade z postrekovačov s dýzami, potrubí, senzorov, ventilov a riadiacej jednotky. Dôležitou technickou vlastnosťou okrom spomínaných parametrov je aj fakt či sa jedná o statický alebo rotačný distribútor vody (*Jobbágy & Štofik, 2011*).

Obr.1 Mikropostrekovače, Rotačný a statický (Jobbágy, Štofik, 2011)
Fig. 1 Microsprinkler, Rotor and Spray type (Jobbágy, Štofik, 2011)

Kvalita zavlažovania sa posudzuje správnou intenzitou a rovnomernosťou zavlažovania. Intenzita vyjadruje množstvo vody v mm dodané zavlažovačom za časovú jednotku (*Jobbágy, 2011*). Pre kvalitné hospodárenie sa však požaduje, aby intenzita zavlažovania bola nižšia ako infiltračná schopnosť

pôdy (*Jobbágy a kol., 2016a; Chyba a kol., 2014; Chyba a kol., 2017*). Rovnomernosť zavlažovania závisí od správnej činnosti zavlažovačov a najmä od:

- vhodného výberu otvoru dýzy zavlažovača,
- tlaku vody v prúdnici,
- vhodnej voľby sponu a vzdialenosti susedných stanovíšť (*Látečka, 2000*).

Cieľom riešenia predkladaného príspevku je prispieť k rozšíreniu poznatkov a preveriť kvalitu v oblasti aplikácie a nastavenia vstupných parametrov mikropostrekovačov.

MATERIÁL A METÓDY

V rámci príspevku sme sa rozhodli otestovať kvalitu práce vybraných troch rôznych mikropostrekovačov Hunter, ktorých technické parametre sú uvedené v tabuľke 1. Terénne merania sa realizovali na vybranom trávniku, kde sa umiestnila nami navrhnutá testovacia konzola. Na KSVB bol teda navrhnutý model pre testovanie kvality práce mikropostrekovačov pod názvom „*Výškovo nastaviteľná testovacia konzola pre mikropostrekovače"(UV 40-2015, Obr. 2).* Pri meraniach bolo treba postupovať podľa normy STN ISO 7749-2, ktorá ustanovuje mechanické a funkčné požiadavky na poľnohospodárske zavlažovacie zariadenia – Otáčavé postrekovače. Výskum pozostával z hodnotenia kvality práce koeficientom rovnomernosti postreku Cu, kde sa namodelovali prekrytia. Na danej konzole je možné pripevniť až 4 mikropostrekovače a s príslušnou riadiacou jednotkou (riadiaca jednotka Hunter, Model EC 401 E) si zvoliť činnosť vybraných mikropsostrekovačov. Pri testoch bolo potrebné konzolu umiestniť tak, aby štvorcová sieť prislúchajúcich nádob bola postačujúca. Výška umiestnenia postrekovača sa upravila podľa výšky umiestnenia nádob.

Tab. 1 Technické parametre mikropostrekovačov, nastavené pri meraniach
Tab. 1 Technical parameter of microsprinkler, Set during measurements
1-Parameter, 2-Spray type microsprinkler, 3-Type, 4-Color, 5-Pressure, 6-Flow, 7-Range, 8-Sector

Parameter (1)	Mikropostrrekovač (2)	Mikropostrrekovač (2)	Mikropostrrekovač (2)
Označenie, Typ (3)	8H	10H	12H
Farba (4)	hnedá	červená	zelená
Tlak, MPa (5)	0,22	0,225	0,25
Prietok, $m^3.h^{-1}$ (6)	0,14	0,21	0,32
Dostrek , m (7)	2,4	3,3	4,0
Sektor, ° (8)	Pevný , 180°	Pevný , 180°	Pevný , 180°

Obr.2 Testovacia konzola pre mikropostrekovače, mikropostrekovač
Fig. 2 Test console for Microsprinkler, microsprinkler

Výpočet sa uskutočňuje podľa nasledovného vzťahu:

$$Cu = 100.\left[1 - \frac{\sum_{i=m}^{n} |Vi - \overline{Vi}|}{n.\overline{Vi}}\right], \quad \% \qquad (1)$$

kde:
Vi - dávka vody na elementárnych plochách, mm
$\overline{Vi}$ - priemerná dávka vody, mm
n - počet rovnako veľkých elementárnych plôch, na ktoré sa zavlažovaná plocha rozdelí, pričom plochy musia byť rovnako veľké, ks,
$\sum_{i=m}^{n} |Vi - \overline{Vi}|$ - absolútna suma odchýliek od priemernej dávky.

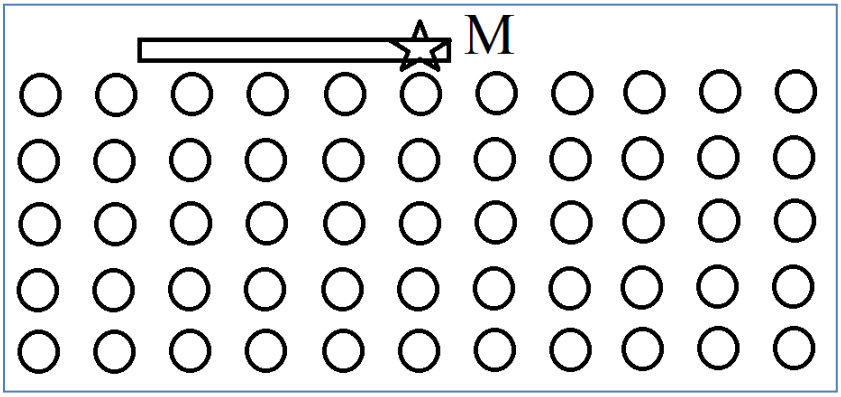

Obr. 3 Princíp merania, M-mikropostrekovač
Fig. 3 Principe of measurement, M-microsprinkler

VÝSLEDKY A DISKUSIA

Na nami navrhnutej konzole sme sa rozhodli otestovať kvalitu práce vybraných mikropostrekovačov, ktorých technické parametre boli uvedené v Tab. 1. Konzola bola navrhnutá na Katedre strojov a výrobných biosystémov, TF, SPU v Nitre, kde jej súčasťou je armatúra, tlakomer, riadiaca jednotka a škrtiaci ventil. V poslednom období sa čím ďalej, tým viac uplatňujú úsporné technológie závlah tohto typu, a aplikujú sa pri zavlažovaní futbalových a iných športových ihrísk, okrasných záhrad a trávnikov. Existuje viac ako 100 rôznych výrobcov a každý z nich vyrába rôzne modifikácie, ktoré sa líšia typom aplikácie závlahy (rotačné alebo statické) a priemerom otvoru dýzy. Nastavenie pracovných tlakov ovplyvňuje dostreky, ktoré môžu byť od niekoľkých centimetrov až do niekoľkých metrov (niekedy viac ako 15 m, ihriska a podobne).

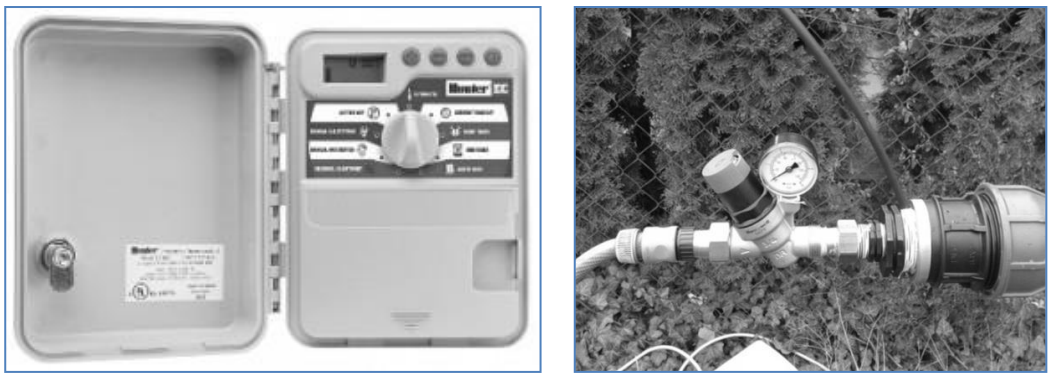

Obr. 4 Riadiaca jednotka a škrtiaci ventil
Fig. 4 Irrigation controller and Shutoff valve

Merania prebiehali pri predpísaných prevádzkových parametroch od výrobcu. Zrážkomerné nádoby sme usporiadali do obdĺžnikovej siete s celkovým počtom kusov 55, s rozstupom 1x1 m (celkovo 5x11, Obr. 3). Dôvodom tvaru obdĺžnika bol fakt, že mikropostrekovač zavlažoval v sektore o uhle 180 °. Grafické zobrazenie výsledkov je uvedené na Obr. 5. Najväčšia závlahová dávka je centralizovaná v okolí mikropostrekovača, v závislosti od vzdialenosti merania klesá. Hodnoty koeficienta rovnomernosti postreku podľa Christiansena Cu sú uvedené v tabuľke 2. Pri výpočtoch sa uvažovali iba

zrážkomerné nádoby, ktoré spadajú do sektoru zavlažovania (závisí od dostreku, zavlažená plocha je teda polkruh). Prakticky možno povedať, že sa pri meraniach dosiahli vyššie dostreky ako boli tabuľkovo udávané hodnoty. Koeficienty rovnomernosti postreku dosiahli nízke hodnoty, kde pri najvyššom dostreku (mikropostrekovač 12H) sa dosiahla hodnota Cu len 7,92 %. Z výsledkov teda vyplýva, že pri aplikácii mikropostrekovačov sa musí jednoznačne zaviesť prekrytie a to dokonca zo všetkých strán. Následne sa namodelovalo prekrytie v hodnotách podľa skutočne nameraných dostrekov. U mikropostrekovača 8H sa výsledky zisťovali pri aplikovaní prekrytia o hodnote 3 m s pozitívnymi výsledkami a jeho zvýšením zo 42,18 % na Cu = 75 %. Pri zavedení prekrytia u mikropostrekovača 10H sa dosiahlo zvýšenie kvality práce až o 26,13 % a u mikropostrekovača 12H 79,62 %. Pri zavedení kombinovaného prekrytia, to znamená že z ľavej a pravej strany mikropsotrekovača to činilo p = 4 m a z čelnej strany o hodnote 3 m, sme dosiahli nepatrné zvýšenie koeficienta rovnomernosti postreku voči prekrytiu o celkovej hodnote (zo všetkých strán rovnaké) p=4m. Výsledky preukázali pozitívny vplyv prekrytia a jednoznačné vyššie hodnoty vo všetkých troch prípadoch skúmania o to minimálne o hodnotu 20 %. Grafické zobrazenie výsledkov s prekrytiami je uvedené na Obr. 6.

Tab. 2 Koeficient rovnomernosti postreku Cu
Tab. 2 Coefficient of irrigation uniformity, Cu
1-Spray Type Microsprinkler, 2-Overlap, 3- Combined Overlap

Mikropsotrekovač (1)	Prekrytie, m (2)	Cu, %
Hunter 8H	0	42,18
Hunter 8H	3	75,00
Hunter 10H	0	47,30
Hunter 10H	4	73,43
Hunter 12H	0	7,98
Hunter 12H	4	79,62
Hunter 12H	Kombinované 4 a 3 (3)	80,25

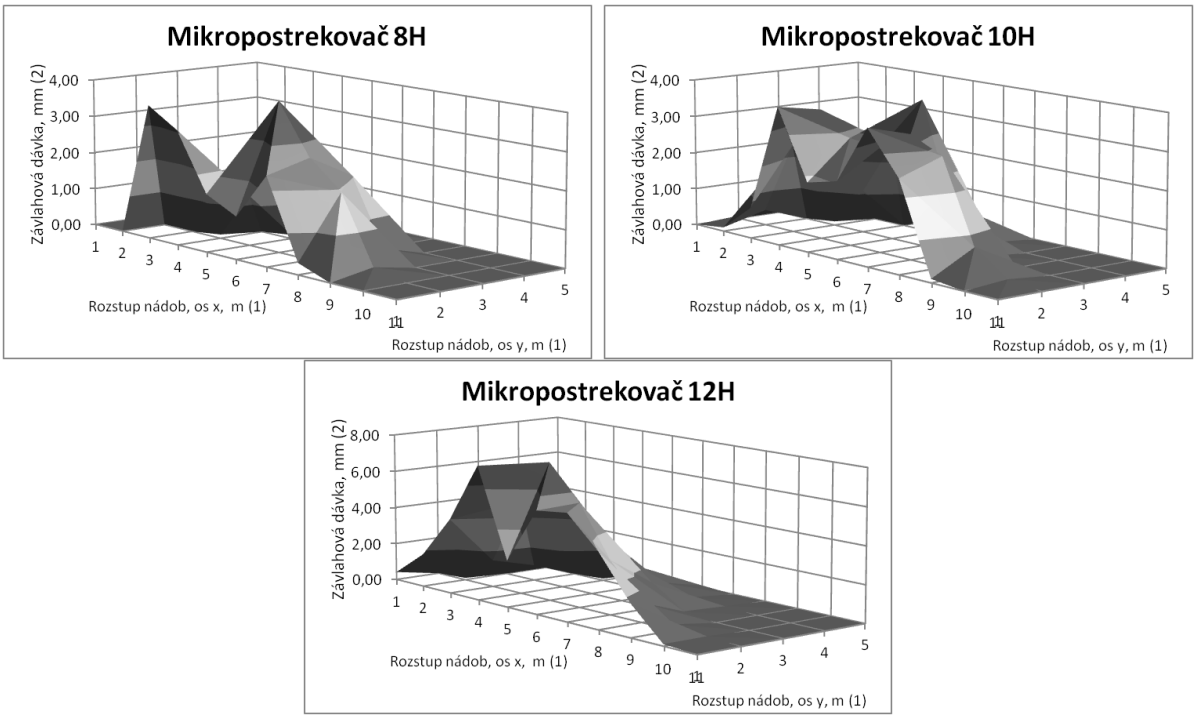

Obr. 5 Kvalita práce – závlahová dávka mikropostrekovačov Hunter 8H,10H a 12H
Fig. 5 Quality of work – irrigation rate of Spray Type Microsprinkler Hunter 8H, 10H and 12H, 1-Spacing of cup, 2-irrigation rate

Výsledky z merania vo forme popisnej štatistiky sú uvedené v Tab. 3. Z výsledkov vyplýva, že pri hodnotení kvality práce s uvažovaním aj s nádobami, v ktorých bola nulová závlahová dávka, je kvalita práce nevyhovujúca. Po odstránení nulových hodnôt, kde postrekovač v podstate nezasahoval, sa znížila hodnota variačného koeficienta, ale jeho hodnota bola aj tak privysoká. Z výsledkov teda vyplýva, že hodnotenie kvality práce mikropostrekovačov zavlažujúcich do kruhu, resp. do výseče, a to bez prekrytia, je vyhodnocovanie s hodnotou koeficienta Cu alebo popisnou štatistikou nesprávna.

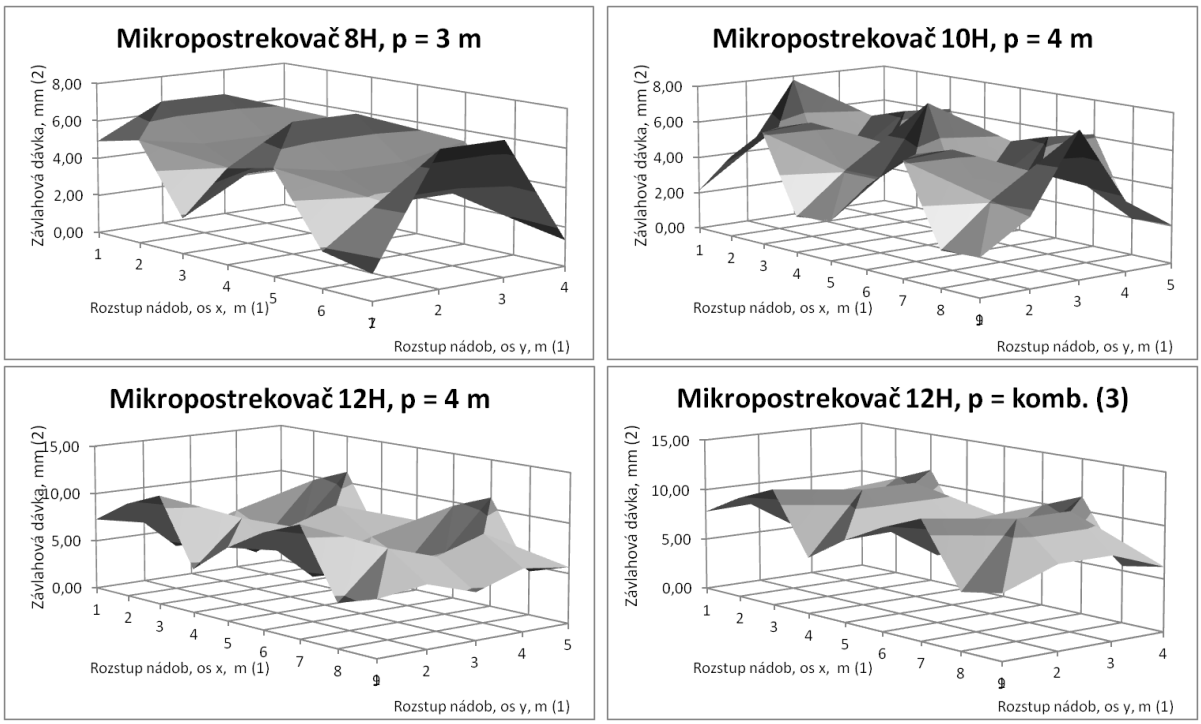

Obr. 6 Kvalita práce – závlahová dávka mikropostrekovačov Hunter 8H,10H a 12H s prekrytiami
Fig. 6 Quality of work – irrigation rate of Spray Type Microsprinkler Hunter 8H, 10H and 12H, 1-Spacing of cup, 2-irrigation rate, with overlap (p), 3-Combined Overlap

Tab. 3 Popisná štatistika
Tab. 3 Descriptive statistic
MP-Spray Type Microsprinkler, 1-Parameter, 2-Overlap, 3-Average, 4-Standard deviation, 5-Variance, 6-Difference max-min, 7-Minimum, 8-Maximum, 9-Sum, 10-Sample size, 11-Coefficient of variation,

Parameter (1)	**MP 8H**		**MP 10H**		**MP 12H**	
Prekrytie (2)	**0**	**3 m**	**0**	**4 m**	**0**	**4 m**
Stredná hodnota (3)	1,25	4,51	16,56	4,32	1,98	6,73
Smerodajná odchýlka (4)	1,33	1,80	13,56	1,80	2,23	2,23
Rozptyl výberu (5)	1,77	3,23	184,01	3,23	4,96	4,99
Rozdiel max – min (6)	3,99	5,53	38,00	5,84	7,37	7,27
Minimum (7)	0,00	1,33	0,00	1,95	0,00	3,89
Maximum (8)	3,99	6,86	38,00	7,78	7,37	11,16
Súčet (9)	27,55	126,19	414,00	194,40	69,14	302,97
Počet (10)	22,00	28,00	25,00	45,00	35,00	45,00
Variačný koeficient, % (11)	106,21	39,86	81,91	41,59	112,70	33,18

Kvalita práce zavlažovania závisí od použitej závlahovej techniky, výsledky sa následne vyhodnocujú prostredníctvom koeficienta rovnomernosti postreku. Pre aplikované mikropostrekovače (tiež aj pre

pásové zavlažovače) sa uplatňuje metóda podľa Christiansena (*Jobbágy a kol. 2016b; Abdul-Razzaq & Jahad, 2014; Udai Adnaid, 2010*). Automatická regulácia závlahového systému teda pozostáva zo základných vstupných informácii ako sú vlastnosti pôdy, plodiny a prostredia (ovzdušie atď.). Závlahová sústava u týchto zariadení pozostáva zo zdroja vody (v prevažnej väčšine vŕtaná studňa), filtrov, mikropočítača (riadiacej jednotky) a čerpadla (*Jobbágy, 2016*).

ZÁVER

V danom príspevku sme sa zamerali na zhodnotenie kvality práce troch vybraných mikropostrekovačov. Skúšky prebiehali na navrhnutej konzole, kde je možné aplikovať až štyri rôzne mikropostrekovač súčasne. Hodnotenie kvality práce podľa koeficienta rovnomernosti postreku vyžaduje namodelovanie prekrytia a tým dosiahnutie uspokojujúcich hodnôt. Práve preto sa aj pri modelovaní a realizácii závlah uplatňuje metodika prekrytí jednotlivých mikropostrekovačov. V našom prípade sme realizovali pokusy u troch rôznych mikropostrekovačov, kde po zavedení prekrytia o hodnote 3 m alebo 4 m sme dosiahli kvalitu práce vyjadrenú koeficientom rovnomernosti postreku v hodnotách nad 70 %. Zavedenie takejto metódy zavlažovania prináša úsporu vody a elektrickej energie.

POUŽITÁ LITERATÚRA

1. Abdul-Razzaq, K. A., & Jahad, U. A. (2014). Evaluation of Uniformity Coefficients for Sprinkler Irrigation System under Traditional and Looped Network Field Conditions. *Journal of Babylon University/Engineering Sciences/* 22(1)
2. Chyba, J., Kroulík, M., Krištof, K., & Misiewicz, P. (2017). The influence of agricultural traffic on soil infiltration rates. *Agronomy Research.* 15(3) 664--673.
3. Chyba, J., Kroulík, M., Krištof, K., Misiewicz, P., & Chaney, K. (2014). Influence of soil compaction by farm machinery and livestock on water infiltration rate on grassland. In *Agronomy Research.* 12(1) 59--64.
4. Hríbik, J., Simoník, J., Jobbágy, J., Hričovský, I., Jankovič, O., & Kollárová, K. (2007). Úsporné technológie zavlažovania z hľadiska ochrany vôd pred znečistením dusičnanmi z poľnohospodárskej výroby. *Vedecká monografia*, Bratislava:VÚPOP, 60s. ISBN 978-80-89128-38-9.
5. Jobbágy, J. (2011). Hodnotenie závlahovej techniky z hľadiska rovnomernosti závlahy postrekom. *Vedecká monografia*, SPU ES v Nitre, 123 s. ISBN 978-80-552-0617-2
6. Jobbágy, J. (2016). Zavádzanie automatizácie do procesu zavlažovania. *Moderná mechanizácia v poľnohospodárstve*. ISSN 1335-6178, 19 (4), 28-30.
7. Jobbágy, J., Beloev, Ch. I., Krištof, K., & Findura, P. (2016a). The benefits and efficiency of precision irrigation. *Mechanization in agriculture*., 62(2), 35-43.
8. Jobbágy, J., & Bleho, H. (2015).*Výškovo nastaviteľná testovacia konzola pre mikropostrekovače : úžitkový vzor č. 40-2015 : dátum zverejnenia 4.8.2015*. Banská Bystrica : Úrad priemyselného vlastníctva Slovenskej republiky, 4 s.
9. Jobbágy, J., Krištof, K., Findura, P. (2016b). Soil compaction caused by irrigation machinery. *Agronomy Research.*, 14 (3), 790-800 .
10. Jobbágy, J, & Štofik, D. (2011). Automatizácia prevádzky zavlažovania. Roľnícke noviny. ISSN 1335-440X, 14.12. 81(50), 18.
11. Látečka, M. (2000). Rovnomernosť postreku pri závlahe otáčavými postrekovačmi. *Monografia*. Nitra, 58 s. ISBN 80-7137-678
12. Rehák, Š., Bárek, V., Jurík, Ľ., Čistý, M., Igaz, D., Adam, Š., Lapin, M., Skalová, J., Alena, J., Fekete, V., Šútor, J., & Jobbágy, J. (2015). Zavlažovanie poľných plodín, zeleniny a ovocných sadov. Bratislava : Veda, 2015. 640 s. ISBN 978-80-224-1429-6.
13. Udai Adnain Jahad. (2013). Study the emission uniformity coeficients for sprinkler irrigation system with different layouts. *Euphrates Journal of Agriculture Science*. 5(4), 256-266

Corresponding author:
Ing. Henrich Bleho., Katedra strojov a výrobných biosystémov, Slovenská poľnohospodárska univerzita v Nitre, Technická fakulta Tr. A. Hlinku 2, Nitra 949 76, Slovenská republika. inex@inexhausgarden.sk

BRIQUETTE BIOFUEL FROM FRUIT ORCHARDS WASTE BIOMASS

Anna BRUNEROVÁ, Milan BROŽEK

Department of Material Science and Manufacturing Technology, Faculty of Engineering, Czech University of Life Sciences Prague

Abstract
Present study described potential of wood waste biomass from fruit orchards for briquette fuel production. Namely, mix of new shoots and old branches of cherry (Prunus avium), apricot (Prunus armeniaca) and plum (Prunus domestica) trees were collected. Within the experimental measurements two kinds of briquette samples were produced (diameter of 50 mm and 65 mm). Suitability of chosen feedstock material for briquette fuel production was stated by set of procedures which determined mechanical parameters of produced briquette samples, thus, briquettes final quality. Evaluation of obtained result values proved very high level of mechanical durability of tested briquette samples: 94.87% (50 mm); 91.06% (65 mm). As well as, satisfactory level of volume density: 951.40 kg·m^{-3} (50 mm); 886.18 kg·m^{-3} (65 mm) and rupture force: 94.30 N·mm^{-1} (50 mm); 60.24 N·mm^{-1} (65 mm). Overall evaluation of obtained result values proved suitability of such briquette production for commercial purposes.

Key words: *fruit trees; volume density; mechanical durability; pruning residues, renewable energy.*

INTRODUCTION

Fruit trees play important role in humans and animals nutrition, as well as, represent major economical subject in agriculture sector worldwide (*Zhang, 2011*). Fruit orchards cover more than 1.29 million hectares in the European Union. Between countries with largest areas covered by orchards belongs Spain (432,612 ha), Italy (285,625 ha) and Poland (150,992 ha) (*Eurostat, 2012*). Focused on Czech Republic, more than 3,000 growers, which produce fruit mainly for commercial production, were monitored. Total area of orchards in Czech Republic is equal to 21,347 ha and average area of one orchard is 8.94 ha. Cherry (*Prunus avium*), apricot (*Prunus armeniaca*) and plum (*Prunus domestica*) trees are one commonly cultivated crops in Czech orchards. Specifically, cherry trees occupy areas of 1,278.17 ha, apricot trees areas of 1,636.88 ha and plum trees areas of 2,545.10 ha. Whereas, an average planting density in cherry orchards is 350 trees/ha, in apricot orchards is 357 trees/ha and in plum orchards is 420 trees/ha (*ČSÚ, 2013*). If we consider mentioned numbers and information, it indicates a huge amount of waste wood biomass which is produced within the fruit orchards life cycle. One of the important step in fruit orchards treatment is annual spring trees pruning while new unwanted shoots and old dead branches are removed from trees. Such a residues represent waste wood biomass, thus, possible feedstock material for solid biofuel production, consequently, for clean renewable energy generation. Previous investigations about subsequent utilization of residues from fruit orchards for energy generation in the form of solid biofuel were already performed with satisfactory results in the form of briquette and pellet biofuels (*Zavrazhnov & Syasin, 2014; Živković et al., 2013*). Further, the potential of fruit orchards pruning was also investigated in the relation to its energy potential, again with satisfactory results. Chemical analyses of pruned wood biomass from fruit orchards indicated gross calorific values (average values) equal to 16.76 ± 2.02 MJ·kg^{-1} for cherry trees, to 17.19 ± 2.58 MJ·kg^{-1} for apricot trees and to 17.12 ± 2.51 MJ·kg^{-1} for plum trees (*Bilandzija et al., 2012*).
Therefore, the main aim of present paper was to determine the potential of waste wood biomass from fruit orchard as a feedstock material for production of briquette fuel with two different diameters (50 mm and 65 mm) by statement of their mechanical parameters and subsequent evaluation of final quality of such a briquette biofuel.

MATERIALS AND METHODS

Whole methodology of present investigation (proper feedstock preparation, briquette samples production, experimental testing) was conducted to related mandatory technical standards, namely, EN

15234–1 (2011), EN ISO 16559 (2014), EN ISO 17225–1 (2015), EN ISO 17831–2 (2015) and EN ISO 18134–2 (2015).

Materials and samples

Feedstock material used in present research for subsequent briquette production was collected in fruit orchard in Central Bohemian Region, Czech Republic. Unprocessed feedstock material consisted of mixed waste wood biomass from cherry (*Prunus avium*), apricot (*Prunus armeniaca*) and plum (*Prunus domestica*) trees. Such a waste biomass was collected during spring trees pruning, specifically, new shoots and old dead branches were chosen. Raw unprocessed material in its initial form was primarily crushed into wood chips by garden shredder Bosch, type AXT 25 D (Stuttgart and Renningen, Germany) equipped with drum cutting system. Wood chips were subjected to initial moisture content determination by laboratory dryer LAC, type S100/03 (Rajhrad, Czech Republic) and subsequently were dried into the proper level of moister content; both according to standard EN 18134–2 (2015).

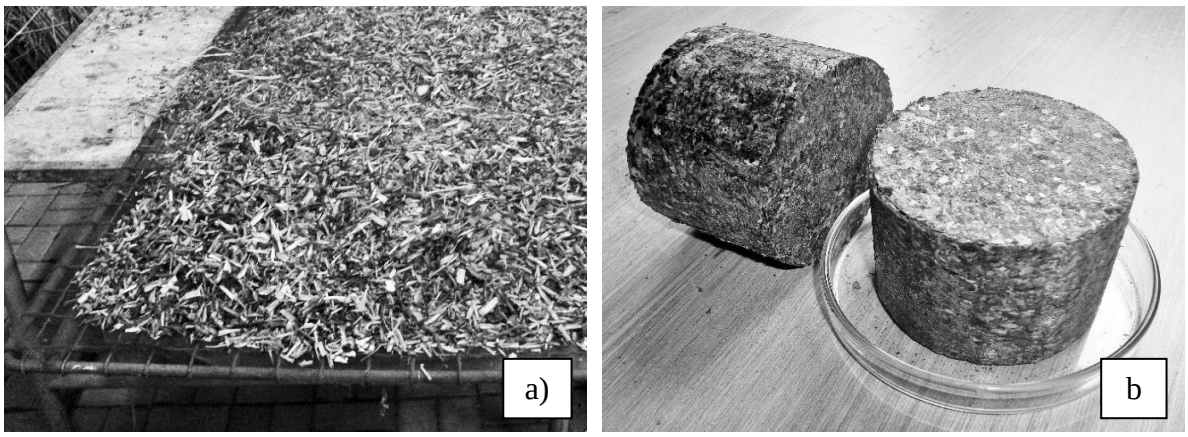

Fig. 1 Investigated feedstock materials in: a) bulk form, b) briquette form (authors data)

In next step, properly prepared feedstock material (particle size, moisture content) was compressed into cylindrical shaped briquettes by using of two high–pressure hydraulic piston briquetting presses Briklis, types BrikStar 50 and BrikStar 30–12 (Malšice, Czech Republic). Used presses were equipped with pressing chambers with different diameters, namely 50 mm and 65 mm, therefore two different types of briquette samples were produced and tested (identified as a Sample D50 and Sample D65). Detail information about produced briquette samples dimensions are presented in Tab. 1.

Tab. 1 Parameters of produced briquette samples in average

	Weight	St. Dev.	Diameter	St. Dev.	Length	St. Dev.
	g	g	mm	mm	mm	mm
Sample D50	108.86	14.49	51.96	0.38	53.90	6.59
Sample D65	120.80	35.62	66.97	0.35	42.28	11.53

(St. Dev. – standard deviation)

Experimental measurement

Produced briquette samples were subjected to determination of volume density, rupture force and mechanical durability immediately after their production; set of used experimental tests represented evaluation of level of briquette samples mechanical properties, thus, their final quality.

To determine the efficiency of densification process (briquetting), thus, the suitability of investigated material for briquette fuel production, the volume density ρ (kg·m^{-3}) of briquette samples were stated by using briquette samples basic dimensions and following equation (1):

$$\rho = \frac{m}{V} \tag{1}$$

where ρ is volume density (kg·m^{-3}), m is mass of briquette sample (kg), V is volume of briquette sample (m^3)
In next step, the briquette samples were subjected to two different deformation tests which stated their mechanical quality, specifically, mechanical durability (%) and rupture force (N·mm^{-1}).
Process of mechanical durability (%) measurement is stated by standard EN ISO 17831–2 (2015). Briquette samples are tested by using of powered by special dustproof rotating drum powered by electricity which is expressed in Fig. 2.

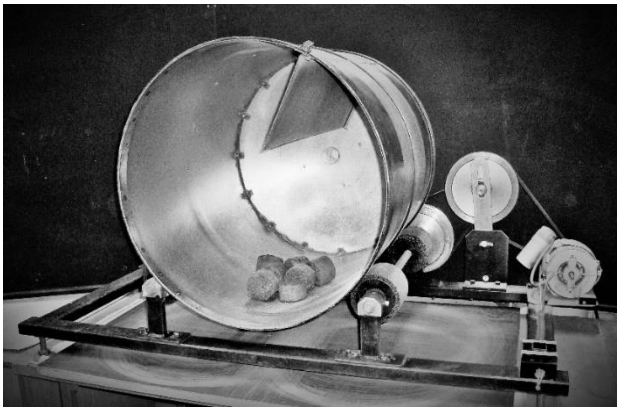

Fig. 2 Laboratory equipment for mechanical durability (DU) determination (authors data)

After experimental testing, result values of mechanical durability were stated by using of following equation (2):

$$DU = \frac{m_a}{m_e} \cdot 100 \quad (2)$$

where DU is mechanical durability (%), m_a is weight of briquette samples after testing (g), m_e is weight of briquette sample before testing (g)

Rupture force (N·mm^{-1}) of briquette samples was performed by using of plate–loading test method. The source of energy represented universal hydraulic tensile compression testing machine type ZDM 50 (Dresden, Germany) with following parameters: maximal force – 500 kN and loading speed – 20 mm·min^{-1}.

All measured data were primarily sorted by Microsoft Excel program, subsequently, the data were analysed by STATISTICA CZ software which stated basic features of measured data by using of descriptive statistics.

RESULTS AND DISCUSSION

If compare all result values obtained during experimental measurements (in detail are shown in Tab. 2) of two different kinds of briquette samples, it was proved that briquette samples with bigger diameter (65 mm) exhibited lower level of all investigated quality indicators.

Tab. 2 Result values of mechanical properties of investigated briquette samples in average

	W	St. Dev.	ρ	St. Dev.	RF	St. Dev.	DU	St. Dev.
	%	%	kg·m^{-3}	kg·m^{-3}	N·mm^{-1}	N·mm^{-1}	%	%
Sample D50	10.9	0.4	951.40	34.70	94.30	23.58	94.87	0.82
Sample D65	11.2	0.3	886.18	29.92	60.24	20.51	91.06	1.76

(W – moisture content, ρ – volume density, RF – rupture force, DU – mechanical durability, St. Dev. – standard deviation)

Focused on specific quality indicators, level of moisture content occurred at level suitable for production of high quality briquettes according to standard EN ISO 18134–2 (2015). Volume density

(ρ) evaluation indicated satisfactory level in compare with result of other authors; *Brožek & Nováková* (2016) proved volume density of briquettes from lime chips equal to 919.4 kg·m^{-3} for 50 mm diameter and equal to 610.3 kg·m^{-3} for 65 mm diameter. Further, authors proved result values of volume density of briquettes from pine shavings equal to 968.4 kg·m^{-3} for 50 mm diameter and equal to 838.9 kg·m^{-3} for 65 mm diameter.
Observed level of rupture force (RF) achieved also high level in compare with other kinds of briquettes; *Brožek et al.* (2012) proved RFs of briquettes with 65 mm diameter from following feedstock materials: birch chips – 26.8 N·mm^{-1}, pine bark – 31.5 N·mm^{-1}, spruce sawdust – 58.7 N·mm^{-1}. According to other studies the RF of briquettes with 50 mm diameter from various feedstock material were following: poppy residues– 58.73 N·mm^{-1}, wheat husk – 44.18 N·mm^{-1} and Japanese knotweed – 112.1 N·mm^{-1} (*Brunerová et al., 2017a*, *Brunerová et al, 2017b*).
If consider the fact, that mechanical durability is main indicator of briquette mechanical quality, its result values are very important for the overall evaluation of investigated briquette samples. As is visible from Tab. 2 both kinds of briquette samples corresponded to high level of mechanical durability, i.e. > 90% which is highly recommended and also necessary for commercial production of briquettes (EN ISO 17831–2, 2015).

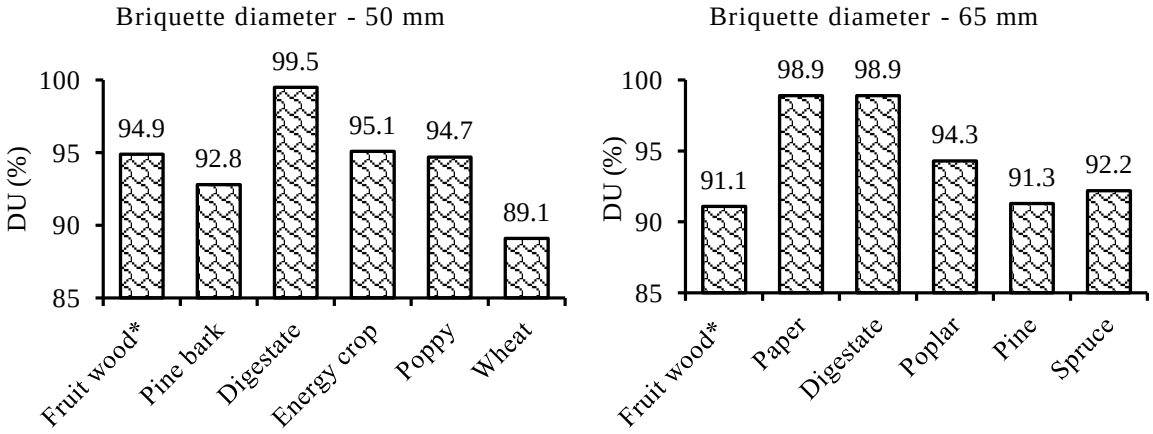

Fig. 3 Comparison of mechanical durability (DU) of briquettes from different biomass kinds (*authors data*; Brožek et al., 2012; Brožek & Nováková, 2016; Brunerová et al., 2016a; Brunerová et al., 2016b; Brunerová et al., 2016c; Brunerová et al., 2017a; Brunerová et al., 2017b*)

As is visible from Fig. 3, comparison of obtained result values with briquettes produced with the same diameters but from different kinds of biomass indicates satisfactory level of both briquette samples investigated in present paper.

CONCLUSIONS

According to all proved result values, the residues (mixed waste biomass) from fruit orchard (cherry, apricot and plum trees) has great potential for production of high quality briquette biofuel. Possibility of commercial production of such densified products was proved especially by achieving of high mechanical durability level (>90 %). Comparison of different diameters proved better result values for briquettes samples with smaller diameter (50 mm). Moreover, the process of spring orchard pruning is an annual integral part of orchards treatment, thus, production of such residues (waste biomass) is inevitable. Consequently, subsequent utilization should be supported within the proper waste management.

ACKNOWLEDGMENT

This study was supported by Internal Grant Agency of the Faculty of Engineering, Czech University of Life Sciences Prague, grant number 2017:31140/1312/3112 and further then by the Internal Grant Agency of the Czech University of Life Sciences Prague, grant number 20173005 (31140/1313/3108).

REFERENCES

1. Bilandzija, N., Voca, N., Kricka, T., Matin, A. & Jurisic V. (2012). Energy potential of fruit tree pruned biomass in Croatia. *Spanish Journal of Agricultural Research 10(2),* 292–298.
2. Brožek, M. & Nováková, A. (2016). Properties evaluation of briquettes made using different briquette presses. *15th International Scientific Conference Engineering for Rural Development*. (pp. 62–67).
3. Brožek, M., Nováková, A. & Kolářová, M., (2012). Quality evaluation of briquettes made from wood waste. *Research in Agricultural Engineering 58(1),* 30–35.
4. Brunerová, A, Brožek, M. & Müller. M. (2017)a. Utilization of waste biomass from post – harvest lines in the form of briquettes for energy production. *Agronomy Research 15(2),* 344–358.
5. Brunerová, A, Müller. M. &. Brožek, M. (2017)b. Potential of wild growing Japanese knotweed (*Reynoutria japonica*) for briquette production. In: *16th International Scientific Conference Engineering for Rural Development* (pp. 561–568).
6. Brunerová, A. & Brožek, M. (2016)a. Optimal feedstock particle size and its influence on final briquette quality. In *6th International Conference on Trends in Agricultural Engineering* (pp. 95–101).
7. Brunerová, A., Ivanova, T. & Brožek, M. (2016)b. Mechanical durability of digestate briquettes mixed with mineral additives. In: *15th International Scientific Conference Engineering for Rural Development*. (pp. 971–976).
8. Brunerová, A., Pecen, J., Brožek M. & Ivanova, T. (2016)c. Mechanical durability of briquettes from digestate in different storage conditions. *Agronomy Research 14(2),* 327–336.
9. Český statistický úřad (ČSÚ) (2013). Sady 2012. (online) Available from: https://www.czso.cz/csu/czso/ovocne-sady-strukturalni-setreni-2012-fdwxsg6ahd Accessed: 7 July 2017.
10. EN 15234–1 (2011): *Solid biofuels – Fuel quality assurance – Part 1: General requirements.*
11. EN ISO 16559 (2014): *Solid biofuels – Terminology, definitions and descriptions.*
12. EN ISO 17225–1 (2015): *Solid biofuels – Fuel specifications and classes – Part 1: General requirements.*
13. EN ISO 17831–2 (2015): *Solid biofuels – Determination of mechanical durability of pellets and briquettes – Part 2: Briquettes.*
14. EN ISO 18134–2 (2015): *Solid biofuels – Determination of moisture content – Oven dry method – Part 2: Total moisture – Simplified method.*
15. Eurostat, statistics explained (2012). Agricultural production – orchards. (online) Available from: http://ec.europa.eu/eurostat/statistics-explained/index.php/Agricultural_production_-_orchards#Publications. Accessed: 7 July 2017.
16. Zavrazhnov & Syasin. (2014). Research process for producing fuel briquettes from waste uprooting orchards. *Вестник Мичуринского Государственного Аграрного Университета 2,* (46–49).
17. Zhang, Y., Jiang, L. & Tian, Ch., (2011). Potential of Perennial Crop on Environmental Sustainability of Agriculture. *Procedia Environmental Sciences 10,* (1141–1147).
18. Živković, M., Živković, M., Urošević, S. O., Mićo, O., Gligorević, K., Zlatanović, I., Koprivica1, R. (2013). Aspects Of Using Potential Energy Products Of Biomass After Pruning Fruit And Grape Plantations In The Republic Of Serbia. *Agriculture & Forestry 59(1),* 167–182.

Corresponding author:
Ing. Anna Brunnerová, Department of Material Science and Manufacturing Technology, Faculty of Engineering, Czech University of Life Sciences Prague, Kamýcká 129, CZ 165 00 Prague, Czech Republic, e-mail: brunerova@tf.czu.cz

COMPARISON OF TWO METHODS FOR MEASURING DRAUGHT FORCE OF THE TRACTOR

Milan BUŘIČ

Department of Agricultural machines, Faculty of Engineering, Czech University of Life Sciences Prague

Abstract
The aim of this paper is compares two methods of draught force measurement during field tests. Energy demands of the soil tillage machines are important factor for choice of machinery, further development and improvement. A common method of measurement is to use a rod with a tensometric sensor. Using of two tractors (pulling one and pulled one equipped with soil tillage machine) is a disadvantage of this method. Inaccuracy is also is entered due to rolling resistance of the drawn tractor. A special frame has been developed for the replacement of conventional methods. The frame was developed in cooperation CULS and Bednar FMT companies. For the evaluation of measuring frame function was used sets of machines: track tractor John Deere 8320 RT as a pulling device, measuring frame mounted on its three point hitch, measuring rod connecting measuring frame and pulled wheel tractor New Holland T7050 and Köckerling Exact Gruber Vario combinator with 5 m working width. When comparing draught force results from strain gauge load cell placed into measuring frame with those from classic measuring rod it was found that there existed no statistically significant difference between the data from measuring frame and measuring rod. Measuring frame can be used for the aim of soil tillage machines draught force measurement and pulled tractor is not necessary in this case. This measurement is much easier. It also eliminated errors in the application classical methods (rolling resistance of the drawn tractor).

Key words: *soil, soil characteristic, soil qualities, soil processing, pulling power, polling power measurement.*

INTRODUCTION

Soil mechanical resistance is influenced by many factors. For example soil compaction, water content, soil texture and other (*Adamchuk et al., 2008; Novák et al., 2014*). The force of soil tillage machines could be affected by parameters as are tool type, working width, working depth and working speed. The other factors influencing draught force could be the factors dependent on the place as are soil types, soil bulk density, soil moisture and other (*Novák et al., 2014*). Current knowledge of draught force could be a useful tool in many ways (*Procházka et al., 2015*).

Novák et al. (*2014*) performed the draught force measurement by load cell with measuring range up to 200 kN. This load cell was mounted between draw able and drawn tractor which was connected the measured cultivator. These measurements were carried out for three different speeds (6, 8, 10 km h^{-1}) and two working depths (0.1 and 0.15 m) at two different soil types (sandy and loam soils). The result of this study (*Novák et al., 2014*) measurement was a confirmation of the influence of soil type on the draught force however the impact of speed on draught force was not proven.

McLaughlin and Burtt (2000) defined his work main sources of measurement errors such as: soil roughness, tractor and tool oscillations, speed differences, soil moisture content differences, and variability of plot. Similar results are also described in other studies (*Novák et al., 2014*; *Procházka et al., 2015*).

Kheiralla et al.(2004) for experiments used three octagonal ring-analog converters to place on the three-point hitch. The experiment was carried out on the sand, clay and loam soil, where they were used in the following devices: mouldboard plow, disc plow, disc gate and rotary tiller. The similar experiment was conducted by *Chen et al.(2013*). Experiments were performed at working speed of 3.19 km h^{-1} on different soil types. The measured values showed that the minimum tensile strength was measured in the soil with coarse sand. Subsequent comparison of soil loamy-sand and the highest values were found in soils sandy-loam.

Determining soil compaction profiles requires fast sampling systems due to change moisture conditions with time. Soil mapping techniques currently used are too costly for soil mapping units (*Rooney, D. J., Lowery, B,. 2000*). Soil cone penetrometers are commonly used for this purpose, but acquiring the data can take a long time (*Raper, et al., 1999*). Cone penetrometer testing (CPT) is a fast and effective system for collecting soils parameters during a site investigation. When used in conjunction with conventional drilling and sampling methods, it provides a complete description of the subsurface conditions.

The aim of this thesis is the processing and analysis of measured data draught force tractor utilization of the potential power of the tractor.

MATERIALS AND METHODS

Measurements took place in the field in Sloveč, near Městec Králové in Nymburk in Central Bohemia Region in October 3. The soil type was identified as clayey-sandy rendzina. Pulling power was carried after harvesting of sugar beets and aerating the soil before the subsequent trailed cultivator Exaktgrubber-Vario. There were a lot of sugar beets on the field in form of rest (Fig. 1).

Fig. 1 Harvest residues, sugar beets.

The measurement was carried out on limited portions of a plot size of 100x50 m. Undisturbed soil samples were taken. It was used Kopecky cylinders with volume 100 cm^3. Samples were taken from three depths.The set for measurement was wheeled tractor New Holland T7050 which trailed cultivator Köckerling Vario 480 with a working width of 4.8 meters with 37 tines pull and track tractor John Deere 8320 RT. Track tractor John Deere has been a source of pulling power (Fig. 2).

Fig. 2 Measuring set. From right: Crawler tractor John Deere 8320 RT, measuring frame and New Holland T7050 with cultivator Köckerling Gruber Vario with 4,8 m working width.

The basic element of the measurement was strain gauge load cell S-38 with range up to 200 kN. A detailed description can be found at (*Novák et al*., *2014*). Its construction can be seen in Fig. 3. The frame was connected to three point hitch (1) of pulling tractor. Strain gauge load cell (3) and horizontal penetrometer (2) were also integrated to the frame. Two point hitch (4) serves for the connection of tillage machine.

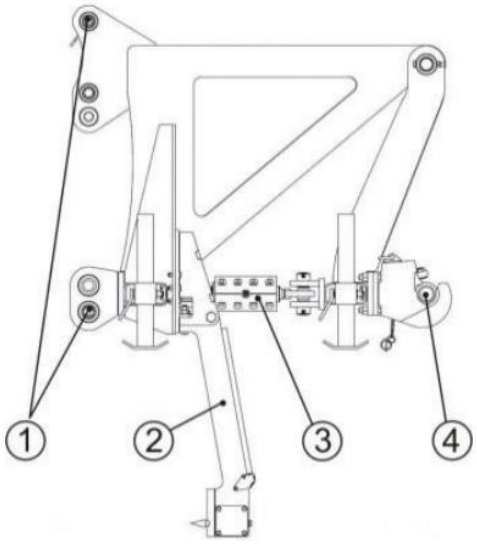

Fig. 3 Measuring frame: (1) connection to three point hitch, (2) horizontal penetrometer, (3) strain gauge load cell, (4) two point hitch.

Measurement of tensile force was performed by two basic methods. The first method for measuring the tensile force was assembled kit pair of tractors connected to the measuring device. It was used measuring rod with sensor. The second tractor did not have gear and had releasing the wheel. Tractor New Holland served only to harness of combinator. In a second method of measurement, the measuring devices (see Fig.3) have linked the John Deere track tractor-drawn combinator.
It was chosen working depth 0.15 m working speed of 6 km h^{-1}. Setting speed was monitored using GPS**.** After completion of the test (all passes) was uncovered upper soil profile to determine the quality parameters of the tillage by chosen cultivator.
Measuring frame has a horizontal penetrometer. For control this device was used standard penetrometer PN-10 which was developed at CULS Prague. The penetrometer had a probe with a cone angle of 30° and area of 100 mm^2. Penetrometer measurements were done at 204 places of above mentioned area up to 0.4 m depth. Cone index was estimated for each 50 mm depth during each measurement.

RESULTS AND DISCUSSION
Fig. 4 shows a comparison of the two tensile forces of the measured values of strain gauges on the frame and on the rod at an average driving speed kit 6.24 $km.h^{-1}$.
Error, or deviation values from each other, is in the sequence of measurements within tolerance. The average value of the error is 0.5%.
On Fig. 5 shows the progress of the penetration resistance depending on the depth. This progress was measured by vertical penetrometer PN 10.

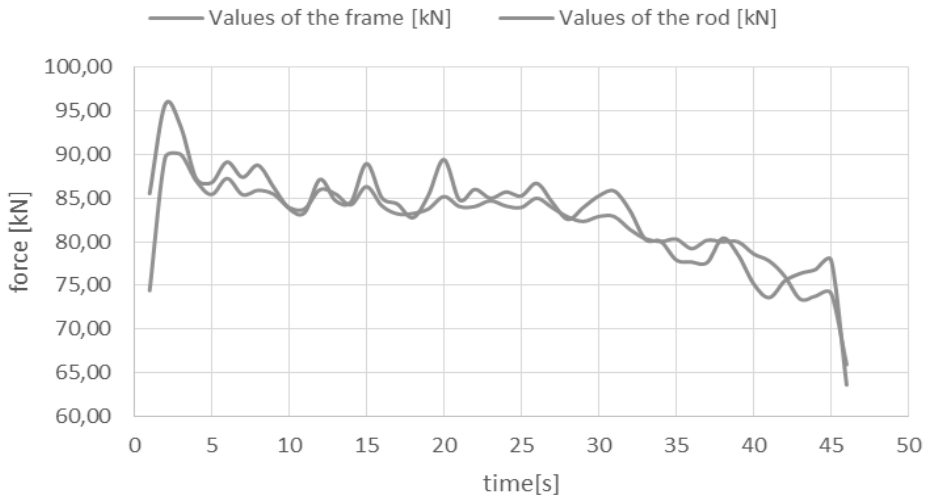

Fig. 4 Comparison of tensile forces on the frame and the rod.

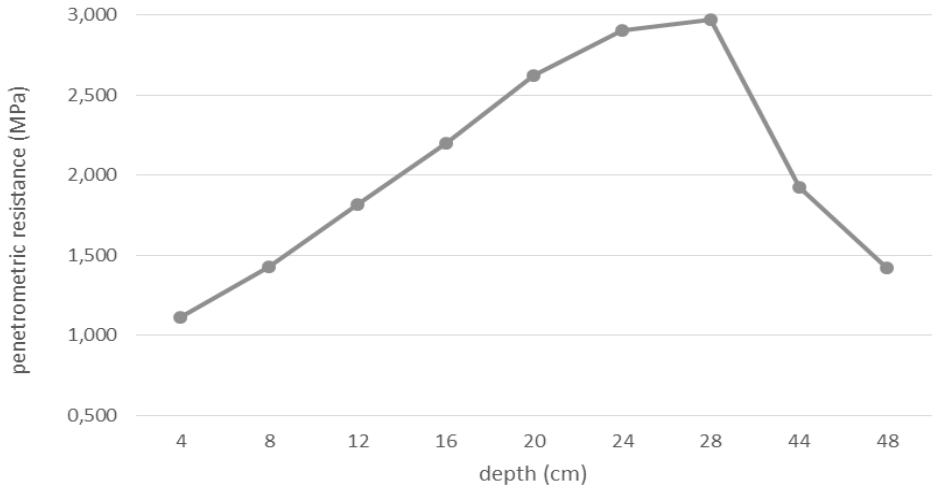

Fig. 5 Cone index- vertical penetrometer.

Fig. 6 shows the measurement of cone index by vertical and horizontal penetrometer.

Fig. 6 Comparison of vertical and horizontal penetrometer.

Horizontal penetration resistance at the marked plot varies from 3 to 4 MPa at an approximate depth of 0.2 m. Unfortunately, the measurement failed to make a comparison with less moist soil, so we cannot from these graphs accurately determine whether the penetration resistance mainly affected by soil moisture. However, we can say that with increasing depth of cone index grows (Fig. 5). Horizontal measurement method achieves higher values of resistance than vertical measurements (Fig. 6), which decides upon the type of tillage. Furthermore, we can say that speed does not affect cone index. This is relatively surprised.
Similar measurements were engaged by other authors. The results of this study confirm Novák et al. *(2014)*. *McLaughlin & Burtt (2000*) emphasize the influence of the moisture. Other authors describe the influence of soil physical properties (*Procházka et al., 2015*). Subsequent research will lead toward improving the calibration of the measuring frame in terms of force transmission.

CONCLUSIONS

The tensile force has considerable influence on the development and construction of machines for soil tillage. Measured data are the basis for theoretical calculations for the construction of machines frames and working tools. Measurements showed the possibility of direct measurement draught force with the use the frame. So there is no need to use a second tractor, as with traditional methods. Horizontal penetrometer measurements may to some extent replace the classic penetrometer in vertically direction.

ACKNOWLEDGMENT

This study was supported by supported by the CULS Prague – Project no. IGA no. 2017:31160/1312/3117.

REFERENCES

1. Adamchuk, V. I., Ingram, T. J., Sudduth, K. A., Chung, S. O., & Ingram, T. J. (2008). On-the-go mapping of soil mechanical resistance using a linear depth effect model. Trans. ASABE, 51 (6), pp. 1885–1894.
2. Novák, P., Chyba, J., Kumhála, F., & Procházka, P. (2014). Measurement of stubble cultivator draught force under different soil conditions. *Agronomy Research*., 12 (1), pp. 135–142.
3. Procházka, P., Novák, P., Chyba, J., & Kumhála, F. (2015). Evaluation of measuring frame for soil tillage machines draught force measurement. *Agronomy Research*., 13 (1), pp. 186–191.
4. McLaughlin, N. B., & Burtt, S. D. (2000). Spatial mapping of tillage energy. Proc. 5th Int. Conf. Precis. Agric. Bloom. Minnesota, USA, 16-19 July, pp. 1–14.
5. Kheiralla, A., Yahya, A., Zohadie, M., & Ishak, W. (2004). Modelling of power and energy requirements for tillage implements operating in Serdang sandy clay loam, Malaysia. Soil Tillage Res., 78 (1), Jul., pp. 21–34.
6. Chen, Y., Munkholm, L. J., & Nyord, T. (2013). A discrete element model for soil–sweep interaction in three different soils. *Soil Tillage Research*., vol. 126, Jan., pp. 34–41.
7. Rooney, D. J., & Lowery, B. (2000). A profile cone penetrometer for mapping soil horizons. Soil Sci. Soc. Am. J., 64 (6), p. 2136.
8. Raper, R. L., Washington, B. H., & Jarrell, J. D. (1999). Technical notes: a tractor-mounted multiple-probe soil cone penetrometer. Appl. Eng. Agric., 15 (4), pp. 287–290.

Corresponding author:
Ing. Milan Buřič, Department of Agricultural machines, Faculty of Engineering, Czech University of Life Sciences, Kamýcká 129, 165 21 Prague-6 Suchdol, Czech Republic, buricm@tf.czu.cz

MICROCLIMATIC CONDITIONS IN THE SPORT FACILITIES

Van Doan CAO

Department of Technological Equipment of Buildings, Faculty of Engineering, Czech University of Life Sciences Prague

Abstract
The aim of this paper is to present the microclimatic research focused on the indoor conditions in several sport facilities for training and competition. In the frame of this research, the main parameters of internal and external properties of climate were measured and evaluated. The construction of the buildings together with technological equipment that can influence the microclimatic conditions inside the building were also measured and analyzed. The measurement results of the air temperature, humidity, concentration of CO_2, show internal microclimate in the building when the HVAC (Heating, Ventilation and Air Conditioning) system was not activated and in the other building (the swimming pool) with operation of this system to regulate temperature and humidity using fresh air from outdoors. Results of different indoor conditions were generalized. The results of the practical measurements show the importance of the HVAC system to provide thermal comfort and acceptable indoor air quality in the residential building for people with several sport activities.

Key words: *air temperature; CO_2 concentration; relative humidity; thermal comfort.*

INTRODUCTION

Microclimatic denotes the meteorological conditions local only to a particular place, like the radiation, air currents at ground level, temperature, humidity and precipitation peculiar only to a limited area. It is the latter which architects have to encounter and intimately know, so that they do not compete against it, but go along with it and derive the best results from its beneficial qualities, and guard against the ravages of its undesirable qualities (*Ghadiali, 1959*). Indoor thermal environment is part of the indoor environmental quality component that close influence by the climatic condition. Nowadays, the climate change phenomenon has caused a threat to the human environment (*Ismail et al., 2012*). Human thermal comfort is found to be related with several factors such as air temperature, air movement, amount of clothing worn, and activity level including a human body itself (*Randall, 2006*). A successful indoor environment much depends on an understanding of the environmental factors, including building design and setting (*Yeang, 2006*).

Energy-efficient buildings are only effective when the occupants of the buildings are comfortable (*Awan & Rahid, 2015*). If they are not comfortable, then they will take alternative means of heating or cooling a space such as space heaters or window-mounted air conditioners that could be substantially worse than typical HVAC systems (*Pritoni et al., 2017*).

Thermal comfort is difficult to measure because it is highly subjective (*Petersen & Knudsen, 2017*). It depends on the air temperature, humidity, radiant temperature, air velocity, metabolic rates, and clothing levels and each individual experiences these sensations a bit differently based on his or her physiology and state (*Ghahramani, A. et al., 2014*).

According to the ANSI/ASHRAE Standard 55-2010, thermal comfort is defined as "that condition of mind which expresses satisfaction with the thermal environment and is assessed by subjective evaluation." (*John, 2012*). Also known as human comfort, thermal comfort is the occupants' satisfaction with the surrounding thermal conditions and is essential to consider when designing a structure that will be occupied by people.

The sport facilities that were mentioned above be focused on the teaching of physical education of students and on the organization of sports and physical activities of the students. The inside of this building, the dust pollution was also evaluated in another research work (*Kic, 2016*). That research showed influences of the rooms' dimensions and intensive ventilation to the dust pollution: very big

influence on the indoor air cleanness and reduction of air pollution by dust has the intensive ventilation, which can reduce the total dust concentration and therefore also the concentration of all dust particles, intensive ventilation is more important if the room has small dimensions and number of sportsmen is high. And the next influences of the equipment buildings to the microclimate in these facilities will be evaluated in this research paper.

The aim of this paper is to show the measurement results of internal environment in several sport facilities used for physical education and sport activities at the Czech University of Life Sciences Prague. During the sport activities in the room, people breathe very intensively and their amount of heat radiation is greater than normal activities. Microclimatic results are important to know what is the situation inside the sport facilities.

MATERIAL AND METHOD

This research work and measurements of the actual values were carried out in buildings and rooms of Department of Physical Education at the Czech University of Life Sciences Prague. All rooms are situated in two buildings, three of them in the same building (two conventional gyms GA, GB and one fitness centre GC). The first gym GA has the following dimensions: floor area about 525 m^2, volume 4,200 m^3 and it is used mainly for different ball games. The second gym GB has the following dimensions: floor area about 204 m^2, volume 1,632 m^3 and it is used mainly for sports games, floor exercise, aerobics, table tennis, etc. The third gym GC has the following dimensions: floor area about 98 m^2, volume 258 m^3 and it is used as a fitness centre. The last building is swimming pool centre SP (pool is 25 m long), which has the following dimensions: floor area about 628 m^2, volume 4,084 m^3.

The measurements of the air temperature, humidity, concentration of CO_2 were carried out initially when all gym rooms were empty, without students and without ventilation and in the swimming pool when 16 students swim with activation of ventilation that the air was supplied and exhausted by 18 air diffusers for supply and 12 air diffusers for exhaust of the air. In the same measurement that were carried out in the gym rooms during the normal function, with students and with standard ventilation. There were following number of persons during the measurement inside the rooms: GA 20 students play floor ball, GB 27 students doing aerobic exercise, GC 18 students in fitness training, SP 20 students swim.

The thermal comfort in the space of buildings was measured during the short-time experiments by globe temperature which includes the combined effect of radiation, air temperature and air velocity (measured by globe thermometer FPA 805 GTS with operative range from –50 to +200 °C with accuracy ± 0.1 °C and diameter of 0.15m) together with temperature and humidity of surrounding air measured by sensor FHA 84 646–21 including temperature sensor NTC type N with operative range from –30 to +100 °C with accuracy ± 0.1 °C, and air humidity by capacitive sensor with operative range from 5 to 98% with accuracy ± 2%. Furthermore the concentration of CO_2 was measured by the sensor FY A600 with operative range 0 – 0.5% and accuracy ± 0.01%.

All these data were measured within the GA,GB,GC and SP in the installed meteorological station and stored at intervals of ten seconds to measuring instrument ALMEMO 2590–9, ALMEMO 2690–8 and ALMEMO 5990–2 during approximately fifteen minutes in every room. In the every room, data were measured in three locations at intervals five minutes that are uniformly distributed in the room. The first measurement was done in July and the second one was carried out in December in the same year and the same way.

RESULTS AND DISCUSSION

The main objective of this research paper is a presentation of results of measurement of main microclimatic parameters sport facilities in summer when the rooms were without activation of HVAC and in the winter (with activation of HVAC). Then, the obtained results were compared with the values recommended in relevant standards.

From the measurement results, while the temperatures inside GA, GB and GC are almost the same, the temperature in the SP is higher. That phenomenon happened because the sun has directly sunk into the big glass surface on the wall of the SP and it heated up itself and then the internal temperature also increased

in small amount. To maintain better thermal comfort inside the SP, we can use blinds on the outside of the glass surface, this way it reduces the light from the sun, which shines directly into the glass. Also it will keep the temperature of glass similar with the outside temperature and does not increase inside temperature during highest external temperatures.

Tab. 1 Average values and standard deviation of air temperature t, relative humidity RH and CO_2 concentration in four rooms and outside during the short-time measurements.

Place of measurement	t °C ± SD	RH % ± SD	CO_2 % ± SD
External	26.1 ± 0.8	46.9 ± 4.4	0.040 ± 0.000
GA	25.9 ± 0.1	56.2 ± 0.3	0.056 ± 0.001
GB	25.9 ± 0.1	55.7 ± 0.4	0.052 ± 0.001
GC	26.1 ± 0.1	57.1 ± 0.6	0.065 ± 0.002
SP	28.9 ± 0.4	53.4 ± 3.0	0.051 ± 0.004

SD – Standard deviation.

In case of CO_2 concentration, in the GA, GB there are no athletes while in the GC there are 8 people who exercise and all rooms have not ventilation activation. This is the reason why the concentration of CO_2 in the GC is higher than in GA and in GB. To maintain accepted level of concentration CO_2 inside the rooms, the activation of ventilation system is very important because during the sport activities, they use a bigger amount of O_2 and breathe out a greater amount of CO_2 than normal. For example, in the SP there are 16 athletes when the ventilation is activated, the amount of CO_2 emissions decrease significantly with comparing to GC. In case that the windows are not opened, ventilation activities help to improve intake of oxygen and decrease carbon dioxide of the internal microclimate for athletes during physical activities.
In the winter, when outside temperature ranks between 7 °C and 7.3 °C, the measurements were carried out during the normal function of rooms, with students and with standard ventilation and heating. The comparison of the temperatures in all rooms is summarized in Fig. 1.

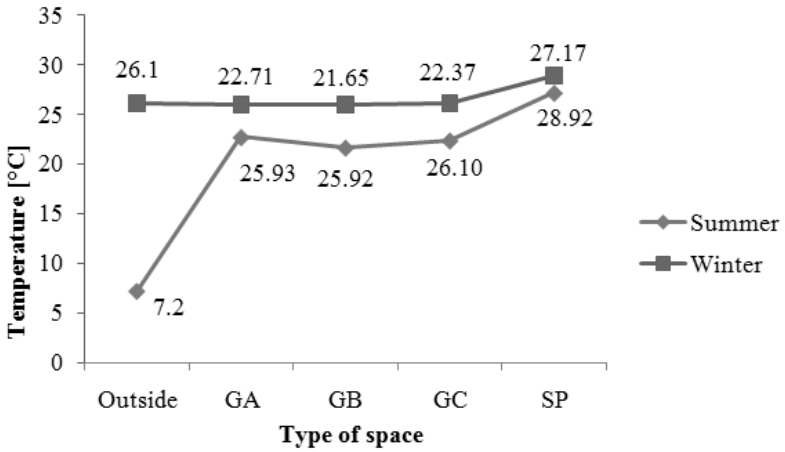

Fig. 1 The comparison of the air temperature outside and inside the rooms in the summer and winter.

From Fig. 1, apparently it is a very significant effect of heating system on temperature´s augmentation in the rooms. Temperature in the all rooms (in range from 21.6 °C to 27.1°C) increased significantly in comparison with outside temperature. This way maintains thermal comfort inside the rooms for all students with sport activities.
Recommendations for summer and winter may vary; a suggested typical range for summer is 23 °C (73 °F) to 25.5 °C (78 °F), with that for winter being 20 °C (68 °F) to 23.5 °C (74 °F), although by other

considerations the maximum should be below 24 °C (75 °F) – and for sick building syndrome avoidance, below 22 °C (72 °F) (*Burroughs, Hansen & Shirley, 2011*). It shows that obtained results of the temperature in GA, GB, GC (25.9 – 26.1 °C) are in range of recommended values.
For SP, the FINA (The international governing body of swimming, diving, water polo, synchronized swimming and open water diving), have set the water temperature for competitive swimming between 77° to 82 °F (25 – 28 °C), and 81 °F (27 °C) for synchronized swimming. For commercial swimming pool, for competitive pools the water should be no higher than 82 °F (28 °C), for recreational pools the recommended maximum is 84 °F (29 °C). Therefore, measurement results in SP (at around 28.9 °C) are also good for students to swim.
When the inside was heated and ventilated, the humidity decreased. The comparison of the humidity in the summer and in winter is showed in Fig. 2.

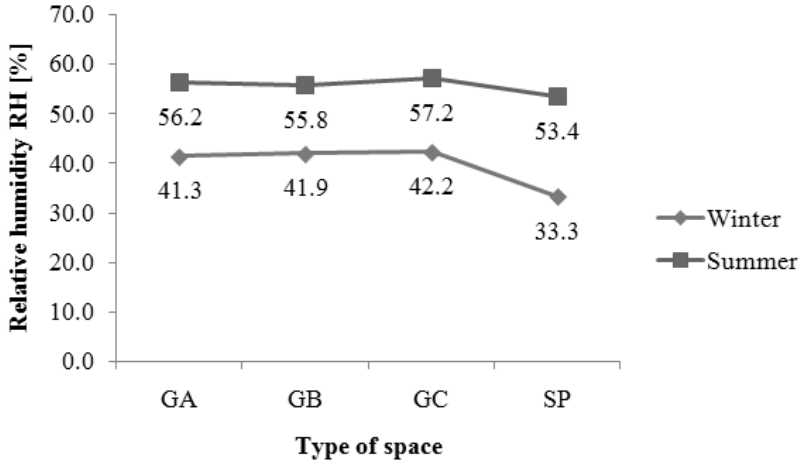

Fig. 2 The comparison of the relative humidity inside the rooms in the summer and winter.

The results of measurement of the CO_2 concentration in the summer and in winter were also showed and compared in Fig. 3.

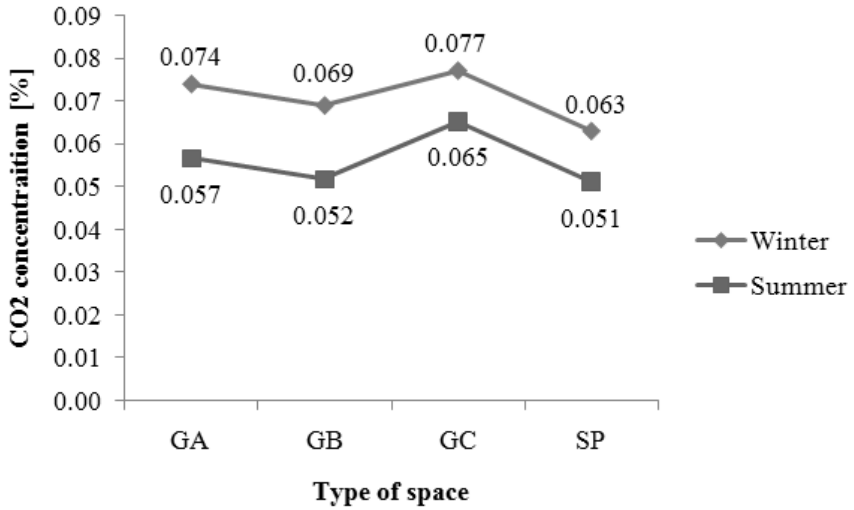

Fig. 3 The comparison of the CO_2 concentration inside the rooms in the summer and winter.

According to the American Society of Heating, Refrigerating and Air-Conditioning Engineers (ASHRAE), a good humidity range for humans is between 30 to 60 percent relative humidity and ideal is around 45-55% (*John, 2012*). From the measurement results, although the ventilation systems in all rooms

were activated, however CO_2 concentration is still higher than concentration outside (0.03%) and higher than concentration in case of empty rooms. It proves that ventilation in all rooms is not enough to reduce CO_2 concentration to the standard level (< 600 ppm). Therefore, in this case with given quantity of students, we need to increase intensity of the ventilators to maintain enough amounts O_2 for students and exhaust CO_2 from inside. Even though, that level above is quite normal to evaluate effects of CO_2 on healthy adults, maximum level may occasionally happen from time to time. In general - ventilation rates should keep carbon dioxide concentrations below 1000 ppm to create indoor air quality conditions acceptable to most individuals. Therefore, the measurement results of CO_2 concentration show that, it is in the acceptance and comfort level for students at good health.

CONCLUSIONS

The results of measurements in both winter and summer in the University sport facilities showed that:

- To maintain or regulate the temperature and intake of natural light for swimming pool, we can use regulated blinds outside the glass wall.
- In the summer, when the windows are not opened, to improve intake of oxygen and decrease carbon dioxide of the internal microclimate for athletes during physical activities in the facilities, we need to activate ventilators.
- In the winter, when outside temperature is lower, HVAC system helps to regulate and maintain thermal comfort for sport actions of the students.
- When HVAC system is activated to heat and ventilate inside temperature in the facilities, the humidity is also changed to the lower level.

REFERENCES

1. Awan, R., & Rahid, A. (2015). HVAC design considerations for energy efficiency in commercial buildings. In *2014 International Conference on Energy Systems and Policies, ICESP 2014*, Islamabad, Pakistan.
2. Burroughs, H. E.; &Hansen, S. (2011). Managing Indoor Air Quality. Fairmont Press. 149-151.
3. Ghahramani, A., Jazizadeh, F., & Becerik-Gerber, B. (2014). A knowledge based approach for selecting energy-aware and comfort-driven HVAC temperature set points. In Energy and Buildings, 85, 536-548.
4. Ghadiali, J.H. (1959). Effect of Climate on Architectural Expression. In *Seminar On Architecture*. New Delhi: Lalit Kala Akademi.
5. Ismail, A., Abdul Samad, M. H., Rahman, A. M. A., & Yeok, F. S. (2012). Cooling Potentials and CO2 Uptake of Ipomoea Pescaprae Installed on the Flat Roof of a Single Storey Residential Building in Malaysia. In *Social and Behavioral Sciences, 35*, 361-368.
6. John, D.A. (2012). Designing air-distribution systems to maximize comfort. *ASHRAE Journal*. *54 (9)*, 20-26.
7. Kic, P. (2016). Dust pollution in the sport facilities. *Agronomy Research 14(1)*, 75–81.
8. Petersen, S., & Knudsen, M.D. (2017). Method for including the economic value of indoor climate as design criterion in optimisation of office building design. In *Building and Environment, 122*, 15-22.
9. Pritoni, M., Salmon, K., Sanguinetti, A., Morejohn, J., & Modera, M. (2017). Occupant thermal feedback for improved efficiency in university buildings. In *Energy and Buildings, 144*, 241-250.
10. Randall, T. (2006). Environmental Design (3th ed.). New York: Taylor & Francis Inc. Robinson.
11. Yeang, K. (2006). Ecodesign - a manual for ecological design. London: Wiley-Academy.

Corresponding author:
Ing. Van Doan Cao, Department of Technological Equipment of Buildings, Faculty of Engineering, Czech University of Life Sciences Prague, Kamýcká 129, CZ 165 00 Prague, Czech Republic, e-mail caodoan2006@gmail.com.

APPLICATION OF ANOVA FOR OPTIMIZE OF CNC MACHINING PARAMETERS

Judita CSERVENÁKOVÁ, Jozef HRUBEC, Ján ŽITŇANSKÝ

Department of Quality and Engineering Technologies, Faculty of Engineering, Slovak University of Agriculture in Nitra, Slovak Republic

Abstract
In statistics, analysis of variance (ANOVA) is a collection of statistical model, and their associated procedures, in which the observed variance in a particular variable is partitioned into components attributable to different sources of variation. The aim of the present investigation is to find the effect of cutting parameters on workpiece surface roughness by employing Taguchi's orthogonal array design and analysis of variance (ANOVA).

Keywords: *ANOVA, CNC Turning, Optimization, Surface Roughness, Taguchi Method.*

INTRODUCTION

The quality of the surface plays a important role in the performance because a good quality turned surface surely improves fatigue strength, corrosion resistance and creep life (*Kučerová & Lestyánska, 2011*). Surface roughness also affects on some functional attributes of parts, such as, contact causing surface friction, wearing, light reflection, ability of distributing and also holding a lubricant, load bearing capacity, coating and resisting fatigue. As we know in actual machining, there are many factors which affect the surface roughness i.e. cutting conditions, tool variables and work piece variables. It is very difficult to take all the parameters that control the surface roughness for a particular manufacturing process. In a turning operation, it is very difficult to select the cutting parameters to achieve the high surface finish.

Taguchi experimental design

The Taguchi experimental design method is a one of the well known, unique and powerful technique for product or process quality improvement. It is widely used for analysis of experiment and in optimization problems. This method uses a design of orthogonal arrays to study the entire parameter space with small number of experiments only. Taguchi recommends analyzing the mean response for each run in the inner array, and he also suggests to analyze variation using an appropriately chosen signal-tonoise ratio (S/N) (*Kolohan, et al., 2011*).
Taguchi introduces his concepts to (*Fratila & Caizar, 2011*):
- Quality should be designed into a product and not inspected into it.
- Quality is best achieved by minimising the deviation from a target.
- The cost of quality should be measured as a function of deviation from the standard and the losses should be measured system wide.

Analysis of variance (ANOVA)

Analysis of variance (ANOVA) is a collection of statistical models used to analyze the differences among group means and their associated procedures, developed by statistician and evolutionary biologist Ronald Fisher. In the ANOVA setting, the observed variance in a particular variable is partitioned into components attributable to different sources of variation. In its simplest form, ANOVA provides a statistical test of whether or not the means of several groups are equal, and therefore generalizes the *t*-test to more than two groups. ANOVAs are useful for comparing (testing) three or more means (groups or variables) for statistical significance. It is conceptually similar to multiple two-sample t-tests, but is more conservative (results in less type I error) and is therefore suited to a wide range of practical problems (*Kemény & Deák, 2000*).

MATERIALS AND METHODS

Work Piece Material

The workpiece material was a shaft from gray iron from Albero 103F5703 shown in the Fig. 1 taken in the form of round bars each of 15 mm dia. and 70 mm length. This shaft has a wide range of applications in the field of compressor´s manufacturing.

Fig. 1 Shaft from gray iron from Albero 103F5703

Experimental Procedure

The turning tests on the workpiece were conducted on a CNC (Computer Numerical Control) lathe (MORI SEIKI NL2500/1250) having maximum spindle speed of 4000 rpm and maximum power of 4.5 kW. The rust layers were removed by 0.5 mm depth of cut in order to minimize any effect of homogeneity on the final results. Machined component after machining was shown in the Fig. 2.

Fig. 2 Component after machining

The aim of the work was to analyze the effect of cutting parameters on surface roughness in turning of 103F5703. It was planned as per Taguchi's L9 Orthogonal array. The surface roughness depends on several parameters like cutting conditions (speed, feed and depth of cut), tool conditions (Tool nomenclature, nose radius) and mechanical properties (hardness, tensile strength) etc (*Veber, 2002*). To reduce the experiments, the cutting speed, feed and depth of cut were used as inputs at three different levels. The control parameters and the levels used in experiment, experimental setup and conditions are given in the Tab. 1.

Tab. 1 Parameters with Levels

Speed (rpm)	Feed (mm/rev)	Depth of cut (mm)
1000	0,2	0,5
1000	0,3	0,75
1000	0,4	1
1500	0,2	0,75
1500	0,3	1
1500	0,4	0,5
2000	0,2	1
2000	0,3	0,5
2000	0,4	0,75

RESULTS AND DISCUSSION

A series of experiments are conducted on a shaft from gray iron . Signal-to-Noise characteristics given by Taguchi are (*Taguchi & Konishi, 1987*):

a) Larger-the-better: it is used where the larger value of response is desired.
   S/N ratio = -10 log10 [1/Yi2]
b) Smaller-the-better: it is used where the smaller value of response is desired.
   S/N ratio = -10 log10 [Yi2] Where, Yi is observed response.

S/N ratios for surface roughness values in this work were calculated using Smaller-the-better characteristic proposed by Taguchi and given in the Tab. 2.

Tab. 2 Experimental Results of Surface Roughness

Surface roughness	S/N Ratio	Mean
6,45	-16,3132	6,5167
9,54	-19,4382	9,41
12,13	-21,708	12,1933
6,9	-16,8078	6,9633
9,12	-19,3219	9,1867
12,2	-21,5744	12,07
6,98	-16,7243	6,85
9,11	-19,2211	9,1733
12,56	-22,1018	12,6267

Analysis of Variance (ANOVA)

The results of surface roughness values were analyzed with Analysis of variance (ANOVA), used to identify the factors significance on the response. It is focused around the correlation of the normal estimation of a typical segment. Analysis of variance is a statistically based, on object resolution making tool used for identify any divergence in standard performing of collections of objects are testing (*Hebák, P. a kol., 2005*).

The result of ANOVA of surface roughness was given in the Tab. 3. This analysis was carried out for a significance level of $\alpha = 0.5$ i.e., for a confidence level of 95%. The sources with a P-value less than 0.05 are considered to have a statistically significant contribution to the performance measures.

Tab. 3 ANOVA Results of Surface Roughness

Source	DF	SS	MS	F	P
Speed	2	0,0529	0,0264	0,31	0,747
Feed	2	45,8624	22,9312	271,91	0,000
Error	4	0,3373	0,0843		
Total	8	46,2526			
S = 0,2904 R-Sq = 99,27% R-Sq(adj) = 98,54%					
Source	DF	SS	MS	F	P
Feed	2	45,8624	22,9312	711,41	0,000
Depth of cut	2	0,2613	0,1306	4,05	0,109
Error	4	0,1289	0,0322		
Total	8	46,2526			

From the results, it is clear that the feed is the most significant parameter followed by depth of cut and cutting speed. From the analysis of the Tab. 3, p-value of feed (0.000) which is less than 0.05, means, that feed's influence significantly on surface roughness between three cutting parameters.

Main Effect Plots Analysis

The data were further analyzed to study the effect of cutting parameters on surface roughness. From the S/N ratios given in the Tab. 4 and 5 main effect plots were drawn using MINITAB-16 software and shown in the Fig. 4 and 5 respectively. The plots show the variation of response with the change in cutting parameters. In the plots 4 and 5, the X-axis indicates the value of each process parameters at three levels and y-axis the response value. These main effect plots are used to determine the optimal design conditions to obtain the low surface roughness.

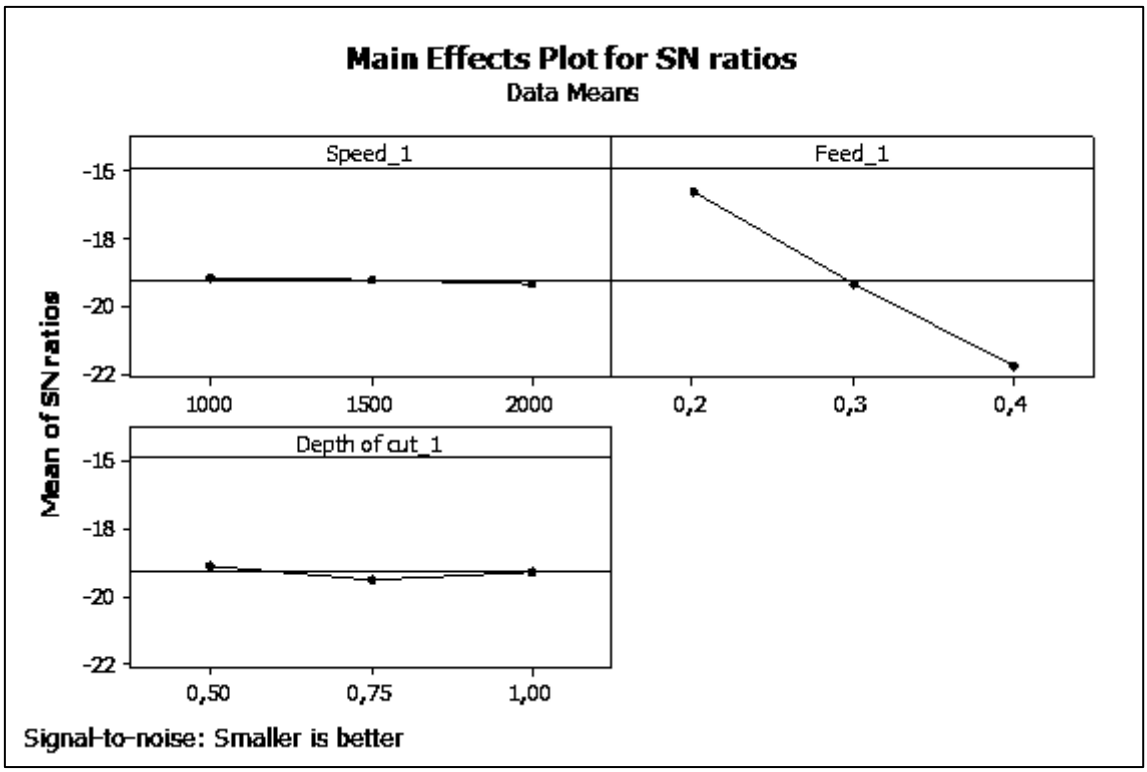

Fig. 4 Main Effects Plot for S/N Ratios of Ra

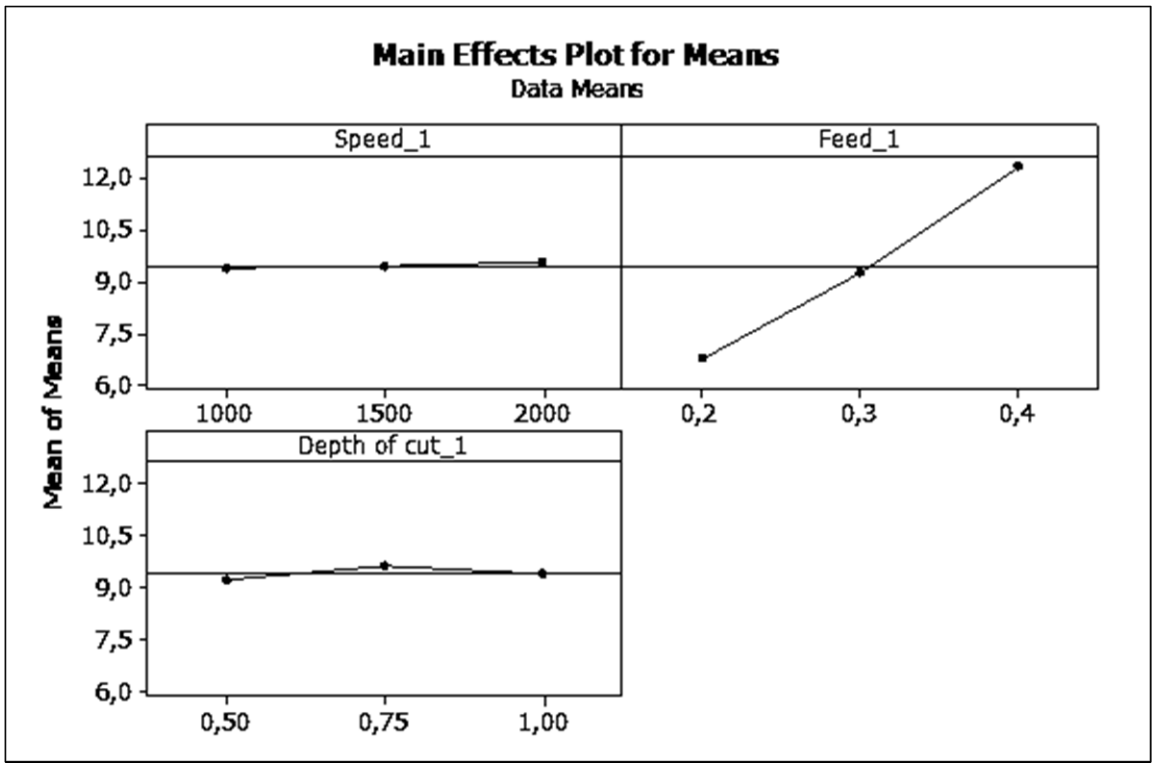

Fig. 5 Main Effects Plot for Means of Ra

From the Fig. 4 and 5 is observed, that with the increase in cutting speed and depth of cut levels there is a less change in response. But with the increase in the levels of feed significant change in the response can be observed. Based on the analysis the low value of surface roughness was obtained at cutting speed of 1000 rpm (level 1), feed of 0.2 mm/rev (Level 1) and depth of cut of 0.5 mm (level 1).

CONCLUSION

From the study and predictd results the following conclusions can be drawn:

1. From Taguchi results: the optimal combination of cutting parameters for low surface roughness was found at v1-f1-d1 i.e., speed at 1000 rpm, feed at 0.2 mm/rev and depth of cut at 0.5 mm.
2. From ANOVA results: parameters making significant effect on surface roughness. For achieving minimum surface roughness values, feed has high influence followed by speed and depth of cut has low influence.
3. Errors between experimental and regression values are within the acceptable range (±7).

The parameters taken in the experiments are optimized to obtain the minimum surface roughness possible. The optimum setting of cutting parameters for high quality turned parts is as speed at 1000 rpm, feed at 0.2 mm/rev and depth of cut at 0.5 mm.

REFERENCES

1. Evans, J. R., & Lindsay, W. M. (2005). The management and control of quality. 6th ed. Mason: Thomson South-Western, 2005. ISBN 03-2420-224-5.
2. Fratila, D., & Caizar, C. (2011). Application of Taguchi method to selection of optimal lubrication and cutting conditions in face milling of AlMg3.Journal of CleanerProduction 19, 640e645.
3. Hebák, P. a kol. (2005). Vícerozměrné statistické metody (3). Praha: Informatorium, 2005. 241 s. ISBN 80-7333-039-3.
4. Kemény, S., & Deák, A. (2000). Kísérletek tervezése és értékelése. Budapest: Muszaki Konyvkiadó. 2000. ISBN 963 16 3073 0.
5. Kolohan, F., Manoochehri, M., & Hosseini, A. (2011). Application of Taguchi method and ANOVA analysis for simultaneous optimization of machining parameters and tool

geometry in turning. Eng. Tech., 74(2011), 82-85.
6. Kučerová, M., & Lestyánska, K. (2011). Štatistické metódy kontroly kvality. 1. Vyd., Trnava: AlumniPress MTF STU, 2011, 150 s. ISBN 978-80-8096-146-6.
7. Sinay, J., et. al. (2007). Nástroje zlepšovania kvality. Prešov 2007. ISBN 978-80-89040-32-2.
8. Taguchi, G., & Konishi, S. (1987). Taguchi methods, orthogonal arrays and linear graphs: Tools for quality engineering. Dearbom: American supplier institute (1987), pp. 35-38.
9. Veber, J. (2002). Řízení jakosti a ochrana spotřebitele. 1. vyd. Praha: Grada Publishing, 2002. ISBN 80-247-0194-4.

Corresponding author:
Ing. Judita Cservenáková, Department of Quality and Engineering Technologies, Faculty of Engineering, Slovak University of Agriculture in Nitra, Tr. Andreja Hlinku 2, 949 76 Nitra,Slovak Republic,
e-mail: cservenakova.judit@gmail.com

IDENTIFIKÁCIA ZVYŠKOVÉHO ZNEČISTENIA TLMIČA NÁRAZOV

Zuzana CSILLAGOVÁ, Martin BALÁŽ, Gabriel POLÓ, Maroš KORENKO, Erik GÓCS

Katedra kvality a strojárskych technológii, Technická fakulta, SPU v Nitre, Slovak Republic

Abstrakt
V článku sa budeme venovať implementácii postupu pre zisťovanie technickej kontroly čistoty alebo zvyškového znečistenia, ktorý sa používa pre určenie čistoty komponentov nových, ešte nepoužitých dvojtrubkových tlmičov nárazov. Jedným z najhlavnejších a dlhodobých cieľov je vytvoriť a udržať štandardnú úroveň čistoty produktov vo výrobnej organizácií. Pri tomto procese sprievodnej technickej kontrole sa hodnotia len vnútorné povrchy tlmičov, ktoré prichádzajú do styku s tlmiacim olejom.

Kľúčové slová: *tlmič, tlmič nárazov, kontrola, zvyškové znečistenie.*

ÚVOD

Každá organizácia musí zamerať svoju pozornosť hlavne na kvalitu svojich výsledných produktov, z tohto dôvodu je potrebné zabezpečiť ich neustálu kontrolu. Jednou z týchto kontrol produktov je aj technická kontrola čistoty, tzv. zistenie zvyškového znečistenia.
Vyhodnotenie zvyškového znečistenia, podľa VDA19.1 z roku 2015, sa zameriava na kritické hodnoty znečistenia, ktoré by mohli negatívne ovplyvniť správnu funkčnosť finálneho produktu. Pri analyzovaní vyhodnocujeme nasledovné hodnoty: celková hmotnosť znečistenia, veľkosť najväčšej kovovej čiastočky, veľkosť najväčšej nekovovej čiastočky. Každá z vyhodnocovaných hodnôt má svoje špecifické požiadavky- hranice, ktoré nesmú byť prekročené.

MATERIÁL A METÓDY

Pri analýze zvyškového znečistenia dochádza ku kontrole troch hlavných komponentov tlmiča, ktoré sú vykonávané na zvlášť filtroch.
Sú to:

1. Vonkajšia rúra
2. Olej (olej z vonkajšej aj vnútornej rúry)
3. Ostatné komponenty :
    - Vnútorná rúra.
    - Piestna tyč.
    - Spodný ventil.
    - Vedenie piestnej tyče (bez tesnenia).

Jednotlivé vyššie spomenuté komponenty môžeme vidieť na Obr.1.

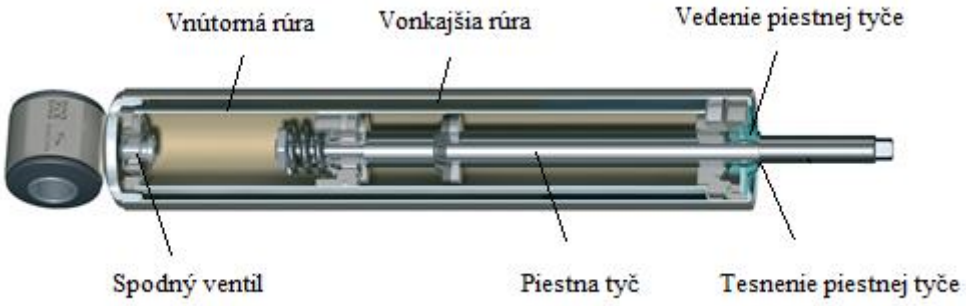

Obr.1 Komponenty tlmiča nárazov

Postup kontroly:

1. Čistenie zariadení- filtračného zariadenia, pinzety a všetky nádoby musia byť taktiež dôkladne vyčistené (oplachovanie studeným postrekom) a vysušené (maximálne 200 μm). Použitá premývacia kvapalina musí byť predfiltrovaná pomocou filtra ≤ 1,2 μm.
   Na extrakciu častí tlmičov a zistenie zvyškového znečistenia budeme potrebovať nasledovné štyri nádoby:

Obr.2 Štyri nerezové nádoby- piestna tyč(piston rod), olej (oil), vonkajšia rúra (container), komponenty(components)

2. Určenie nulovej hodnoty – táto hodnota musí byť určená ešte pred samotným testom jednotlivých dielcov tlmiča.
3. Demontáž tlmiča:
   - Vytiahneme piestnu tyč z vonkajšej rúry a premiestnime ju do nerezovej nádoby v polohe vzpriamenej, aby sme zabránili k úniku oleja.
   - Pomocou využitia skrutkovača oddelíme vedenie piestnej tyče, tesnenia a spolu s vnútornou rúrou ich vložíme do príslušnej nádoby.
   - Zhromaždíme olej z vnútornej aj vonkajšej rúry do nádoby určenej pre olej.
   - A posledným krokom je vybratie piestnej tyče z vnútornej rúry.
4. Extrakcia testovacích komponentov – povrchy súčiastok v nádobách, sú pomocou studeného čistiaceho postreku prepláchnuté tak, aby všetko médium ostalo v nádobách.
   Parametre postreku:
   - Tryska: 1,5 mm
   - Prietok: 1 l / min
   - 1500 ml média
5. Doplníme médium do nádob tak, aby boli komponenty ponorené.
6. Vložíme nádoby do ultrazvukového kúpeľa (6min.).
   Parametre pre ultrazvukový kúpeľ podľa WN 70/13 U:
   - Frekvencia: 40 kHz
   - Výkon: 25 W / l
   - Teplota okolia

   Po vytiahnutí nádob z ultrazvukového kúpeľa, vyberieme jednotlivé komponenty z nádob a opláchneme ich, aby sme odstránili prípadné zadržané častice na ich povrchu. Všetko toto médium sa udržiava v príslušných nádobách.
7. Filtrácia kvapalín z nádob- budeme mať 3 filtre:
   - 1x nádoba pre vonkajšiu rúru
   - 1x komponenty
   - 1x olej
8. Sušenie filtrov – štyri filtre (nulová hodnota, vonkajšia rúra, komponenty, olej) sušíme v rúre bez re-cirkulácie vzduchu pri 100°C počas jednej hodiny.

9. Filtre je potrebné nechať vychladiť v exsikátore jednu hodinu. (Pri mokrých filtroch by mohlo dôjsť ku chybným meraniam hlavne hmotnosti)
10. Analýza filtrov pomocou zisťovania váhy filtru a vizuálne pomocou mikroskopu Jomesa (Obr.3).

Obr.3 Jomesa mikroskop

11. Dokumentácia výsledkov.

VÝSLEDKY

Extraction & Gravimetry			
Extraction Method:		Parts on Filter:	1
Liquid:	Desolvit	Filter Type:	SEFAR 41µm / Ø47mm
Amount [ml]:		Weight [mg]:	1,45

Microscopic Analysis			
Scale:	X:6.4 µm/Pxl Y:6.5 µm/Pxl	Evaluated Ø [mm]:	44
Filter occupancy [%]:	0.374228	allowed Occupancy:	1,5 % (Cellulose), 3 % (Nylon)

Largest metallic particle	Length [µm]:	188	Width[1] [µm]:	58
Largest nonmetallic particle[2]	Length [µm]:	462	Width[1] [µm]:	47

Stretched length of longest fiber				L_{str} [µm]:	2426	Total [mm]:	56.6
Length [µm]				Code	per Filter Membrane	per Part/Component	per 1000 cm²
		Non metallic[2]	Metallic	Non metallic[2]	Metallic	Non metallic[2]	Metallic

Summary:							
> 600	J-N	0	0	0.0	0.0		
200…600	H-I	83	0	83.0	0.0		
100…200	F-G	269	23	269.0	23.0		
15...100	C-E	1517	16	1517.0	16.0		

[1] Šírka častíc v tejto správe sa vždy udáva v ortogonálnom reze.
[2] častice bez vlákien.

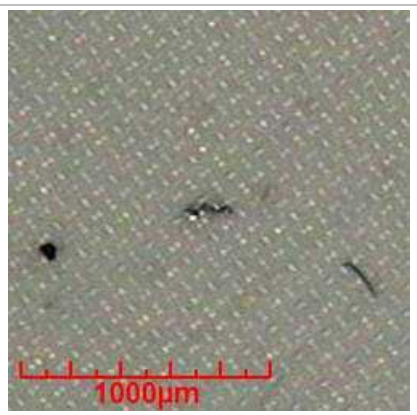

Najväčšia kovová častica
188 µm x 58 µm

Druhá najväčšia kovová častica
176 µm x 84 µm

Najväčšia nekovová[2] častica
462 µm x 47 µm

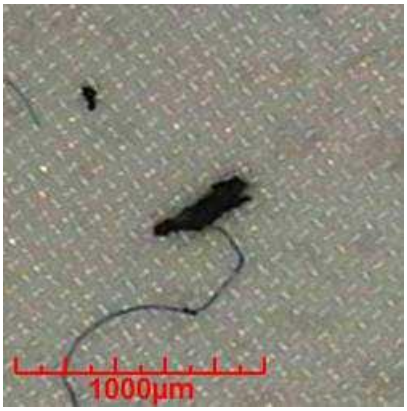

Druhá najväčšia nekovová[2] častica
442 µm x 147 µm

Pohľad na membránu
0.37 % výskyt pri Ø = 44 mm

Najdlhšie vlákno
$Feret_{max}$ = 1592 µm / L_{str} = 2426 µm

Obr. 4 Vizuálna kontrola častíc

Vyhodnotenie analýzy zvyškového znečistenia

Hmotnosť znečistenia: Hmotnosť znečistenia nesmie prekročiť hodnotu 5mg. V našom prípade je hodnota hmotnosti znečistenia 1,45mg. Výsledok hmotnosti je viac než prijateľný a nepoukazuje na nič nezvyčajné.

Veľkosť najväčšej kovovej čiastočky: Veľkosť najväčšej kovovej čiastočky nesmie prekročiť hodnotu 200µm. V našom prípade bola nájdená kovová čiastočka o veľkosti 188µm, ktorá spĺňa požiadavku na maximálnu veľkosť kovovej čiastočky. Vznik takejto čiastočky mohlo spôsobiť lisovanie krúžku

spätného dorazu, kde takýto typ kovových čiastočiek vzniká veľmi často. Eliminovanie takéhoto typu kovových čiastočiek je možné opraním dielov po zalisovaní krúžku spätného dorazu.
Veľkosť najväčšej nekovovej čiastočky: Veľkosť najväčšej nekovovej čiastočky nesmie prekročiť hodnotu 500µm. V našom prípade bola nájdená nekovová čiastočka o veľkosti 462µm, ktorá spĺňa požiadavku na maximálnu veľkosť nekovovej čiastočky. Nekovové čiastočky boli identifikované ako zvyšok laku, ktorý sa pravdepodobne zachytáva na prípravkoch uchytávania dielov v práčke. Eliminovanie takéhoto typu nekovových čiastočiek je možné zvýšením frekvencie preventívnej údržby so zameraním sa na problematické prípravky.

ZÁVER

Na záver by sme mohli zhodnotiť, že vybraný analyzovaný diel spĺňa požiadavku na maximálnu hmotnosť znečistenia, požiadavku na maximálnu veľkosť kovovej čiastočky a tiež požiadavku na maximálnu veľkosť nekovovej čiastočky. Týmto pádom vieme zhodnotiť celkovo celú analýzu zvyškového znečistenia a to, že analyzovaný diel spĺňa požiadavku na čistotu podľa VDA 19.1: 2015.

POUŽITÁ LITERATÚRA

1. Causemann, P. (2001). Automotive shock absorbers. Features, designs, applications. Second edition, 2001. ISBN 3-478-93230-0.
2. STN EN ISO/IEC 17025 (2005). Všeobecné požiadavky na kompetentnosť skúšobných a kalibračných laboratórií; SÚTN, 2005.
3. ZF Levice. Work Instruction Product Line. WI-C 902.
4. ISO 16232 (2007). Road Vehicles – Cleanliness of Components and systems.
5. ISO/IEC Guide 99 (2007**).** International Vocabulary of Metrology — Basic and General Concepts and Associated Terms, 3rd edition.
6. VDA 19.1 (2015). Quality Managemetn in the Automotive Industry,Technical Cleanliness, Part 1.

Corresponding author:
Ing. Zuzana Csillagová, Katedra kvality a strojárskych technológii, Technická fakulta, SPU v Nitre, Tr. A. Hlinku 2, 949 76 Nitra, e-mail: xcsillagova@uniag.sk

SOLAR ENERGY POTENTIAL IN INDONESIA

Minh-Quan DANG

Department of Physics, Faculty of Engineering, Czech University of Life Sciences Prague

Abstract
Abstract Indonesia is the largest archipelagic country in the world which is located in the South-East Asia area. The geographical condition of Indonesia is extremely suited for developing of renewable energy in general and solar energy in specific. This report aims to review the solar energy potential in Indonesia and using PVGIS to study the feasibility of fixed stand solar photovoltaic system as well as sun tracking system in Indonesia conditions. The result from the case studies shows that the crystalline silicon solar panel can collect about 12.8% energy from sunlight. The sun tracking system has impact on yearly energy yield, the most suitable system is the inclined tracking system.

Key words: *Solar energy, Sun tracking system, fixed stand, Indonesia.*

INTRODUCTION

Indonesia is the largest archipelagic country in the world which is located in the South-East Asia area. According to Indonesia's National Coordinating Agency for Survey and Mapping, the total number of islands in the archipelago is 13,466, of which 922 are permanently inhabited. The equator crosses through Indonesia providing them abundance solar irradiation necessary for developing and exploiting solar energy.This report aims to review the solar energy potential in Indonesia and using PVGIS to study the feasibility of fixed stand solar photovoltaic system as well as sun tracking systems in Indonesia conditions.The International Renewable Energy Agency estimated the potential for solar PV in Indonesia is 532.6 GW (*Irena & Sener, 2017*). The most energy can be harvested in Sumatra, Java and Papua islands.

By the end of 2012, the total solar PV capacity installed in Indonesia is estimated at 80 MW and the potential for solar photovoltaic is up to 500GW(*Irena, 2016*). For the on-grid component, the installed capacity is estimated at around 10 MW. The largest power plants are located in Bali (2 MW), Kupang (5 MW) and Gorontalo (2 MW) (*Kosasih, 2016*). By mid-2016 there was over 700 MW in memorandums of understanding as well as commitments by PLN to develop utility-scale solar PV systems in Indonesia. announcement in July 2016 of a new feed-in tariff to support 250 MW of solar PV installation is likely to further support the market in the coming years (*Fathoni et al., 2014; Susanto, 2016*).

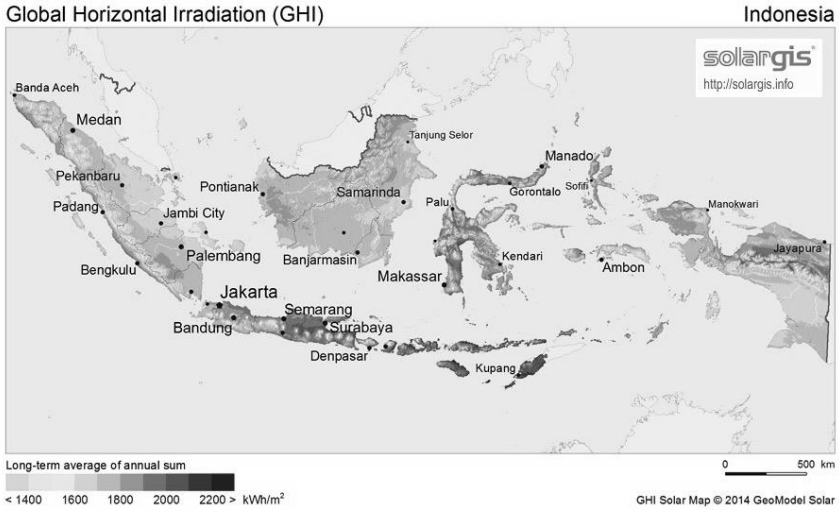

Fig. 1 Global Horizontal Irradiation in Indonesia

The global horizontal irradiation in Indonesia (Fig. 1) shows that the irradiation in Indonesia is equally distributed. Most of the regions have higher that 1600 kWh/m2 per year compare to under

1100kWh/m2 in the Czech Republic (*Libra & Poulek, 2010*). The Southern islands of Indonesia including Java and Bali island have very high direct irradiation. The Eastern parts such as Papua also have high irradiation. These regionshave biggest potential for developing the solar PV power plant because of its remote, low people density and large land field available.

METHODOLOGY

The location for case study is the city of Medan (3.590, 98.674) and elevation is 27 m in the upper left corner of the Fig. **1**. Medan is one of the biggest city in Indonesia which have population over 2 million people and density 7900/km^2 Medan is the capital of North Sumatra province in Indonesia, located along the north-eastern coast of Sumatra Island.

The tool will be used to evaluate the solar potential of Medan is Photovoltaic Geographical Information System (PVGIS) (*Huld, 2017*). PVGIS provides a map-based inventory of solar energy resource and assessment of the electricity generation from photovoltaic systems in Europe, Africa, and South-West Asia.

With the supporting of PVGIS, the power yield from a 1.4 kWp photovoltaic solar system will be evaluated with following cases:

1. Solar energy in Medan collected on horizontal and optimal plane.
2. Photovoltaic solar system with fixed stand with horizontal and optimal cases
3. Photovoltaic solar system with tracking systemwith vertical, inclined and two-axis tracking

Fig. 2 Vertical axis, Inclined axis and Two-axis sun tracking system concepts (from left to right)

The solar module is Canadian Solar 280 Mono with the technical specification as in the Tab. **1**.

Tab. 1 Technical specification of solar module

Electrical Data	Value
Nominal Max. Power	280 W
Opt. Operating Voltage (Vmp)	31.5 V
Opt. Operating Current (Imp)	8.89 A
Open Circuit Voltage (Voc)	38.5 V
Short Circuit Current (Isc)	9.43 A
Module Efficiency	17.11 %

Number of module is 4 and the total area for module is 8.2 m^2. The electrical losses of the PV system will be assumed14% of total energy production.

RESULTS AND DISCUSSION

Solar irradiation in Medan

The PVGIS provide the option to find optimum slope and azimuth for fixed stand PV system and in the case of Medan the optimum slope is 1^0 and azimuth -8^0. Fig. **3** indicates the average solar energy in Medan from 2005 to 2016. The different between solar irradiation on horizontal plane (dark grey) and optimal plane (light grey) is minor. Solar irradiation around the year is stable with minimum in Decemberis 126.9 kWh/m^2 and maximum in March is 170.2kWh/m^2.Standard deviation of solar irradiation during the year is about 11 kWh/m^2. The irradiation on horizontal plane during April to July is

higher than on optimal plane that indicate in order to harvest the most energy from the sun, the solar module's slopecould be adjust twice a year on March and October.

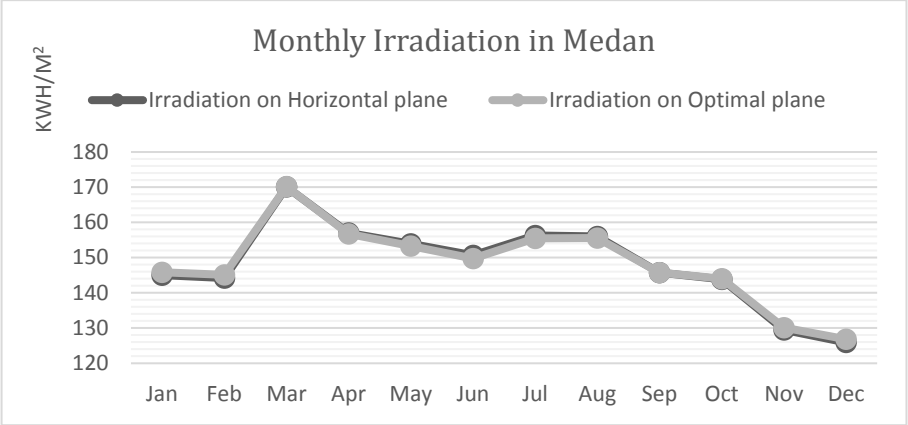

Fig. 3 Monthly Irradiation on horizontal and optimal plane

Photovoltaic solar system with Fixed Stand

The solar photovoltaic system with fixed stand collect about 12.8% energy from the sun every into usable electricity, which is in average 155/1213.6 kWh per month. The deviation of energy production due to year to year variation is 3.35%. The total energy production from the PV system is 1864 kWh/year. The system yield is 1331.4 kWh/kWp per year or 3.64 kWh/kWp per day. This energy yield is higher than most of Europe and many other part of Asia (Ismail, Ramirez-Iniguez, Asif, Munir, & Muhammad-Sukki, 2015).

Photovoltaic solar system with Tracking system

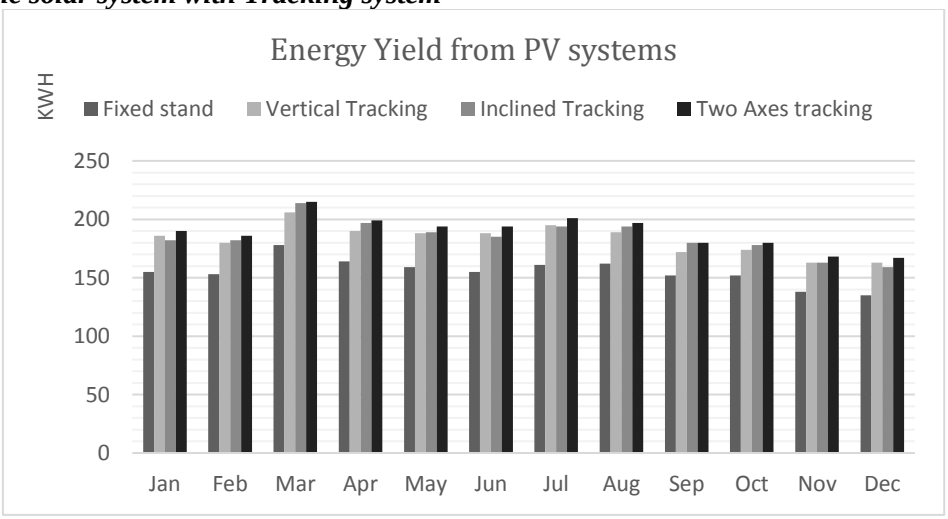

Fig. 4 Energy yield from PV systems

Tab. **2** below shows energy production from solar PV with sun tracking system. Sun tracking system improve the energy efficiency by about 2% in general. The more significant improvement is daily energy yield. It improved from 3.64 kWh/kWp of fixed stand up to 4.44 kWh/kWp with two-axis tracking system. Between tracking systems, the two-axis system results to the highest energy yield follow by inclined tracking system and then vertical axis system. Because of the location of Medan and Indonesia in general, the sun elevation during the year vary with much smaller amount compare to Europe. Therefore, different between type of tracking system were not much different. Actually, the daily energy yield from two-axis tracking only 0.11 kWh higher than inclined axis system and 0.15 kWh vertical axis system.Consider to the complexity and cost of the two-axis system, the inclined axis is more convenience to be applied.

Tab. 2 Results from solar PV with sun tracking systems

	Average monthly energy production [kWh]	*System efficiency [%]*	*Total energy production per year [kWh]*	*Daily yield [kWh/kWp]*	*Yearly yield [kWh/kWp]*
Vertical axis system	*183*	*15.08 %*	*2194*	*4.29*	*1567*
Inclined axis system	*185*	*15.24 %*	*2217*	*4.33*	*1583*
Two-axissystem	*189*	*15.57 %*	*2271*	*4.44*	*1622*

CONCLUSIONS

The paper reviews the current situation of utilizing solar energy in Indonesia. The installed capacity of solar power plant in Indonesia is still small (80MW) compare to its potential more than 500GW. The case studies indicate some advantages for solar PV in Indonesia. Because of the location near to the equator, solar modules can be installed in the horizontal plane without losing energy production capability. The sun tracking system could be installed to improve the energy yield; however, the improvement is only about 2% even for the two-axis tracking system. If for any reason the tracking system would be deployed then the inclined axis tracking seems to be the correct option.

ACKNOWLEDGMENT

I would like to show my gratitude to professor Martin Libra and doc. Ing Vladislav Poulek for sharing their wisdom with me during this research. I also would like to express my grateful to professor David Herak for giving me the opportunity to conduct this research.

REFERENCES

1. Fathoni, A. M., Utama, N. A., & Kristianto, M. a. (2014). A Technical and Economic Potential of Solar Energy Application with Feed-in Tariff Policy in Indonesia. *Procedia Environmental Sciences*, *20*, 89–96. https://doi.org/10.1016/j.proenv.2014.03.013
2. Huld, T. (2017). PHOTOVOLTAIC GEOGRAPHICAL INFORMATION SYSTEM. Retrieved from http://re.jrc.ec.europa.eu/pvg_static/en/contacts.html
3. IRENA. (2016). *Renewable Energy Statistics 2016*. IRENA. Retrieved from www.irena.org/Publications
4. IRENA, & SENER. (2017). *Renewable Energy Prospects: Indonesia*.
5. Ismail, A. M., Ramirez-Iniguez, R., Asif, M., Munir, A. B., & Muhammad-Sukki, F. (2015). Progress of solar photovoltaic in ASEAN countries: A review. *Renewable and Sustainable Energy Reviews*, *48*, 399–412. https://doi.org/10.1016/j.rser.2015.04.010
6. Kosasih, F. U. (2016). Kupang Houses Indonesia's Largest Solar Power Plant. *Global Indonesian Voices*. Retrieved from http://www.globalindonesianvoices.com
7. Libra, M., & Poulek, V. (2010). *Photovoltaics - Theory and practice of solar energy utilization*. Prague.
8. Susanto, A. (2016). New government decree to accelerate the Indonesian solar market. *Solarplaza*,. Retrieved from www.solartrademissionindonesia.com

Corresponding author:
Ing. Minh-Quan Dang, Department of Physic, Faculty of Engineering, Czech University of Life Sciences Prague, Kamýcká 129, Praha 6, Prague, 16521, Czech Republic, e-mail: dang@tf.czu.cz

EXPERIMENTAL DESCRIPTION OF DEGRADATION OF SHEAR STRENGTH OF RESINS FILLED WITH PARTICLES FROM THE PHOENIX DACTYFILERA

Karolína HABROVÁ

Department of Material Science and Manufacturing Technology, Faculty of Engineering, Czech University of Life Sciences Prague,

Abstract
Reaction resins filled with organic particles can be considered as biocomposites - materials that are formed by at least one phase on a natural basis. These materials are particularly interesting especially because of the possibility of replacing primary raw materials with secondary raw materials, being environmentally friendly and inexpensive. However, it is also important to mention the negative aspects of natural materials, and that is their natural character. Degradation is one of the limits of natural materials. This paper describes an experimental program that evaluates the decrease in shear strength of resin filled with date seeds particles of the plant Phoenix Dactyfilera by the degradation of test bodies in the climatic chamber for 4 weeks. The remains of the date processing, the stones from Phoenix Dactyfilera, can be considered as a secondary raw material, usage of which may be desirable. Degradation resulted in a 41.1% reduction in shear tensile strength for concentration 2.5% and a 38.4% tensile shear strength reduction for concentration 5.0%.

Key words: *Composite system, mechanical characteristics, natural filler, particle.*

INTRODUCTION

Composite materials can be characterized as materials composed of two or more phases (*Taddei et al., 2016; Dědičová et al., 2016)*. Biocomposites are then materials composed of different phases that can combine natural materials with inorganic materials. It is primarily an inorganic matrix filled with organic fibers or particles. Natural materials have been used more and more in recent years, one of the reasons being their low cost *(Müller et al., 2017)*. The expansion of biocomposite materials is primarily due to the fact that they are known as green materials that can replace materials from petroleum *(Shivamurthy et al., 2014)*. Organic fillers have many advantages including availability, price, good mechanical properties and low weight. The disadvantages include their natural character, e.g. natural fibers have different diameter and length, which affects their mechanical properties and hence the mechanical properties of the resulting composite system *(Renner et al., 2010).*The presence of particles can optimize the adhesion and cohesion characteristics of polymeric materials *(Ruggiero et al., 2016)*.
Degradation is an irreversible process that causes a weakening of the material at the interface between the filler and the matrix. It is a change in properties over time when molecular weights and material structures are affected *(Grassie et al., 1985)*. Composite adhesive bonding degrades primarily due to temperature, humidity, and microorganisms *(Soykok et al., 2017; Chocholouš & Müller, 2013; Müller 2013; Cidlina & Müller, 2015)*. The natural filler in a composite system with an epoxy resin matrix can adversely affect the degradation process - for example by its water absorption or faster decomposition.
The aim of the experiment is the experimental description of the degradation process of epoxy resin filled with date seeds particles prepared from Phoenix Dactyfilera plants. The particle size was adjusted by screening and ranged from 200-300 μm. The addition of such natural particles does not significantly affect the shear strength - this hypothesis has been verified by the experimental program and statistical methods. The decrease in shear strength in relation to the degradation length in the climatic chamber was described.

MATERIALS AND METHODS

The two-component epoxy resin with a polyamide based hardener was used as a matrix. The particles used as a filler were processed from seeds of dates from the Phoenix Dactylifera plant - the country of origin of China. It is a biomass produced by the processing of a fruit, where the seeds are a secondary product. The seeds were processed on a knife mill at a speed of 20,000 rpm. The particles were dried at 105 °C and further sorted by analytical sieves. The fractions used in this experiment were collected between top sieve with mesh sizes of 300 μm and bottom sieve with mesh size 200 μm. The prepared particles were mechanically mixed with the epoxy resin of the desired concentration.

Mechanical mixing of the prepared particles and the epoxy resin resulted in a composite system which was further applied to steel adherents. Two different weight concentrations of 2.5 and 5.0 wt. % were used in the experiment.

In the course of this work, the composite mixture was applied to carbon steel sheets S235J0. Prior to application, the sheet surface was blasted and degreased. Surface roughness was measured on the Surftest 301 for the roughness test. The prepared bonded joints were placed in the degradation chamber which was set to the degradation cycle, see Figure 1. The temperature (70 °C and - 40 °C) and humidity (90% and 50% - ČSN EN ISO 9142) were controlled during the degradation process. Samples were taken from the chamber at each end of 7 cycles (1 cycle - 24 hours). Overall, 4 x 7 cycles were repeated (28 cycles - 672 hours).

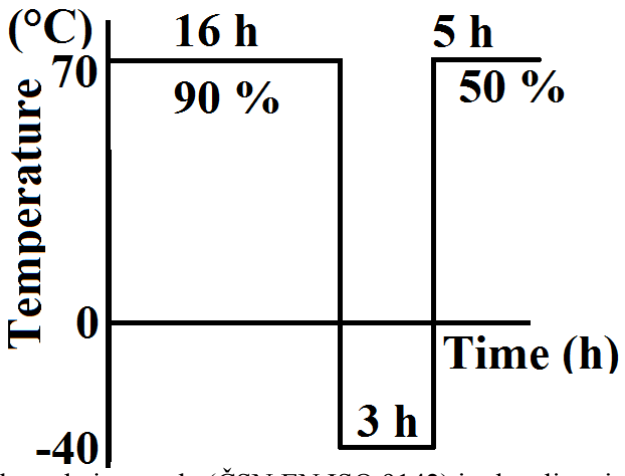

Fig. 1 The course of the degradation cycle (ČSN EN ISO 9142) in the climatic chamber (temperature, time, humidity)

After degradation process in the climatic chamber, the samples were taken out and left at room temperature. The shear strength was tested according to ČSN EN 1465.

The type of failure was evaluated in accordance with ISO 10365. Statistical analysis of the data was performed using an ANOVA and T-test with a level of significance $\alpha = 0.05$. A zero hypothesis (H_0) was expressed, its validity showing a statistically insignificant difference of observed statistical data.

Electron microscopy Tescan Mira 3 GXM equipped with dispersion X-ray (Oxford X-MaxN) was used for optical sample analysis and interphase interaction analysis.

RESULTS AND DISCUSSION

Prior to preparing the filled resin and preparing the test samples, the size of the individual particles was evaluated by stereoscopic microscopy. The histogram was selected for presenting the measured data - Fig. 2, which shows that the average particle size at 31% corresponded to the interval 240-260 μm, 25% of the particles falling within the range of 220-240 μm. 12% of the particles were outside the chosen range of 200-300 μm, due to the fact that not all particles less than 200 μm fell through the bottom sieve and particles were slightly smaller than 300 μm in the fraction. Therefore, 88% of the particles were in the required set interval. The particles were dried and blended prior to

application to the epoxy resin to completely resolve the particles in the resin. The composite mixture thus prepared was applied to steel adheres.

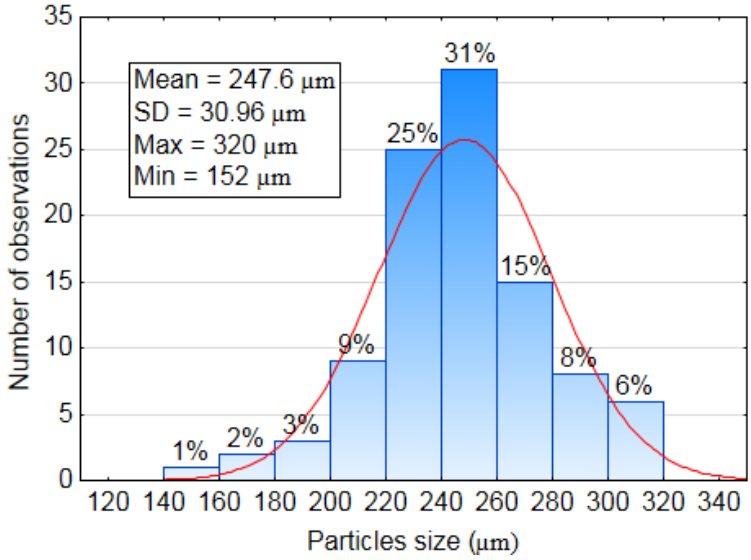

Fig. 2 Evaluation of the particle size used in the experiment

The roughness was evaluated through the Ra and Rz parameters prior to application of the composite system to steel adheres. The parameter Ra was 2.4 ± 0.21 µm and the Rz parameter was 10.59 ± 1.11 µm. The shear strength of the non-filled resin on the treated adherent with the specified roughness was 12.15 ± 0.65 MPa.

To verify the hypothesis that the used organic particles did not affect the shear strength of the epoxy resin on steel adherents, a statistical comparison of the non-filled resin with the resin filled with 2.5 and 5.0 weight percent of the particles from dates was used. Statistical verification of hypothesis at significance level 0.05 was performed - parameters p = 0.35 (2.5 wt%) and p = 0.53 (5 wt%), see graphical comparison Fig. 3.

The strength of the non-filled resin decreased in proportion to the degradation time, up to 7.71 ± 0.42 MPa, i.e. a decrease of 4.43 MPa (see Figure 3). For the resin filled with 2.5 wt% filler, the shear strength before degradation was 12.56 ± 0.51 MPa, this value decreased after 4 weeks of degradation to 7.36 ± 1.07 MPa, i.e. a decrease of 5.17 MPa. For a resin filled with 5.0 wt% filler, the shear strength before degradation was 11.82 ± 0.88 MPa, this value decreased after 4 weeks of degradation to 7.29 ± 0.62 MPa, i.e., a decrease of 4.54 MPa.

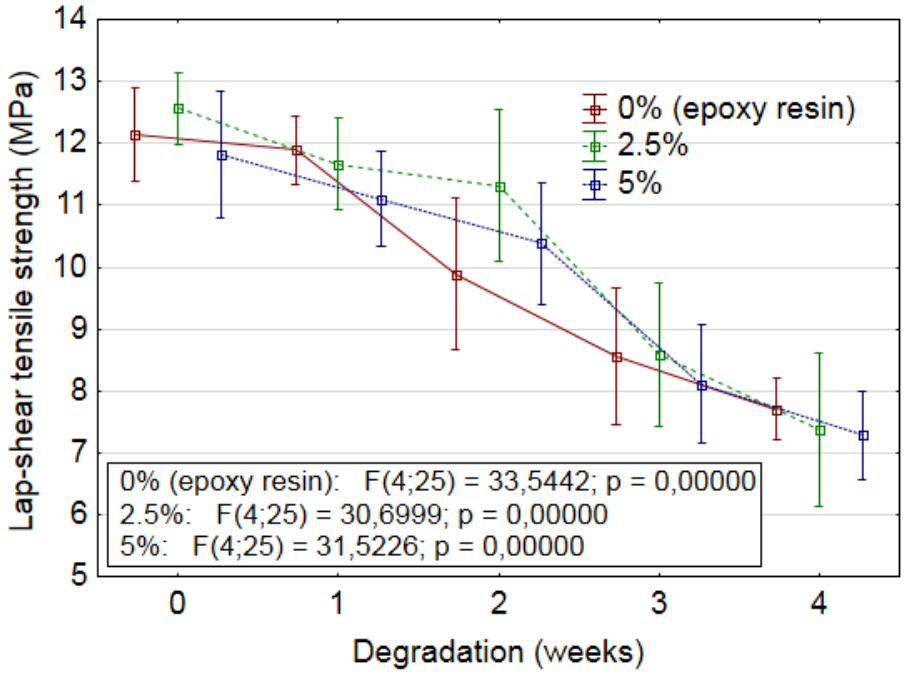

Fig. 3 Decrease in shear strength depending on duration of degradation

From the point of view of formed composite systems, the interaction between filler and resin is important. This interaction was evaluated by electron microscopy. The particulate filler from the dates was well wetted with the used resin. Figure 4 describes this interfacial interaction before degradation of the test samples.

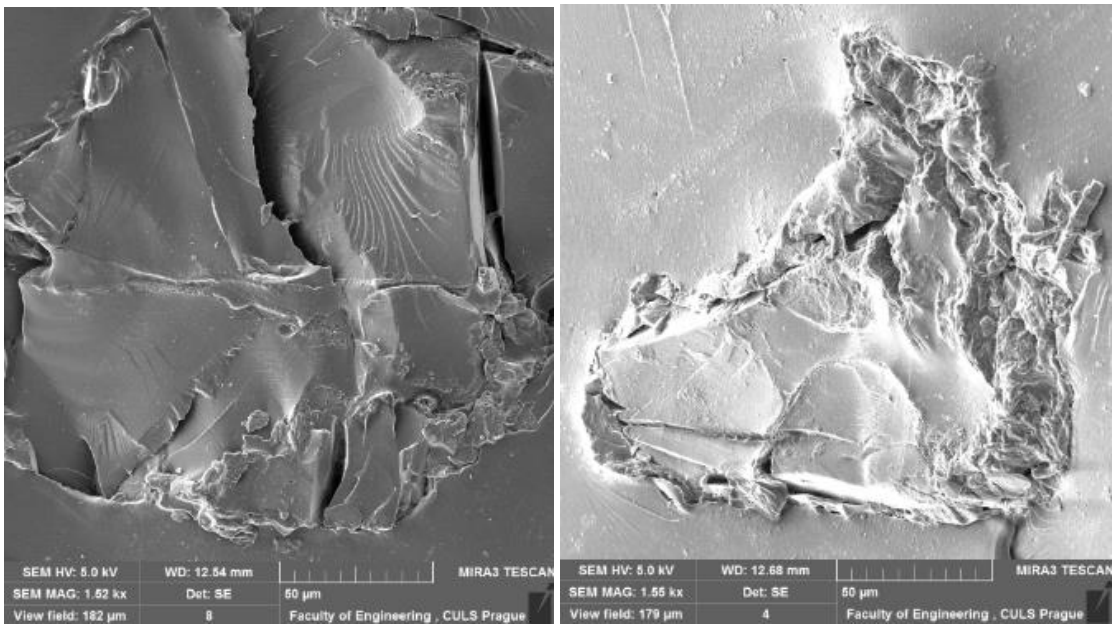

Fig. 4 Interphase interaction: Mag. 1.52 kx (left), Mag. 1.54 kx (right)

The course of degradation of the test samples is described in Fig. 5, which shows the test sample after 1 to 4 weeks of degradation when the corrosion of the steel adherents is evident. In the course of the experiment, the type of failure was assessed - the failure was in most cases of adhesion type. Some of the test specimens showed corrosion of the bonded joint after 4 weeks of degradation.

Fig. 5 Course of degradation of test samples - 1 - one week, 2 - two weeks, 3 - 3 weeks, 4 - 4 weeks

CONCLUSIONS

The shear strength was influenced by degradation in both the non-filled resin and resin filled with particles of dates - the shear strength dropped. The experiment has shown that inclusion of inorganic particles with size 200-300 μm does not significantly affect the shear tensile strength compared to the non-filled resin. The most important conclusions of the experiment can be summarized as follows:

1. The tensile shear strength dropped by 36.5% after 4 weeks of degradation of non-filled resin.
2. The shear tensile strength dropped by 41.4% after 4 weeks of degradation of the resin filled with 2.5% of the particles prepared from the date seeds.
3. The shear tensile strength decreased by 38.4% after 4 weeks of degradation of the resin filled with 5% of the particles prepared from the date seeds.

ACKNOWLEDGMENT

This study was supported by the grant IGA TF 2017 (31140/1312/3113).

REFERENCES

1. Chocholouš, P., & Müller, M. (2013). Mechannical surface treatment for adhesive bonding technology in sandwitch production. In *5th International Conference on Trends in Agricultural Engineering 2013, TAE 2013 03.09.2013, Prague.* Prague: Czech University of Life Sciences Prague, pp. 249-253.
2. Cidlina, J., & Müller, M. (2015). Influence of overlapping length on peeling strength of adhesive bonds. *In 14th International Scientific Conference on Engineering for Rural Development 2015 20.05.2015, Jelgava. Jelgava: Latvia University of Agriculture, s. 761-765.*
3. Dědičová K., & Valášek, P. (2016). Influence of glass powder size sorting on properties of composite systems. *Scientia Agriculturae Bohemica, 47, pp. 25-31.*
4. Grassie N., Guy M.I., & Tennent, N.H. (1985). Degradation of epoxy polymers: Part 1-Products of thermal degradation of bisphenol-A diglycidyl ether. *Polymer Degradation and Stability, 12, pp. 65-91.*
5. Müller M., Valášek P., Rudawska, A. (2017). Mechanical properties of adhesive bonds

reinforced with biological fabric. *Journal of Adhesion Science and Technology, 9, pp. 1-13.*

6. Müller, M. (2013). Influence of Specific Degradation Liquid Contaminants of Agricultural Production on Shear Impact Strength of Adhesive Bond. In *6th International Scientific Conference on Rural Development - Innovations and Sustainability 28.11.2013, Kaunas, Akademija, Lithuania. 10-406, s. 89-94.*
7. Renner K., Kenyó C., et al. (2010). Micromechanical deformation processes in PP/wood composites: Particle characteristics, adhesion, mechanisms. *Composites Part A: Applied Science and Manufacturing, 41(11), pp. 1653-1661.*
8. Ruggiero, A., Valášek, P., & Müller, M. (2016). Exploitation of waste date seeds of Phoenix dactylifera in form of polymeric particle biocomposite: Investigation on adhesion, cohesion and wear. *Composites Part B: Engineering, 104, pp. 9-16.*
9. Shivamurthy B., Murthy K., et al. (2014). Mechanical properties and sliding wear behavior of Jatropha seed cake waste/epoxy composites. *Journal of Material Cycles and Waste Management, pp. 1-13.*
10. Soykok I.F. (2017). Degradation of single lap adhesively bonded composite joints due to hot water ageing. *Journal of Adhesion, Vol. 93, pp. 357-374.*
11. Taddei P, Ruggiero A., Pavoni E., & Affatato, S. (2016). Transfer of metallic debris after in vitro ceramic-on-metal simulation: Wear and degradation in Biolox® *Delta composite femoral heads. Composites Part B: Engineering, in-press.*

Corresponding author:
Ing. Karolína Habrová M.Sc., Department of Material Science and Manufacturing Technology, Faculty of Engineering, Czech University of Life Sciences Prague, Kamýcká 129, Praha 6, Prague, 16521, Czech Republic, phone: +420 721 801 716, e-mail: habrovak@tf.czu.cz

TRANSPORT OF DANGEROUS GOODS IN SLOVAKIA FROM THE VIEW OF ENVIRONMENTAL

Marek HALENÁR, Peter KUCHAR, Vladislav HAJDÁK

Department of Transport and Handling, Faculty of Engineering, Slovak University of Agriculture, Slovak Republic

Abstract
The paper isfocused onpossible solutions ofroad transport on adefined territoryof the Slovak Republicin terms of potential environmental pollution in case of ADR vehicles crash. The article illustratestheseriousness situation related transport of dangerous goods effecting significantdamage of theecosystem because the utilizedroadsare not suitablefor thetransport of dangerous goods. Atthe monitoredsection of the road, wedescribedthe risks affecting vehicle crash and then proposed solutions to reduce its. These solutionswill increase thesafety of ADR transport and eliminateadverseeffects on theenvironment and population.

Key words: *road transport; ADR agreement; dangerous goods; environment.*

INTRODUCTION

ADR Agreement is an international agreement on the transport of dangerous goods, categorized into nine classes with a corresponding degree of hazard. Part of the agreementare twosubclasses,which deals with all elementsdirectlyrelated to thetransport of hazardous materials. Transport of dangerous goodsaremainlychemicals, which by theirtoxicity, flammabilityand infectivitythreaten the environmentand in direct contacthave a negativeimpact on public health, but any accidenttransport unit carryingharmful substancehas adisastrousimpact on the environmentinwhich we live.(Law no. 56/2012 abaut road transport). Transportin each countryis influencedby a variety ofsocio-economic factors, amongwhich may beincludeddemographics, urban planning, standard of the population and ultimately the country's integration into international trade (*Hujo et al., 2013*).Difficultyof road transporthas long beenan important topicof various economicandenvironmentaldebates, and in fact thestarting pointfor determiningthe amount of emissionsproduced bytransport andcalculating the energy performance of transport (*Hegedüš et al., 2012*;*Janoško et al., 2014*). We see the problem with the transport of dangerous goods in an increase in the international transport of dangerous substances, more dense and congested roads, the quality of crews transporting dangerous materials, in dealing with emergency situations in case of accidents. Currently ADR transport makes up 30% of the total transport on roads in Slovakia, where it is foreseeable, that the percentage share of dangerous goods will go up with the increase in production of the chemicals (*Žitňák & Korenko, 2011*). The total amount of dangerous goods in the European Union is about 110 billion tonne-kilometers per year, of which 58% is by road, 25% by road and 17% by inland waterway. The trend for road and inland waterway transport of dangerous goods is increasing, but decreasing for rail transport. The share of dangerous goods transport in total freight transport is about 8% (*Statistics of transporting ADR, 2014*).
The goal of this paper is to assess the risks of the damage to the ecosystem due to the transport of ADR in emergency situations based on available input data and to propose solutions to eliminate damage to the environment by establishing an appropriate transport corridor.

MATERIALS AND METHODS

The term optimization of transport routes is understood to create a structure of the transport corridors in road transport, which will be designed in accordance with the terms of the ADR and the applicable local laws of the road and the road. By optimizing the transport corridors of transportation of dangerous goods, creating a case study in dealing with bottlenecks we minimize adverse impacts in a traffic accident on the environment. Preparatory studies have been described in the risk segments in the defined territory of the Slovak Republic, focusing on the protection of groundwater reservoirs on the Žitný ostrov, analyzing the passage of roads across the river Hron. The last described risk section is

the field of mineral resources of major spa town Piešťany, whose solution is used as a case study set out to circumvent a city with resource-rich mineral springs.

2.1 ADR analysis on Žitný ostrov

Žitný ostrov belongs to the largest ground water reservoir in Central Europe. There fore, there is increased attention on thequality of thegroundwater. The area isalmostimpassablewith substancesthat may causepollution of groundwater, soil and waterways. The trucks wittingly use traffic diversion coming through the area mentioned above to pay no road fee however it is not excluded that some trucks transport hazardousmaterials. Figure 1 shows the corridor: Dunajská Streda – Topoľníky – Veľký Meder with a total length 29 km.

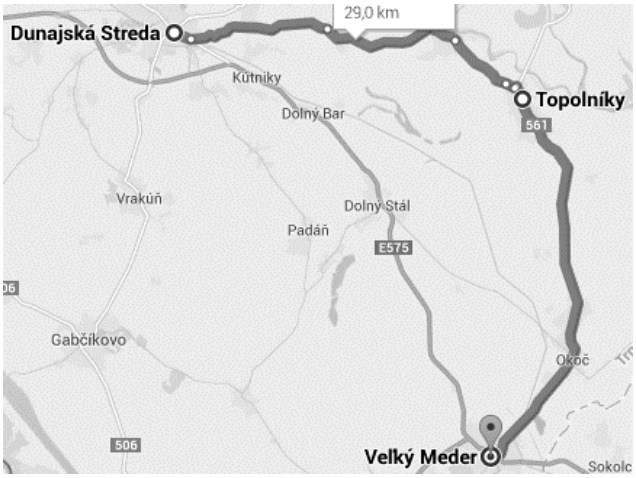

Fig. 1 Dunajská Streda – Veľký Meder

2.2 Analysis of crossing the river Hron

A crossing the river Hron is a problematic road section on the territory of Slovakia. The road has become a risk due to exceed the clearance limit because trucks use it instead the fee international communication. Road communication of II. class path is also used by carriers for the transport of dangerous goods. Bridge over the river Hron is not equipped with sedimentation tanks and thus creates a risk area in extenso. Comparing the distance passing through the point it is clear that truck drivers in the use of lines outside the R1 in FIG. 2 Scroll to a greater distance, but also to avoid paying tolls. This II. Class road is not ensured sedimentation tanks and drainage canal retaining leak of hazardous substances getting into in the groundwater and the river Hron during an accident.

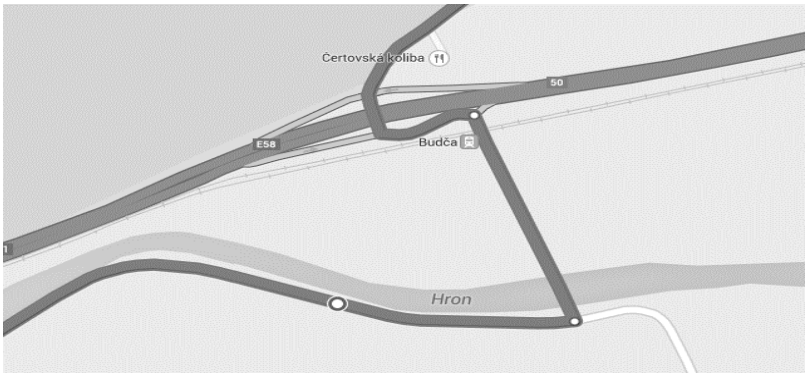

Fig. 2 The section crossing the river Hron for payment alternative

Fig.3 The section crossing the river Hron in circumventing (unpaid) alternatives

2.3. Transport hub of Piešťany

The problematic area of ADR transport in the district of Piešťany is the transport hub of Piešťany. According to Law 8/2009 Z.z. on road traffic and in accordance with the Collection of Laws No.56 / 2012 on road transport are adopted provisions for the detour of Piešťany for vehicles transporting pollutants, because the city is a spa city, which has an underground water resources and significant sources of natural springs and healing mud. FIG. 4 map is shown with traffic signs defining the transport of dangerous substances determinescommandment the direction of transport of dangerous materials (C19) and No entry for vehicles carrying cargo (B22), which may cause water and soil pollution. The transport of dangerous goods flow is diverted from the highway D1, the first class roads [61] and the path II. Class [499], given the fact that, on circumventing route are built sedimentation tanks, thus roads are drained in the case of biological disasters. Detour of highway D1 is on the specified communication paths I and II. Class with the length of 8.6 km by 1.7 km longer than the direct route along the highway, where the passage of vehicles carrying cargo that may cause pollution of water is prohibited (*Gnap & Jagelčák, 2009*).

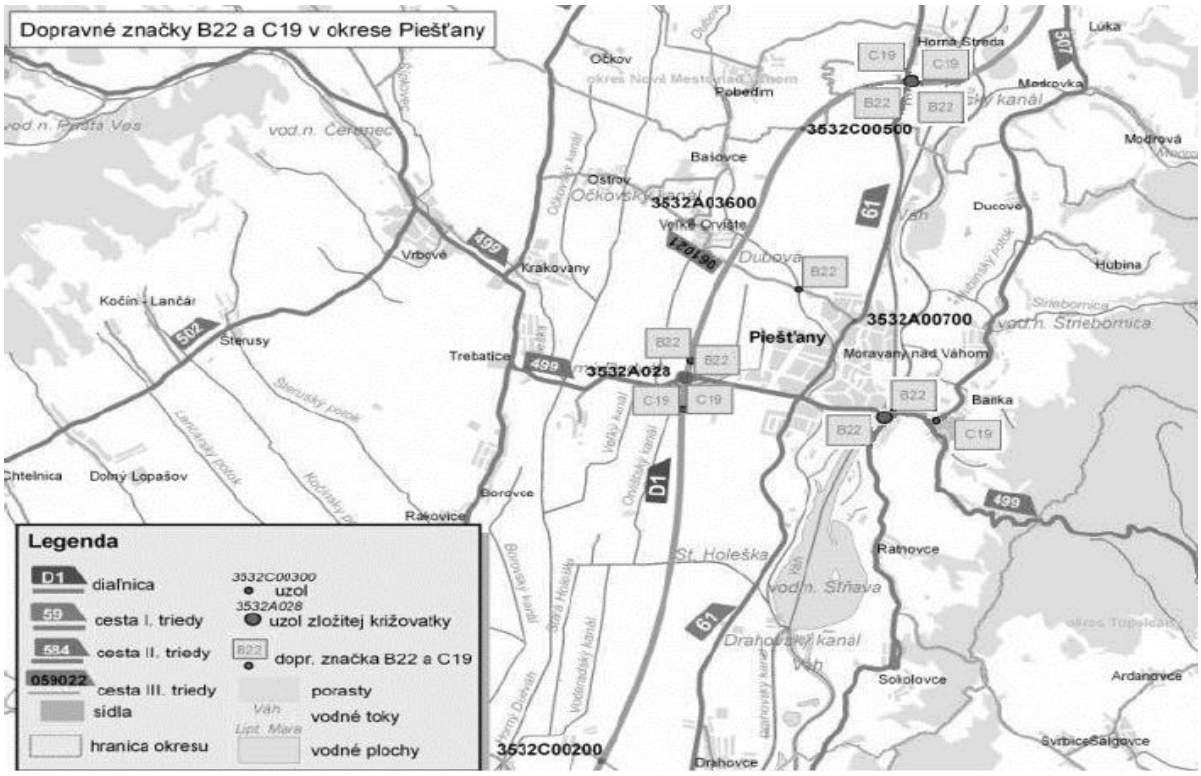

Fig.4 Traffic signs B22 and C19 near the town of Piestany (*Gnap* & *Jagelčák, 2009*)

RESULTSAND DISCUSSION

In the first part we analyzed transport corridor Dunajska Streda - VelkyMeder, where shippers of dangerous goods by truck deliberately bypass the tolls, thus creating a risk area for the environment. Given the state of the communicationsection, the communicationstatus (route II. Class), and in particular the position of the Transport Corridor (Žitný ostrov), we propose a complete ban on entry of trucks carrying hazardous materials vehicles and vehicles, whose gross weight exceeds 7.5 t. Proposed a narrowly defined transport route, suitable for the transport ADR see Fig. 5, passings Dunajská Streda - Kútniky – Dolny Stal – Veľký Meder with a total length of 20.4 km. The proposed alternative will contribute to the security environment since the routes leading first-class roads. We further propose the given road to equip with sedimentation tanks, which will minimize the percentual risk of pollution in case of leakage of hazardous substances.

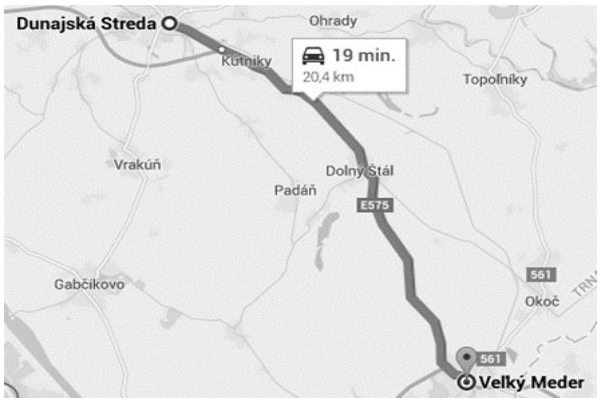

Fig. 5 Dunajská Streda – Veľký Meder

In the next section we paid attention especially to passages through a river flows, specifically analyzing the crossing of the river Hron. The road is excessively overloaded and inadequate. Carriers use the given communicationmainly to circumvent the toll section along expressway R1. We propose a prohibition for trucks to enter this road, whose gross weight exceeds 7.5t and completely divert transport of dangerous goods on the expressway. Consequently, we propose an overall reconstruction of the bridge. An important factor is a detailed analysis of individual road sections circumventing due to chargingand thus generate hazard areas from the perspective of a possible dangerous situation. In the last section, we used as an example a solution to transport hub of the town Piešťany, which by their scope may serve as a model for various spa towns in different countries. Based on the current development of the carriage of dangerous substances it can be assumed, that the amount of dangerous substances will continue to rise and risks for the environment by dangerous substances in the transport of ADR will grow.

CONCLUSIONS

In the present paper, we analyzed the three problem areas in terms of transport of dangerous goods and provided alternative solutions to ensure ADR transport. In the first part of the scientific article, we drewattention to the problematic area of Žitný ostrov, where is increased attention to the transport of dangerous goods, especially in the use of groundwater. For these reasons, a detailed analysis of transport corridors is necessary, Long-term monitoring of trucks carrying dangerous materials and the consequent drawchanges in traffic, leading to an increase in environmental safety. Next, we analyzed transport corridor, which creates a bottleneck across the river Hron, where we designed the reconstruction and individual no entry. In the last part of the paper, we paid attention to the spa town Piešťany, from the view of and divertion of traffic, because of significant sources of healing springs in this area. A solution of individual analyzes serves as a model for a similar bottlenecks.

Development of transport in the monitored area must comply with safety and environmental protection. The transport sector makes economic growth, contributes significantly to the functioning of the Slovak economy, the various regions, thus creating conditions for optimal economic potential (*Hujo et al., 2014;Majdan et al., 2014*).

ACKNOWLEDGMENT
The contribution was made under the grant project of the Ministry of Education of the Slovak Republic VEGA1/0464/17 „Research aimed at influence of agricultural, forest and transport machinery on environment and its elimination on the basis of ecological measures application“.

REFERENCES

1. Hegedüš, T., Janoško, I., et al. (2012).Assessment ofthe monitoring systemDynafleet.. In *XIV*. International ScientificConference of Young2012*:* 1. edition. 1 CD-ROM (263 s.). ISBN 978-80-228-2342-5. International ScientificConference of Young. Zvolen :Technical University in Zvolen, 2012, p. 93-98.
2. Hujo, Ľ. (2014). ADR transport on proposed lines of selected area in Slovak Republic et al.. -- ilustr.In: Naučnitrudove. -- ISSN 1311-3321. -- Tom. 53, seria 1.1 (2014), pp. 142-144.
3. Hujo, Ľ., Jablonický, J., et al. (2014).EkonomicIdiocators Evaluation of Transport Company in Terms of Individully Composite Indexes. In. Agricultural, Forest and Technologies (ISSN: 2367 – 5888) Volume I – Issue 1, 2014
4. Jagelčák, J., (2009).Solution of driving bansin relation to thetransport of dangerous goodsaccording toADR [online] available on: http://www.chemlog.info/ [2014-17-02]
5. Law no. 56/2012 abaut road transport (2017).Dangerous things, [online] available on: www.adr.sk [2017-17-02]
6. Majdan, R., Szabó, M., et al. (2014).Impact ofhuman factorsonfueltrucks [electronic resource] = The influence of human factor on the fuel consumption of lorries, - ISSN 978-80-248-3499-9 International Conferencedepartmentsof transport, handling, construction and agricultural machinery. -- Ostrava : Technical university of Ostrava, 2014. 10 s.
7. Polonec, T., Janoško, I., et al. (2015). The design of equipment for testig and optimization of parameters of cumbustion engines, XL. VI. International scientific conference of the Czech and Slovak universities and institutions dealing with research of internal combustion engines. ISBN: 978-80-227-4425-6
8. Statistical Office Slovak Republic, (2016).available [online]: http://slovak.statistics.sk
9. Statistics oftransporting dangerous goods available (2009) [online]: http://www.europarl.europa.eu/meetdocs/2004_2009/documents/com/com_com%282006%290852_/com_com%282006%290852_sk.pdf
10. Žitňák, M., & Korenko, M. (2011). Technical-economical indicators in the sugar beet transportation management / Miroslav Žitňák, Maroš Korenko. -- obr.,tab.In: Research in agricultural engineering. -- Vol 57, no. 2 (2011), s. S63-S71. -- ISSN 1212-9151.

Corresponding author:
Ing. Marek Halenár, Department of Transport and Handling, Faculty of Engineering, Slovak University of Agriculture in Nitra, Tr. A. Hlinku 2, 949 76 Nitra, Slovak Republic, phone: +421376414616, email: xhalenarm@is.uniag.sk

UTILIZATION OF THE SHAPE GENERATOR IN THE DESIGN OF THE STRUCTURAL PARTS

Michaela HNILICOVÁ[1], Jaroslav MATEJ[2], Richard HNILICA[3]

[1]*Department of Forest Harvesting, Logistics and Ameliorations, Faculty of Forestry, Technical University in Zvolen, Slovak Republic*
[2]*Department of Mechanics, Mechanical Engineering and Design, Faculty of Environmental and Manufacturing Technology, Slovak Republic*
[3]*Department of Manufacturing Technology and Quality Management, Faculty of Environmental and Manufacturing Technology, Slovak Republic*

Abstract
This post represents the new Autodesk Inventor model package, namely the shape generator. It evolves and imitates the evolutionary approach of nature in the form of generative design. The use of the shape generator package is presented in the design of carry frame a fire body on a forest wheeled skidder.

Key words: *shape generator; design; software; construction.*

INTRODUCTION

The Shape Generator, introduced in Autodesk Inventor R2 2016, is technology in some features similar to topological optimization. It uses the principles of generative design, in which it is necessary to define a set of parameters, respectively rules, while the internal Shape Generator algorithm in the cycle generates the component design itself unless an optimal solution is found. Topology optimization is a tool based on the finite element method and defined criteria to optimize the initial solution in order to achieve the goal. However, the result may be expensive or unmanageable by common production techniques, although with the continued development of technology, the manufacturing criteria can also be applied. At present, the solution is an additive manufacturing technology, 3D printing. (*Thomas, 2015*)

Generative design simulates the natural evolutionary approach. Designers or engineers inserted aims to software for generative design, along with parameters such as materials, production methods and cost requirements. Then, using cloud computing, the software examines all possible permutations of the solution and generates design alternatives. It tests and learns from every iteration what works and what does not. Using a generic design does not result in one solution but a potentially large number. (*Autodesk, 2017*)

Generic design covers these optimization methods (*Autodesk, 2017*):

- Form synthesis - With this approach, designers or engineers input their goals and constraints, and the software runs artificial intelligence-based algorithms to produce a wide range of design alternatives.
- Lattice and surface optimization - This method applies internal lattices and optimized surface structures to an existing component to make it lighter and stronger.
- Topology optimization - This approach reduces the weight of an existing component by running analysis to remove unnecessary material, while meeting or exceeding performance criteria.
- Trabecular structures - This method precisely scales and distributes tiny pores through solid materials, and creates surface roughness to mimic bone in medical implants to help patients heal.

For more information on this topic can be found in the project Dreamcatcher (Autodesk Research, 2017).

MATERIALS AND METHODS

By solving the submitted paper, we mainly tried to present a new approach to the design of light-weight, structurally efficient parts. The Shape Generator provides an intelligent strategy to maximize the stiffness of the parts based on the specified limitations.
Work methodology consisted of the following partial plan:

- defining the model envelope (volume),
- carry out a geometry is optimized based on user input, such as loading condition, anticipated pressure, and targeted weight reduction threshold,
- detailed construction design.

RESULTS AND DISCUSSION

Scheme frame holder tanks were processed in Autodesk Inventor using the Shape Generator. This tool works quite differently from conventional optimization tools, so in short lists and its use. A common optimization task optimizes the parameters of the finished model. It can be of dimensions such as length, cross-section, type cross-section, material, etc. However, the basic structure of the model must already be known and the optimization only improves it. The result is good but only if the quality and original design. Shape Generator uses a different approach based on locally adding material only where it is needed. It requires the definition of boundary conditions, ergo places where the model will be mounted where they work force and their size. Next, it is necessary to define the maximum possible envelope of the model, i.e. volume model that can take in all directions. As a result, we have obtained an amorphous volume, in the form of a finite element network, which we have used as a guide for the frame holder construction of a standard material (Fig. 1 to Fig. 4).

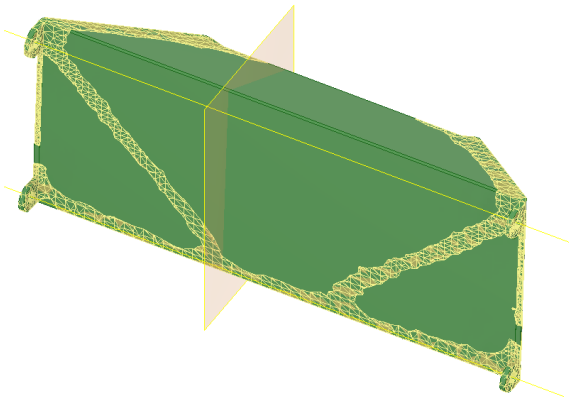

Fig.1 The front view of the defined envelope of the model and the resulting network created by the Shape Generator.

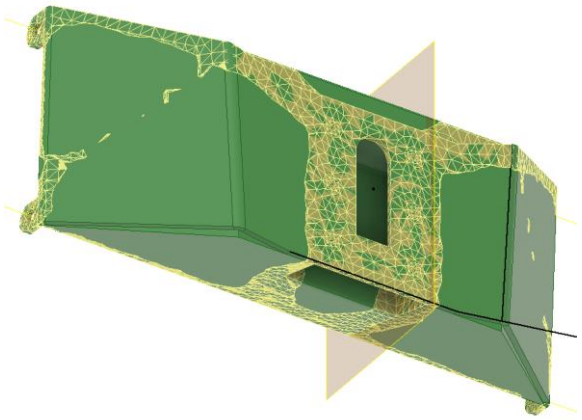

Fig. 2 Rear view of the defined envelope of the model and the resulting network created by Shape Generator.

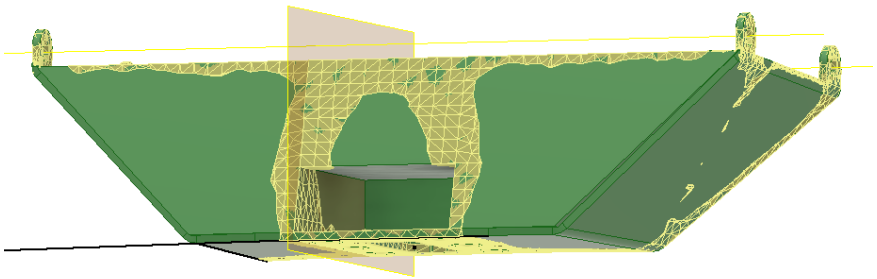

Fig. 3 The bottom view of the defined envelope of the model and the resulting network created by the Shape Generator.

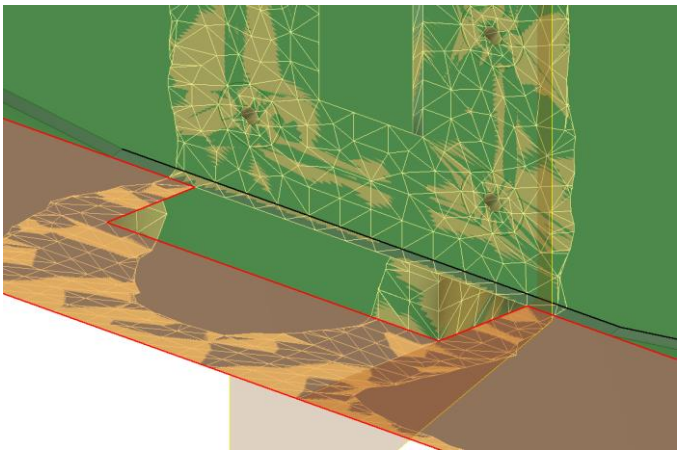

Fig. 4 A detailed view of the defined envelope of the model and the resulting network created by the Shape Generator.

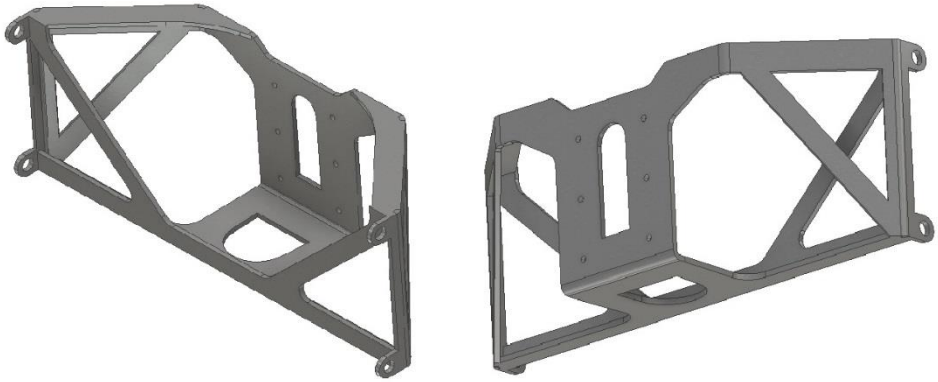

Fig. 5 Design of the frame for the fire-fighting adapter.

CONCLUSIONS

Based on the procedures and results presented in this post, we can conclude that the presented software package is an excellent tool for designing and creating structural parts of different constructions. The basics of designing now consist in creating the structure of the model and its subsequent optimization. By using the shape generator, it is enough to define its maximum volume bounded by boundary conditions. Output is then an indication of the structure of the model that can be take form in all directions. We have verified this fact on the part proposed by us, and we will address this solution also in the future. After determining the boundary conditions Shape Generator own algorithms determine where you need to add mass and where it is unnecessary.

ACKNOWLEDGMENT
This work was supported by the Slovak Research and Development Agency under the contract No. APVV-14-0468 „Development of an auxiliary device and its technological employment to increase the efficiency of extinguishing forest fires“.

REFERENCES

1. Autodesk: Generatívny dizajn. [cit. 3.7.2017] Dostupné online: https://www.autodesk.com/solutions/generative-design
2. Autodesk Research: Project Dreamcatcher. [cit. 3.7.2017] Dostupné online: https://autodeskresearch.com/projects/dreamcatcher
3. Michael Thomas: The More Things Change - Generative Design. [cit. 3.7.2017] Dostupné online: https://designandmotion.net/autodesk/the-more-things-change-generative-design/

Corresponding author:
Ing. Michaela Hnilicová, PhD., Department of Forest Harvesting, Logistics and Ameliorations, Faculty of Forestry, Technical University in Zvolen, T. G. Masaryka 24, 960 53 Zvolen, Slovak Republic, phone: +421456206289, e-mail: michaela.hnilicova@gmail.com

SOIL ELECTRICAL CONDUCTIVITY DATA ACQUISITION BY UAV

Jaroslav HOLUB, Milan KROULÍK

Department of Agricultural Machines, Faculty of Engineering, Czech University of Life Sciences

Abstract
One of the main obstacles of precision farming is high requirement on information about the field itself. Gathering all of the information is time consuming and demands specialized one-purpose equipment. Soil apparent electrical conductivity presents viable multipurpose parameter as it can be used not only for description of the field, but for optimization of sampling grid. Remote sensing presents a way of acquiring large amount of spatial data in short window of time. Therefore, we tried to utilize remote sensing for assessing soil apparent electrical conductivity. RGB images of research field were taken by a drone mounted with a camera and electrical conductivity was measured by conductivity probe. Results were statistically analyzed and a correlation has been found.

Key words: *remote sensing, electrical conductivity, soil, UAV, digital mapping.*

INTRODUCTION

Soil is one of the fundamental resources for plant production and as such it must be protected and used reasonably, responsibly and most importantly sustainably. Precision agriculture technologies have been introduced several years ago. Despite all the potential of these technologies, there are still many problems that impede their higher usage and adoption. Implementation of precision agriculture implies relatively high level of expertise and technical skills required by the users (*Dobos et al., 2010*). Most farmers see this approach as too complicated. As also shown in studies from the Denmark, Germany, Great Britain and USA, and it is one of the reasons for the low rate of spreading of technologies of precision agriculture compared to the assumptions (*Reichardt et al., 2009*). The same was concluded in 2005 by *McBratneyet al.,* who states that precision farming is developing, but not as fast as expected 5 years prior. The development of appropriate decision support systems and systems for performing accurate decisions remain a major obstacle to the adoption of these technologies. The key idea of precision agriculture is based on the premise that the variability of conditions for plant growth is one of the main reasons to the differences in yields and therefore also different inputs under different soil conditions could present viable means to approach the situation. Number of growers already has, for example, yield data from several seasons. However, the effectiveness of the decision–making process can be guaranteed only when we operate with high quality information on the spatial variability of soil, which on the other hand limits yield in certain parts of the field. Lack of knowledge about which information is significant and economically acceptable is the most limiting factor(*Adamchuk and Rossel, 2010*). That is where apparent soil electrical conductivity comes into play as it is among the easiest properties to measure (*Fortes et al., 2015*) and farmers can devise a lot of information about the field just from this one parameter. Electromagnetic induction (EMI) is common way of measuring apparent electrical conductivity nowadays, but this method requires specialized one-purpose equipment and a lot of field time to acquire the information.

EMI is widely used for proximal soil electrical conductivity determination based on the radiation of a very low frequency electromagnetic wave into the soil. Depending on soil electrical conductivity, eddy currents are generated and it produces a secondary EM field which is recorded by the EMI system, specifically by receiver coil. This method works at frequencies ranging from 1–100 kHz. EMI applications are very diversified, it is used for salinity mapping and monitoring in agricultural fields (*Amezketa, 2006; Cameron et al., 1981; Hendrickx et al., 1990; Leschet al., 1998*). The conductivity measurement of soil becomes one of the most widely used techniques for field variability mapping for the needs of precision agriculture technologies *(Corwin & Lesch, 2003; Terrón et al., 2011*) and farmers can use the measurement for fast and accurate characterization of soil environment (*Doerge, 2001*). Among other applications of electrical conductivity measurements is soil water content estimation (*Kachanoski et al., 1988; Reedy & Scanlon, 2003*), soil texture mapping (*Hedley et al., 2004; Triantafilis & Lesch, 2005*), soil acidity assessment *(Dunn & Beecher, 2007*), detection of buried metallic

bodies like unexploded ordnance (UXO) *(Pasion et al., 2007*), detection of contaminants in soils and shallow aquifers (*Hoekstra et al., 1992; Ladwig, 1983*), clay content estimation (*McBratney et al., 2005; Triantafilis & Lesch, 2005)* and characterization of the vadose zone (*Everett et al., 2006*). Measurement of the electrical conductivity of the soil is also suitable for detection of many soil parameters and variables description (*Fortes et al., 2015*) or yields potential prediction (*Johnson et al., 2003*).
The high price of the sampling and laboratory analysis supports the deployment of sensors which will evaluate required soil properties; such as during towing of sensors over plot (*Adamchuk et al., 2004; Viscarra Rossel et al., 2011*) or remote sensing (*Dobos et al., 2010*). Variable sampling applications require significant number of samples, but where there is a possibility the hand sampling should be replaced by an autonomous or semi–autonomous data collection. Indirect measurement of soil properties has many promising applications, which should be further developed and improved.
Remote sensing applications in agriculture are based on the interaction of electromagnetic radiation with soil or plant material. Typically, remote sensing involves the measuring reflected radiation, rather than absorbed or transmitted radiation. The platforms for making these measurements include tractors, satellites, aircrafts and hand-held sensors. In addition to reflectance, transmittance and absorption, plant leaves can emit energy by fluorescence (*Apostol et al., 2003*) or thermal emission (*Cohen et al., 2005*). The constraints of traditional aerial imagery platforms can be addressed by low altitude remote sensing (LARS) using UAVs. Two popular UAV platforms for LARS are the quadcopter and the fixed wing UAV. Unlike traditional remote sensing systems, UAVs have high spatial and temporal resolutions and can operate below clouds. At high spatial resolution, the area of the smallest pixel decreases, thus the homogeneity of the crop or soil within the pixel increases (*Mulla, 2013*).
The purpose of the measurements was to determine whether it is possible to use remote sensing to assess levels of soil apparent electrical conductivity on the field, thus speeding up the process of collecting the data significantly and lowering the procurement cost of the data.

MATERIALS AND METHODS

The measurement and verification of the measurement electronics was done on the field, which manages agriculture company ZD Dolany (geographical coordinates: 50°22'48"N, 15°57'40"E). Field experiments were carried out during seeding of spring wheat. The soil is Haplic Luvisol(Anon n.d.). The highest part of the field is at the northern part an altitude of 325 m a.s.l. and further field is sloped to the lowest altitude 29 m a.s.l. Field acreage was 14.25 ha (see Fig. 1).

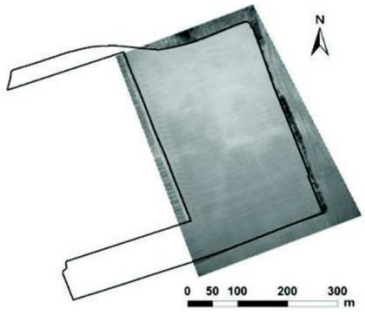

Fig. 1 Aerial picture of the experimental plot, which was taken after sowing by UAV

The most commonly used electrical and electromagnetic sensors for field–scale on– the–go measurements are electrical resistivity (ER) and electromagnetic induction (EMI) *(Corwin and Lesch, 2003*). ER and EMI measure the electrical conductivity of the bulk soil, which is referred to as the apparent soil electrical conductivity (ECa).
The eight-propeller unmanned aerial vehicle of the Department of Agricultural Machinery at the Faculty of Engineering of the Czech University of Life Sciences in Prague was used to scan the land. This is the Asctec Falcon 8 model with camera attachment and control equipment. The airplane can be fitted either with a classical RGB still camera or a multispectral camera, which is able to capture images in the near infrared spectrum.

To obtain a validation set of measurements of electrical conductivity from platform which was installed on seeder, the measurement using reference probe EM38 MK2 (Geonics Limited, Ontario, Canada) on the same date was carried out as well. Probe EM38 MK2 is a commercially sold product utilizing non-contact electromagnetic induction measurements. The validation data were measured in vertical mode of the probe in spacing of 12 m between parallels. Data were acquired and stored together with GPS position with storage interval of 1 sec. Scheme of moving trajectories and sampling patterns is illustrated in Fig. 2.

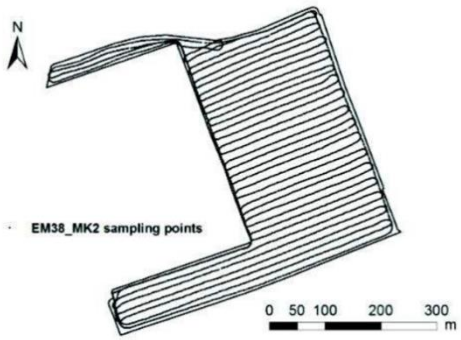

Fig. 2 Sampling patterns and moving trajectories of EM38 MK2 device

Software Statistica 12 (StatSoft, Inc., Tulsa, OK, USA), ENVI (Exelis VIS, McLean, VA, USA), ArcGIS 10.2 (ESRI, Red lands, USA) and Microsoft office (Microsoft Corporation, Redmond, USA) were used.

RESULTS AND DISCUSSION

Values larger or less than three times the standard deviation from the mean value were also excluded from the initial data set of validation data. The ECa data series was smoothened during the subsequent modification. A simple running average method was applied to smooth the ECa data series of all measurements. Aerial image of the research field was adjusted by the method of unsupervised image classification. Colors were assigned to six different levels (1-6), while the darker the color, the lower the number (1=darkest, 6=lightest).

Ordinary Kriging interpolation method was used for spatial interpolation of measured values. On the basis of regression and correlation analysis, the significance of variogram modelling for the subsequent interpolation was proved. For the purpose of data set comparison, if the points do not have identical coordinates, both maps were resampled to the grid of 5 x 5 meters and data from both sets were paired. That enabled comparison and assessment of values recorded. Resampled maps are presented in Fig. 3.

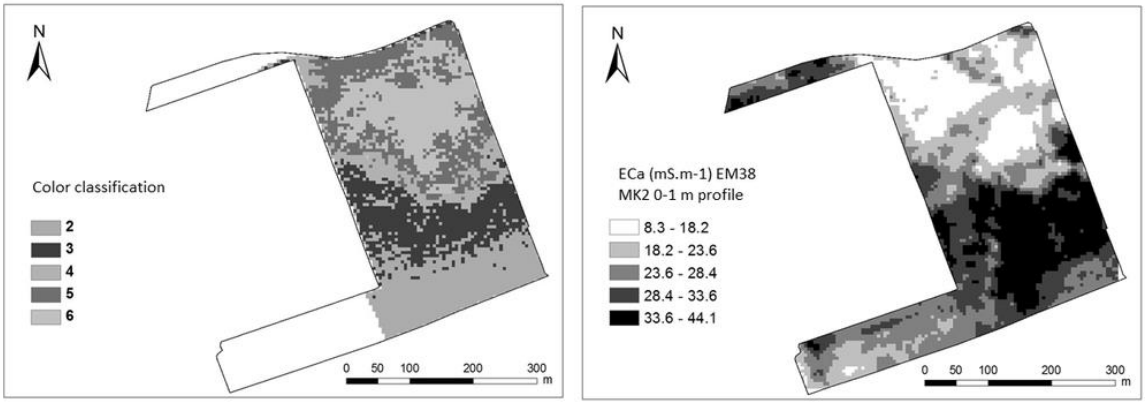

Fig. 3 Resampled maps, color classification of aerial image (left), ECa measurements by EM38 MK2 (right)

Presented resampling of data sets allowed a mutual comparison. The comparison and evaluation of these two data sets were carried out by means of regression and correlation analysis. Fig. 4 shows the results of this analysis. In the legend of the chart, it is also possible to read determination and correlation coefficient values (R2 = 0.54 and R = -0.74 respectively), including significance test ($p < 0.05$).

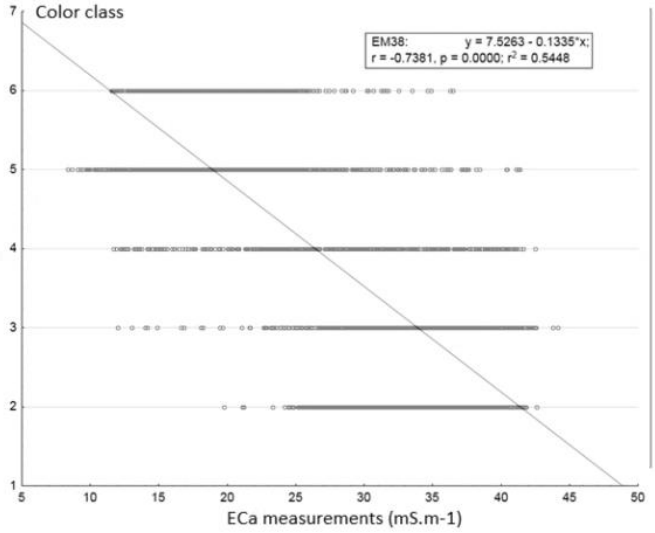

Fig. 4 Relationship between color classified data from UAV and outputs from EM38 MK2

The results can be used to partially overcome temporal and financial requirements of precision agriculture as specified by McBratney et al., in 2005. This form of ECa map can be used as a basis for optimization of sampling grid and following measurements (*Dunn & Beecher, 2007*). Even though small scale aerial imaging is considered most useful for grid size around 250 m (*Dobos et al., 2010*) and authors prefer different measurements methods for finer spatial resolution maps, but they highlight other benefits of aerial imaging, as speed and price, as well.

CONCLUSIONS

The rapid development of sensor technology and data processing, which frequently contribute to the efficient and sustainable agricultural production, along with the development of the internet and telecommunications are nowadays the key innovative processes. Currently, the data collection is associated mainly with individual and independent activity, that requires additional entrance on the field, acquisition costs of the measuring device and time for data collection. Outputs from measuring platform and aerial images acquired by UAV Asctec Falcon 8 showed a significant correlation with the data from sensor EM 38. As such, it has been proven, that aerial imaging is viable supplement technology for gathering information about spatial variability of ECa on the field in fraction of time required in comparison to traditional measurement method.

ACKNOWLEDGMENT

This study was supported by the Grant Agency of the Czech University of Life Sciences Prague (CIGA No. 20163005).

REFERENCES

1. Adamchuk, V. I., J. W. Hummel, M. T. Morgan, and S. K. Upadhyaya. (2004). "On-the-Go Soil Sensors for Precision Agriculture." *Computers and Electronics in Agriculture* 44(1):71–91.
2. Adamchuk, V. I. & Viscarra Rossel, R. A.. (2010). *Development of On-the-Go Proximal Soil Sensor Systems*. edited by R. A. Viscarra Rossel, A. B. McBratney, and B. Minasny. Dordrecht: Springer Netherlands.
3. Amezketa, E. (2006). "An Integrated Methodology for Assessing Soil Salinization, a Pre-Condition for Land Desertification." *Journal of Arid Environments* 67(4):594–606.
4. Anon. n.d. "World Reference Base for Soil

Resources (2014) International Soil Classification System for Naming Soils and Creating Legends for Soil Maps."
5. Apostol, S., Viau, A.A., Tremblay, N., Briantais, J.M., Prasher, S., Parent, L.E., Moya, I. (2003). "Laser-Induced Fluorescence Signatures as a Tool for Remote Monitoring of Water and Nitrogen Stresses in Plants." Pp. 57–65 in *Canadian Journal of Remote Sensing*, vol. 29. Taylor & Francis.
6. Cameron, D. R., D. W. L. Read, E. DE Jong, and M. Oosterveld. (1981). "Mapping Salinity Using Resistivity and Electromagnetic Inductive Techniques." *Canadian Journal of Soil Science* 61(1):67–78.
7. Cohen, Y., V. Alchanatis, M. Meron, Y. Saranga, and J. Tsipris. (2005). "Estimation of Leaf Water Potential by Thermal Imagery and Spatial Analysis." *Journal of Experimental Botany* 56(417):1843–52.
8. Corwin, D. L. & S. M. Lesch. (2003). "Application of Soil Electrical Conductivity to Precision Agriculture." *Agronomy Journal* 95(3):455.
9. Dobos, E., T. Hengl, & Hi Reuter. (2010). "Digital Soil Mapping." *Office for Official Publications of the European Communities* 68.
10. Doerge, T. (2001). "Fitting Soil Electrical Conductivity Measurements Into the Precision Farming Toolbox." *Wisconsin Fertilizer, Aglime and Pest Management Conference.* 1–7.
11. Dunn, B. W. & H. G. Beecher. (2007). "Using Electro-Magnetic Induction Technology to Identify Sampling Sites for Soil Acidity Assessment and to Determine Spatial Variability of Soil Acidity in Rice Fields." *Australian Journal of Experimental Agriculture* 47(2):208–14. Retrieved July 5, 2017
12. Fortes, R., S. Millan, M. H. Prieto, & C. Campillo. (2015). "A Methodology Based on Apparent Electrical Conductivity and Guided Soil Samples to Improve Irrigation Zoning." *Precision Agriculture* 16(4):441–54.
13. Hedley, C. B., I. J. Yule, C. R. Eastwood, T. G. Shepherd, & G. Arnold. (2004). "Rapid Identification of Soil Textural and Management Zones Using Electromagnetic Induction Sensing of Soils." *Australian Journal of Soil Research* 42(4):389–400.
14. Hendrickx, J. M. H., B. Baerends, Z. I. Raza, M. Sadig, & M. Akram Chaudhry. (1990). "Soil Salinity Assessment by Electromagnetic Induction of Irrigated Land." *Soil Science Society of America Journal* 56(6):1933–41.
15. Hoekstra, Pieter, Raye Lahti, Jim Hild, C.Richard Bates, & David Phillips. (1992). "Case Histories of Shallow Time Domain Electromagnetics in Environmental Site Assessment." *Groundwater Monitoring & Remediation* 12(4):110–17.
16. Johnson, Cinthia K., David a Mortensen, Brian J. Wienhold, & John Doran. (2003). "Site-Specific Management Zones Based on Soil Electrical Conductivity in a Semiarid Cropping System Site-Specific Management Zones Based on Soil Electrical Conductivity in a Semiarid." *Agronomy journal* 95(2):303–15.
17. Kachanoski, RG, E. G. Gregorich, & I. J. Van Wesenbeeck. (1988). "Estimating Spatial Variations of Soil Water Content Using Noncontacting Electromagnetic Inductive Methods." *Canadian Journal of Soil Science* 68(4):715–22.
18. Ladwig, Kenneth J. (1983). "Electromagnetic Induction Methods for Monitoring Acid Mine Drainage." *Ground Water Monitoring & Remediation* 3(1):46–51.
19. Lesch, S. M., J. Herrero, & J. D. Rhoades. (1998). "Monitoring for Temporal Changes in Soil Salinity Using Electromagnetic Induction Techniques." *Soil Science Society of America Journal* 62(February):232–42.
20. McBratney, A., B. Whelan, T. Ancev, & J. Bouma. (2005). "Future Directions of Precision Agriculture." *Precision Agriculture* 6(July 2004):7–23. Retrieved July 5, 2017
21. Mulla, David J. (2013). "Twenty Five Years of Remote Sensing in Precision Agriculture: Key Advances and Remaining Knowledge Gaps." *Biosystems Engineering* 114(4):358–71.
22. Pasion, Leonard R., Stephen D. Billings, Douglas W. Oldenburg, &Sean E. Walker. (2007). "Application of a Library Based Method to Time Domain Electromagnetic Data for the Identification of Unexploded Ordnance." *Journal of Applied Geophysics* 61(3–4):279–91.
23. Reedy, Robert C. & Bridget R. Scanlon. (2003). "Soil Water Content Monitoring Using Electromagnetic Induction." *Journal*

of Geotechnical and Geoenvironmental Engineering 129(11):1028–39.
24. Reichardt, M., Jürgens, C., Klöble, U., Hüter, J., & Moser., K. (2009). "Dissemination of Precision Farming in Germany: Acceptance, Adoption, Obstacles, Knowledge Transfer and Training Activities." *Precision Agriculture* 10(6), pp. 525–45.
25. Terrón, J. M., Marques da Silva, J. R, Moral, F. J., & García-Ferrer., A. (2011). "Soil Apparent Electrical Conductivity and Geographically Weighted Regression for Mapping Soil." *Precision Agriculture* 12(5):750–61.
26. Triantafilis, J. & Lesch., S. M. (2005). "Mapping Clay Content Variation Using Electromagnetic Induction Techniques." *Computers and Electronics in Agriculture* 46(1–3 SPEC. ISS.):203–37.
27. Viscarra Rossel, R. A., A. Chappell, P. De Caritat, & Mckenzie., N. J. (2011). "On the Soil Information Content of Visible-near Infrared Reflectance Spectra." *European Journal of Soil Science* 62(3):442–53.

Corresponding author:
Ing. Jaroslav Holub, Department of Agricultural Machines, Faculty of Engineering, Czech University of Life Sciences Prague, Kamýcká 129, Praha 6, Prague, 16521, Czech Republic, phone: +420608242883, e-mail: holubjaroslav@tf.czu.cz

,

THE COMPARATIVE ANALYSIS OF THE ORGANIZATION OF WORK ZONES ON MOTORWAYS - TRAFFIC SIGNS IN THE WORK ZONE

Lukáš Jan HRABÁNEK

Department of vehicles and ground transport, Faculty of Engineering, Czech university of Life Sciences Prague

Abstract
The main aim of paper is to describe the occurrence of motorway's optimal work zone safety and its appearance during different times of the day. It depends on the particular maintenance or the safety of an extraordinary event. The further aim is to pay an attention to newly implemented safety elements and recommendations. These ones include, in particular, alert thresholds, illuminating arrows or safety lateral distances. Next and more progressive implementation is the automatic setting up of a work zone and traffic signs.

Key words**:** *work zone, safety, maintenance, traffic signs, retroreflection.*

INTRODUCTION

The high density of traffic, the climatic factors, material aging, freight vehicles overloading and sometimes poor quality of motorways design and the removal of consequences of traffic accidents implies the need to a greater or lesser extent, regular servicing, carry on their maintenance, inspections and measurement of these roads. That always requires a greater or lesser interference with the traffic and road safety. Dual carriageway are very dangerous due to above mentioned for this activities, because traffic disposition and organization affirms drivers, that it is a road without pedestrians and slow moving vehicles. Traffic signs must be clear, comprehensible and visible so that they can be timely and responsive to the driver. This is particularly important in the work zone where the traffic is often changed.

Work on the motorway is always dangerous *(Urwyler et al., 2015; Young et al., 2009)* and there is a significant risk of traffic accidents and threats to road workers, as evidenced by many studies *(Domenichini et al., 2017).* Very risky appears to be the implementation of work zone, which is evidenced by research conducted in Italy, in which it was found, that during the time the work zone is implemented, the increases of about 33 % for FI crashes and 66 % for PDO crashes as compared to the crash frequency in the "before" period *(La Torre et al., 2017).*

Another factor that may increase the risk of traffic accidents in the work zone is a temporary adjustment of the width of traffic lanes. It was found that the tested provisional geometric characteristics of traffic lanes width of 2, 50 m, 2, 75 m a 3,0 m did not influence the behavior of drivers when overtaking other vehicle in the working zone *(Petzoldt et al., 2016)*, but the width of the traffic lanes, that are less than 3, 0 m already results in a relatively effective speed reduction in the working zone *(La Torre et al., 2017).*

The work on the motorway during low volume of traffic doesn´t automatically mean less danger to road workers and road users *(De Waard et al., 2009; De Waard et al., 2008)*. In poor visibility in different age groups varies (getting worse) the evaluation of speed and distance, the road workers become less visible and they can be blinded by the headlights of vehicles *(Zhou et al., 2009)*. Nighttime motorway construction is according to research conducted Arditi about five times more dangerous than daytime construction *(Arditi et al., 2007).*

It was found *(Arditi et al., 2005)*, the two most important factors influencing the risk of traffic accidents at night are the state of the vehicle driver and good lighting conditions *(Dukic et al., 2013; Åkerstedt et al., 2013)*. However, both of these factors are very closely related to visibility. Arditi in this context assessed eg *(Arditi et al., 2004)*.

A study from 2001 states, that motorway lighting *(Hyari et al., 2016)* reduces traffic accidents about 49 % compared to dark motorway *(Bruneau et al., 2001)* to the same conclusion came also *(Wanvik Po, 2009)*, but the percentage decrease in the number of traffic accidents is different in countries like UK, Sweden and Netherlands *(Debnath et al., 2015).* And so it is necessary to consistently ensure that such work zones are well secured, sufficiently and properly lighted and the work is carried out by appropriately qualified personnel and resed road workers.
Traffic signs are designed to be reflective during the nighttime under the illumination of vehicles' headlights so that drivers can read vital roadway information without other external lighting. Special sheeting materials with retro-reflective features are used for traffic signs so that light can be reflected back to its original source and perceived effectively by drivers. The objective of traffic sign retroreflectivity condition assessment is to evaluate the retro-reflective capability of traffic signs in support of traffic sign replacement or maintenance *(Tsai et al., 2016; Balali et al., 2015; Hummer et al., 2013; Khalilikhah et al., 2016; Obeidat et al., 2016).*

MATERIALS AND METHODS

For partial samples measuring 0.1 m × 0.1 m, the retroreflection values of the Zenther 6060 or Delta will be always measured at three points (CIE). A single sample of 0.1 m × 0.1 m will always be unobstructed and will not be covered in any way. Once the values are entered in the pre-prepared form, the surfaces of the remaining five areas will be covered with an orange-black scraping band of 50 mm, in other cases the samples will be covered with magnetic tape or sheet metal construction.
During the observed period of 1, 4, 10, 18, 24 weeks will these tades be peeled off, cleaned with a damp cotton cloth and appropriate retroreflection values will be measured. In the final stage all the values will be measured including previous sub samples and also the uncovered sample.

RESULTS AND DISCUSSION

The retroreflection sheeting measurement will begin at the end of July 2017 to determine whether the use of orange - black stripping tapes or magnetic tapes in the traffic closures has a negative effect on the retroreflection of traffic signs and on the functional life of traffic signs.

CONCLUSIONS

Orange – black stripping tapes in the traffic closures has a negative effect on the retroreflection of traffic signs and on the functional life of traffic signs.

ACKNOWLEDGMENT

This paper was supported by CULS Prague, faculty engineering project IGA 2017:31150/1312/3120.

REFERENCES

1. Åkerstedt, TorbjÖrn et. al. (2013). Having to stop driving at night because of dangerous sleepiness - awareness, physiology and behaviour. *Journal of Sleep Research* (online). 8., vol. 22, no. 4, s. 380–388 (vid. 2016 11 19). ISSN 09621105. Available from: doi:10.1111/jsr.12042
2. Arditi, David, Mehmet A. Ayrancioglu a Jonathan SHI (2004). Effectiveness of Safety Vests in Nighttime Highway Construction. *Journal of Transportation Engineering* (online). 11., vol. 130, no. 6, s. 725 732 (vid. 2016 11 13). ISSN 0733 947 X. Available from: doi:10.1061/(ASCE)0733 947X(2004)130:6(725)
3. Arditi, David, Mehmet A. Ayrancioglu a Jonathan Jingsheng SHI (2005). Worker safety issues in night-time highway construction. *Engineering, Construction and Architectural Management* (online). B.m.: Emerald Group Publishing Limited, 11. 10., vol. 12, no. 5, s. 487–501 (vid. 2016-11-13). ISSN 0969-
9988. Availablefrom: doi:10.1108/09699980 510627171
4. Arditi, David, Dong-Eun Lee a Gul Polat (2007). Fatal accidents in nighttime vs. daytime highway construction work zones. *Journal of Safety Research* (online). vol. 38, no. 4, p. 399 405. ISSN 00224375.A vailablefrom: doi:10.1016/j.jsr.2007.04.001

5. Bergel-Hayat, Ruth, Mohammed Debbarh, Constantinos Antoniou a George Yannis (2013). Explaining the road accident risk: weather effects. *Accident; analysis and prevention* (online). 11., vol. 60, p. 456–65 (vid. 2016-11-13). ISSN 1879-2057. Available from: doi:10.1016/j.aap.2013.03.006
6. Bruneau, J. F., Denis Morin a Marcel Pouliot (2001). Safety of motorway lighting. *Journal of the Transportation Research Board* (online). vol. 1758, no. 1758, p. 1–5. ISSN 0361-1981. Available from: doi:DOI: 10.3141/1758-01
7. De Waard, Dick, Chris Dijksterhuis a Karel A. Brookhuis (2009). Merging into heavy motorway traffic by young and elderly drivers. *Accident Analysis & Prevention* (online). vol. 41, no. 3, p. 588–597. ISSN 00014575. Available from: doi:10.1016/j.aap.2009.02.011
8. De Waard, Dick, Anje Kruizinga a Karel A. Brookhuis (2008). The consequences of an increase in heavy goods vehicles for passenger car drivers' mental workload and behaviour: A simulator study. *Accident Analysis & Prevention* (online). vol. 40, no. 2, p. 818 828. ISSN 00014575. Available from: doi:10.1016/j.aap.2007.09.029
9. Debnath, Ashim Kumar, Ross Blackman a Narelle Haworth (2015). Common hazards and their mitigating measures in work zones: A qualitative study of worker perceptions. *Safety Science* (online). vol. 72, p. 293 301. ISSN 09257535. Available from: doi:10.1016/j.ssci.2014.09.022
10. Domenichini, Lorenzo, Francesca Latorre, Valentina Branzi a Alessandro Nocentini (2017). Speed behaviour in work zone crossovers. A driving simulator study. *Accident Analysis and Prevention* (online). vol. 98, p. 10–24. ISSN 00014575. Available from: doi:10.1016/j.aap.2016.09.018
11. Dukic, Tania, Christer Ahlstrom, Christopher Patten, Carmen Kettwich a Katja Kircher (2013). Effects of Electronic Billboards on Driver Distraction (online). 7., vol. 14, no. 5, p. 469–476. ISSN 15389588. Available from: doi:10.1080/15389588.2012.731546
12. Godley, Stuart T, Thomas J Triggs a Brian Nfildes (2004). Perceptual lane width, wide perceptual road centre markings and driving speeds. *Ergonomics* (online). B.m.: Taylor & Francis Ltd , 26. 2., vol. 47, no. 3, p. 237 256 (vid. 2016 11 19). ISSN 00 14 0139. Available from: doi:10.1080/00140130310001629711
13. Hyari, Khalied, Khaled El-rayes a Khaled El-rayes (2016). Construction Management and Economics Field experiments to evaluate lighting performance in nighttime highway construction Field experiments to evaluate lighting performance in nighttime highway construction (online). (vid. 2016-11-18). Available from: doi:10.1080/01446190600601669
14. La Torre, Francesca, Lorenzo Domenichini a Alessandro Nocentini (2017). Effects of stationary work zones on *motorway* crashes. *Safety Science* (online). 2.,vol. 92,p. 148 159(vid. 20161113).ISSN 09257535.Available from: doi:10.1016/j.ssci.2016.10.008
15. Petzoldt, T, P Rossner, C Mair a Ac Bullinger (2016). How does left lane width in motorway work zones affect driver behaviour and perception? *Advances in Transportation Studies an international Journal* (online). no. 1, p. 51–58 (vid. 2016-11 19). Available from: https://www.tuchemnitz.de/hsw/psychologie/professuren/allpsy1/pdf/Petzoldt et al. (2016) - author's.pdf
16. Urwyler, Prabitha et. al., (2015). Age-dependent visual exploration during simulated day- and night driving on a motorway: a cross-sectional study. *BMC Geriatrics* (online). B.m.: BioMed Central, 28. 12., vol. 15, no. 1, p. 18 (vid. 2016 11 19). ISSN 1471 2318. Available from: doi:10.1186/s12877-015-0015-2
17. Wanvik Po (2009). Effects of road lighting on motorways. *Traffic Inj Prev* (online). 6., vol. 10,no. 3, p. 279 289. ISSN 15389588.Available from: doi:10.1080/15389580902826866
18. Young, Mark S., Janina M. Mahfoud, Neville A. Stanton, Paul M. Salmon, Daniel P. Jenkins Enkins a Guy H. Walker, (2009). Conflicts of interest: The implications of roadside advertising for driver attention. *Transportation Research Part F: Traffic Psychology and Behaviour* (online). vol. 12, no. 5, p. 381 388. ISSN 13698478. Available from: doi:10.1016/j.trf.2009.05.004

19. Zhou, Huaguo, Fatih Pirinccioglu a Peter HSU (2009). A new roadway lighting measurement system. *Transportation Resear ch Part C: Emerging Technologies* (online). vol. 17, no. 3, p. 274–284. ISSN 0968090X. Available from: doi:10.1016/j.trc.2008.11.00 1
20. Ai, C. a Y.J. Tsai (2016). An automated sign retroreflectivity condition evaluation methodology using mobile LIDAR and computer vision. *Transportation Research Part C: Emerging Technologies* (online). roč. 63. Available from: doi:10.1016/j.trc.20 15.12.002
21. Balali, V., M.A. Sadeghi a M. Golparvar-fard (2015). Image-based retro-reflectivity measurement of traffic signs in day time. *Advanced Engineering Informatics* (online). roč. 29, č. 4. Available from: doi:10.1016/j.aei.2015.08.003
22. Hummer, J.E., E.A. Harris a W. Rasdorf (2013). Simulation based evaluation of traffic sign retroreflectivity maintenance p ractices. *Journal of Transportation Engineeri ng* (online). roč. 139, č. 6. Available from: do i:10.1061/ (ASCE)TE.1943-5436.0000526
23. Khalilikhah, Majid a Kevin Heaslip (2016). The effects of damage on sign visibility: An assist in traffic sign replacement. *Journal of Traffic and Transportation Engineering (E nglish Edition)* (online). 12., roč. 3, č. 6, s. 57 1 581 (vid. 2017 03 09). ISSN 20957564. Av ailable from: doi:10.1016/j.jtte.2016.03.009
24. Obeidat, Mohammed Said, Malgorzata J. Rys, Andrew Rsy a Juan Du (2016). Evaluation of overhead guide sign sheeting materials to increase visibility and safety for drivers. *Applied Ergonomics* (online). 9., roč. 56, s. 136–143 (vid. 2017-03-11). ISSN 00036870. Available from: doi:10.101 6/j.apergo.2016.03.016

Corresponding author:
Ing. Lukáš Jan Hrabanek, Department of vehicles and ground transport, Faculty of Engineering, Czech University of Life Sciences Prague, Kamýcká 129, Praha 6, Prague, 16521, Czech Republic, phone: +420 22438 3106, e-mail: hrabanek@tf.czu.cz

ASSESSMENT OF HYDRAULIC FLUID PROPERTIES BY PHYSICO-CHEMICAL ANALYSIS

Michaela JÁNOŠOVÁ[1], Ana PETROVIĆ[2], Peter OPÁLENÝ[1]

[1]*Department of Transport and Handling, Faculty of Engineering, Slovak University of Agriculture in Nitra, Slovak Republic*
[2]*Department of Physics, Faculty of Engineering, Slovak University of Agriculture in Nitra, Slovak Republic*

Abstract
The submitted contribution is focused on the evaluation of hydraulic fluids used as power sources in hydraulic presses. Hydraulic fluid has its lifetime, after which it can no longer fulfill the required functions. The assessment of the condition of the oil filling can be carried out according to predefined intervals or continuously. The first method often leads to frequent exchange of oil. The second method is more demanding on the number of analyzes, but it allows for early intervention in a sudden change and an exchange at the time the oil is actually worn out. According to the contribution of the oils analysis in hydraulic presses can reveal the amount of pollutants as well as the physico-chemical parameters of hydraulic oils. To determine the technical parameters of the oil filling it is necessary to use appropriate diagnostic methods. The aim of our paper is to analyze the properties of the withdrawn hydraulic fluids in terms of dynamic viscosity, acidity, water content, ferrographic analysis, and evaluate the results in tabular and graphical form.

Key words: *hydraulic oil; physico-chemical properties; contamination.*

INTRODUCTION

Target of each sector of the economy is to reduce wear and within that of prolong lifetime (*Tulik, 2013*). Hydraulic systems have a wide application in high efficient mechanisms, ground roads and construction machineries, in agricultural and forestry technologies as well as in many other areas. Each functional hydraulic mechanism is part of liquid, that is its main and most important element (*Hujo et al., 2017*). There are high demands on the working fluid and it form basic element in the hydraulic system. Physically, hydraulic fluids are characterized in that, their particles are relatively close to each other, but they are not bound in fixed positions. Hydraulic fluid can move in the entire volume. Hydraulic fluids have the following characteristics: the liquids have no permanent shape, the liquids have their own volume, the liquids have a free surface, the liquids are droplets, the liquids are hardly compressible, the heat is flowing in the fluids. The hydrostatic pressure transmission system and usege of the hydrodynamic principle requires a perfect medium, and therefore the hydraulic fluid must meet all the conditions that occur in the operation of the hydraulic systems. The new development of current hydraulic components is aimed at increasing the power output, reducing energy intensity, minimizing environmental pollution and increasing technical lifetime and reliability (*Jablonicky el al., 2012*).
By detection and analyzing the properties of liquids we can examine its impact and also the impact on the elements of the hydraulic system, especially the hydrostatic transducers (*Tulik, 2013*). At present, technical means are at such a high level that new space has been created to find and apply the innovation and usege of used hydraulic fluids by adding additives (*Majdan et al., 2010*).

MATERIALS AND METHODS

The main function of the fluid in the hydraulic mechanism is transfer of pressure energy from the hydrogenerator to the hydraulic motor, the lubrication of the friction parts of the hydraulic mechanism, the removal of residues penetrating into the hydraulic system and the generated hydraulic systems, the heat removal, the extraction of excess heat generated during operation in the hydraulic system, protection against corrosion, creating oil film on the internal metallic elements of the hydraulic mechanism, and feeding the hydraulic elements of the information transmission system (*Hujo et al., 2017*).

Evaluation of cleanliness of the hydraulic oil is still developing, which is directing by trends even smaller residues of contamination. It is a natural response to the increasing accuracy of production of control and regulating elements in hydraulic systems (*Tkáč et al., 2010*).
In most cases, damage of machines are the causes of oil pollution by either hard (wear particles) or soft dirt (sludges and oil oxidation products). Another major cause of lubrication failure is the degradation of the base oil. Lower quality of the base oil results in deterioration of lubricating properties due to decomposition of unstable components due to operating conditions such as temperature and load. Resistance of the base oil to degradation is given to the liquid during production and the primary affects its life under operating conditions. Each oil has its limited lifetime. The main causes of oil aging are:

- polutions
- lifetime and usage of additives
- degradation of the base oil (*Tkáč et al., 2014*)

Analysis of oils in hydraulic presses can reveal a number of metal wear, oil pollution, additive quantities, and physico-chemical parameters of hydraulic oils. To determine the technical parameters of the oil filling, it is necessary to use appropriate diagnostic methods to analyze the physicochemical properties of the used hydraulic fluids (*Majdan et al., 2014*). The samples of hydraulic oils taken from the operating tests were proceeded to the following laboratory analysis:

- dynamic viscosity
- TAN number
- Water contamination
- Ferrographic analysis

The aim of article is to analyze the physicochemical properties of taken hydraulic fluids used in hydraulic presses on lines 8 and 9 with evaluation of changes in hydraulic fluids. Mentioned devices worked without changing the hydraulic fluid in the working mode shown in Tab. 1.

Description of manipulation devices:

In manufacturing plant DS SMITH are operating 53 injection moulding machines consist of ARBURG, NETSAL, DEMAG, KRAUSSMAFFE. Mentioned machines operate on the hydraulic principle and two pressing lines on the electric. Based on plant request, we investigated the contamination of hydraulic fluids by physicochemical analysis on NETSAL lines 8 and 9 and designed a suitable oil change interval. The parameters for each line are described in Tab. 1.

Tab. 1 Parameters of production press line

DS SMITH								
NETSAL synergy 1500								
Line No.	Oil	Date of filling	Date of sampling	Volume (L)	Pressure (10^5 Pa)	Flow (L.min^{-1})	Cycle (s)	Products/Cycle
8	OSO S 46 AGIP	07/11 2014	05/05/2016	260	59.6	143	46.86	8
9	OSO S 46 AGIP	07/11 2014	05/05/2016	260	54	72.6	47,8	8

Hydraulic oils OSO S 46 AGIP samples were subjected to the following laboratory analysis:
Ferrographic analysis - using mentioned analysis with magnetic separation of particles, which are separated during wear of friction pairs in the lubrication system, we investigated the size and the morphology of the particulates of wear.
Temperature dependence of viscosity - viscosity is defined as the resistance of a fluid to flow. Viscosity of most of the liquids decreases with increasing temperature according to Arrhenius equation (*Figura & Teixeira, 2007*):

$$\eta = \eta_0 e^{\frac{E_A}{RT}}, \quad (1)$$

where η is, dynamic viscosity (Pa.s), η_0 is reference value of dynamic viscosity (Pa.s), E_A is activation energy (J.mol^{-1}), R is gas constant (J.K^{-1}.mol^{-1}) and T is absolute temperature (K). Presented data have been obtained by rotation viscometer DV2T fy Brookfield. We used ULA (0) spindle for our measurements.

Measurement of acid value - the total acid number (TAN) is an important indicator of the quality of the used oil, and indicates the quantity of such acid in the oil, to determine the degree of degradation of the oil.

Measurement of the content of water - the water in oil is undesirable factor which arises during operation of the machine and causes unfavourable degradation processes which can result in various degrees of failure of the device. For this measurement, we used devices from HYDAC.

RESULTS AND DISCUSSION

Analysis of physico-chemical properties of hydraulic oils was conducted in the laboratories of the Department of Transport and Handling, and in the laboratories of the Department of Physics at the Slovak University of Agriculture in Nitra. The Department of Transportation and Handling carried out the analysis, which results are shown in Tab. 2.

Tab. 2 The results of chemical analyses

Line No.	Ferrographic analysis	Acid value (mg.KOH.g^{-1})	Content of water (%)
8	clean	0.86	0
9	clean	1.05	0

Ferrographic analysis – after two years of hydraulic oil use, in the lines 8 and 9, no metal particles were found in the test oil.

TAN number – oil manufacturer indicates oil use up to 1.3 mg.KOH.g^{-1} as hydraulic oil does not exceed this number is still suitable for use.

Water contamination – Since the hydraulic circuit closed water analysis in all three samples was 0%.

Dynamic viscosity in dependence on temperature was measured. Range of temperatures was from 25 °C – 90 °C. Three samples were measured. First one was new oil for comparison, and the second and third oils OSO S 46 AGIP were from press lines 8 and 9. Results obtained in this work are presented on Fig. 1.

It is possible to observe that dynamic viscosity of hydraulic oils is decreasing exponentially with increasing of temperature, what was expected and corresponds with conclusions reported in literature (*Vozárová et al., 2015; Hlaváč et al., 2014; Hlaváč & Božiková, 2014; Severa et al., 2012*).

Regression equations and determination coefficients for individual samples are in the Tab. 3.

The analysis of viscosity determines the quality and the purity of hydraulic oils, since contaminants increase the viscosity of the fluid, which can be indirectly monitored by determining the dynamic viscosity in above specified range of temperatures. As it can be seen on Fig.1 in both cases of used oils (8 and 9) were observed increase in viscosity which can be caused by several factors: presence of impurities (metal or non-metal) and/or structural changes in hydraulic oils during operation. Therefore, the samples of the hydraulic oils further will be analyzed to find out which kinds of impurities or other factors are influencing the viscosity.

Tab. 3 Determination coefficients and regression equations

Sample	Regression equation	Determination coefficient R2
New OSO S 46 AGIP	$205.77e^{-0.037x}$	0.9925
Used OSO S 46 AGIP 8	$265.84e^{-0.028x}$	0.9305
Used OSO S 46 AGIP 9	$263.46e^{-0.033x}$	0.9862

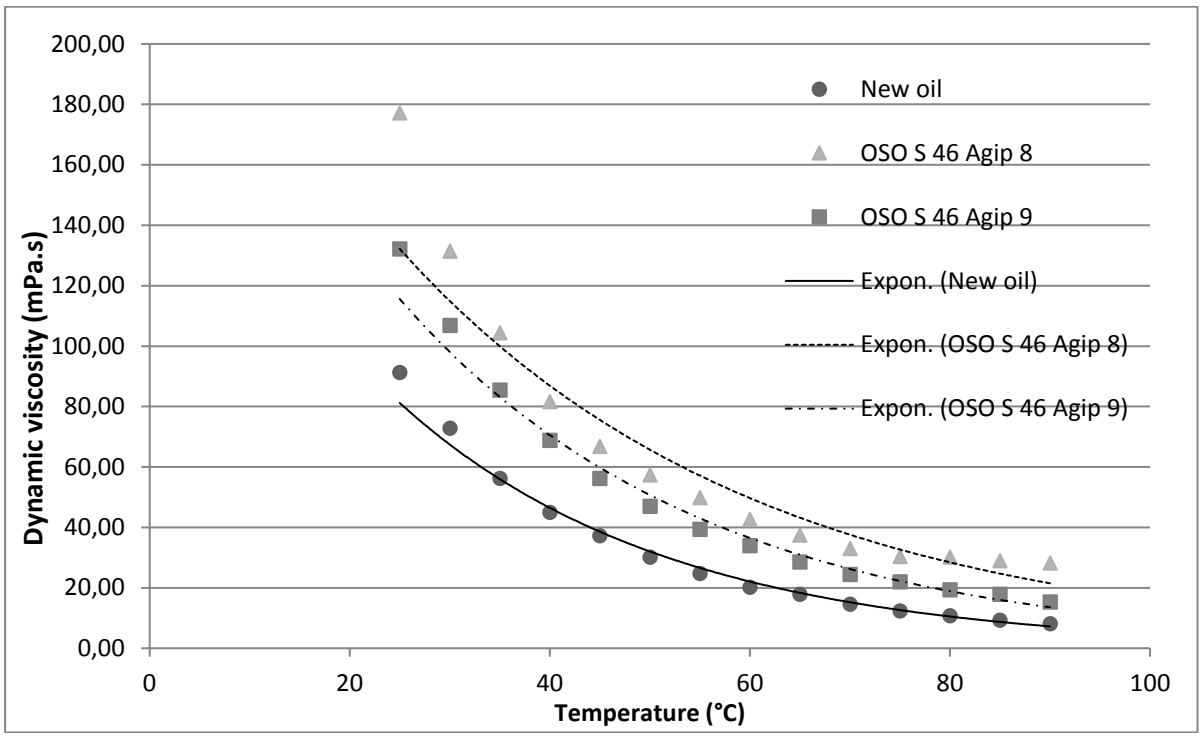

Fig. 1 Dependences viscosity on temperature

CONCLUSIONS

Hydraulic devices are widely used in the powerful mechanisms of agricultural and forestry machinery as well as in many other areas. The development of modern hydraulic components is aimed at enhancing transmission performance, reducing energy severity, minimizing environmental pollution and increasing machine life and reliability (*Máchal et al., 2013; Tkáč et al., 2007*).

From the point of view of the use of hydraulic fluid in the mobile machine, it is important to know the operating properties of the liquid, To know the influence of the fluid on elements of the hydraulic system (*Tkáč et al., 2008*). Attention was paid to the laboratory methods and procedures which can be used to evaluate the properties of hydraulic fluids (*Tkáč et al., 2014*).

Results of ferrographic analysis showed no metal particles, in oil in hydraulic presses, even after two years of use. All samples of hydraulic oils were clean. Values of the acid number of the used hydraulic oils does not exceed number which the oil producers indicates (up to 1.3 mg KOH/g), oils are still suitable for use. The water content of all examined samples of used oils was 0%.

Viscosity influences the oil's ability to flow through the hydraulic system, therefore affects the pressure required to push the oil sufficiently to develop the necessary flow. The rate of oil flow is important to the life of the hydraulic system.

As the Ferrographyc analysis for both used samples was clean from metal particles, it may be that there are contaminants of other origin (non-metal) that measurement of viscosity showed. Further research will be focused on detecting of origin of the impurities and on determining other factors influencing increase of dynamic viscosity.

ACKNOWLEDGMENT

This work was co-funded by European Community under project no 26220220180: Building Research Centre „AgroBioTech“ and contribution was made under the grant project of the Ministry of Education of the Slovak Republic VEGA1/0337/15 „Research aimed at influence of agricultural, forest and transport machinery on environment and its elimination on the basis of ecological measures application.

REFERENCES

1. Figura, L. O., & Teixeira, A. A. (2007). Food physics, Physical properties - measurement and applications. USA: Springer. 550 p.
2. Hlaváč, P., & Božiková, M. (2014). Effect of Temperature on Dynamic Viscosity and Activation Energy of Milk and Acidophilus Milk. *Advanced Materials Research*, 1059, 53-59.
3. Hlaváč, P., Božiková, M., & Presová, R. (2014). Temperature relations of selected engine oils dynamic viscosity. *Acta technologica agriculturae*, 17, 104-107.
4. Hujo, Ľ., Jablonický, J. & Tkáč, Z. (2017). Návrh inovatívneho laboratórneho simulačného zariadenia na skúšanie hydrostatických prevodníkov hydraulických kvapalín. Nitra Slovenská poľnohospodárska univerzita.
5. Jablonický, J., Tkáč, Z., Majdan, R., Uhrinová, D., Hujo, Ľ. & Vozárová, V. (2012). Hodnotenie vlastností biopalív a biomazív. 1st ed. Nitra: Slovenská Poľnohospodárska Univerzita.
6. Máchal, P., Tkáč, Z., Kosiba, J., Jablonický, J., Hujo, Ľ., Kučera, M. & Tulík, J. (2013). Design of a laboratory hydraulic device for testing of hydraulic pumps. *Acta Universitatis Agriculturae et Silviculturae Mendelianae Brunensis*, 61 (5), 1313-1319.
7. Majdan, R., Tkáč, Z., Drabant, Š., Pap, M., Tulík, J., Chrastina, J. & Zigiň, P. (2010). Simuiácia tlakového rázu a jeho tlmenie. *XXIX. Setkání kateder mechaniky tekutín a termomechaniky: mezinárodní konference.* Ostrava: Vysoká škola báňská - Technická univerzita, (pp. 179-182).
8. Majdan, R., Tkáč, Z., Stančík, B., Abrahám, R., Štulajter, I., Ševčík, P. & Rášo, M. (2014). Elimination of ecological fluids contamination in agricultural tractors. *Research in agricultural engineering*, 60 (1), 9-15.
9. Severa, L., Kumbár, V., Buchar, J., Čorňák, Š., Glos, J., Hlaváč, P., & Čupera, J. (2012). On the engineering flow properties of used and new engine oils. *Applications of physical research in engineering: The renewable energy sources and physical properties of selected industrial materials*. Nitra : Slovak University of Agriculture. ISBN 978-80-552-0839-8.
10. Tkáč, Z., Drabant, Š., Majdan, R. & Cvíčela, P. (2007). Design and realisation of testing device for laboratory tests of hydrostatic pumps. In 3rd international conference Trends in agricultural engineering, Prague, September 12-14, (pp. 450-454).
11. Tkáč Z., Drabant Š., Majdan R., Cvíčela P. (2008). Testing stands for laboratory tests of hydrostatic pumps of agricultural machinery. *Research in Agricultural Engineering*, 54, 183–191.
12. Tkáč, Z., Majdan, R., Drabant, Š., Abrahám, R., Vozárová, V. & Jablonický, J. (2010): Hodnotenie vlastností hydraulických kvapalín na základe skúšok s použitím hydrogenerátora (Performance evaluation of hydraulic fluids based on test susing hydraulic generator). Nitra, Slovenská poľnohospodárska univerzita.
13. Tkáč, Z., Majdan, R. & Kosiba, J. (2014). Výskum vlastností ekologických kvapalín a nových testovacích metód mazacích olejov : (postupy, metódy a ich aplikácie). 1st ed. Nitra: Slovenská poľnohospodárska univerzita.
14. Tulík, J., Kosiba, J., Hujo, Ľ., Jablonický, J. & Šinský, V. (2013). The durability of a tractor gear-hydraulic circuit. *Trends in agricultural engineering*, 1st ed., 617-621.
15. Vozárová, V., Kardjilova, K., Híreš, L., Valach, M., & Wollner, A. (2015). Temperature Dependence of Dynamic Viscosity and DSC Analysis of the Plantohyd samples. *Journal of Central European Agriculture*, 16, 221-230.

Corresponding author:
Ing. Michaela Jánošová, Department of Transport and Handling, Faculty of Engineering, Slovak University of Agriculture in Nitra, Tr. A. Hlinku 2, Nitra, 949 01, Slovakia, phone: +421 908 190 338, e-mail: xjanosova@is.uniag.sk

DRY SORPTION STABILIZATION OF ACIDIC COMPOUNDS IN FLUE GASES

Petr JIRSA, Jan MALAŤÁK

Department of Technological Equipment of Buildings, Faculty of Engineering,Czech University of Life Sciences Prague

Abstract
The article focuses on a technology of flue gases stabilization in hospital waste incinerating facility. Hazardous particles and compounds formed in flue gas during the process of thermal waste degradation need to be stabilized according to an enacted legislation. The aim of the research is to examine an efficiency of sorbents $Ca(OH)_2$ and $NaHCO_3$ to stabilize HCl and SO_2 in flue gases. Experiments were performed in semi operation in a hospital waste incinerating plant with heating power 1.5 MW and capacity 250 kg. h^{-1}. Both sorbents were injected into the system in different volumes to determine refining effect. With every 1 kg of $Ca(OH)_2$ injected to the system, observed concentrations linearly decrease; SO_2 by 24.43 $mg.m^{-3}$ and HCl by 10.07 $mg.m^{-3}$. With every 1 kg of $NaHCO_3$ injected to the system concentration linearly decrease; SO_2 by 27.85 $mg.m^{-3}$ and HCl by 15.39 $mg.m^{-3}$.

Key words: *Hospital waste, Calcium hydroxide, Sodium bicarbonate, HCl, SO_2.*

INTRODUCTION

Elimination of sulphur oxides and halogen hydrogens in flue gas can be done by several methods such as a wet, semi-dry and dry process *(Wey et al., 2001).* Dry refining technology is based on a sorbent injection that is in a form of finely crushed dry powder. The agent is sprayed directly into the flue gas flow *(Allen et al., 2001)* or mixed with waste going into the reactor *(Cunill et al., 1991).* Neutral compounds are formed by sorbent reaction with acid components. Solid particles are captured on solid particles separators. Sorbents can be calcium or sodium based. There are other synthesized sorbents at the market that can achieve better efficiency in flue gases stabilization under specific condition *(Cao et al., 2014).*

The research focuses on the dry sorption refining technology in a hospital waste incinerating plant with a heating power under 5 MW. The dry sorption refining technology seems to be very efficient for such application. However, such technology is not commonly used for plants with higher power output because of high volume gas transfer in the system. Wet or semi-dry sorption technologies are usually used for plants with greater thermal output.

The aim of the study is to determine the refining effect of calcium hydroxide and sodium bicarbonate on HCl and SO_2 in relation with process conditions in the dry sorption refining system.

MATERIALS AND METHODS

Experimental tests were conducted at the incinerating facility for hospital waste treatment Johnson Controls Fabrics Strakonice a.s., Czech Republic. The incinerating plant consisted of a pyrolysis-incinerating furnace Hoval – Schiestl GG 24, thermoreactor TR 24 and a steam boiler THD IV 0580 with heating power 1,508 kW. The capacity of the plant was 250 $kg.h^{-1}$ and the burned material was dosed discontinuously 60-65 kg per every 15 minutes. The input material was hospital waste.

In the furnace chamber, the temperature was set in range of 900 to 950 °C. Two burners for natural gas automatically control the heat to the required temperature. The waste was carbonized and formed gas was mixed with the air and burned in thermoreactor at the temperature 1,100 to 1,150 °C. Formed flue gases flowed to the boiler where the temperature was reduced to 200 to 250 °C. A device for dosing tested sorbent was placed after a boiler. Flowingly the flue gas passed through the first pipe labyrinth which was 8 m long and a heat exchanger where the temperature was reduced to 130 to 135 °C. Then flue gas went through the second pipe labyrinth which was 17 m long. All solid particles involving hazardous compounds and sorbents injected into the system were captured on a tied filter subsequently.

Emissions measuring in flue gas was taken according to appropriate legislative *(Act No. 201/2012 Coll. Air Protection. Czech Republic., 2012).* The measuring point was placed at the horizontal flue pipe with diameter 355 mm after a ventilator according to ISO 9096 and EN 13284-1.

Flue gas properties and the concentration of particulate matter (PM), hydrogen chloride (HCl), sulfur-dioxide (SO_2), oxygen (O_2) were determined according to technical standards:

- Gravimetric determination of the mass concentration of particulate matter (ISO 9096 EN 13284-1);
- Determining flow velocity and volume flow (ISO 10780);
- Paramagnetic determination of oxygen (EN 14789);
- Photometric determination of the mass concentrations in inorganic chloride compounds (EN 1911);
- Determination of sulphur dioxide mass concentration, automated system – UVF fluorescence NDUV (ISO 7935, EN 14212);

Volumes, weights of combustion air and emission concentration are given for normal conditions, i.e., at t = 0 °C, p = 101.325 kPa and the reference oxygen content in the flue gases O_r = 11 %.
For the experimental measurement, two different sorbents were tested on efficiency to eliminate hazardous particles in flue gases.

- Calcium hydroxide: $Ca(OH)_2$,
- Sodium Bicarbonate: $NaHCO_3$.

Sorbents react with acidic components of flue gas according to following chemical equations:

$$SO_2 + Ca(OH)_2 = CaSO_4 + H_2O \quad (1)$$

$$2HCl + Ca(OH)_2 = CaCl_2 + 2H_2O \quad (2)$$

$$SO_2 + 2NaHCO_3 + 1/2\ O_2 = Na_2SO_4 + 2CO_2 + H_2O \quad (3)$$

$$HCl + NaHCO_3 = NaCl + CO_2 + H_2O \quad (4)$$

Estimated consumption of the sorbent was calculated for every experiment according to stoichiometric relation expressed in following equations:

$$G^T_{Ca(OH)_2} = M_{Ca(OH)_2} \times V \times \left(\frac{c_{SO_2}}{M_{SO_2}} + \frac{c_{HCl}}{\frac{1}{2}M_{HCl}}\right) \quad (5)$$

$$G^T_{NaHCO_3} = M_{NaHCO_3} \times V \times \left(\frac{c_{SO_2}}{\frac{1}{2}M_{SO_2}} + \frac{c_{HCl}}{M_{HCl}}\right) \quad (6)$$

where: $M(SO_2)$ = 64.066 g.mol^{-1}; $M(HCl)$ = 36.461 g.mol^{-1}; $M(Ca(OH)_2)$ = 74.093 g.mol^{-1}; $M(NaHCO_3)$ = 84.007 g.mol^{-1}; V = flue gas flow [Nm^3.h^{-1}]; C_{SO2}, C_{HCl} = concentration [mg.m^{-3}].

Both sorbents $Ca(OH)_2$ and $NaHCO_3$ were injected into a flue gas pipe after the heat exchanger. Concentration of hydrogen chloride and sulphur dioxide was measured in relation to various volume of sorbent dosed into the system.
The flue gas went through the first pipe labyrinth where the mean residence time was 0.6 s. Then it went through the cooler with the mean residence time of 1.1 s. The flue gas went through the second pipe labyrinth with the mean residence time of 1.3 s. The total time of possible reaction between the sorbent and acid flue gas elements in the system was approximately 3 s. The measuring point was after a heat exchanger where the temperature of flue gas was 225 °C.
Calcium hydroxide was tested during the first set of measurement with following parameters. The mean volume of flue gas was 3,629 Nm^3.h^{-1} and mean volume of O_2 was 10.1 ± 0.98 %. Theoretical consumption of $Ca(OH)_2$ was calculated according to equation (5). The theoretical sorbent consumption was determined at level 2.553 kg.h^{-1} for stated conditions. During the test 2.5 to 7 kg.h^{-1} of $Ca(OH)_2$ was dosed into the system and the concentration of HCl and SO_2 was measured in relation with volume of injected sorbent.
Sodium Bicarbonate was tested during the second set of measurement with following parameters. The mean volume of glue gas flow was 3,380 Nm^3.h^{-1} and mean volume of O_2 was 10.5 ± 1.13 %. Theoretical consumption of $NaHCO_3$ was calculated according to equation (6). The theoretical sorbent consumption was determined at level 2.341 kg.h^{-1} for stated conditions. During the test 1.8 to 5 kg.h^{-1} of $NaHCO_3$ was dosed into the system and the concentration of HCl and SO_2 was measured in relation with volume of injected sorbent.

RESULTS AND DISCUSSION

The dependence of HCl and SO_2 concentration in flue gas on volume of $Ca(OH)_2$ injected into the system is shown on the graph (Fig 1). The first value represents the reference point for evaluation when no sorbent was injected into the system.

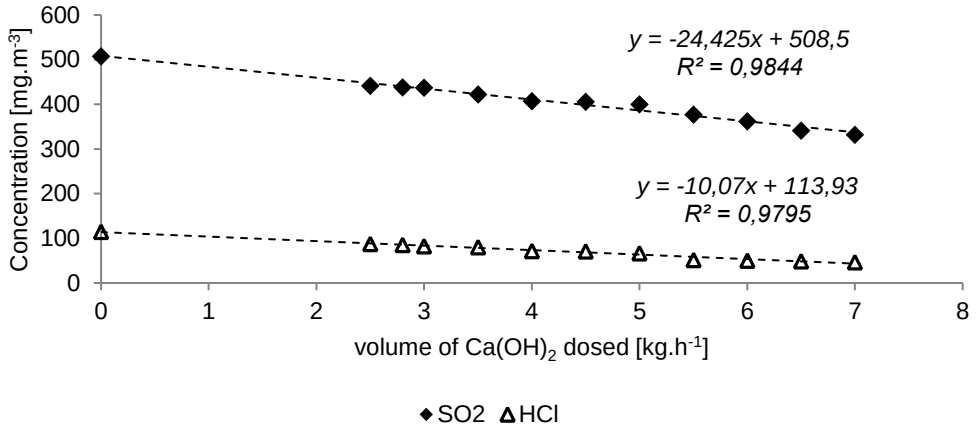

Fig. 1 Reduction of HCl and SO_2 concentration in flue gas based on dosing $Ca(OH)_2$

The results show that calcium hydroxide reacts with both hydrogen chloride and sulphur dioxide. The concentration of SO_2 linearly decreases by 24.43 $mg.m^{-3}$ and the concentration of HCl linearly decreases by 10.07 $mg.m^{-3}$ with every 1 kg of $Ca(OH)_2$ injected to the system. By dosing $Ca(OH)_2$ 7 kg per hour the concentration of SO_2 decreased by 34.5 % and the concentration of HCl decreased by 59.0 % referring to the initial concentration when no sorbent was added. In different study, similar results were observed. Conversion of SO_2 and HCl linearly dependence on molar excess of $Ca(OH)_2$ dosed into the flue gas *(Veselý et al., 2016).* Other study suggests that even better results in HCl stabilization can be reached by dosing calcium oxide (CaO). Removal 76 % of HCl by CaO at temperature of 600 °C *(Shemwell et al., 2001).*

The dependence of HCl and SO_2 concentration in flue gas on volume of $NaHCO_3$ injected into the system is shown on the graph (Fig 2). The first value represents the reference point for evaluation when no sorbent was injected into the system.

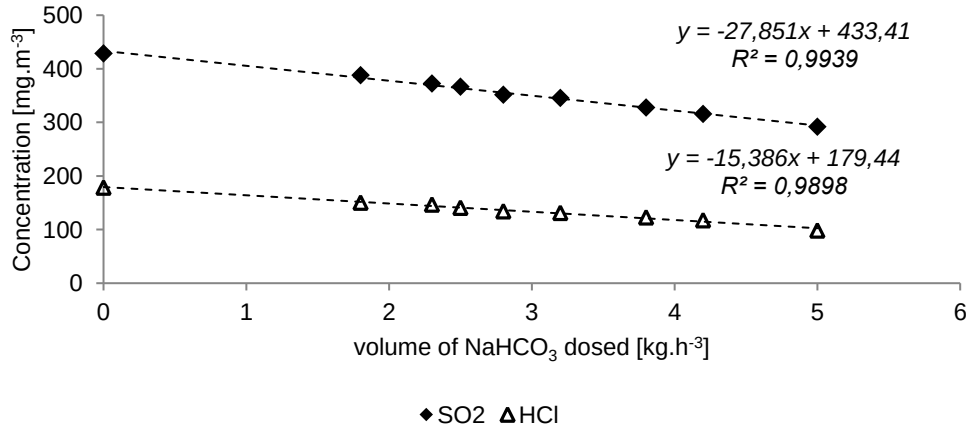

Fig 2. Reduction of HCl and SO_2 concentration in flue gas based on dosing $NaHCO_3$

The results show that sodium bicarbonate reacts with both hydrogen chloride and sulphur dioxide. The concentration of of SO_2 linearly decreases by 27.85 $mg.m^{-3}$ and the concentration of HCl linearly decreases by 15.39 $mg.m^{-3}$ with every 1 kg of $NaHCO_3$ injected to the system. By dosing $NaHCO_3$ 5 kg per hour the concentration of SO_2 decreased by 32 % and the concentration of HCl by 44.8 % referring to an initial concentration when no sorbent was added. Similar results were observed in different study. Experimental results demonstrate that concentration of SO_2 and HCl decreased monotonously

with increasing quantity of dosed bicarbonate *(Veselý et al., 2016).* Previously was published that $NaHCO_3$ is more efficient in SO_2 stabilization that other sorbents such as Na_2CO_3 *(Keener & Davis, 1984)*.

CONCLUSIONS

The paper presents technology process of flue gas stabilization for hospital waste combustion. It takes into account reduction of SO_2 and HCl by adding different agents directly into the flue gas flow. It is dry sorption based process which can be effective for a small scale incinerating plants referring to obtained results. The experiments were conducted in a semi operation of hospital waste incinerating plant with two-stage combustion system with heating power 1.5 MW. Material was dosed discontinuously 60-65 kg per 15 minutes and burned in a burning chamber at the temperature of 900-950 °C. Formed gas was mixed with air and burned at the thermoreactor for 2 sec at the temperature 1,100-1,150 °C. Tested sorbents calcium hydroxide ($Ca(OH)_2$) and sodium bicarbonate ($NaHCO_3$) were injected directly into the flue gas flow after a boiler where the temperature decreased to 200-250 °C. Results shows that both sorbents eliminate concentration of observed acidic gases in the exhaust. The concentration of SO_2 linearly decreases by 24.43 $mg.m^{-3}$ with every 1 kg of $Ca(OH)_2$ and linearly decreases by 27.85 $mg.m^{-3}$ with every 1 kg of $NaHCO_3$ injected to the system. Regarding elimination of HCl the concentration linearly decreases by 10.07 $mg.m^{-3}$ with every 1 kg of $Ca(OH)_2$ as well as linearly decreases by 15.39 $mg.m^{-3}$ with every 1 kg of $NaHCO_3$ injected to the system. It was observed that the theoretical amount of sorbent calculated according to chemical equations (1-4) was not enough to reduce the concentration of SO_2 and HCl to expected levels. It is presumably caused by low number of collisions in flue gas flow between sorbent and eliminated substances. However, with 2-3 times excess of dosed sorbent, both calcium hydroxide and sodium bicarbonate achieved sufficient efficiency in SO_2 and HCl elimination. Using combination of both sorbents for flue gas stabilization would be probably the most suitable approach that will be examined in following experiments of this research.

ACKNOWLEDGMENT

This study was supported by Internal Grant Agency of the Czech University of Life Sciences Prague, Czech Republic, Grant No. 20173002.

REFERENCES

1. Act No. 201/2012 Coll. Air Protection. Czech Republic. (2012).
2. Allen, R. W., Archer, E., & MacInnes, J. (2001). Adsorption by particles injected into a gas stream. Chemical Engineering Journal, 83(3), 165–174.
3. Cao, J., Zhong, W., Jin, B., Wang, Z., & Wang, K. (2014). Treatment of Hyd-rochloric Acid in Flue Gas from Municipal Solid Waste Incineration with Ca–Mg–Al Mixed Oxides at Medium–High Tempera-tures. Energy & Fuels, 28(6), 4112–4117.
4. Cunill, F., Izquierdo, J. F., Martínez, J. C., Tejero, J., & Querol, J. (1991). Influence of different additives on the reaction between hydrated lime and sulfur dioxide. Environmental Progress, 10(4), 273–277.
5. Keener, T. C. & Davis, W. T. (1984) Study of the Reaction of SO_2 with $NaHCO_3$ and Na_2CO_3. Journal of the Air Pollution Control Association, 34(6), 651-654.
6. Veselý V., Jirsa P., Szeliga Z., & Kovač D. (2016). Removal of Acid Gases in an Incinerator of Hospital Waste. Journal of Energy and Power Engineering, 10, 681-691.
7. Shemwell, B., Levendis, Y. A., Simons, G. A. (2001). Laboratory study on the high-temperature capture of HCl gas by dry-injection of calcium-based sorbents. Chemosphere, 42(5), 785-796.
8. Wey, M.-Y., Ou, W.-Y., Liu, Z.-S., Tseng, H.-H., Yang, W.-Y., & Chiang, B.-C. (2001). Pollutants in incineration flue gas. Journal of Hazardous Materials, 82(3), 247–262.

Corresponding author:
Ing. Petr Jirsa., Department of Technological Equipment of Buildings, Faculty of Engineering, Czech University of Life Sciences Prague, Kamýcká 129, Praha 6, Prague, 16521, Czech Republic, phone: +420 607 616 711, e-mail: pjirsa@ft.czu.cz

ENDURANCE LIFEPO4 BATTERY TESTING

Milan JURKA

Department of Electrical Engineerign and Automation, Faculty of Engineering, Czech University of Life Science Prague

Abstract
Lithium-iron-phosphate ($LiFePO_4$) are currently considered to be one of the best battery types. $LiFePO_4$ has a longer battery life than other types of batteries, especially for deep discharge, they can be discharged with high currents and are several times safer than regular lead batteries (Chang, 2012). Since battery life and safety are both the main problem, the parameters specified by the battery manufacturer must be precisely defined and verified (Shrestha & Goel, 1998). This article focuses on the battery test by winston, more precisely the WB-LYP40AHA type, especially by the comparison of the actual measured parameters with the manufacturer's data.

Key words: *Battery, $LiFePO_4$, depth of discharge, balancers.*

INTRODUCTION

The main obstacle to the use of all types of accumulators is their service life, manufacturers and wholesalers provide information on low depth discharge parameters and, above all, emphasize the advantages of individual cells - the possibility of charging and discharging with high currents (*Wang X et al., 2012*). Lifetime, according to the manufacturer's specifications, is performed in cycles according to a pre-defined DOD cell discharge, while the service life is being observed after many discharging and charging cycles where worsening of parameters begins to appear (*Cenek et al., 2003*). Sometimes, the measured values differ from those reported by 100%. The most important criterion for assessing the quality of supplied batteries is to find out the real life of $LiFePO_4$ cells (*Scrosati et al., 2013; Thundersky 2017*). Testing of selected accumulators is carried out on a special test station, on which the discharging and charging cycle is optimized (*Papez & Papezova, 2016*).

MATERIALS AND METHODS

Most $LiFePO_4$ battery parameters will only be reflected after long-term measurements, when discharged deeply. Therefore, the discharging and charging cycle is fully automated and controlled by a computer. The individual electrical parameters of the cells are gradually recorded and processed. The cells are equipped with balancing and protection circuits (in particular balancers), which ensure uniform discharge of individual cells and other protection circuits are used to prevent tamping. The measuring equipment consists of a control unit, balancers, input-output cards for La-bWiev recording, DC power supply and electrical load. The Statron 3227, which has a maximum load of 80V at a current of 20A, was used as a power source. The output current can be set manually and the setting stability is 1%. The power supply also includes a circuit to prevent the cell from dropping below a predetermined level, thereby ensures battery recharging.
The balancers have been designed to ensure that the battery cells are discharged / charged evenly. The balancer can be loaded up to 80W. When using load 10A, the balancers seamlessly ensure charging at a maximum voltage of 4V single cells and at the same time, during the discharge cycle, they prevent the battery from being lowered.

RESULTS AND DISCUSSION

Measurement of parameters is performed by cyclic discharge of the cells to a predetermined depth discharge value of DOD = 50%; DOD = 100% and their re-acquisition at maximum voltage. All battery parameters have been recorded and evaluated during the measurements.
The WB-LYP40AHA batteries with four 40AH rated cells (*Winston Battery, 2017a*) were tested for use as a backup source of an electric fire system that consumes 10A in case of fire. In both cases the

discharge and charging currents were set to this value. The charging process was controlled by balancers to ensure the same discharge / charge of individual cells.
The temperature of the batteries was monitored by means of a thermocouple which did not exceed 20 ± 1 ° C throughout the test.
In the first case, the batteries were discharged to DOD = 100%, the charging cycle was terminated when all cells were charged above 3.5V and discharged when the voltage at one cell dropped below 2.9V. The batteries were discharged to the lowest possible value indicated by the manufacturer.
The measured electrical parameters are shown in Tab. 1.

Tab. 1 Test results of 4 cells WB-LYP40AHA Winston Battery with DOD = 100%.

After (cycles)	Dischar. voltage (V)	Charging voltage (V)	Full discharge (Ah)	Full discharge (%)	Full charge (Ah)	Charging efficiency (%)	Charging efficiency (Ah)
0	11.94	15.8	46.3	115.8%	46.6	99.4%	
100	11.94	15.9	44.4	111.0%	45.0	98.7%	1.9
200	11.93	15.9	42.3	105.8%	42.8	98.9%	4.0
300	11.87	15.9	41.3	103.3%	41.7	99.0%	5.0
400	11.88	15.8	39.6	99.0%	40.0	99.0%	6.7
500	11.89	15.8	37.2	93.0%	37.9	98.2%	9.1
600	11.88	15.9	35.8	89.5%	36.2	98.9%	10.5
700	11.87	15.9	35.0	87.5%	35.4	98.9%	11.3
800	11.87	15.9	33.8	84.5%	34.1	99.1%	12.5
900	11.86	15.9	32.6	81.5%	32.9	99.1%	13.7
1000	11.86	15.8	31.4	78.5%	31.7	99.1%	14.9
1100	11.85	15.8	30.4	75.9%	30.7	99.0%	15.9
1200	11.85	15.8	29.4	73.5%	29.6	99.3%	16.9
1300	11.86	15.8	28.4	71.0%	28.7	98.8%	17.9
1400	11.85	15.8	27.4	68.5%	27.6	99.3%	18.9
1500	11.84	15.8	26.5	66.2%	26.7	99.2%	19.8

The measured results can be evaluated as follows: After the first charge, the battery value was 46.6A corresponding to 116.5% of the capacity reported, after 30 cycles the battery capacity dropped by 0.03% per cycle, then the drop was down to 0.02% per cycle. 1000 cycles, the drop value stabilized to 0.11% per cycle and remained until the end of the test. The drop in capacity to 70% occurred after 1340. The charging efficiency was almost constant at about 99% throughout the test.
In the latter case, the discharge DOD = 50% was used, the charging and discharging current was the same as in the previous case, ie 10A. The charging cycle was terminated when the voltage across all cells exceeded 3.95V and discharged when the voltage dropped below 3.2V on one cell. At this voltage, the remaining battery capacity was 20Ah, or 50% of the total battery capacity.
The measured parameters are shown in Tab. 2.

Tab. 2 Test results of 4 cells WB-LYP40AHA Winston Battery with DOD = 50%.

After (cycles)	Dischar. voltage (V)	Charging voltage (V)	Full dis-charge (Ah)	Full dis-charge (%)	Full charge (Ah)	Charging efficiency (%)	Charging efficiency (Ah)
0	12.87	15.24	45	112.50%	45.5	98.90%	
100	12.87	15.28	44.55	111.38%	45.08	98.82%	0.45
200	12.86	15.26	44.1	110.25%	44.56	98.97%	0.9
300	12.85	15.13	43.67	109.18%	44.15	98.91%	1.33
400	12.86	15.2	43.26	108.15%	43.72	98.95%	1.74
500	12.86	15.18	42.86	107.15%	43.33	98.92%	2.14
600	12.87	15.22	42.48	106.20%	42.98	98.84%	2.52
8700	12.87	15.15	42.11	105.28%	42.53	99.01%	2.89
800	12.86	15.15	41.74	104.35%	42.23	98.84%	3.26
900	12.87	15.09	41.39	103.48%	41.83	98.95%	3.61
1000	12.86	15.1	41.05	102.63%	41.49	98.94%	3.95
1100	12.86	15.13	40.72	101.80%	41.18	98.88%	4.28
1200	12.87	15.15	40.4	101.00%	41.86	96.51%	4.6
1300	12.86	15.18	40.09	100.23%	40.49	99.01%	4.91
1400	12.86	15.19	39.79	99.48%	40.2	98.98%	5.21
1500	12.85	15.18	39.49	98.73%	39.85	99.10%	5.51
1600	12.86	15.09	39.21	98.03%	39.56	99.12%	5.79
1700	12.86	15.11	38.92	97.30%	39.23	99.21%	6.08
1800	12.85	15.13	38.65	96.63%	39.12	98.80%	6.35
1900	12.86	15.07	38.37	95.93%	39.19	97.91%	6.63
2000	12.87	15.08	38.1	95.25%	38.67	98.53%	6.9
2100	12.86	15.11	37.85	94.63%	38.33	98.75%	7.15

Measured values can be evaluated as follows: After initial charge, the battery value was 45.5A, corresponding to 113.8% of the stated capacity, after 30 cycles the battery capacity dropped by 0.015% per cycle, then the drop decreased to 0.01% per cycle, after 1500 cycles the value of the loss stabilized at about 0.007% per cycle and remained until the end of the test. A 95% capacity drop occurred after 2040 cycle. Charging efficiency was almost constant at about 99% throughout the test.

CONCLUSIONS

Batteries were tested on two test devices that were fully automated by the stations (*Papez & Papezova, 2016);* these equipments were enriched with low internal and galvanic separation balancers. For the control of charging / discharging cycles, the program was equipped with a continuous evaluation of the used charge based on the selected DOD. Two long-term tests were performed on Winston WB-LYP40AHA batteries with four 4V cells with a total capacity of 40Ah. The first one was performed at 100% DOD discharging and 1500 cycles, the other at 50% DOD discharging and 2400 cycles. During charging and discharging cycles, the current voltages of each battery have been verified by a constant current of 10A, the efficiency of the charging and their capacity have been determined. Battery life at discharge DOD = 50% with respect to 70% nominal capacity was calculated from the measurement results to about 5000 cycles. For the second battery, 100% DOD, it was measured that the drop to 70% capacity (here battery life) occurs after 1340 cycles. The maximum battery capacity was above 46Ah (approximately 116%), and the manufacturer has probably chosen a higher primary capacity to ensure

the required life of the $LiFePO_4$ batteries due to their physicochemical properties, where the battery's capacity is decreasing significantly in the first cycles. (*Winston-Battery, 2017b*).
12 V, 40 Ah (*Reddy, 2010*) lead-acid batteries (VRLA batteries) have a life of 300 cycles at 100% DOD and a life of 900 cycles at 50% DOD. The purchase price of VRLA is approximately 45%

ACKNOWLEDGMENT
Acknowledgments belong to the Department of Electrical Engineering and Automation especially to doc. Ing. Stanislava Papežová CSc.

REFERENCES

1. Cenek, M., Jindra, J., Jon, M., Kazelle, J., Kozumplík, J. & Vrba, J. (2003). Accumulator from principle to practice. FCC Public, Praha, 248 pp. (in Czech).
2. Chang WY. State of charge estimation for $LiFePO_4$ battery using artificial neural network. (2012) Oct;7(5):5874–80
3. Papez, V. & Papezova, S. (2016). Automated measuring station for accumulator testing. Agronomy Research 14(S1), 1212–1221.
4. Scrosati, B., Abraham, M., Schalkwijk, W. & Hassoun, J. (2013). Lithium Batteries Advanced Technologies and Applications. Wiley. New Jersey. 392 pp.
5. Shrestha GB, & Goel L. (1998) A study on optimal sizing of stand-alone photovoltaic stations.;13(4):373–8.
6. Thundersky Product Manual http://www.thunderstruckev.com/Manuals/Thundersky_Product_ Manual.pdf , Accessed 23.1.2017.
7. Wang X, Adelmann P, & Reindl T. (2012) Use of $LiFePO_4$ batteries in stand-alone solar system. In Elsevier BV;. p. 135–40.
8. Winston-Battery. http://en.winston-battery.com/index.php/products/power-battery/category/lyp-battery. Accessed 23.3.2017.
9. Winston-Battery. http://en.winston-battery.com/index.php/products/power-battery/item/wb-lyp-40aha, Accessed 11.4.2017.

Corresponding author:
Ing. Milan Jurka, Department of Electrical Engineering and Automation, Faculty of Engineering, Czech University of Life Sciences Prague, Kamýcká 129, Praha 6, Prague, 16521, Czech Republic, e-mail: jurkam@tf.czu.cz

EVALUATION OF THE GNSS RECEIVERS PROPERTIES

Jan KADEŘÁBEK

Department of Agriculture Machines, Faculty of Engineering, Czech University of Life Science Prague

Abstract
The article is focused at the evaluation of technologies for localization and navigation of the robotic machines in the agriculture. The evaluation of the horizontal position accuracy is presented for three low-cost GNSS receivers where one of them use RTK technology. The measurement with static and dynamic position of antennas was conducted. From results follows, that two the same receivers Adafruit Ultimate GPS Breakout can survey-ing different under the same conditions. The receiver u-Blox M8P can determine the position up to one meters, nevertheless it was not possible arise of the accuracy 0,025 m + 1 ppm witch is noticed by manufacturer.

Keywords: *localization, position accuracy, GNSS, RTK, robotics, agriculture.*

INTRODUCTION

The progress in areas of robotics, automatization and information technology causes the incentives for implementation of these new technologys and process to agriculture for a vision of optimization of quality and quantity outputs (products) and at the same time for a vision of reduce of resources need. The sources obtained from the nature can be to reduce thanks to development of the precision farming (*Brantley, 2011; Perez-Ruiz &Upadhyaya, 2012; Moravec et al., 2017),* with is helping the processes thanks to these new technologies. These technologies are deployed for needs of the data collection (*Tsukor, 2012*) and the intervention are performed basis on this data (*Vega, 2014*). The capability of the localization and the navigation requiring the localization is expected for most cases of the robotic machines like UAV (Unmanned aerial vehicle) (*Dlouhý, 2016*), autonomous tractor (*Gan-Mor, 2007*), other agriculture machines (*Rossmann et al., 2010*). In case of the deployment of the robotics machines in a local closed area (for example the animal farms, the glasshouses, the warehouses etc.), it is possible to use the meters determining the relative position (the odometry, the inertion systems, the triangulation or the trilateration, the radar systems, the video navigation etc.). We can to use the GNSS (Global Navigation Satellite System) receivers for the purposes of the obtaining of the absolute position on the earth where the unshaded signal is. Nevertheless, the position accuracy of survey-ing by GNSS receivers is discutable.
The goal of this study is the provide comparison of horizontally accuracy of two GPS receivers Adafruit Ultimate GPS Breakout (UGPSB1 and UGPSB2) and one GPS receiver u-blox NEO M8P (M8P) which use the RTK corrections.

MATERIALS AND METHODS

The measurement was conducted under semi-cloudy sky without precipitation at temperature 6° C in the area 50°14'08", 14°54'50". It was conducted the static and the dynamic measurement for purposes of verification of the position accuracy of the three GNSS receivers. The complete automotive system Dewesoft RTK S-BOX+SIRUS with the inertial unit Dewesoft IMU/GYRO and pair of antennas Novatel OEM 701(DEWESOFT) was used for purposes as the reference information for detereming of distance deviations. This system received the correction messages from the Dewesoft basestation VGPS-HS in RTCM 3.1 format through wireless transmission at ISM band (868 MHz).
Three GNSS receivers were verified: the pair of the small low-cost receivers (USGPS1 and USGPS2) and next one of low-cost RTK receivers (M8P) with was the part of the development kit 2xV94-M8P. The antennas Novatel OEM 701 were connected to all measured receivers and were placed on the roof of the vehicle on the radius 0,2 m around the reference point of Dewesoft system. Only the GPS signal was processed.

The data was recorded from all three receivers to the SD card in the NMEA GGA format with sample rate 5 Hz. Each message had to be verified by checksum, converted and synchronized according the UTC time stamp. The all samples were removed from evaluation if the message was damaged, the time stamp not corresponding or the message was not received. The recorded geographic coordinates from each sample was converted to the relative positions to metric coordinate system NED (North-East-Down). Only the horizontally accuracy was evaluated where the offset 0,2 m had to deducted. The evaluation consisted from determination of the mean values and the dispersions of measured distances between antenna and reference point of Dewesoft system. Further the RMS error value was noticed. The RMS error was calculated as the square root of the average of quadrat of distance error (*Gan-Mor, 2007; Berber, 2013*).
In first step the position accuracy was verified with the static position of the antennas. The Fig. 1 is presented the map of measured points of all receivers including the Dewesoft reference system from 400 s of measurement. The start point of the surface was selected as the basestation antenna placement. Nevertheless, the distances deviation of the points was evaluated measured by the verified receivers and the reference system.
In this map the character of the distances deviations and dispersions is visible for each receivers. The error of the Dewesoft reference system is here also visible. However, the deviation of this system was more than 0,1 m in 5,6% of cases only from this measurement. This error was considered as negligible for presenting of results in this paper. The more detailed examination of the properties of this system will be devoted to the further work of author.

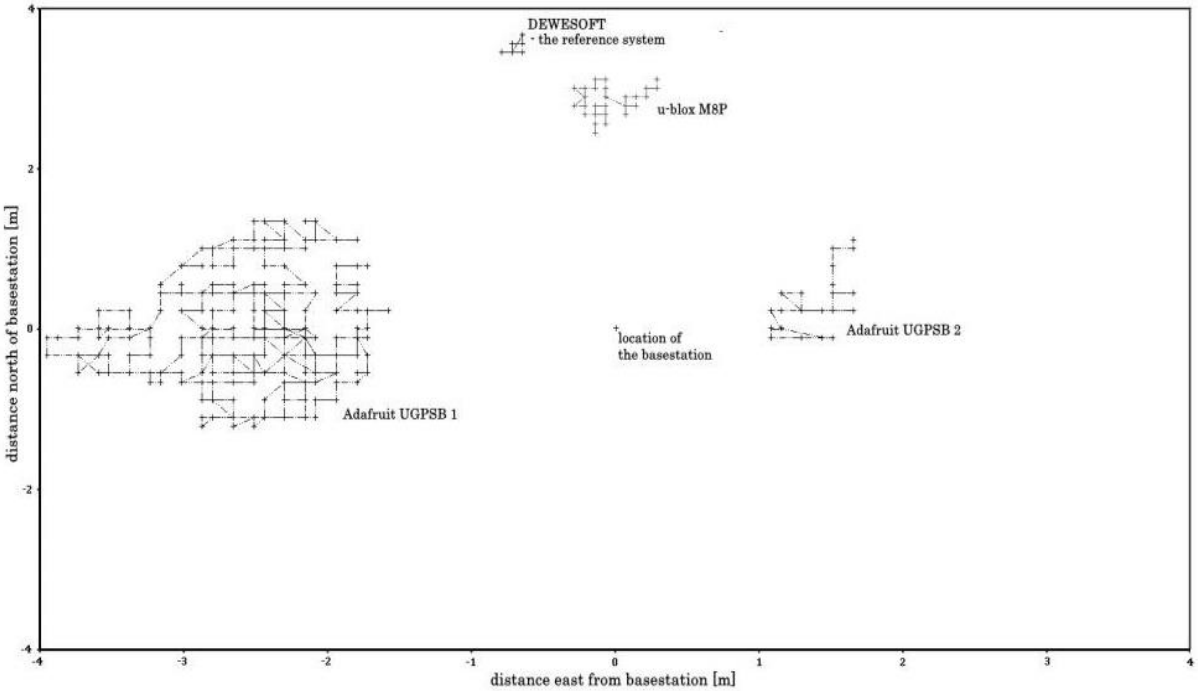

Fig. 1 Map of the static measurement

In the next step the dynamical measurement was conducted. With all measurement equipment was moving (without base station) along the randomize trajectory selected by the car driver. The points of measured trajectory were rendered to Fig. 2. The measurement took 320 s and the distance deviation was measured here with the same way as in first measurements.

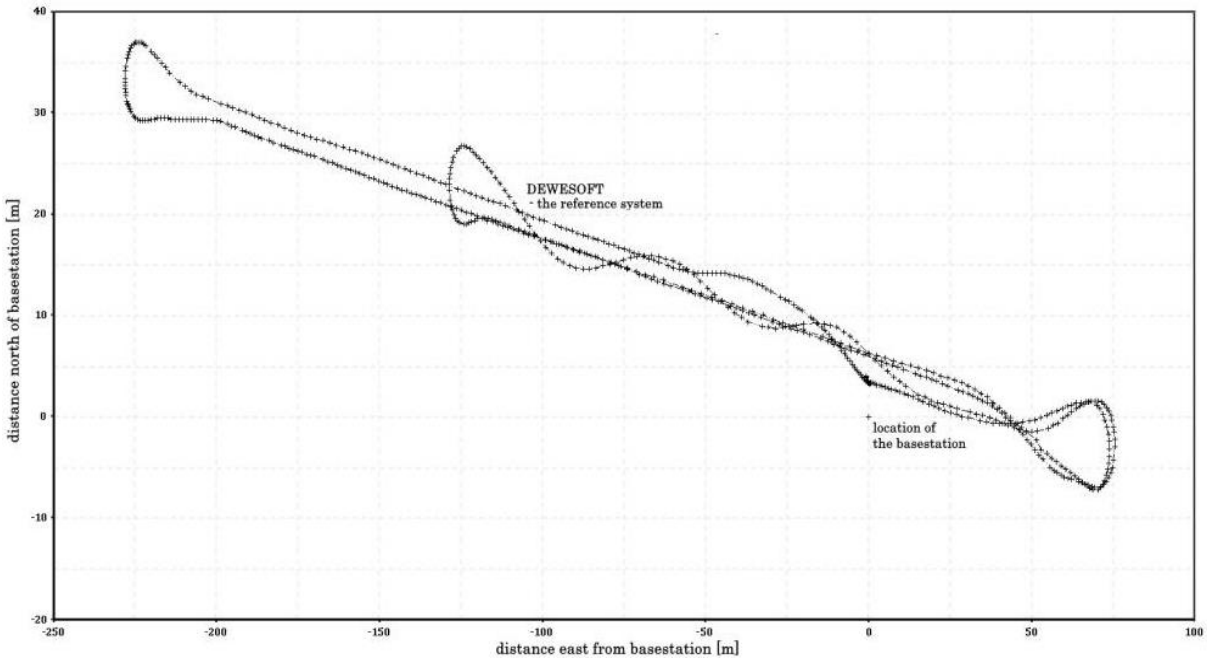

Fig. 2 Map of the dynamic measurement

RESULTS AND DISCUSSION

The similarity of results (Fig. 3) is evident from the static measurement of the USGPS1 and USGPS2 receivers (identical product) in the mean values of deviations and RMS error. Nevertheless, the area and the dispersion of measured points is different (Fig. 1). The M8P receiver had measured points nearest to the reference system and its values of the deviation, dispersion and RMS error was better. All three receivers was receiving the GPS signal from 11 – 12 satellites in the all time of this measurement.

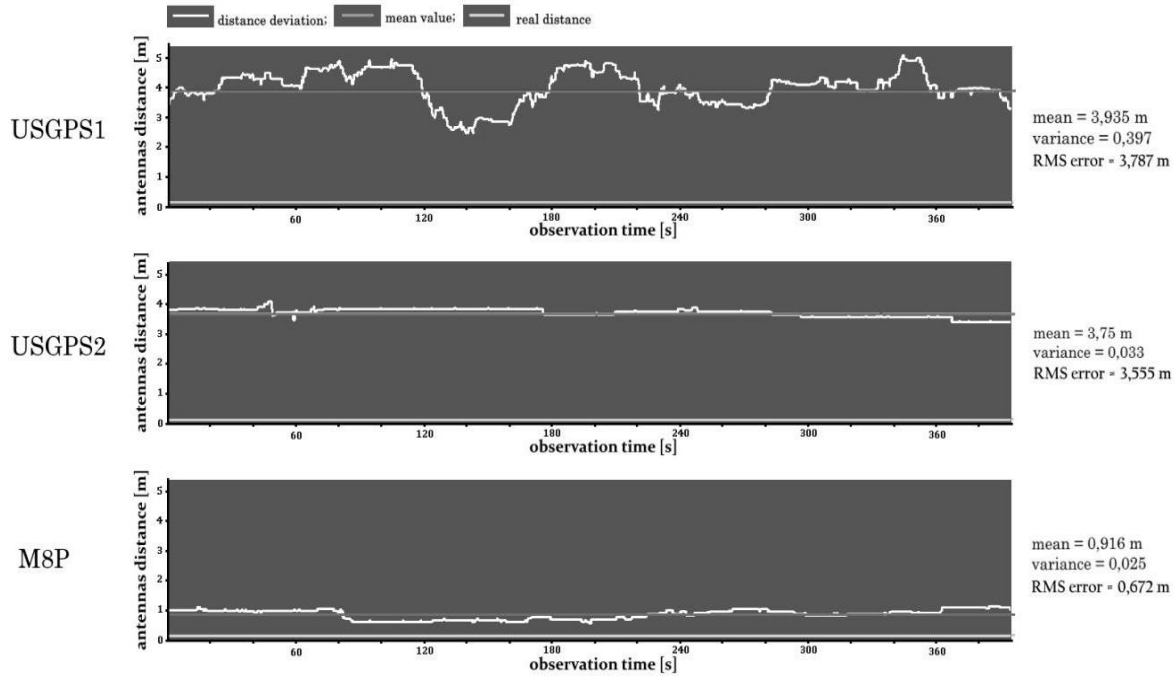

Fig. 3 Rresults of the static measurement

The dynamical measurement (Fig. 4) showed paradoxically the better result of the deviations but the move of all measurement equipment was reflecting in its dispersion values. The better values had the

M8P receiver than the USGPS1 and USGPS2 receivers in all cases. It could be that the M8P had the signal from more satellites, concretely 12 in the time of measurement and the receivers USGPS1 and USGPS2 received irregularly 9 – 12 satellites.

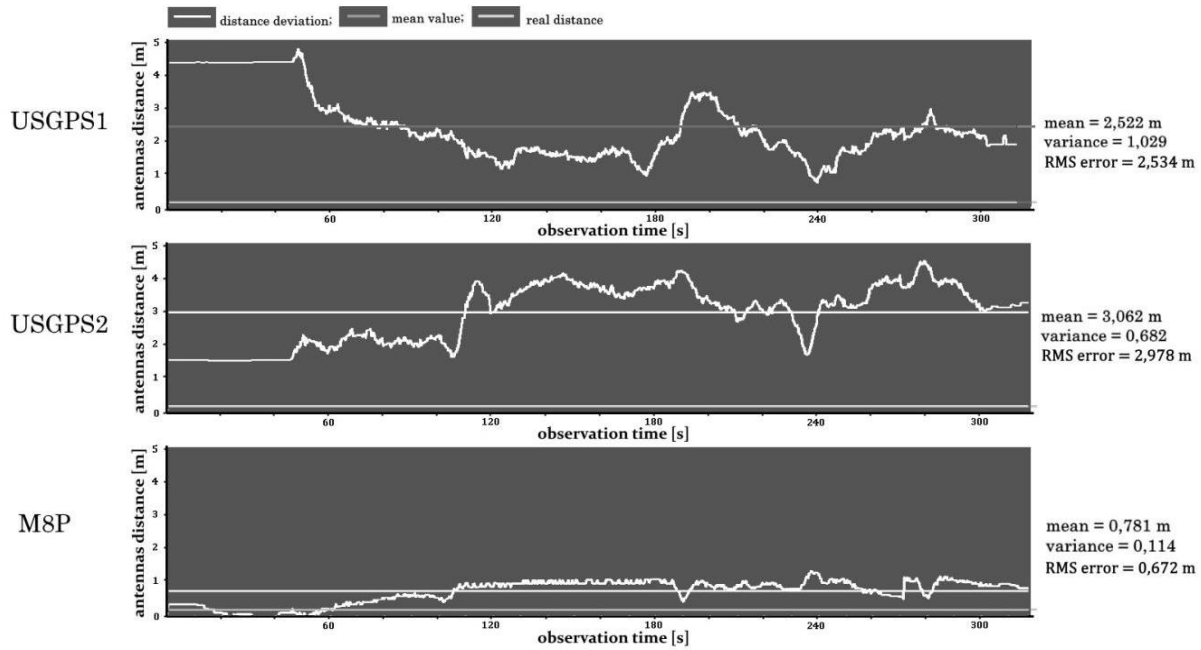

Fig. 4 Results of the dynamic measurement

The receiver U-Blox M8P with RTK performed better accuracy, however, according od this results still not arise the value RMS error 0,025 m + 1 ppm (*u-Blox, 2017*) specified by the manufacturer. This accuracy was probably given by the receiver inability to solve the problem of ambiguity phases. Generally, the RTK receivers are capable to provide information about position with the centimeter precision only assuming that they are capable to calculate the integer value of the phases of carrier waves including the decimal component of phasis (*Geng, 2010*). In this case, we are talking about so called the "RTK fix mode". If is the receiver capable to solve only the decimal component then the receiver is in so called "RTK float mode". During all measurement in this work the M8P receiver was able to achieve the "RTK fix mode" only once at the beginning of the static measurement in time between 3 and 4 second (5 samples) which makes approximately 0,139 % from all time of both measurement.

Generally, the localization by GNSS is loads the error consist from combination of factors of influences: ephemeris data error, satellite clock error, ionosphere influence, troposphere influence, antennas construction and placement (including multipath error) (*Parkinson, 2001*). These factors could affect the verified receivers in this work, nevertheless, these influences disruptive at GNSS receivers in the variable rate constantly and determine its properties.

Regarding the usual accuracy of GNSS receivers using RTK correction, these receivers typically achieve centimeter precision. In work (*Vega, 2014*) the author achieved the RMS error 13,6 mm with receiver Trimble BX982. The author (*Tamura, 2002*) verified the caliber Leica MC1000 with result of horizontally displacement 15 mm. The work (*Feng, 2008*) proves the dependence of distance of the basestation location on the RMS error. The work (*Geng, 2010*) compares measured accuracies with the phase ambiguity solution.

CONCLUSIONS

The comparison of two different technologies for localization was presented in this work. From the results of horizontal accuracy it was was found that the two identical product (Adafruit Ultrastar GPS) were determining the position differently. Its RMS error ranged between two to four meters.

The RTK system u-Blox M8P presented better results of the localization, nevertheless, but not according to the manufacturer specification. This receiver was capable to determine the position with RMS

error less than one meter. The reason of this deviations was probably given by the receivers inability to solve the problem of ambiguity phases. These areas of research and verification will be the further work of author.

ACKNOWLEDGMENT
This study was supported by GA no. 2017/31160/1312/3123 with topic "Evaluation of Determined Position Accuracy by RTK Receivers".

REFERENCES

1. Berber, M. & Arslan, N. (2013). Network RTK: A case study in Florida. *Measurement*, 46, 2798-2806.
2. Brantley, S. T., Zinnert, J. C., & Young, D. R. (2011). Application of hyperspectral vegetation indices to detect variations in high leaf area index temperate shrub thicket canopies. *US Army Research*, 114.
3. Dlouhý, M., Lev, J. & Kroulík, M. (2016). Technical and software solutions for autonomous unmanned aerial vehicle (UAV) navigation in case of unavailable GPS signal. *Agronomy Research*, 14(3), 733-744.
4. Feng, Y. & Wang, J. (2008). GPS RTK Performance Characteristics and Analysis. *Journal of Global Positioning Systems*, 7, 1-8.
5. Gan-Mor, S., Clark, R. L. & Upchurch, B. L. (2007). Implement lateral position accuracy under RTK-GPS tractor guidance. Computers and Electronics in Agriculture, 59, 31-38.
6. Geng, J., Meng, X., Dodson, A. H., Ge, M. & Teferle, F. N. (2010). Rapid re-convergences to ambiguity-fixed solutions in precise point positioning. *Journal of Geodesy*, 84, 705–714.
7. Moravec, D., Komárek, J., Kumhálová, J., Kroulík, M., Prošek, J., & Klápště, P. (2017). Digital elevation models as predictors of yield: Comparison of an UAV and other elevation data sources. *Agronomy Research*, 15(1), 249-255.
8. Parkinson, B. & Spilker, J. (2001). Global Positioning System: Theory and Applications.
9. Perez-Ruiz, M. & Upadhyaya, S. K. (2012). GNSS in Precision Agricultural Operations. *InTech*.
10. Rossmann, J., Schlette, C., Emde, M., & Sondermann, B. (2010). Discussion of a Self-Localization and Navigation Unit for Mobile Robots in Extraterrestrial Environments. *i-SAIRAS*.
11. Tamura, Y., Matsui, M., Pagnini, L., Ishibashi, R. & Yoshida A. (2002). Measurement of wind-induced response of buildings using RTK-GPS, *Journal of Wind Engineering and Industrial Aerodynamics*, 90, 1783-1793.
12. Tsukor, V., Klose, R. & Ruckelshausen, A. (2012). Multi-sensor simulation method for outdoor plant phenotyping based on autonomous field robots. *CIGR*.
13. u-Blox. (2017). NEO-M8P u-blox M8 High Precision GNSS Modules Data Sheet, https://www.u-blox.com/sites/default/files/NEO-M8P_DataSheet_%28UBX-15016656%29.pdf.
14. Vega, A. J. (2014). Comparison of positional accuracy between RTK and RTX GNSS gased on the autonomous agricultural vehicles under field conditions. *Applied engineering in agriculture*, 30(3), 361-366.

Corresponding author:
Ing. Jan Kadeřábek., Department of Agriculture Machines, Faculty of Engineering, Czech University of Life Sciences Prague, Kamýcká 129, Praha 6, Prague, 16521, Czech Republic, phone: +420 22438 3149, e-mail: jkaderabek@tf.czu.cz

VLIV BAINITU A MARTENZITU NA ABRAZIVNÍ OPOTŘEBENÍ OCELI

Adam KEŠNER[1], Miloslav LINDA[2], Monika HROMASOVÁ[2]

[1]*Katedra materiálu a strojírenské technologie, Technická fakulta, Česká zemědělská univerzita v Praze*
[2] *Katedra elektrotechniky a automatizace, Technická fakulta, Česká zemědělská univerzita v Praze*

Abstrakt
Tento článek je zaměřen na problematiku abrazivního opotřebení ocelí používaných u zemědělských nástrojů. Abrazivní opotřebení bylo testováno na oceli 25CrMo4. Pro experiment byla navržena bainiticko-martenzitická struktura oceli. Pro zjištění velikosti abrazivního opotřebení oceli byla zvolena normalizovaná metoda ASTM G65. Výsledky ukazují, že složení mikrostruktury ovlivňuje velikost abrazivního opotřebení.

Klíčová slova: *mikrostruktura ocelí; ASTM G65; abrazivní opotřebení.*

Abstract
This article is focused on abrasive wear of steels used for agricultural tools. Abrasive wear was tested on 25CrMo4 steel. The bainitic-martensitic steel structure was designed for experimentation. The standardized method ASTM G65 was chosen to determine the amount of abrasive wear of steel. The results show that the composition of the microstructure affects the amount of abrasive wear.

Key words: *microstructure of steels; ASTM G65; abrasive wear.*

ÚVOD

Společným zájmem výrobců součástí, které jsou namáhány na abrazivní opotřebení, je zvyšovat odolnost proti abrazivnímu opotřebení za současného zachování nebo snižování nákladů na výrobu (*Jankauskas et al. 2014; Jankauskas & Skirkus, 2013a*). Technologie zvyšující odolnost proti abrazivnímu opotřebení jako je navařování, povlakování, apod. nelze aplikovat na všechny součásti (*Thakare et al,. 2012; Herian et al., 2014; Sabet et al., 2011; Vite-Torres et sl., 2011*). Jedná se o součásti, na které jsou kladeny další požadavky jako je tvrdost, houževnatost, dodržení přesných rozměrů, apod (*Jankauskas & Skirkus, 2013b; Oladijo et al., 2012*). Právě tyto vlasnosti nelze dodržet s výše zmíněnými technologiemi. Z tohoto důvodu je nutné se zaměřovat na zvyšování abrazivní odolnosti proti opotřebení samotných ocelí (*Konyashin & Ries, 2014*). Toho může být dosaženo volbou oceli s vhodným chemickým složením (přidání boru, chromu, křemíku) (*Béjar & Moreno, 2006; Jankauskas et al., 2008*) a tepelným zpracováním (*Baburaj et al., 2013; Liu et al., 2014; Bhakat et al., 2007*). Tepelné zpracování umožňuje vznik různých mikrostruktur, které mají odlišné vlastnosti jako jsou tvrdost, houževnatost a právě odolnost proti abrazivnímu opotřebení (*Chotěborský & Hrabě, 2013; Chotěborský et al., 2009; Chotěborský & Linda, 2016*). Kombinace bainitu a martenzitu je vhodná pro součásti, které jsou namáhány na abrazivní opotřebení (*Das Bakshi et al., 2013; Zhou, Wu & Fu, 2013*). Pro vznik bainiticko-martenzitické struktury je vhodné použití izotermického kalení (*Salman et al., 2007; Kim et al., 2008*).
Je známo mnoho metod pro zjištění velikosti abrazivního opotřebení (*Kamdi et al., 2011; Hyttel et al., 2013; Doering et al., 2011*). Metoda ASTM G65 je normalizovaná metoda s přesně definovanými parametry zkoušek ocelí pro zjištění velikosti abrazivního opotřebení. Princip metody spočívá v aplikaci písku s velikostí zrn 0,200 až 0,315 μm mezi vzorek a kotouč s pryžovým obvodem. Tento mechanimus je podobný působení abrazivních částic na zemědělský nástroj v půdě (*Oladijo et al., 2014; Elalem & Li, 1999; Chacon-Nava et al., 2010*).
Cílem této práce bylo zjistit vliv baitinicticko-martenzitické struktury vybrané oceli na velikost abrazivního opotřebení. Někteří autoři uvádí, že tvrdost je hlavní parametr pro abrazivní opotřebení. Z tohoto důvodu byl ověřován vliv tvrdosti na velikost abrazivního opotřebení.

MATERIÁL A METODY

Pro experiment byla vybrána ocel 25CrMo4, která je používána pro zemědělské součásti, na které působí abrazivní opotřebení. Chemické složení oceli je uvedeno v Tab. 1. Vzorky byly připraveny o velikosti 25 x 10 x 50 mm. Velikost vzorků odpovídá normě pro abrazivní testy ASTM G65.

Tab. 1 Chemické složení oceli 25CrMo4 (hm. %)

ocel	C	Mn	Si	P	S	Cr	Ni	Cu	Al	Mo	Sn	V	Ti
25CrMo4	0.25	0.71	0.23	0.018	0.022	1.03	0.09	0.23	0.023	0.21	0.011	0.004	0.015

Bylo připraveno 6 vzorků, které byly zpracovány izotermickým kalením. Izotermické kalení bylo navrženo tak, aby kombinace bainiticko-martenzitické struktury byla co nejvíce rozdělena (od 100 % bainitu až ke 100 % martenzitu). Parametry izotermického kalení byly odečteny z IRA digramu dodaného od výrobce oceli. Všechny vzorky měly teplotu ohřevu 800°C. Pro ochlazování byla použita solná lázeň 50 hm.% $NaNO_2$ + 50 hm.% $NaNO_3$. Parametry ochlazování pro jednotlivé vzorky jsou uvedeny v Tab. 2.

Tab. 2 Parametry ochlazování vzorků oceli 25CrMo4

Číslo	1. ochlazování			2. ochlazování			3. ochlazování		
vzorku	teplota	médium	čas	teplota	médium	čas	teplota	médium	čas
1	400°C	solná lázeň	35 s	400°C	vzduch	160 s	20°C	vzduch	do 20°C
2	400°C	solná lázeň	35 s	20°C	voda	do 20°C	—	—	—
3	300°C	solná lázeň	40 s	300°C	vzduch	1000 s	20°C	vzduch	do 20°C
4	300°C	solná lázeň	40 s	20°C	voda	do 20°C	—	—	—
5	400°C	solná lázeň	40 s	400°C	vzduch	1200 s	20°C	vzduch	do 20°C
6	400°C	solná lázeň	40 s	20°C	voda	do 20°C	—	—	—

Po tepelném zpracování byly vzorky připraveny na abrazivní testy. Příprava všech vzorků probíhala následujícím způsobem: všechny vzorky byly zbaveny oxidů po izotermickém kalení, plocha 25 x 10 mm byla broušena na kotouči Struers MD Piano o velikost 0.1 mm. Po broušení každé plochy byla měřena tvrdost (HRC). Broušení plochy o 0.1 mm bylo opakováno do doby, než byla tvrdost stejná. Následně byla plocha přebroušena kotoučem Struers MD Allegro s přidáním diamantové suspenze Struers 9 μm.

Metoda testování odolnosti proti abrazivnímu opotřebení ASTM G65 byla prováděna na broušené ploše. Mezi vzorek a kotouč s pryžovým obvodem (ø210 mm, šířka kotouče byla 12.5 mm) dopadaly částice písku o velikosti 0.200 až 0.315 μm. Kotouč byl přitlačován na vzorek silou 100 N. Měření bylo 10x opakováno. Před a mezi každým měřením byla na analytických vahách změřena hmotnost vzorku.

Příprava vzorků na obrazovou analýzu probíhala následujícím způsobem: vzorky byly rozříznuty ve své polovině. Rozříznutá plocha byla broušena kotouči Struers MD Piano s přidáním vody, Struers MD Allegro s přidáním diamantové suspenze Struers 9 μm, Struers MD Dac s přidáním diamantové suspenze Struers 3 μm. Následovalo leštění kotoučem Struers MD Chem s přidáním suspenze Struers OP-S. Leptání plochy bylo provedeno 2% nitalem (1 ml HNO3 + 50 ml ethanolu). Obrazová analýza byla provedena od středu vzorku k jeho okraji po vzdálenosti 0.5 mm. Analýza probíhala na elektronovém mikroskopu SEM (Tescan Mira 3 GXM) vybaveného energiově disperzním detektorem X-ray (Oxford X-MaxN). Z mikroskopu byly ukládány snímky o velikosti 104x104 μm.

Snímky byly analyzovány v programu QuickPHOTO INDUSTRIAL 3.1., kde bylo zjištěno zastoupení ploch jednotlivých fází.

Tvrdost (HV) byla měřena ve stejných místech, odkud byly ukládány snímky.

VÝSLEDKY A DISKUZE

Závislost hmotnostních úbytků jsou ukázány na Obr. 1. Výsledky byly pro lepší přehlednost vyneseny do dvou grafů. Největší hmotnostní úbytky a tedy nejmenší odolnost proti abrazivnímu opotřebení byly naměřeny u vzorku 1. Naopak největší odolnost proti abrazivnímu opotřebení byla naměřena u vzorku 4. Výsledky byly statisticky porovnány pomocí F-testu. Izotermické kalení nemělo vliv mezi vzorky 3 a 5, 3 a 6, 5 a 6. Rozdíly hmotnostních úbytků ostatních kombinací vzorků jsou statisticky významné.

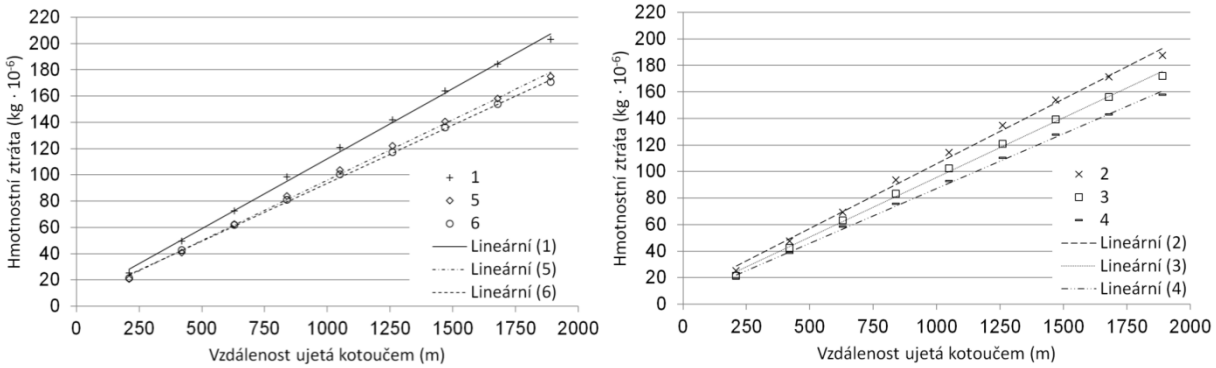

Obr.1 Závislost hmotnostní ztráty na vzdálenosti ujeté kotoučem

Výsledky mikrostruktury pro jednotlivé vzorky jsou ukázány na Obr. 2 a 3. U všech vzorků byla zjištěna kombinace bainitu a martenzitu. Příklady fáze bainitu je ukázána na Obr. 2 a 3, kde bainit je označen písmenem B a martenzit písmenem M. Výsledky poměru fází bainitu a martenzitu jsou uvedeny v Tab. 3.

Tab. 3 Zastoupení fází bainitu a martenzitu pro jednotlivé vzorky

	Označení vzorku					
	1	2	3	4	5	6
Bainit (%)	12	26	99	66	98	73
Martenzit (%)	88	74	1	34	2	27

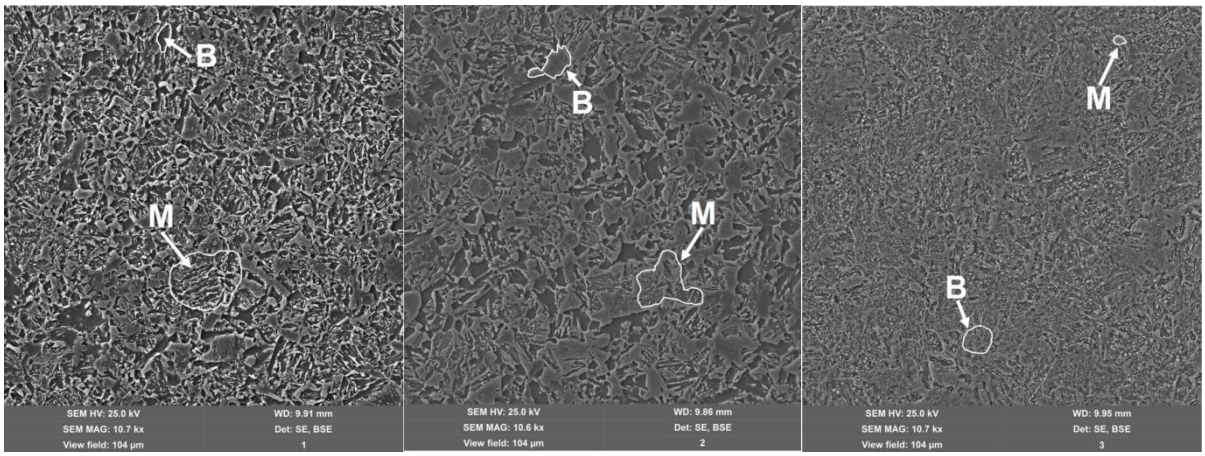

Obr. 2 Mikrostruktury pro vzorky 1, 2, 3 oceli 25CrMo4

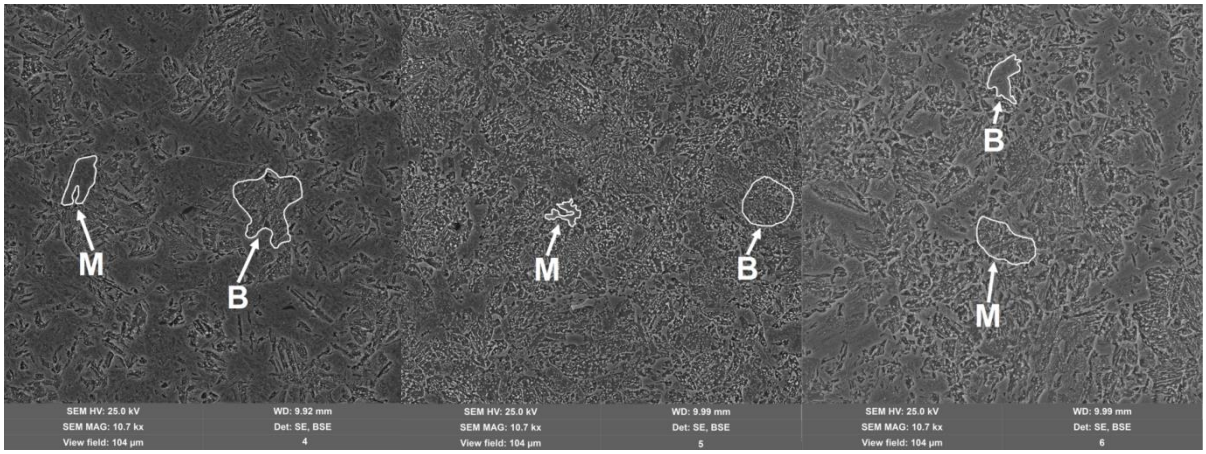

Obr. 3 Mikrostruktury pro vzorky 1, 2, 3 oceli 25CrMo4

Závislost mikrostruktury na hmotnostní ztrátě je ukázána na Obr. 4. Nejmenší hmotnostní ztráty naměřených metodou ASTM G65 jsou zjištěny u mikrostruktury s objemovým podílem 60 % až 80 % bainitu a zbytkovým martenzitem. Právě u tohoto objemového podílu mikrostruktury je nejvyšší odolnost proti abrazivnímu opotřebení oceli 25CrMo4. U objemového podílu mikrostruktury s 10 % až 30 % bainitu a zbytkového martenzitu je naměřen nejvyšší hmotnostní úbytek a je zde nejmenší odolnost proti brazivnímu opotřebení oceli 25CrMo4.

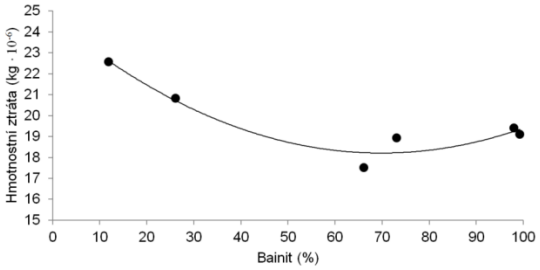

Obr. 4 Závislost hmotnostní ztráty na podílu bainitu v mikrostruktuře

Tvrdost byla zkoumána v závislosti na mikrostruktuře – viz Obr. 5 vlevo. Nejvyšší tvrdosti bylo dosaženo u mikrostruktury s 66% bainitu a zbytkového martenzitu. Nejmenší tvrdosti proti opotřebení bylo dosaženo u mikrostruktury s podílem 12 % a 26 % bainitu a zbytkového martenzitu. Tento trend odpovídá hmotnostním ztrátám na Obr. 4. Z výsledku je tedy patrné, že mikrostruktura ovlivňuje tvrdost ocelí a odolnost oceli proti abrazivnímu opotřebení. Velikost hmotnostního úbytku zjištěného metodou ASTM G65 je ukázán na Obr. 5 vpravo. S většími hodnotami tvrdosti klesá hmotnostní úbytek oceli.

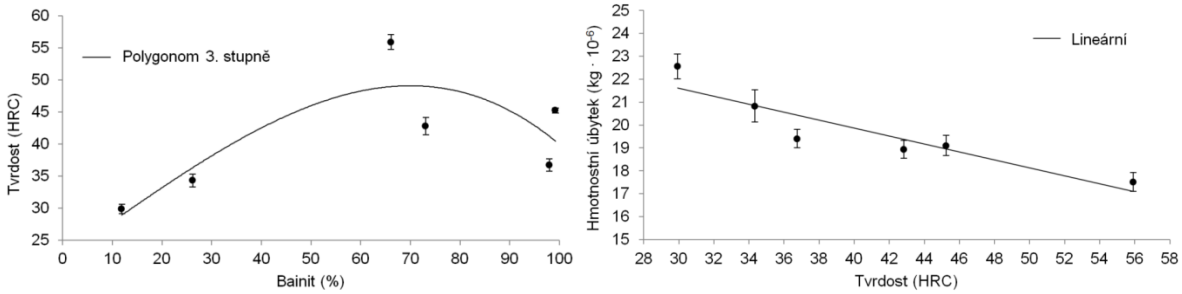

Obr. 5 Vlevo - Závislost tvrdosti na podílu bainitu v mikrostruktuře, vpravo - Závislost mezi hmotnostním úbytkem a tvrdostí oceli 25CrMo4

Autoři *(Bhakat et al., 2004; Sabet et al., 2011; Vite-Torres et al., 2011*) uvádějí, že tvrdost je nejdůležitější pro velikost abrazivního opotřebení ocelí. Naopak autoři *(Xu et al., 2016; Šolić et al., 2016; Varga & Badisch, 2017*) uvádějí, že mikrostruktura má největší vliv na velikost abrazivního opotřebe-

ní ocelí. Jak ukazují výše uvedené výsledky této práce, mikrostruktura má významný vliv na velikost abrazivního opotřebení. Bylo by však dobré práci rozšířit o další podíly bainitu a martenzitu. Také jiné oceli by mohly být zkoumány a porovnány s výsledky této práce.

ZÁVĚR

Na základě výsledků této práce lze konstatovat následující tvrzení:

- Nejvyšší odolnost proti abrazivnímu opotřebení je u mikrostruktury s podílem bainitu 66 % a 73 %. Nejmenší odolnost proti abrazivnímu opotřebení byla zjištěna u bainitu 12 % a 26 % a zbytkového austenitu.
- Různý podíl bainitu a martenzitu má významný vliv na tvrdost a velikost abrazivního opotřebení. Různý podíl bainitu a martenzitu je dosažen i malými změnami ochlazovacích parametrů izotermického kalení.
- Tvrdost je závislá na mikrostuktuře oceli. Nejvyšší tvrdost (56 HRC) byla zjištěna u 66 % bainitu. I malé změny podílu bainitu (66 % a 73%) a martenzitu mohou mít vliv na velikost tvrdosti – rozdíl 15 HRC.
- S rostoucími hodnotami tvrdosti se zvyšuje odolnost proti abrazivnímu opotřebení.

PODĚKOVÁNÍ

Tento článek vznikl díky podpoře Interní grantové agentury 31140/1312/3114 na Technické fakultě, České zemědělské univerzity v Praze.

LITERATURA

1. Baburaj, A., Chaudhary, S. S. K. B., Khatirkar, R. K., & Sapate, S. G. (2013). Abrasive Wear Behaviour of Heat Treated En31 Steel. *ISIJ International*. *53*(8), (pp. 1471–1478).
2. Béjar, M.A., & Moreno, E. (2006). Abrasive wear resistance of boronized carbon and low-alloy steels. *Journal of Materials Processing Technology*. *173*(3), (pp. 352–358).
3. Bhakat, A. K., Mishra, A. K., & Mishra, N. S. (2007). Characterization of wear and metallurgical properties for development of agricultural grade steel suitable in specific soil conditions. *Wear*. *263*(1–6), (pp. 228–233).
4. Bhakat, A. K., Mishra, A. K., Mishra, N. S., & Jha, S. (2004). Metallurgical life cycle assessment through prediction of wear for agricultural grade steel. *Wear*. *257*(3–4), (pp. 338–346).
5. Das Bakshi, S., Shipway, P. H., & Bhadeshia, H. K. D. H. (2013). Three-body abrasive wear of fine pearlite, nanostructured bainite and martensite. *Wear*. *308*(1–2), (pp. 46–53).
6. Doering, A., Danks, D., Mahmoud, S., & Scott, J. (2011). Evaluation of ASTM G65 abrasive —Spanning 13 years of sand. *Wear*. *271*(9–10), (pp. 1252–1257).
7. Elalem, K., & Li, D. Y. (1999). Dynamical simulation of an abrasive wear process. *Journal of Computer-Aided Materials Design*. *6*(2), (pp. 185–193).
8. Herian, J., Aniolek, K., Cieśla, M., & Skotnicky, G. (2014). Shaping the structure during rolling and isothermal annealing, and its influence on the mechanical characteristics of high-carbon steel. *Materials Science and Engineering: A*. *608*, (pp. 149–154).
9. Hyttel, M.W., Olsson, D.D., Reisel, G., & Bøttiger, J. (2013). Comparison of a newly developed compression-twist abrasive wear test with the ASTM G65 test method. *Wear*. 307(1–2), (pp. 134–141).
10. Chacon-Nava, J. G,, Martinez-Villafañe, A., Almeraya-Calderon, F., Cabral-Miramontes, J. A., & Stack, M. M. (2010). Some remarks on particle size effects on the abrasion of a range of Fe based alloys. *Tribology Internationa*. 43(8), (pp. 1307–1317).
11. Chotěborský, R., & Hrabě, P. (2013). Effect of destabilization treatment on microstructure, hardness and abrasive wear of high chromium hardfacing. *Research in Agricultural Engineering*. *59*(4).
12. Chotěborský, R., Hrabě, P., Müller, M., Savková, J., Jirka, M., & Navrátilová, M. (2009). Effect of abrasive particle size on abrasive wear of hardfacing alloys. *Research in Agricultural Engineering*. *55*(3).
13. Chotěborský, R., & Linda, M. (2016). Determination of chemical content of soil particle for abrasive wear test. *Agronomy Research*. *14*

14. Jankauskas, V., Katinas, E., Skirkus, R., & Aleknevičiene, V. (2014). The method of hardening soil rippers by surfacing and technical-economic assessment. *Journal of Friction and Wear*. 35(4), (pp. 270–277).
15. Jankauskas, V., Kreivaitis, R., Milčius, D., & Baltušnikas, A. (2008). Analysis of abrasive wear performance of arc welded hard layers. Wear [online]. November 2008. Vol. 265, no. 11–12, p. 1626–1632.
16. Jankauskas, V., & Skirkus, R. (2013a). Steel abrasive wear forecasting by wearing surfaces microgeometric parameters. *Mechanika*. 19(4).
17. Jankauskas, V., & Skirkus, R. (2013b). Investigations of abrasive wear of steel surfaces strengthened by vibro-arc carbonization/layering. *Surface Engineering and Applied Electrochemistry*. 9(5), (pp. 396–400).
18. Kamdi, Z., Shipway, P. H., Voisey, K. T., & Sturgeon, A. J. (2011). Abrasive wear behaviour of conventional and large-particle tungsten carbide-based cermet coatings as a function of abrasive size and type. *Wear*. *271*(9–10), (pp. 1264–1272).
19. Kim, Y. J., Shin, H., Park, H., & Lim, J. D. (2008). Investigation into mechanical properties of austempered ductile cast iron (ADI) in accordance with austempering temperature. *Materials Letters*. *62*(3), (pp. 357–360).
20. Konyashin, I., & Ries, B. (2014). Wear damage of cemented carbides with different combinations of WC mean grain size and Co content. *International Journal of Refractory Metals and Hard Materials*. *46*, (pp12–19).
21. Liu, S.G., Dong, S.S., Yang, F., Li, L., Hu, B., Xiao, F.H., Chen, Q., & Liu, H.S. (2014). Application of quenching–partitioning–tempering process and modification to a newly designed ultrahigh carbon steel. *Materials & Design*. *56*, (pp. 37–43).
22. Oladijo, O.P., Sacks, N., Cornish, L.A., & Venter, A.M. (2012). Effect of substrate on the 3 body abrasion wear of HVOF WC-17wt.% Co coatings. *International Journal of Refractory Metals and Hard Materials*. *35*, (pp. 288–294).
23. Oladijo, O.P., Venter, A.M., & Cornish, L.A. (2014). Correlation between residual stress and abrasive wear of WC–17Co coatings. *International Journal of Refractory Metals and Hard Materials*. *44*, (pp. 68–76).
24. Sabet, H., Khierandish, S., Mirdamadi, S., & Goodarzi, M. (2011). The Microstructure and Abrasive Wear Resistance of Fe–Cr–C Hardfacing Alloys with the Composition of Hypoeutectic, Eutectic, and Hypereutectic at Cr /C6. *Tribology Letters*. 44(2), (pp. 237–245).
25. Salman, S., Findik, F., & Topuz, P. (2007). Effects of various austempering temperatures on fatigue properties in ductile iron. *Materials & Design*. *28*(7), (pp. 2210–2214).
26. Šolić, S., Godec, M., Schauperl, Z., & Donik, Č. (2016). Improvement in Abrasion Wear Resistance and Microstructural Changes with Deep Cryogenic Treatment of Austempered Ductile Cast Iron (ADI). *Metallurgical and Materials Transactions A*. *47*(10), (pp. 5058–5070).
27. Thakare, M.R., Wharton, J.A., Wood, R.J.K., & Menger, C. (2012). Effect of abrasive particle size and the influence of microstructure on the wear mechanisms in wear-resistant materials. *Wear*. *276–277*, (pp. 16–28).
28. Varga, M., & Badisch, E. (2017). Temperature and load influence on in-situ formed layers during high temperature abrasion. *Wear*. *384–385*, (pp. 114–123).
29. Vite-Torres, M., Vite, J., Laguna-Camacho, J. R., Castillo, M., & Marquina-Chávez, A. (2011). Abrasive wear on ceramic materials obtained from solid residuals coming from mines. *Wear*. *271*(9–10), (pp. 1231–1236).
30. Xu, X., Van Der Zwaag, S., & Xu, W. (2016). The effect of ferrite and martensite morphology on the scratch and abrasive wear behaviour of a dual phase construction steel. *Wear*. *348–349*, (pp. 148–157).
31. Zhou, H., Wu, Z.W., & Fu, H. (2013). A study of self-hardening bainitic cast steel. *Materialwissenschaft und Werkstofftechnik*. *44*(9), (pp. 753–759).

Autor pro korespondenci:
Ing. Adam Kešner, Katedra materiálu a strojírenské technologie, Technická fakulta, Česká zemědělská univerzita v Praze, Kamýcká 129, Praha 6, Praha, 16521, Česká republika, telefon: +420 721 608 926, e-mail: kesner@tf.czu.cz

THE CONSUMPTION OF TRANSPORT ENERGY – PERSPECTIVES OF ELECTRIC VEHICLES

Miroslav KRUMBHOLC

Department of Vehicles and Ground Transport, Faculty of Engineering, Czech University of Live Sciences Prague

Abstract

This paper is aimed to provide a literature overview on a topic of a construction of electro-vehicles, usage of energy mix, vehicles' advantages and disadvantages. It contains a description of components of the electric devices. The paper compares advantages and disadvantages of the electric vehicles with combustion engine vehicles.

Key words: *construction of electro vehicles, energy mix, vehicle´s advantages and disadvantages.*

INTRODUCTION

The first standard dealing with exhaust fumes was developed in California in 1968. The first emission standard in 1971 - EEO 15 was introduced in Europe. It is a binding European Union (EU) standard setting limits for exhaust emissions of petrol and diesel engines for motor vehicles depending on the weight of the pollutant over the distance traveled. Standards set limits for carbon monoxide (CO), hydrocarbons (HC), nitrogen oxides (NOx) and particulate matter (PM); Norms does not deal with carbon dioxide or sulfur compounds. The standard is issued in gradually tightening numbered versions. Currently, in 2017 the EURO 6 standard is in force (September 2014). However, the monitored substances are not the only ones that are discharged by the combustion engine. There is, for example, carbon dioxide CO_2, which is often mentioned in connection with global warming. The reason for monitoring this greenhouse gas is a significant increase in vehicle sales in the developing world and a strong position within the EU, where individual passenger transport occupies an exclusive position as compared to other modes of transport. Tracking and regulation of emissions of new vehicles to the EU market, particularly passenger cars, is an important task for which it is necessary to lay down appropriate implementing regulations and decrees leading to a sound development of vehicle technology and reducing exhaust emissions, including carbon dioxide, leading to reduced fuel consumption of such vehicles and increase their energy efficiency.

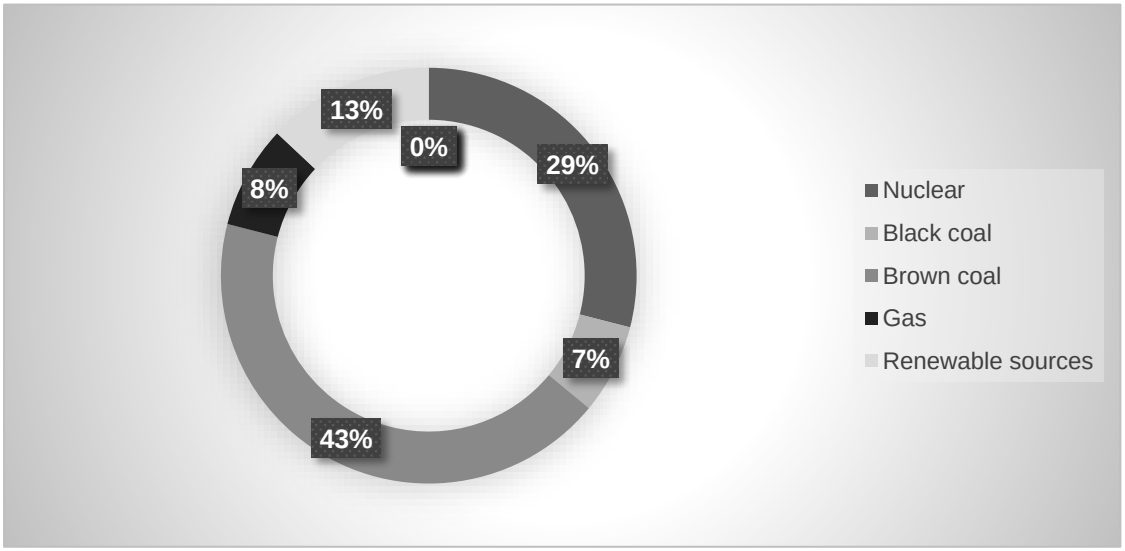

Graph 1 The share of fuels and technologies for production electricity in the Czech Republic in 2016 (*Blythe et al., 2017*)

MATERIALS AND METHODS

Electro vehicles charging technology. The charging design is available in three versions:
The first type is low speed with a conventional 230 V home type socket, where a vehicle charging module is used that transforms the gain to direct current (DC) to the vehicle's traction batteries. This type of charging is used in practice when recharging traction batteries in the home environment. Recharging is used by the vehicle manufacturer to supply the interconnecting recharge cable with a special control module that limits the maximum charge current so that the electrical installation of the house is not overloaded (in the Czech Republic, the maximum rated current of the 230 V mains socket is 16 A, the charging module setting of the vehicle cable usually 10 A). Because this rechargeable wire is often supplied as the only type for a new car, public charging stations are also equipped with this possible way of interconnection. This embodiment has a recharge time of about 12 hours.
The second type is for fast recharging and is the most widespread. Compared to the previous low-speed recharging, the interconnect cable does not contain a constraint module to control the electrical wiring of the house. Special sockets called Mennekes (according to socket manufacturer) are used and maximum current consumption is permitted according to the requirement of the vehicle charger. Thus, the charging time is reduced to only half compared to the previous variant. However, the charging time is still in the order of hours, based on the total energy capacity of the traction accumulators.
The third type of charging is the fastest, in tens of minutes. This method requires a special charging device that is highly energy-intensive and therefore it is not possible to install such a device in domestic conditions. The only one uses a rechargeable DC voltage that is fed directly to the vehicle's traction accumulator. However, this method is the least appropriate for the battery life cycle.

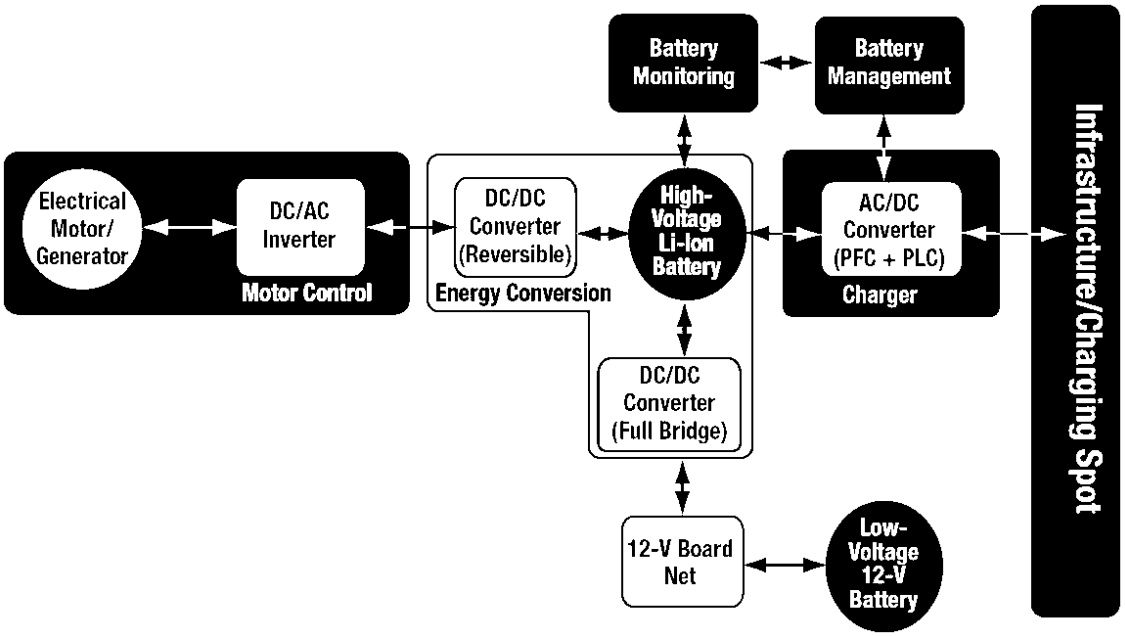

Fig. 1 Block diagram of an electric car (First et al., 2008)

The construction of an electric vehicle is related to the design of a conventional vehicle with an internal combustion engine as we know it. This is mainly a vehicle with a self-supporting body, rather small in size for easy movement in urban agglomerations, allowing easy maneuvering and parking or the dimensions of sports cars where the torque of the electric motor is very favorable. According to the drive configuration, the torque of the electric motor is transmitted to the front, rear or all wheels. The high operating speed range provided by the electric motor, its design and technical characteristics, and above all its favorable performance characteristics, allow for the absence of hydrodynamic or friction clutches and transmissions, which greatly simplifies the technical concept of the drive and, above all, user control and vehicle assistance systems. The output shaft of the electric motor is this connected directly to the end-gear reducer and the differential, which ensures the transmission

of the torque on individual axles. A synchronous three-phase electric motor is used for the drive where the efficiency, weight, overload and reliability ratio is excellent. An important advantage is the design of the rotor of the electric motor. It is not formed by the winding and eliminates the need for brushes that are subject to wear due to traffic. The electric motor is maintenance-free from a regular service point of view. Drive traction accumulators are located under the floor of the vehicle and / or in the luggage compartment. Due to the current rate of evolution of traction accumulators, where there is still a large proportion of available energy per unit mass and volume, the storage of large and heavy accumulators under the floor of the vehicle is particularly advantageous from a practical point of view, where the volume of the luggage compartment is not reduced. In terms of driving characteristics, such a placement means a significant reduction in the center of gravity of the vehicle.
The traction accumulator provides for passenger cars a voltage range of 350 - 400 V, which is carefully monitored by a number of electronic components and systems. For users a much higher level of protection against electric shock is ensured than with normal home or apartment use, where the 230 V voltage is normally used. In addition there is no electric shock when touching one pole of the electrical wiring due to the absence of earthing part of the divorce as is the case with domestic electricity distribution.

The most widespread design of currently used batteries is despite their relatively high lithium ion price. The main benefits of this type of battery include zero memory effect. It can therefore be recharged at any stage of discharge into any charging state, eg from 5% charge up to 82% charge of the battery. The disadvantage is the rapidly decreasing capacity due to temperature outside the optimum range, which ranges from 5 to 30 ° C. For operating under unfavorable climatic conditions such as a temperature range, manufacturers of some electric vehicles can supply batteries with heating elements or connect the battery body to the heating and air conditioning circuit of the vehicle interior. In general, we can expect a dynamic shift in the development of electric power sources for electric drives in the coming decades, whether in the form of accumulators, hydrogen fuel cells or other sources.
Low-energy vehicle on-board systems are powered by a second 12 V on-board battery, which is recharged while the vehicle is running from the traction battery while charging traction batteries from the vehicle's charger. This concept allows the power supply of 12 V system and vehicle sensors before switching on the traction battery contactors that are in the open state when the vehicle is switched off. In the event of a fault in the power distribution of the drive, the battery contactors will not be switched on and therefore the possible consequences of faults will be avoided. The fundamental difference in the construction of electric vehicles is the heating solution to ensure the thermal comfort in the passenger vehicle. The use of heat losses of the combustion space, drained by the coolant to the water / air heat exchanger in the interior of the vehicle, is very limited in the case of an electric device. The electric motor and its accessories are connected in the same way as the combustion engine to the cooling circuit, the coolant heat values in relation to the electric drive performance do not reach temperatures above 75 ° C and at low engine load the coolant temperature does not reach 40 ° C. This does not suffice for sufficient and timely heating of the interior of the vehicle. Vehicle comfort is thus provided by electric heating, hot-water heating (electric heating spirals heat up the liquid supplied to the water / air exchanger) or hot-air (electrical heating resistors heat the exchanger body through which air is fed into the interior of the vehicle). In the summer season air cooling is provided by an air conditioning compressor that is driven directly by a special electric motor, which ensures greater power efficiency compared to drive belt drive and pulley assembly. The electric motor is designed in a brushless three-phase design. Such an engine is an inverter that converts the DC voltage of the traction accumulator into alternating three-phase voltages. In addition to an electric motor are the heating and air conditioning system the most important electrical appliance and the extent of its use greatly influenced by the electrification range.
Crew safety must be at the same level as for internal combustion engine vehicles, so the traction accumulator and its electrical wiring bundles in the vehicle are located outside the deformation zones. Independent body resistance testing (eg EURO NCAP) in impact is the same as conventional vehicles. The components of the rescue integrated system (in particular the Fire Rescue Corps) are informed at the national level by the importer / manufacturer of the electrical device about the way of its identifica-

tion, procedures for neutralizing the electrolyte of the batteries and the possibilities of division of the body for the needs of rescue of the vehicle after an accident.

RESULT AND DISCUSSION

An electric car is often associated with eco-friendly operation. The electric car has zero emissions at the point of its operation but it is necessary to consider the way electric cars are consumed. Electricity originates in the Czech Republic from various sources, which can be expressed by the so-called energy mix. That is by a mix of resources which in proportion to the whole supply electricity to the power system. In each country. This energy mix differs according to the available natural resources and the state concept of electricity generation.

CONCLUSION

The environmental benefits of electrified vehicles need to be taken from a wider perspective, is not only to evaluate the production of vehicle emissions as such. The power generation from which the traction accumulator is charged can be produced with completely different methods and their harmful gas production is markedly different (coal / wind power). The benchmark between electric vehicle and the combustion-engine vehicle can be used to select emissions per kilometer of distance traveled. In the case of an electric car, this is recalculated from the emissions produced by the power plants in the energy mix in the given location (state, continent, etc.). For comparison, vehicle operation is required under the same conditions, so you can choose the New European Driving Cycle (NEDC) driving test used in vehicle approval. After determination of rolling resistance, air resistance and acceleration resistance, it is possible to calculate the instantaneous power output in each second of the driving cycle. From the total cumulative energy requirement during a driving test, one kilometer of energy can be determined, both in the Urban Cycle (UDC) and in the Extra-Urban Cycle (EUDC). The ratio of the individual cycles in the NEDC test can be expressed as the combined consumption per kilometer traveled.

ACKNOWLEDGEMENT

The paper was supported by ULS Prague, Faculty of engineering - IGA project 2017: 31150/1312/3121

REFERENCES

1. Blythe, P. T., Dawson R. J., Heidrich, O., Hill G. A., Huebner, Y., & Neaimeh, M. (2017). How do cities support electric vehicles and what difference does it make?, *Technological Forecasting & Social Change*, http://dx.doi.org/10.1016/j.techfore.2017.05.026
2. First, J. a kolektiv (2008). Zkoušení automobilů a motocyklů, *S&T C s.r.o., Praha*, ISBN 978-80-254-1805-5
3. Hromádko, J., & Miler, P. (2012). Environmental benefits analysis of electric vehicles in the Czech Republic, *Transportation Research Part D: Transport and Environment*, volume 17, issue 2, ISSN: 1361-9209, p. 251-255
4. Košťál, J. (2016). Elektromobilita – budoucnost již začala
5. Kotek, M., Lukeš, M., & Růžička, M. (2015). Comparison of transport systems in rural and suburbanized areas with regards to energy consumption and travel speed, *Engineering for Rural Development*, ISSN 1691-5976, p. 342-347
6. Matoušková, L. (2015). Strategie Evropského společenství ke snižování emisí skleníkových plynů z dopravy
7. Ministerstvo průmyslu a obchodu: Národní akční plán čisté mobility *(NAP CM)*, (2015)
8. www.eru.cz
9. www.pendatron.cz

Corresponding author:
Ing. Miroslav Krumbholc, Department of Vehicles and Ground Transport, Czech University of Life Sciences Prague, Kamýcká 129, Praha 6, Prague, 165 21

EVALUATION OF DIFFERENT KIND OF REMOTE SENSING TECHNIQUES BY ESTIMATION OF SUGAR BEET YIELD

Kateřina KŘÍŽOVÁ[1]

Department of Agricultural Machines, Faculty of Engineering, Czech University of Life Sciences Prague

Abstract
Despite the rapid decline in the second half of 20th century, sugar beet is still one of the main crops cultivated in Czech Republic. Since it is a crop with high requirements for soil nutrition content, agricultural management must be planned utmost properly. Use of remotely sensed data became relatively common in agricultural practice. Technologies developed rapidly over recent decades and therefore there are plenty of options. Input data selection and their processing may be adjusted to a particular research. Vegetation Indices are common tool for vegetation cover evaluation based on remotely sensed data. However, their suitability for yield prediction was tested mostly on grain field data. Thus, this study was focused on determination of relation between different kind of remotely sensed data and actual yield of sugar beet pulp. Satellite WoldView-3 data and data from multispectral camera Parrot SEQUOIA were utilized to derive three kinds of indices (NDVI, SAVI and OSAVI) over the experimental field of Crop Research Institute in Prague–Ruzyně. Input data variability was provided by 24 different ways of fertilization on 96 parcels. Relation between yield from every particular parcel and values of vegetation indices in the same zones was then examined. Correlation analysis indicated strong relation between all indices derived from both kind of remotely sensed data and sugar beet yield. The initial assumption that UAV data with finer spatial resolution should provide more accurate results was not confirmed. Moreover, conclusion was drawn that satellite and UAV data provided very similar information despite significantly different spatial resolution. Thus, low-cost UAV method may be sufficiently used to predict yield of sugar beet pulp.

Key words: *field experiment, satellite, WorldView-3, UAV, SEQUOIA, vegetation indices.*

INTRODUCTION

Sugar beet cultivation has a long tradition in Czech Republic. There were almost four hundred sugar factories in the past. However, social and political changes caused dramatic decline in recent decades, so there are only seven sugar factories left. Despite this fact sugar beet is still one of the main agricultural crops cultivated in this area (*Krejčí et al., 2016*). Besides it as a staple crop for many branches of food industry, sugar beet gains more importance also in an energetic sector. According to *Draycott* (2008) the worldwide demand for sugar increased fivefold over past 60 years. However, this crop has relatively high requirements for soil nutrition sufficiency, especially for nitrogen. Therefore, it is recommended for sugar beet to be sown on one agricultural plot in a period not shorter than four years. Thus, to utmost precise agricultural management is needed to be applied to provide high yield.
Since the remote sensing (RS) techniques became commonly used in agriculture, it is possible to examine the vegetation status in many ways in a non-destructive mode (*Richards, 1993*). This approach is commonly known as Precision Agriculture (PA). Various plant characteristics, such as lack of water or nutrients or biomass content, can be described based on spatially related distance data containing information about electromagnetic radiation. By combining values of reflectance within different bands vegetation indices (VIs) are derived. VIs are the most common tool used to examine current vegetation status. At present, more than 150 VIs is described in scientific literature, however only a small part has a real use. Authors develop new indices that are best suitable for their research, e.g. the study *of Hunt Jr. et al.* (2013), where Triangular Greenness Index (TGI) was developed and successfully used to indicate leaf chlorophyll content in maize. However, in general VIs fit best on grains vegetation cover (*Zhang, 2015*). There is still limited information about utilization of VI on sugar beet data in terms of yield prediction. There is a study of *Clevers* (1997), where optical methods were utilized to improve existing growth models. In results Clevers suggested to do more research despite the fact that his experiment had satisfactory results. Moreover, since 1997 technologies

developed rapidly and therefore it was indispensable to undertake further research. Most of current studies focus on use of RS techniques for detection of vegetation attacked either by pests or by weed. Five VIs, including the basic Normalized Difference Vegetation Index (NDVI), were derived from RS data to identify parts of sugar beet canopy stressed by *Heterodera schachtii* and *Rhizoctonia solani*. To get RS images for this study near-range spectroradiometers carried by aircraft was utilized (*Hillnhütter et al., 2011*). One of the most important weed in sugar beet canopy is the creeping thistle (*Cirsium arvense*) (*Andreasen & Stryhn, 2012*). Its identification within the agricultural plot is therefore crucial. Classical RGB images captured by unmanned ground vehicle (UGV) may be used to detect thistle in sugar beet fields (*Kazmi et al., 2015*). However, latest trend in this field of study are unmanned aerial vehicles (UAV) (*Houborg et al., 2015*). These can carry different types of cameras and they are therefore able to capture various kinds of images. Very common is combination of UAV with multispectral camera. *Garcia-Ruiz et al.* (2015) were testing this combination when trying to identify thistle in within the sugar beet field. His team was also searching ideal spatial resolution of multispectral images to provide most accurate information in terms of weed detection. It was concluded that very detailed resolution is indispensable, 6 mm per pixel or finer.
Remotely sensed data in general capture the information about objects on Earth surface. All mentioned studies were focused on processes that take place above the ground. Therefore, this study aimed to describe the relation between remotely sensed data and sugar beet yield with regard to the fact that main product of sugar beet cultivation is actually a pulp that grows under the surface. Thus, the relation between beet leaves and beet pulp was aimed to be described in the first place. Moreover, the objective of this study is to determine whether UAV data with finer spatial resolution provide more accurate results than commercial satellite as the source for VIs calculation.

MATERIALS AND METHODS

Field experiment for this study was conducted within an experimental plot of Crop Research Institute in Prague–Ruzyně (50°05'21.1"N, 14°18'00"E). On this 1.4 ha location sugar beet was grown in 2016 season. To get higher input data variability, the plot was splitted into 96 parcels and different agricultural management was applied. Thus, there were 24 variants of fertilization in 4 repetitions (see Tab. 1).
Remotely sensed data were used to evaluate the vegetation cover before harvest. Commercial WorldView-3 (WV-3) satellite imagery was put into comparison with simple multispectral camera Parrot SEQUOIA. Satellite data with 1.2 m spatial resolution were captured on 13th September 2016. UAV-embedded SEQUOIA imagery was captured from 30 m height on 7th October 2016. This approach provides finer spatial resolution than the satellite, i.e. 0.025 m per pixel.
Based on these images selected VIs were derived using software ENVI (ENVI 5.4). Calculations were undertaken according to equations given by Tab. 2. NDVI as the basic indicator of green and healthy vegetation was calculated in the first place. However, the structure of sugar beet vegetation cover has a different character than a grain vegetation cover. Depending on aboveground biomass of beet leaves, the soil is more or less visible in the imagery. Therefore, other type of indices had to be calculated as well. Soil Adjusted Vegetation Index (SAVI) and Optimized Soil Adjusted Vegetation Index (OSAVI) were developed for this kind of canopies where soil pixels contribution is more significant. These are very similar indices that differ only in the value of adjusting factor (L). L=0.5 should be the optimal value to eliminate soil contribution over a wide range of vegetation covers (Rondeaux, 1996). According to studies of Huete (1988) the value of L should be decreasing with denser vegetation in order to provide most accurate results. Thus, L=0.16 in equation for OSAVI calculation should make it more sensitive specifically for canopy with ≥ 50 % density.

Tab. 1 Fertilization management

Parcels	Manure [t/ha]	Compost [t/ha]	Slurry+straw [t/ha]	N [kg/ha]	P_2O_5 [kg/ha]	K_2O [kg/ha]
111-114	0	0	0	0	0	0
121-124	0	0	0	40	20	30
131-134	0	0	0	70	40	60
171-174	0	0	0	0	40	60
181-184	0	0	0	100	60	90
191-194	0	0	0	130	40	60
211-214	10.5	0	0	0	0	0
221-224	10.5	0	0	40	20	30
231-234	10.5	0	0	70	40	60
271-274	10.5	0	0	0	40	60
281-284	10.5	0	0	100	60	90
291-294	10.5	0	0	130	40	60
311-314	0	10.5	0	0	0	0
321-324	0	10.5	0	40	20	30
331-334	0	10.5	0	70	40	60
371-374	0	10.5	0	0	40	60
381-384	0	10.5	0	100	60	90
391-394	0	10.5	0	130	40	60
611-614	0	0	30	0	0	0
621-624	0	0	30	40	20	30
631-634	0	0	30	70	40	60
671-674	0	0	30	0	40	60
681-684	0	0	30	100	60	90
691-694	0	0	30	130	40	60

Tab. 2 Selected VIs calculated in this study

VI	Equation	Reference
NDVI	*(NIR-Red)/(NIR+Red)*	*Rouse et al. (1973)*
SAVI	*(1.5*(NIR-Red))/(NIR+Red+0.5)*	*Huete (1988)*
OSAVI	*(1.5*(NIR-Red))/(NIR+Red+0.16)*	*Rondeaux et al. (1996)*

SW ENVI enables to calculate various indices simply by putting required equation to a *Band Math* tool and assigning particular band of electromagnetic spectrum. There are raster layers as on output that may be processed in Geographic Information Systems (GIS). Rasters of NDVI, SAVI and OSAVI were thus further analyzed in ArcGIS software (ArcMap 10.5). A simple vector representing a net was created above the VIs to identify parcel borders. 1 m inner buffer was added to eliminate a margin effect. Finally, six rows of sugar beet were selected in every parcel. These zones corresponded with those, where the later yield data were acquired from (see Fig. 1). To get the numerous data from VI raster, a tool *Zonal Statistics as table* was utilized. The resulting tables contained information about mean value of particular VI in every zone of interest. Since the yield data for every parcel were available, correlation analysis could be done. The relation between the mean value of VI and yield was examined at two levels. Correlation coefficients (r) were calculated first between VI and beet leaves. But since the beet pulp is the main product of sugar beet cultivation, its relation with VI was the matter of main interest. All levels of correlation analysis were processed using R Studio software.

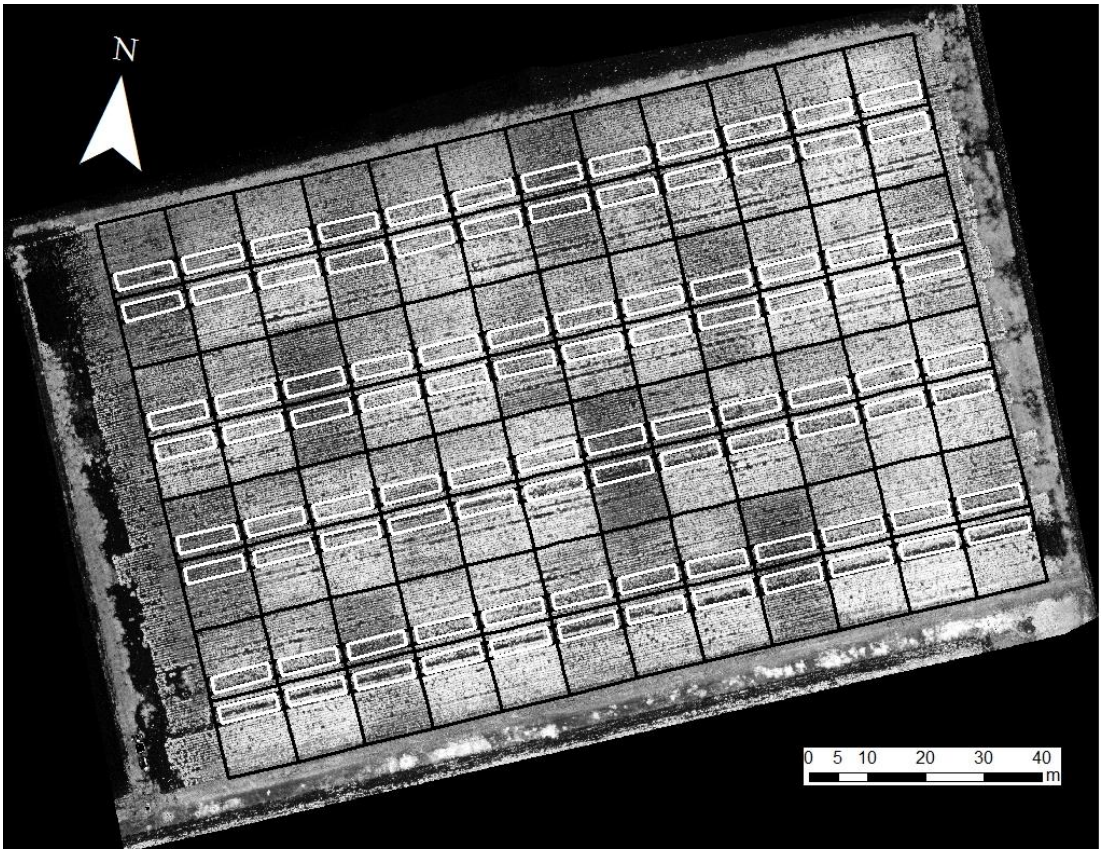

Fig. 1 Six rows zones (white) selected within every parcel (black) above NDVI raster

RESULTS AND DISCUSSION

Graph 1 shows the relation between yield of beet leaves and beet pulp. These two variables are undeniably correlated (r=0.796), which piece of information is crucial for further research in terms of sugar beet yield prediction.

Graph 1 Correlation of beet leaves and beet pulp yield data

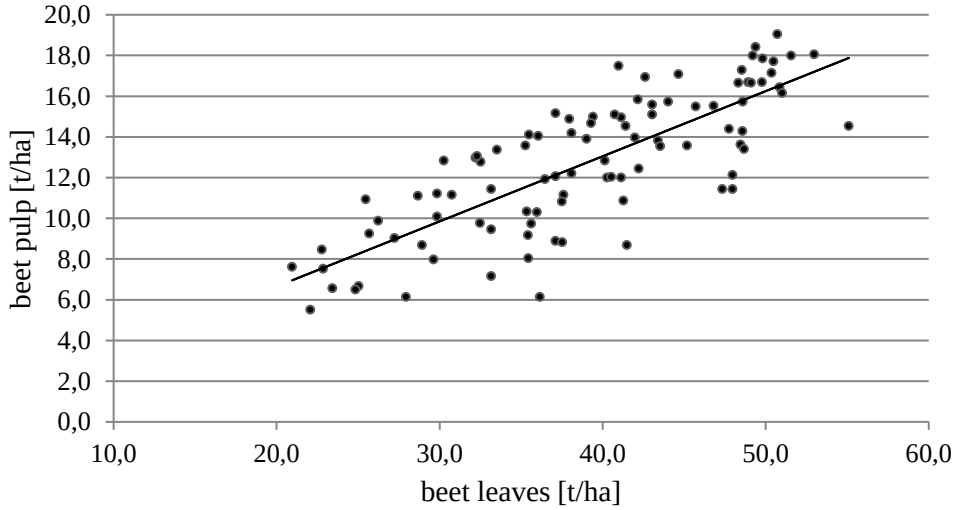

Statistical analysis was done to determine the relation between both kinds of remotely sensed data and sugar beet yield. Tab. 3 gives the resulting values of r separately for WV-3 satellite and UAV data.
A significant correlation was examined at all levels. These results support the hypothesis that VIs are applicable on sugar beet data and may be used to predict pulp yield. The main assumption was that finer spatial resolution of an input data could provide more accurate results. With regard to the study

of *Jay et al.* (2017), where it was stated that spatial resolution 4 cm or finer is best performing when studying sugar beet vegetation characteristics, spatial resolution of SEQUOIA (0.025 m = 2.5 cm) should provide better results than WV-3 satellite data. However, results of this study show the opposite trend. Data from WV-3 were in fact more correlated with both kinds of yield data (leaves, pulp). However, the differences between *r* results are so slight that they may be considered as insignificant. Since there are apparently no other studies focused on sugar beet yield prediction, selected VIs performance cannot be compared. As shown in Tab. 3, NDVI derived from WV-3 is best correlated with beet leaves yield, but OSAVI is here better correlated with actual pulp yield. SEQUOIA provides more consistent results. SAVI shows higher *r* at both levels of analysis. This is probably caused by finer spatial resolution of this kind of RS data. Finer spatial resolution here likely makes this index more sensitive to variable vegetation density. According to the statement of *Huete* (1988), SAVI is more suitable for sparse vegetation cover. Therefore, further analysis should be undertaken to determine actual vegetation density of examined agricultural plot.

Tab. 3 Correlation coefficients *r* between yield (leaves, pulp) and particular VI; best performing VIs in bold (*levels of statistical significance: * p<0.05; ** p<0.01; *** p<0.001*)

WV-3	*r*	
	leaves	pulp
NDVI	**0.851*****	0.779***
SAVI	0.839***	0.783***
OSAVI	0.832***	**0.784*****

SEQUOIA	*r*	
	leaves	pulp
NDVI	0.802***	0.675***
SAVI	**0.839*****	**0.716*****
OSAVI	0.828***	0.704***

CONCLUSIONS

Since the concept of PA became more open to low-cost methods and open source data, the role of commercial products should be determined. Nowadays, more farmers decide to analyze their agricultural plots using these methods to provide higher yields from spatially limited area. But, the question of financial costs is here crucial. Therefore, the study of suitability of different kind of input RS data to predict sugar beet yield was undertaken. The results showed that commercial satellite data with coarser spatial resolution provide only negligibly more accurate results than low-cost method based on UAV utilization. Despite this fact, both kinds of data were strongly correlated with real yield data. It was therefore concluded that quite the same information may be gathered from both kinds of RS methods applied on sugar beet vegetation cover while the financial costs differ significantly. Low financial inputs are crucial for opening the PA concept to wider group of farmers that in consequences means the step towards more economical and environmental agricultural practice while increasing its efficiency.

REFERENCES

1. Andreasen, C., & Stryhn, H. (2012). Increasing weed flora in Danish beet, pea and winter barley fields. *Crop Protection*, 36, 11-17.
2. Clevers, J. G. P. W. (1997). A simplified approach for yield prediction of sugar beet based on optical remote sensing data. *Remote Sensing of Environment*, 61, 221-228.
3. Draycott, A. P. (2008). *Sugar Beet*. Hoboken: John Wiley & Sons.
4. Garcia-Ruiz, F. J., Wulfsohn, D., & Rasmussen, J. (2015). Sugar beet (*Beta vulgaris L.*) and thistle (*Cirsium arvensis L.*) discrimination based on field spectral data. *Biosystems Engineering*, 139, 1-15.
5. Hillnhütter, C., Mahlein, A.-K., Sikora, R. A., Oerke, E.-C. (2011). Remote sensing to detect plant stress induced by *Heterodera schachtii* and *Rhizoctonia solani* in sugar beet fields. *Field Crop Research*, 122, 70-77.
6. Houborg, R., Fisher, J. B., & Skidmore, A. K. (2015). Advances in remote sensing of vegetation function and traits. *International Journal of Applied Earth Observation and Geoinformation* 43, 1-6.
7. Huete, A. R. (1988). A soil-adjusted vegetation index (SAVI). *Remote Sensing of Environment*, 25, 295-309.
8. Hunt Jr., E. R., Doraiswamy, P. C., McMurtrey, J. E., Daughtry, C. S. T., Perry,

E. M., & Akhmedov, B. (2013). A visible band index for remote sensing leaf chlorophyll content at the canopy scale. *International Journal of Applied Earth Observation and Geoinformation* 21, 103-112.

9. Jay, S., Gorretta, N., Morel, J., Maupas, F., Bendoula, R., Rabatel, G., Dutartre, D., Comar, A., & Baret, F. (2017). Estimating leaf chlorophyll content in sugar beet canopies using millimeter- to centimeter-scale reflectance imagery. *Remote Sensing of Environment*, 198, 173-186.
10. Kazmi, W., Garcia-Ruiz, F. J., Nielsen, J., Rasmussen, J., & Andersen, H. J. (2015). Detecting creeping thistle in sugar beet fields using vegetation indices. *Computer and Electronics in Agriculture*, 112, 10-19.
11. Krejčí, T., Dostál, I., Havlíček, M., & Martinát, S. (2016). Exploring the hidden potential of sugar beet industry brownfields (case study of the Czech Republic). *Transportation Research Part D*, 46, 284-297.
12. Richards, J. A. (1993). *Remote Sensing Digital Image Analysis: An Introduction.* Berlin: Springer-Verlag.
13. Rondeaux, G., Steven, M., & Baret, F. (1996). Optimization of Soil-Adjusted Vegetation Indices. *Remote Sensing of Environment*, 55, 95-107.
14. Rouse, J., Haas, R., Schnell, J., & Deering, D. (1973). *Monitoring vegetation systems in the Great Plains with ERTS.* In Third ERTS Symposium (pp. 309-3017), NASA.
15. Zhang Q. (2015). *Precision Agriculture Technology for Crop Farming.* Boca Raton: CRC Press.

Corresponding author:
Ing. Kateřina Křížová, Department of Agricultural Machines, Faculty of Engineering, Czech University of Life Sciences Prague, Kamýcká 129, Praha 6, Prague, 16521, Czech Republic, e-mail: krizovak@tf.czu.cz

TECHNICAL - ECONOMIC ANALYSIS AND EVALUATION OF TRANSPORT ORGANIZATION

Peter KUCHAR, Marek HALENÁR, Vladislav HAJDÁK

Department of Transport and Handling, Faculty of Engineering, Slovak University of Agriculture in Nitra, Slovak Republic

Abstract
The contribution focuses on the examination of the transport company, whose main focus lies in the livestock production and transport acts as a transport for own needs and for the transport of products to the customers in the context of international and domestic road freight transport. During the investigation of the organization are utilized the tools of economic analysis, analysis of the performances and the use of the fleet. Then they are compared from year to year for each of the indicators selected cars or the entire enterprise.

Key words: *transport; rolling stock; economic analysis.*

INTRODUCTION

Transport infrastructure and transport services are an integral part of the life of every human being. In the framework of the international division of labour assist in improving the competitiveness of transport, increase prosperity, labour mobility and stimulate economic growth.
The objective of the transport policy of the state is to create transparent conditions, to minimize the risks on the transport market and to ensure a permanently growing need of transport, whether of goods or persons with the required quality and time and at the same time reducing the negative effects of transport on the environment. The Slovak Republic is for the european transport significant country, mainly because of the geographical location of the landscape. Therefore, we can observe an increasing trend over the last 10 years that transportation almost doubled, and this tendency is also foreseen in the future. Taking into account also the growing number of cars on our roads, it is necessary to expand the capacity of the road network and its modernisation in particular in connection with the increased load of motorways, express roads (I), (II) and (III) class. As a good solution appears to be building a motorway and expressway segments, which will result in the removal of capacity and a better link between the regions. This measure will increase the standard of living in the more remote regions, the growth of new jobs and improved transport and transit on our territory *(Hujo et al., 2014a*).
Build an advanced road infrastructure at the same time brings increased competition, whether in the field of transport, or other services. Therefore, it is necessary from the perspective of the organization must be flexible to respond to market changes and apply new technologies. At the same time, it is necessary for these changes to conduct effective and economically, for what it is used the economical analysis of the economic situation of the company and the analysis of the performances of the fleet of the transport undertaking, which deals with this post (*Hujo et al., 2013*).

MATERIALS AND METHODS

The company, which issue we are dealing with in the post has a long tradition as a production organization in the agricultural sector, which focuses mainly on the breeding and production of live animals. Whereas it is necessary to export produced goods to the end customers in a larger volume, organisation acceded to own transport by freight road means of transport. With regard to the topic of work we will focus on just a part of the organization of the transport. Freight transport in an enterprise can be divided into two main parts:
• transport of live animals,
• transport of bulk mixtures.

Transport of live animals forms a primary part of the transport shall be carried out on a long distance driving, the majority outside the territory of the Slovak Republic. Transport of bulk mixtures forms

from the point of view of number of performances and number of the cars a minor part. Rides are as opposed to the transport of live animals to the shorter distance only in the vicinity of the centre and, therefore, exclusively in the territory of the Slovak Republic. The number of journeys are substantially greater than in the above-mentioned section of the carriage.

Economic analysis represents an exploration of economic processes, assessment, evaluation and economic processes depending on other processes and the surrounding area. It also examines economic status, operation and efficiency management undertaking or to a specific section.
In the context of the results of the analysis, the company management or other management structure can make decisions and to draw conclusions on the future direction in the organization.
With enough information and indicators, may serve analysis as diagnostic tool, showing process efficiency, their difficulty, what may accrue decisions on the axle, or forecast trends and appraisal of the situation in the future. (*Konečný et al., 2010*)

In analysing transport in the enterprise in view performance of vehicles are used these absolutely indicators:

- Driving performance - is the distance, that the vehicle pass for a certain period of time. It is divided into driving performance with and without a load, the aim is to ensure the greatest possible number of kilometers with cargo and minimize kilometers unladen vehicle, (*Janoško et al., 2014b*)

Relative indicators in terms of outputs include:

- Coefficient of utilization ride β - represents the exploitation of vehicle in terms of the running vehicle performance with the load to the total running vehicle performance over a period of time. It may be in the range 0 - 1. It can be calculated by equation (1)

$$\beta = \frac{l_z}{l}, \quad (1)$$

where l_z is driving performance of the vehicle, l is driving performance vehicle in total.

- Coefficient of using useful weight γ - represents the useful curb weight in one turnover. It is a dimensionless indicator, the value is between 0 - 1, where appropriate also over 1 when the vehicle is loaded, which is seen as a breach of legislation. It can be calculated by equation (2)

$$\gamma = \frac{q}{K}, \quad (2)$$

where q is weight load transported, K is useful weight of the vehicle.
(*Chrastina, et al., 2014*)
Time analysis - use of means of transport is a necessary tool in the evaluation of efficiency a transport undertaking. Between relative indicators time use of means of transport are:

- Coefficient of time utilization of fleet α - gauge is the use of vehicles with regard to the time of operation. It shall be calculated by equation (3)

$$\alpha = \frac{VD_{pr}}{VD_{ev}} \quad (3)$$

where VD_{pr} is on-board days in operation, VD_{ev} is on-board day on the records. (*Hujo et al., 2014b*)

RESULTS AND DISCUSSION

The first step in the evaluation a transport organization has been collecting and examining data entry. They have been granted to the undertakings concerned in printed or electronic form and some of the data was necessary to find in the system "Dispečer", which records the current status of fuel and movement of the vehicle on the probe in the tank and GPS coordinates. Then we have processed these data in MS Office, where were created table and formulas for calculating necessary parameters.
Among the basic values included:

- Driving performance,
- Costs per unit.

Of which is then calculated their total q.p. All of these data can be seen in Tab. 1.

Tab. 1 The input values needed to calculate the individual composite indexes

Month	Driving performance km		Unit Cost EUR/km		$q_0.p_0$ EUR	$q_1.p_0$ EUR	$q_0.p_1$ EUR	$q_1.p_1$ EUR
	2013 q_0	2014 q_1	2013 p_0	2014 p_1				
January	34534	34432	0.41	0.44	14189,9	14148,0	15107,4	15062,8
February	28178	42134	0.47	0.40	13281,9	19860,1	11216,4	16771,7
March	39582	42861	0.42	0.45	16764,6	18153,3	17899,3	19382,1
April	46818	13139	0.50	0.56	23271,6	18206,0	26008,2	20347,0
May	37135	39590	0.43	0.40	16096,0	17159,3	14709,3	15681,0
June	23889	27356	0.59	0.50	14091,5	16136,6	11852,9	13573,1
July	30951	29374	0.58	0.42	18032,7	17113,9	13148,2	12478,3
August	19182	26762	0.45	0,52	8648,0	12065,4	10039,8	14007,1
September	23989	35040	0.68	0.42	16222,7	23695,9	10077,4	14719,7
October	29258	26127	0.65	0.46	19124,0	17077,5	13368,9	11938,2
November	35627	23901	0.48	0.39	17096,4	11469,4	13750,9	9225,1
December	24822	18729	0.73	0.77	18079,5	13641,6	19152,4	14451,1

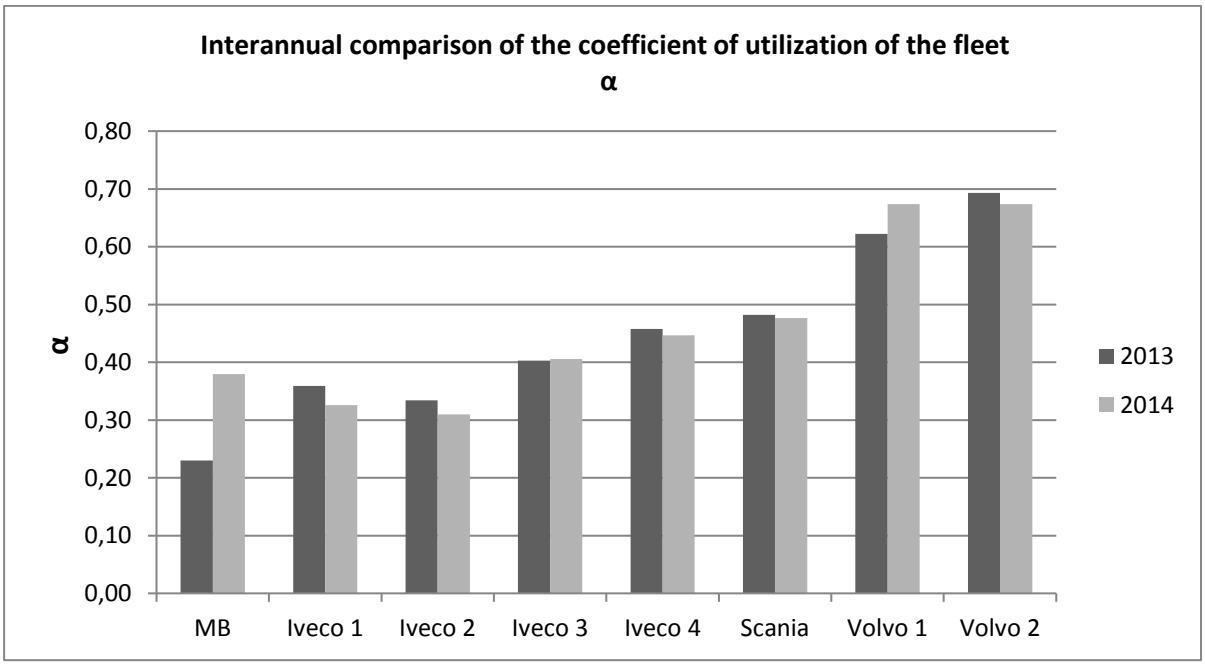

Fig. 1 Interannual comparison of the coefficient of utilization of the fleet

In the assessment of using fleet in terms of the ratio on on-board days in operation at the on-board day in the registration we arrived at the conclusion that year-on-year coefficient use of rolling stock α increased by 2,2%. The main difference was for a vehicle Mercedes-Benz, where it has increased by

65%, which is generated by the sale of vehicle in June and therefore only early half- hourly capacity. Increased also by in vehicle Volvo 1, by 8%, in Iveca 3 by 1%. We have recorded a decrease in the remaining vehicles in the range of 1% to 9%.

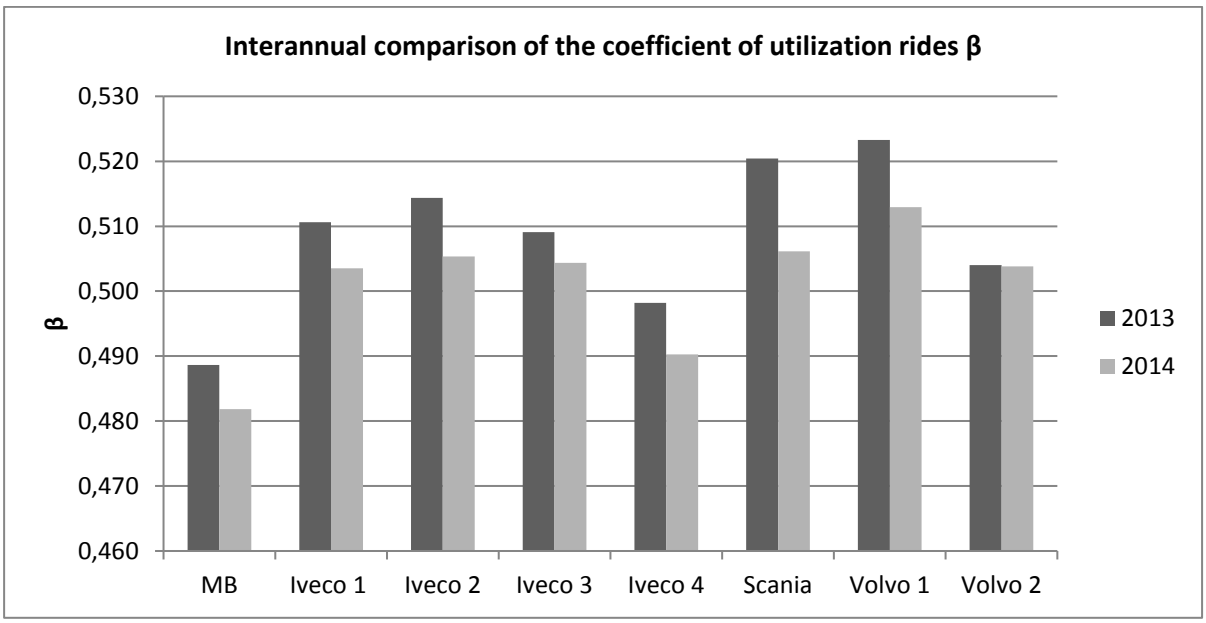

Fig. 2 Interannual comparison of the coefficient of utilization rides

Further the parameter was interannual comparison efficiency of utilization ride β, what is the share of the distance travelled with the load at the total distance travelled. The aims is achieve the coefficient of the closest 1, and thus take the most kilometers of cargo. In its own animal transport this is problematic for safety reasons, since the organization fear to bringing disease into the holding and the possible major damage. Therefore are transported to customers only animals produced in the enterprise concerned and the trip back is unladen. Therefore the moving in coefficient $\beta = 0.5$ we consider to be adequate. Year-on-year came to a reduction coefficient β of 1.57%, and the greatest difference was in Scania vehicles and Volvo 1, 2.7% and 1.9%. (*Janoško el al.2014c*)
Useful vehicle weight coefficient shows how to effectively use the shipping capacity of the vehicle, whether from the perspective of the mass, or store. The result of the compare coefficient of the use of useful weight was that this year have decreased by 4.7%. Vehicle Mercedes-Benz year on year coefficient fell this and the vehicle was used less in 2014. We can also observe the use of Iveco vehicles below 2 and 4, which are used only for smaller shipments, and sometimes they are just an additional vehicle for transport items that are no longer fit into the primary vehicle. (*Janoško et al. 2014a*)

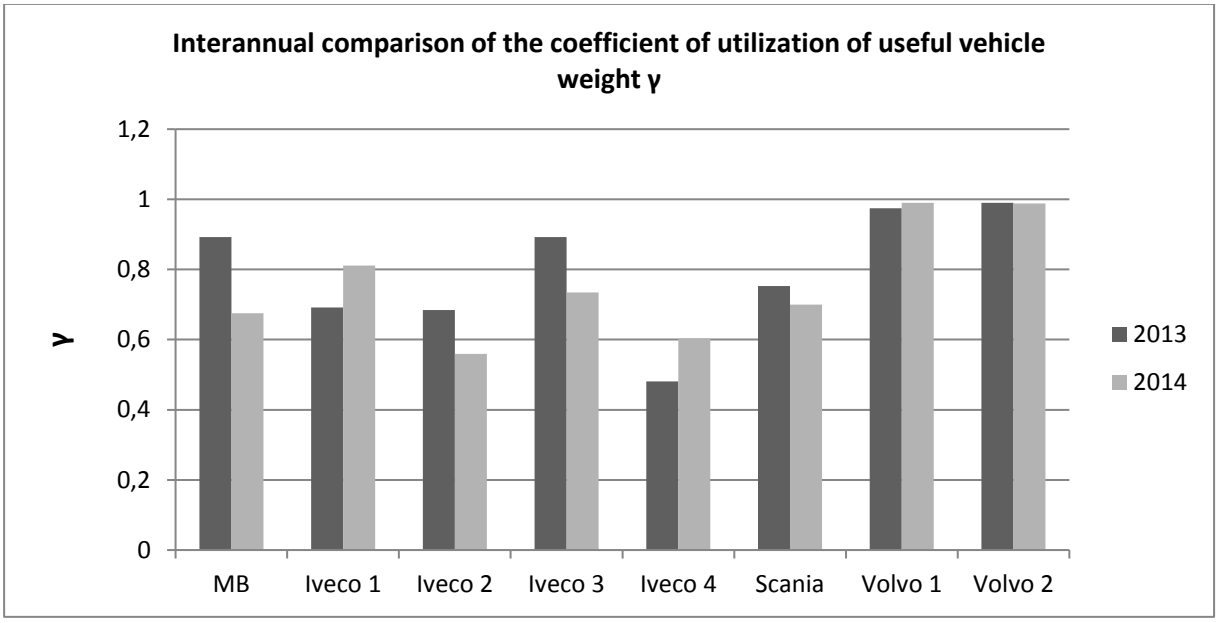

Fig. 3 Interannual comparison of the coefficient of utilization of useful vehicle weight

CONCLUSIONS

Economical use of the resources of the undertaking operating in the field of transport, or any other, is a very important task. It is therefore necessary to examine their use and on the basis of the results of the carried out remedy. In this way it is possible to save a company significant resources, which can then be used for the renewal of the fleet, the introduction of new technology, which ultimately can save resources and further improve the ecological aspect of transport. For this reason we have developed the economic analysis of the transport section of the undertaking concerned, we evaluated the individual compound indices, the result of which was the change in the total cost when you change the driving performance, unit cost, or both at the same time. These changes are expressed through share in % and in financial terms. Then have been assessed selected data through relative indicators and a year-on-year comparison coefficient of use of rolling stock, efficiency rating journeys and efficiency rating useful weight of the vehicle. From the analysis shows that the biggest reserves are in the time vehicle use, whereas vehicles spend in operation for less days and more days will spend in wait time.
In some cases there is insufficient transport capacity vehicle Iveco Eurocargo and is transported rest of goods another vehicle. This case is clearly inefficient and should be subjected to detailed examination, whether it would not be appropriate to carry goods one vehicle, which should have sufficient capacity.

ACKNOWLEDGMENT

This work was supported by AgroBioTech Research Centre built in accordance with the project Building „AgroBioTech" Research Centre ITMS 26220220180.
The contribution was made under the grant project of the Ministry of Education of the Slovak Republic VEGA 1/0464/17 „ Monitoring of the impact of ecological fuels derived from agricultural production and impurities in hydrocarbon fuels to technical and environmental performance of internal combustion engines used in agricultural and transport technology “.

REFERENCES

1. Hujo, Ľ., Halenár, M., Kosiba, J., & Hajdák, V. (2014a). Optimization of transportation routes of dangerous materials by creating an interactive map of ADR in Trnava region. In *Rural buildings in European regions (II) – architecture, constructions, technology, security and logistics.*Nitra. p. 126-138. ISBN 978-80-552-1242-5.
2. Hujo, L., Jablonický, J., Tkáč, Z., Angelovič, M., & Rečková, B. (2013). Assesment of transport company in terms of performance utilisation of vehicle. In *Acta technologica agriculturae*. ISSN 1335-2555, (16)

3. Hujo, Ľ., Jablonický J., Tulík, J., Nikolov, M., & Hajdák, V. (2014b). Economic indiocators evaluation of transport company in terms of individully composite indexes. In *Agricultural, Forest and Technologies*, (1)1, 2367 – 5888.
4. Chrastina, J., Janoško, I. & Kangalov, P. (2014). Monitoring the operating parameters of municipal vehicles. Ruse: Angel Kanchev University of Ruse, Bulgaria, ISBN 978-954-712-629-9.
5. Janoško, I., & Chrastina, J. (2014a). Monitoring parameters of municipal vehicles. Nitra : Slovak University of Agriculture in Nitra, ISBN 978-80-552-1276-0.
6. Janoško, I., Lindák, S., & Kosiba, J. (2014b). Monitoring of theimpact of operating personnel on the transportation efficiency in the intercity bus transpor. *Naučni trudove*. Ruse. Bulgaria. (p. 145-152). ISSN 1311-3321.
7. Janoško, I., Lindák, S., & Polonec, T. (2014c). Technical-economic analysis of the logistics collection of waste in the city of Nitra. *Rural construction in European regions (II) – architecture, construction, technology, security and logistics*. Nitra. p. 139-146. ISBN 978-80-552-1242-5.
8. Konečný, V., Poliak, M., & Poliaková, A. (2010). Economic analysis of a road traffic. I. edition. Žilina : University of Zilina / EDIS – publisher ŽU, ISBN 978-80-554-0253-6.

Corresponding author:
Peter Kuchar, Department of Transport and Handling, Faculty of Engineering, Slovak University of Agriculture in Nitra, Tr. A. Hlinku 2, 949 76 Nitra, Slovak Republic, e-mail: xkuchar@is.uniag.sk

ANIMAL DETECTION USING THERMAL CAMERA CARRYING BY UAV

Jan LEŠETICKÝ

Department of Physics, Faculty of Engineering, Czech University of Life Science Prague

Abstract
The article is focused on the animal detection system carrying by UAVs. The presented system collects thermal images in the area intended for haymaking or harvesting. The captured image is transferred to the laptop, where a Threshold Binary image recognition analysis is performed on the OpenCV platform. During testing, the reliability of the presented system was verified. Results show that the presented system is capable to localize animals autonomously and is beneficial for the reduction of the number of injured or killed animals during haymaking or harvesting.

Key words: *UAV, detection, thermal camera.*

INTRODUCTION

Detection of wildlife during haymaking or harvesting (further "activities") is starting to be a current topic issue. Many commercial companies are dealing with it, because both activities are accompanied with great losses. The application developed recently by the PEF faculty of CULS brought the beneficial improvement under the program called "Protection of animals during harvest". The program is focused on the active interconnection between the farmers, the huntsmen and the volunteers. Web is designed to collect data about dead animals on the field and about actual location of the animals, and it also makes easier to report harvest which is mandatory by law. After log in it is possible for volunteer to help with getting the animals out of the field. One of the detection possibilities is the use of doppler radar (*Kauppinen et al., 2015*), but this method is economically unsuitable because it requires to stop harvesting. For this reason, it seems as if they were to use unmanned vehicles (UAVs). Drones of various shapes, sizes, and functionalities have emerged over the past few decades, and their civilian applications are becoming increasingly appealing.(*Tang & Shao, 2015*) explain in their article about advantages of using drones in forestry industry. Also (*Christensen, 2015*) was studying how to lower the cost of forest fire and how to decrease the number of forest fires by using drones with thermo camera and UAV. Furthermore, this combination is also used to determine the quality of solar panels. Detection of a game using drones and Thermo camera also deals with (*Gonzalezet et al., 2016; Ward et al., 2016*) and they show interesting reliability and use of this technology. Aim of this article was to use image analysis such as automated detection using UAV and thermal camera.

MATERIALS AND METHODS

First, it was necessary to determine what flight level the UAV would be moving, as with the increasing height the value of the information in the individual pixels decreases, thereby reducing the reliability of the detection. Due to the legislation on drones in the Czech Republic, we were limited to a height of 10 m using an anchor system that served as a failed system in the event of fatal UAV failure. The entire detection system is divided into two parts. The first part is a defective part, consisting of the UAV (DJI F330), optical camera (Eachine TX03) for optical scanning of the detected scene, and a mobile phone with an additional thermal imaging module (Seek Thermal CompactPRO) for recording IR spectrum. The second part consists of a laptop to which a video signal receiver (USV 5.8 GHz) is connected for optical flight control. Next, the OpenCV Evaluation Platform with Threshold. After the flight, the detection itself was made from the captured mobile phone record. Binary Threshold was selected for image analysis. This algorithm approaches the problem by using wildlife's heat signature, which creates a good contrast between the background and the target wildlife. This contrast allows for an intensity threshold to be applied which in turn eliminates the background and brings the object of interest to the front. Intensity threshold, also known as binarization or segmentation of an image, assigns 0 to all pixels under or equal to the threshold and 255 to all the pixels above the same threshold where 0 represents the black color and 255 represents the white color. This thresholding operation can be expressed as (1)

$$dst(x,y) = \begin{cases} maxVal & if\ src(x,y) > tresh \\ 0 & otherwise \end{cases} \quad (1)$$

So, if the intensity of the pixel src(x,y) is higher than thresh, then the new pixel intensity is set to a MaxVal. Otherwise, the pixels are set to 0. The threshold was manually set by the track bar. The processing and final detection are shown in Fig. 1,2.

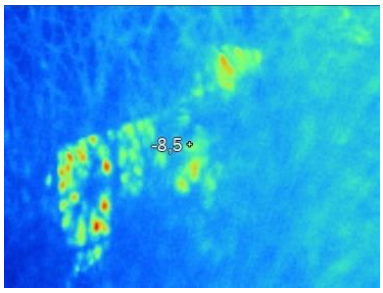

Fig. 1 Original picture in IR spectrum

Fig. 2 Picture after Threshold Binary

RESULTS AND DISCUSSION

Currently, the measurement is not completed and the entire project is planned by the end of this year. In any case, however, several sub-questions and problems have already been solved. A critical factor for the reliability of the entire system is above all the background temperature. This property, therefore, limits detection only to the morning hours when the redundant or disposed material is colder than the detected game. Cumulative measurements are not available as test live video from the thermal camera via rack plate with XBee and an automatically scheduled UAV route that meets the Czech legislative requirements. Repeated trials give a fair assessment in 87% of cases. The scatter of the processed image is about 3%, that is, 3% of the image that was not evaluated as a spiral image, while 23% of the image was evaluated as a virus, although it was not there.

CONCLUSIONS

This paper deals with harvest detection and harvesting. The architecture of the fawn detection system consisting of a thermal camera mounted on a UAV (DJI Phantom 1 F330) was described. Also, the workflow of the whole fawn rescue process was presented. Detection is reliable when the environment is lower than the detected animal. Previous results show the possibility of deploying neural networks for more effective automatic detection.

ACKNOWLEDGMENT

This study was supported by department of Physics, Faculty of Engineering.

REFERENCES

1. Christensen, B. R. (2015). Use of UAV or remotely piloted aircraft and forward-looking infrared in forest, rural and wildland fire management: evaluation using simple economic analysis. *New Zealand Journal of Forestry Science*, *45*(1), 16.
2. Gonzalez, L., Montes, G., Puig, E., & Johnson, S. (2016). Unmanned Aerial Vehicles (UAVs) and artificial intelligence revolutionizing wildlife monitoring and conservation. *Sensors*.
3. Kauppinen, T., Panouillot, P.-E., Siikanen, S., Athanasakou, E., Baltas, P., & Nikopoulous, B. (2015). About infrared scanning of photovoltaic solar plant. In *Proceedings of SPIE - The International Society for Optical Engineering* (Vol. 9485).
4. Tang, L., & Shao, G. (2015). Drone remote sensing for forestry research and practices. *Journal of Forestry Research*, *26*(4), 791–797.
5. Ward, S., Hensler, J., & Alsalam, B. (2016). Autonomous UAVs wildlife detection using thermal imaging, predictive navigation and computer vision. *Conference, 2016 IEEE*. /

Corresponding author:
Ing. Jan Lešetický., Department of Physics, Faculty of Engineering, Czech University of Life Sciences Prague, Kamýcká 129, Praha 6, Prague, 16521, Czech Republic, phone: +420 22438 3149, e-mail: leseticky@tf.czu.cz

POSSIBILITIES OF IMPROVING THE WEAR RESISTANCE OF FUNCTIONAL SURFACES ON THE WINCH APPROACH ROLLER

Veronika ĽUPTÁČIKOVÁ[1], Miroslava ŤAVODOVÁ[1], Michaela HNILICOVÁ[2]

[1]*Faculty of Environmental and Manufacturing Technology, Technical University in Zvolen, Slovak Republic*
[2]*Faculty of Forestry, Technical University in Zvolen, Slovak Republic*

Abstract
The article deals with the improvement of the abrasion resistance properties of the approach roller reel for the approaching of wood used on the underlying machine. Experiments and measurements were made for the experiment to create the bases for applying the method of increasing the surface temperature resistance of its surface. We performed chemical analysis of the material, hardness measurement, notch toughness measurement, material resistance to abrasive wear on the grinding cloth, and evaluation of the roller material microstructure. To increase the wear resistance of the roller surface, we have designed a heat treatment mode according to the steel sheet material data sheet. In order to verify the suitability of this procedure, analyzes and tests were again performed. Based on the obtained data, the conclusion was reached and a recommendation for the procedure in the next experiment.

Key words: *approach roller, steel, heat treatment, microstructure, rope, mechanical properties tests.*

INTRODUCTION

Conveyor machines are predominantly powerful aggregate machines up to 25 tonnes and engine power up to 180 kW. Highest performance and economy are attained in the case of underground mining, but they can also be used differently. When approaching wood, they most often use the reel. The winch, as additional equipment must operate in harsh operating conditions, where occurs the pressure, tension, torsion, dynamic shocks, abrasion, etc. (*Hnilica et al., 2015; Mikleš et al., 2011*).
With the help of the winch, the wood is approaching the machine from inaccessible places. A steel rope that is wound onto a drum coil is used to approach the mass. The rope is wound onto the spool via a series of pulleys, which are routed to the rope and stored on the drum, at the same time fulfilling the protective function, protecting the rope from tearing and tearing the worker in front of the rope. The most energy is transmitted through the steel rope at work (*Janeček et al., 2011; Hnilicová et al., 2016*).
It is very important to choose the right grade of steel in terms of other treatments, such as thermal, surface, mechanical processing. The different types of processing help us to increase the life of the components, thereby saving the economy (*Dvořák et al., 2011*).

METHODS AND MEASUREMENT

The friction and wear processes take place on the surface of the parts. These processes cause surface degradation (degradation), thereby degrading the functional properties of components, construction nodes, and ultimately, the entire system is compromised. In general, surface interactions are associated with material properties, contact conditions, design, operating conditions, chemical, chemical and heat treatment of the material. They result in energy loss (friction) and material loss (wear) (Zdravecká & Ondráč, 2016; Žernovič & Kotus, 2007*)*.
Abrasive wear is characterized by the separation of particles of material from the functional surface by the hardness and roughness of another body or by the action of abrasive particles. It is also necessary to include in the analyzes of the course of abrasive wear the time course of the forces acting between the abrasive particles and the wear surface (Zdravecká & Ondráč, 2016; Blaškovič, et al., 1990; Buckley, 1981).
Basic research on abrasion resistance in abrasive surface friction has been described by several authors (Blaškovič et al., 1990; Hrabě & Chotěborský, 2005; Hrabě et al., 2007). Until now, there is no uniform view of the most appropriate type of material structure in terms of abrasion resistance. Some

authors consider a suitable austenitic-carbide, other martensitic-carbide structure. These differing views stem from the diversity of the abrasive wear process and the wide range of operating conditions.
Mechanical properties are the final characteristics of materials that determine their suitability for use for the purpose and for the given operating conditions (Kalincová et al., 2016). Under the mechanical testing of metallic materials we mean, in particular, the quantitative determination of their mechanical properties - characteristics that allow and limit their mechanical stress during processing (Ľuptáčiková & Ťavodová, 2017).
Heat treatment involves technological processes in which the controlled heat regime achieves structural changes and consequently changes properties in the desired direction. The nature of the heat treatment lies in the phase transformations that take place therethrough. Basic thermal treatment techniques used in technical practice include quenching and subsequent quenching (Kalincová, 2010). The purpose of hardening is to increase the hardness of the steel. Rapid cooling from the quench temperature converts austenite to martensite or bainite. With the increasing drop-in temperature, the strength and the taper of the steel are reduced and its plastic and deformation properties and characteristics increase. Tensioning compensates for differences in the mechanical values of the edge layers and the overlapped core. By fitting appropriate heat treatment modes, or other ways of enhancing and improving mechanical properties, we obtain structures that better resist the operating factor (Jech, 1977; Kalincová, 2010).

EXPERIMENT

As a component of the mechanism used in forestry technologies, the rectifying roller from the winch of the base machine, the universal wheeled tractor was selected for the experiment (Fig. 1).

Fig. 1 Reel on universal wheeled tractor with pulley detail (Babic, 2017)

The pulley was made of 12,060 (C55) steel. It is carbon steel for refining, used for cranked and other shafts, toothed wheels, spindles, pins, latches, etc.
The reel pulley was operated for 40 working days, i.e., j. About 320 hours. Its wear was manifested especially in the groove, the rope (Fig. 2). It is necessary to apply a suitable method to increase the lifetime of this functional area. One of the basic methods, which is often used in practice, was the method of heat treatment of the pulley material. When determining the correct heat treatment mode, it is assumed that the load area will be more resistant to rubbing.

In the first step, a composite input analysis of the pulley material was performed. It consisted of:
• pulley weight measurement,
• chemical analysis of material,
• hardness measurements,
• impact toughness measurements,
• determination of material resistance to abrasive wear on abrasive cloth,
• microscopic analysis of the material structure.

a) b)

Fig. 2 Pulley groove a) unworn, b) worn.

To find out the comparison of the possible weight loss, we have considered the new unused roller and we also considered the roller used in the operation. The difference in pulley weight values is in Tab. 1.

Tab. 1 Difference of pulley weight values

Weight of the new pulley	Weight of the worn roller	Weight difference
3810g	3760g	50g

Chemical analysis

Using chemical analysis, the chemical composition of the pulley was detected. Subsequently, this composition was compared to the chemical composition according to the material sheet. It has been confirmed that it is actually material 12 060 (Tab. 2).

Tab. 2 Chemical composition detected of materials 12 060

Chemical composition of the sample (wt.%)							
C	Mn	Si	Cr	Ni	Cu	P	S
0.471	0.737	0.324	0.096	0.112	0.204	0.0084	<0.150
Chemical composition from material sheet							
0.52–0.60	0.50-0.80	0.15-0.40	max. 0.25	max. 0.30	max. 0.30	max. 0.040	max. 0.040

Hardness measurement

We used the Brinell method $HB_{2.5\ /\ 187.5}$ to find the hardness values. We made three prints on the surface. Hardness values are in Tab. 3. Consequently, the values were compared with the values in the material list.

Tab. 3 Material hardness values (HB)

Number of the imprint	1	2	3	Average value	Value according to Material Data Sheet
Value $HB_{2.5/187.5}$	207	207	202	205	171-253

Neck stiffness test

In the next step, samples were taken from the pulley used, on which we performed a notch test. The test was performed according to STN EN ISO 148-1: 2011 with a notch type V with a nominal hammer energy of 300J. The measured values are in Tab. 4. Norm for semi-finished products, rolled sheet metal does not value HV.

Tab. 4 Toughness values

Measurement number	1	2	3	Average value
Value KCV (J)	18	18	18	18

Evaluation of Abrasion Resistance Abrasion

On 4 standard samples we performed a test to determine the resistance of metallic materials to abrasive wear on the grinding cloth (ČSN 01 5084). The measured values are in Tab. 5.

Tab. 5 Measured values from the test to determine the abrasion resistance of metallic materials on the abrasive cloth

Sample number	1	2	3	4	Average value
Initial weight (g)	6.545	6.585	5.467	6.685	
Final weight (g)	6.428	6.570	5.358	6.572	
Difference (g)	0.117	0.115	0.109	0.113	0.1135

Evaluate the structure of the material

To determine the state of the material structure, we performed a microscopic analysis of the pulley material. The microstructure is composed of ferrite and perlite, with a hint of linearity, ie it corresponds to the basic condition of the material without heat treatment (Fig. 3).

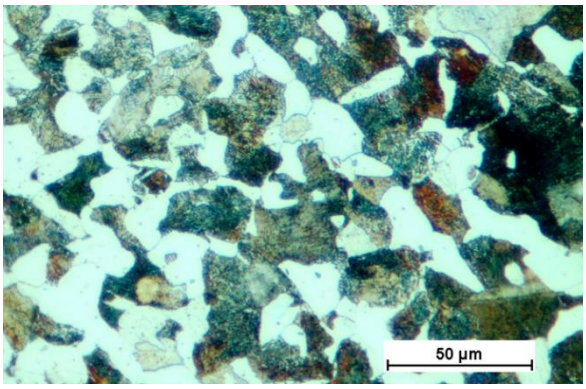

Fig. 3 Microstructure of material 12 060 (magnification 400x)

On the basis of the technological data in the material sheet, we have proposed the heat treatment parameters in the next step. The purpose of the heat treatment is to change the structure, more wear-resistant.

On a sample of material 12 060 we performed heat treatment under laboratory conditions of KVTMK FEVT. According to data from the material sheet, we have selected a tempering temperature of 820 °C for tempering, durability at this temperature for 20 minutes and subsequent cooling in oil. For tempering, we chose a heating temperature of 600 °C, lasting 15 minutes, with free cooling in the oven.

Hardness hardness measurement after heat treatment

From the template chart for steel 12 060, we found that for a given tempering temperature, the tensile strength R_m = 800 MPa was reached, resulting in a hardness of 22 HRC.

After performing the heat treatment, we repeated all the tests to evaluate the effect of the heat treatment of the material to change its structure and mechanical properties.

To determine the hardness values of the material after heat treatment, we used the Rockwell method. We made three prints. The HRC values after the heat treatment of the sample correspond to the values in the material sheet.

Tab. 6 HRC hardness values after heat treatment of the sample

Imprint	1	2	3	Average value	Value according to Material Data Sheet
Value HRC	22	23	21	22	22

Impact toughness test after heat treatment

In the next step, samples were taken from hardened and pulled pulleys, where we performed a notched toughness test. The test was performed according to STN EN ISO 148-1: 2011 with a notch type V with a nominal hammer energy of 300J. The measured energy values are in Tab. 7. Heat treatment results in a higher toughness value, which can improve the material's abrasion resistance. Notched toughness test is in Fig. 4.

Tab. 7 Toughness values after heat treatment of the sample

Measurement number	1	2	3	Average value
Value KCV (J)	26	21	29	25

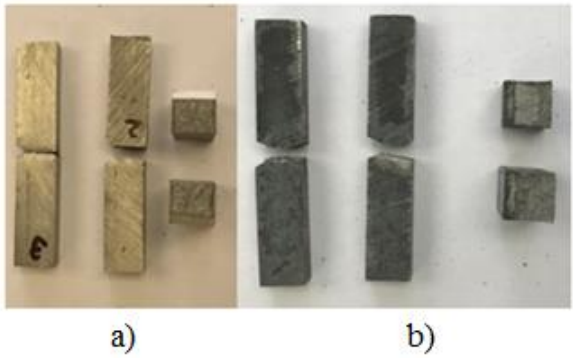

Fig. 4 Notched toughness test a) uncured sample b) hardened specimenst

Evaluation of resistance to abrasion after heat treatment

The test for determining the resistance of abrasive materials against abrasive wear on the grinding cloth (ČSN 01 5084) was performed on 4 standard samples. The measured values are in Tab. 8. Samples used in the test to determine the resistance of abrasive abrasive materials to abrasive cloths is in Fig. 5.

Tab. 8 Measured values from the test to determine the abrasion resistance of metallic materials on the abrasive cloth after heat treatment of the sample

Sample number	1	2	3	4	Average value
Initial weight (g)	6.575	6.698	6.682	6.586	
Final weight (g)	6.471	6.593	6.591	6.449	
Difference (g)	0.104	0.105	0.091	0.137	0.10925

Fig. 5 Samples used in the test to determine the resistance of abrasive abrasive materials to abrasive cloths a) uncured sample b) hardened sample

Evaluation of the structure of the material after heat treatment

Microscopic analysis of the hardened sample is shown in Fig. 6. The microstructure is composed of the martensite. Matches the status of the material after quenching and quitting.

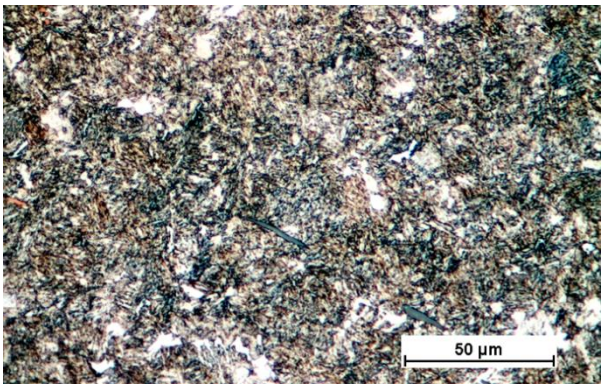

Fig. 6 Microstructure sample of material 12 060 after heat treatment (magnification 400x)

RESULTS AND DISCUSSIONS

The roller, as a component of the forestry equipment, is subject to wear which reduces its functionality. On the circumference of the pulley there is a guide - a groove in which the steel rope is guided. In areas where repeated friction occurs, after a certain period of operation, the functionality of these surfaces is reduced (Mikleš et al., 2011; Ľuptáčiková & Ťavodová, 2017). This also involves the precision of the rope guidance, which reduces the quality of the wood approaching process. By comparing the weight of the pulley before and after its use, we found weight loss.

Authors in many papers documented that there is so far no uniform view of the most appropriate type of structure in terms of abrasion resistance. These differing views stem from the diversity of the abrasive wear process and a wide range of actual operating conditions. The highest resistance to abrasion wear is obtained under the austenitic-carbide structure. Carbide and austenite grid parameters are closer than martensite and carbide lattice parameters, so the combination of these structural components most favorably impacts abrasive wear (Zdravecká & Ondráč, 2016; Hrabě et al., 2007).

Through the input analysis, we have found the mechanical, chemical and structural properties of the pulley material to form the substrates for applying the method of increasing its wear resistance to the functional surfaces of the pulley. On the basis of the technological parameters from the material sheet, we proposed a heat treatment regime and applied it to a sample of material 12 060. We achieved the structure corresponding to the quenching and descent, ie the predominantly ruptured martensite (Fig. 6). Thus, a more suitable structure, such as the ferritic-perlite, is obtained, the basic structure of the roller blank (Fig. 1). However, ferrite (white areas) occurred in the structure. In order to find out if this component really is, it is still necessary to perform a microhardness measurement. Other tests have confirmed that heat treatment applications have their justification for increased thermal resistance. Average loss of material in the abrasive wear test was 0.10925 g, and the notched toughness increased to 25 J.

For more accurate conclusions, however, further experiments are needed to evaluate the wear of the turbid pulley after the operating tests, respectively. Designing other options for increasing the roll resistance of the pulley. These may include, for example, the application of welds to the functional surface of the pulley, the change of material, the design change of the functional part - the pulley groove and the like.

CONCLUSION

A suitable heat treatment of the material used to make the pulley is a prerequisite for increasing abrasion resistance. This can increase the lifetime of functional areas and thus extend their workload and improve the quality of work. In order to verify the proposed roll-over lifting alternative, more experiments need to be carried out, which will be the task of ongoing research.

ACKNOWLEDGMENT

This paper was developed as part of the project APVV-16-0194 "Research on Impact of Innovation in Production Processes on the Lifetime of Tools and Components of Forest Mechanisms."

REFERENES

1. Babic, M. (2017). Možnosti zvyšovania životnosti funkčných plôch komponentov mechanizmov využívaných v lesníckych technológiách: záverečná práca. Zvolen: TUZVO, Fakulta environmentálnej a výrobnej techniky, 61.
2. Blaškovič, P., Balla, J., & Dzimko, M. (1990) *Tribológia.* Bratislava: Alfa, 360 p. ISBN 80-05-00633-0.
3. Buckley, D. H. (1981). Surface Effet in Adhesion, Friction, Wear and Lubrication. Amsterdam – Oxford – New York. 1981.
4. Dvořák, J., Bystrický, R., Hošková, P., Hrib, M., Jarkovská, M., Kováč, J., Krilek, J., Natov, P., Natovová, L. (2011) The use of harvester technology in production forests. Kostelec nad Černými lesy : Lesnická práce, 156 p. obr., tab. - (Folia forestalia Bohemica). - ISBN 978-80-7458-018-5.
5. Hnilica, R., Messingerová, V., Stanovský, M., Slugeň, J., Hnilicová, M., & Ferenčík, M. (2015). Možnosti mechanizácie prác pri zakladaní a výchove lesa. 1. vyd. Zvolen: TUZVO, 2015. 99s. ISBN 978-80-228-2722-5.
6. Hnilicová, M., Hnilica, R., & Dado, M. (2016). Technika a technológie pri výchove a pestovaní lesa. *Zvyšovanie životnosti nástrojov a konštrukčných častí mechanizmov: vedecký recenzovaný zborník.* 1. vyd. Zvolen: TUZVO, pp. 16 – 26, ISBN 978-80-228-2862-8.
7. Hrabě, P., & Chotěborský, R. (2005). *Návary a jejich využití v praxi.* [online]. [cit. 30. 7. 2017]. Dostupné na internete: <http://www.mmspektrum.com/clanek/navary-a-jejich-vyuziti-v-praxi.html>.
8. Hrabě, P., Müller, M., & Chotěborský, R. (2007). Vybrané návarové materiály a jejich laboratorní porovnání proti abrazivnímu opotřebení. In *Strojírenská technologie*, 12, č. zvláštní číslo, pp. 77 – 80. ISSN 1211-4162.
9. Janeček A., Suchomel, J., Štollmann, V., & Mikleš, J. (2011). *Standardy a optimalizace lanových výrobních systémů z hlediska ekonomiky a ekologické čistoty práce.* Brno: Tribun EU, 96 p. ISBN 978-80-263-0054-0.
10. Jech, J. (1977). Tepelné zpracování ocelí. Praha: SNTL – Nakladatelství technické literatury, 400 p.
11. Kalincová, D. (2010). Technické materialy. Zvolen: TUZVO, ISBN 978-80-228-2086-8.
12. Kalincová, D., Ťavodová, M., Hnilicová, M., & Veverková, D. (2016). Machinery for forest cultivation - increase of resistance to abrasive wear of the tool. In *MM science journal.* č. November, pp. 1269 – 1272.
13. Ľuptáčiková, V., & Ťavodová, M. (2017). Opotrebenie funkčných plôch komponentov mechanizmov využívaných v lesníckych technológiách. In *ERIN 2017 – 11th International Conference for Young Researchers and PhD students.* 11, pp. 8 – 14, ISBN 978-80-7561-056-0.
14. Mikleš, M., Tkáč, Z., Jablonický, J., Hujo, Ľ., Mikleš, J., & Krilek, J. (2011). Lesnícke stroje a zariadenia. 1. vyd. Zvolen: TUZVO, 294 p. ISBN 978-80-228-2302-9.
15. Zdravecká, E., Ondráč, M. (2016). Charakterizácia procesov abrazívneho opotrebenia. in *Strojárstvo,* pp. 24 – 26.
16. Žernovič, M., Kotus, M. (2007). Stanovenie veľkosti opotrebenia zo zmeny lineárnych rozmerov v prevádzke. In *Bezepčnosť, Kvalita, Spoľahlivosť*. Košice: Tu, pp. 280 – 285. ISBN 978-80-9073-828-0.

Corresponding author:
Ing. Veronika Ľuptáčiková, Faculty of Environmental and Manufacturing Technology, Technical University in Zvolen. Študentská 26, 960 53 Zvolen. Slovak Republic. e-mail: luptacikovav@gmail.com

DIAGNOSIS OF THE BRAKING RISE

Daniel MADER, Martin PEXA, Lukáš BABIČ

Department of Quality and Dependability of Machines, Faculty of engineering, Czech university of Life Sciences Prague

Abstract
The paper is focused on diagnosis of the braking rise of road vehicle brake systems. This is a very important but hardly measurable parameter of the brake systems of road vehicles. For this reason, the braking rise of the brakes during the technical checks is not measured and is considered to satisfactory. However, for the comprehensive diagnostics of brake systems, it is necessary to focus on this parameter and thus to contribute to increased trouble-free traffic on the road.

Key words*: braking rise, speed, acceleration, braking force.*

INTRODUCTION

The most important factor in road transport, which needs constant attention, it is their safety, not only in the Czech Republic but also worldwide. E.g. In the Czech Republic, according to the Police of the Czech Republic (see Fig. 1), there were 98 864 accidents in total in 2016, which is 5 797 more accidents than in 2015. Accidents increase each year since 2009. The number of killed people slightly decrease, but the current national road safety strategy will determine that in 2020 on the Czech roads can not die more people than the average of EU countries, which is a decrease by about 60% compared to 2009.

The number of accidents and consequences, CZ, 2007-2016	The number of accidens	Consequences for life and health	Killed	Heavily injured	Slightly injured
2007	182 736	23 060	1 123	3 960	25 382
2008	160 376	22 481	992	3 809	24 776
2009	74 815	21 706	832	3 536	23 777
2010	75 552	19 676	753	2 823	21 610
2011	75 137	20 487	707	3 092	22 519
2012	81 404	20 504	681	2 986	22 590
2013	84 398	20 342	583	2 782	22 577
2014	85 859	21 054	629	2 762	23 655
2015	93 067	21 561	660	2 540	24 426
2016	98 864	21 386	545	2 580	24 501

Fig. 1 Road accident statistics over the past 10 years (Police of the Czech Republic)

Nowadays, a several roadside assistants contribute to increase driving safety, including Lane Keeping Support, Brake Assist, etc. However, these assistance systems are dependent on the state and functionality of the brake of the vehicles brake systems. It is therefore necessary to perform a diagnosis of these brake systems (*Biondi, F. et al., 2017, Hecker, F. 2015*).
However, diagnosis is performed on slow roller tester, but they are not able to measure the braking effect at higher speed compared to high speed testing, and thus get closer to real driving conditions on the road (*Bojko, A. et al., 2015*). For this reason, it would be very convenient to develop a multifunctional high speed tester that, in addition to diagnostics of the brake system, would allow loading car's engine and thus to measure performance parameters and emissions.

The main aim of this paper is to analyze the rise of the braking effect. It is the initial braking area, where the braking pressure increases, and therefore the braking effect, up to the maximum achievable or required value. (*Pan, H. et al., 2017*) In standard braking systems testing, this parameter is neglected due to its difficult measurability. The Brake Control Regulation at the Technical Inspection Stations only assumes that the maximum required time required for hydraulic brakes for road vehicles is less

than 0.4 s. However, this is a very significant value that noticeably influences the effect of the entire braking system. (ECE-OSN No. 13)

MATERIALS AND METHODS

In this case the braking effect was measured by a dynamic method, where the test runs go on from the selected speed, when the braking system decrease the kinetic energy accumulated in the rotating parts of the roller tester and the actual rotating parts of the test vehicle. During the measurement, the impulses of rotating cylinders are recorded per unit of time. Depending on these impulses, braking force and other parameters are calculated to assess the condition of the braking system.

First, it is necessary to precisely position and secure the vehicle on the cylinders. Subsequently, the cylinders start running at the desired circumferential speed, which corresponds to the respective vehicle speed. Both the non-driven and the drive axle are driven directly by electric motors connected to cylinder cylinders of the roller tester.
After that the maximum circumference speed of the cylinders is stabilized, the programmable data collector is switched on. Rollers of the roller tester continues 3-5 seconds at a steady circumferential speed. Then follows braking of the vehicle to the stop by an operating, emergency or manual brake.
As soon as this speed is reached, the brake pedal is released and then the time to stabilization the steady speed of the rollers is measured. Then again, 3-5 seconds long measuring with steady running rollers follow. After that is possible to stop the measuring device and the electric motors driving the rollers. This causes that wheels of the vehicle stop automatically due to rolling and mechanical resistance.

The determination of the braking force is based on the formula (1):

$$F_b = G_{hr} \cdot a \tag{1}$$

Where F_b is the braking force [N], G_{hr} is the reduced wheel and wheel weight per wheel circumference [kg], and is the peripheral acceleration of the rollers [m.s^{-2}].

The braked mass of the vehicle on the road and the inertia of the engine are in this case replaced by the mass of the measured wheel and the pair of rollers on which the vehicle is situated reduced to the circumference of the wheel and signed as G_{hr}.

The acceleration and deceleration of the rollers is obtained from the measured pulses per time unit (formula 2 and 3). The pulse generator is an incremental sensor which has 1024 pulses per rotation. Impulses are scanned based on a preset time interval.

$$Ov_i = \frac{(d_{i+1} - d_{i-1}) \cdot 60}{1024 \cdot (t_{i+1} - t_{i-1}) \cdot 0{,}00000002} \tag{2}$$

$$a_i = \frac{(Ov_{i+1} - Ov_{i-1}) \cdot 2 \cdot \pi . r_v}{60 \cdot (t_{i+1} - t_{i-1}) \cdot 0{,}00000002} \tag{3}$$

Where O_{vi} is speed of the test roller in the i-th interval [rpm], d_i is the order of the split in the i-th interval [-], t_i is the time of the passage of the i-th interval [s], 1024 is the number of sensor pieces per rotation [-], i is the deceleration of the test rollers in the i-th interval [ms^{-2}], r_v is the radius of the roller [m].

From the described system comes out that the result is the part where the wheels of the vehicle slow down and the part when the wheels accelerate. From today's point of view, it is necessary to separate these two parts from one another and to obtain a part during which the deceleration occurs and the car brakes are in operation. The wheels of the testing vehicle must overcome all inertia resistances and the power of the electric motors, which is determined by the acceleration part.

RESULTS

First, measurements were made at a scanning frequency of 50 ms, using a brake booster and with disconnected brake booster. Fig. 2 shows the dependence of braking deceleration and roller speed on time

using a brake booster. It is obvious that the initial area of increasing of the braking deceleration until the maximum of the brake force is reached. In order to separate the braking rise from the maximum braking force (deceleration), it is necessary to find the point where the maximum braking deceleration starts to occur.

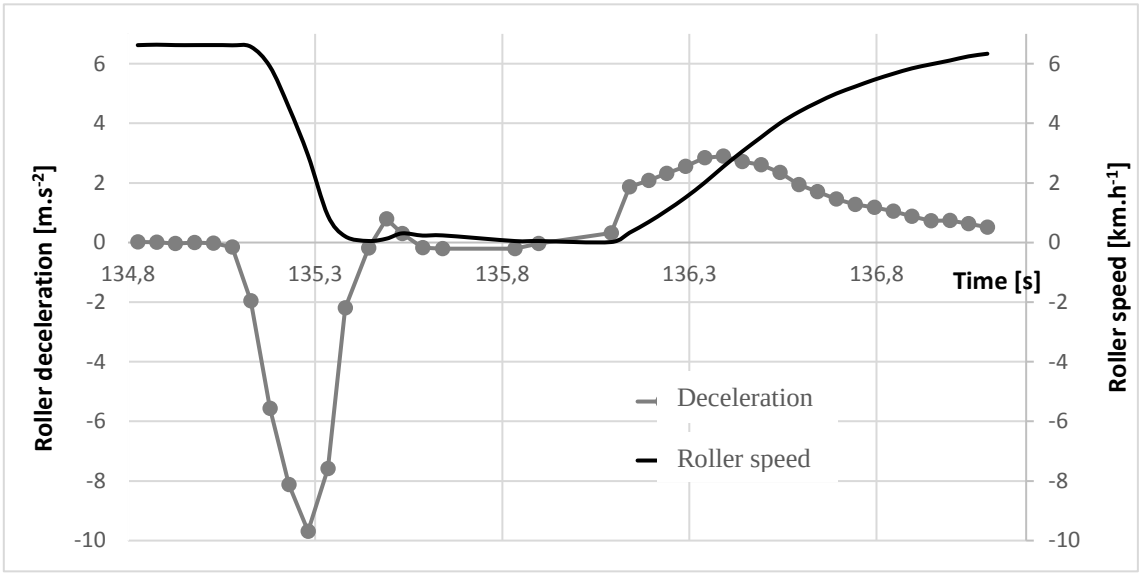

Fig. 2 Speed and acceleration – 50 ms with brake booster

The key issue is to determine the limit where the braking effect can be considered as the maximum. It is possible to break the highest values with a straight line and at the point where the line first crosses the braking force or deceleration curve, this moment shall be marked as the start of maximum braking force. To construct such a line, it is necessary to come up with several values with similar intensity, or to take into account the value at which the braking force is stabilized.

Tab. 1 Braking record 50 ms with brake booster

Channel	Time	Impuls	Time s	Roller speed rpm	Roller acceleration $m.s^{-2}$	Calculated speed $km.h^{-1}$	Braking force N	Speed course %
1	6748856173	363637	134.9771	121.6277	0.0023	6.6231	370.8825	100
1	**6751384976**	**363742**	**135.0277**	**121.6454**	**-0.0198**	**6.6241**	**362.4733**	**100.01**
1	6753916905	363847	135.0783	121.4952	-0.1577	6.6159	310.0553	98.89
1	6756419139	363950	135.1284	120.5954	-1.9616	6.5669	-375.392	99.15
1	**6758959234**	**364044**	**135.1792**	**108.4175**	**-5.5643**	**5.9038**	**-1744.44**	**89.14**
1	6761492398	364116	135.2298	83.27037	-8.1212	4.5344	-2716.06	68.46
1	6764058260	364163	135.2812	53.66435	-9.6844	2.9223	-3310.06	44.12
1	6766692788	364178	135.3339	16.68053	-7.5863	0.9083	-2512.8	13.71

According to ECE R 13, where the maximum braking force is limited by the speed of the rollers, it is interval determined by the abbreviation MFDD. This is the moment when the speed drops to 80% and the lower speed of the rollers decreases to 10%. Therefore, it is necessary to determine the point of sinking to 80% for the determination of the braking time. Due to small number of values at the 50 ms frequency, 80% can not be accurately achieved, because small number of points, the possible interlace is not accurate enough. In tab. 1 is highlighted the interval (150 ms) from the start of braking to value closest to 80%. In this case, it is 89.14%.

In the second measurement was used scanning frequency of 10 ms to obtain a larger relevant data volume to estimate the rise time. Fig. 3 again shows a plot of braking deceleration and cylinder speed depends on time using a brake booster.

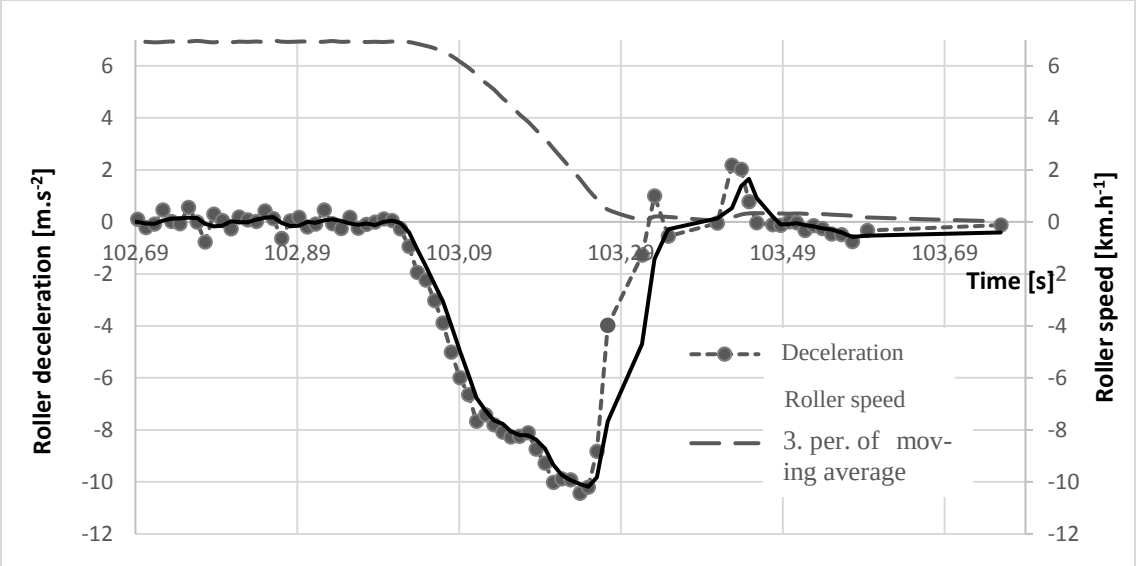

Fig. 3: Speed and acceleration – 10 ms with brake booster

With a 10-ms frequency, it is possible to get closer to measured values to required speed reduction value to 80%. For example, when measuring the booster time without a booster, was reached 81,17 %, which corresponds to the braking rise 0.773 s without brake booster and 0.044 s with brake booster.

From the graphs above, it is clear, that the braking force quickly reaches the maximum and then drops. This is caused by low speed of rollers, when the speed of the rollers approaches zero after reaching the maximum braking force. Roller speed is maintained by the electric motors at approximately 122 rpm, corresponding to approximately 6 $km.h^{-1}$. This speed was chosen with respect to rapidly reaching the maximum braking force, when wheels will be blocked at higher speed. The large inertial force of the rollers would, despite the standing wheels of the test vehicle, rotate the rollers, thus damaging tires of the car.

CONCLUSION

For evaluate the acceleration of brakes, 50ms scanning frequency seems to be less suitable than the 10ms scanning frequency because of the insufficient number of values for its analysis. It is come out that the sensing frequency has an effect to determining the rise time. During the measurement, a scanning frequency of 0.5 ms was also used, but it is not reported in the measurement results because of low predictive value and difficult evaluation. At the scanning frequency, the rise time was 0.073 s without a booster and 0.084 s with a booster.

This scanning frequency, however, disproved the prime premise of more accurate measurement with higher scanning frequency. Using a 0.5ms frequency, there was a significant fluctuation in the measured values. Because of the fluctuation of the speed around the constant value, the acceleration also varies. Therefore, speed changes, instead of acceleration, within a very small range of values. For this reason, at a higher scanning frequency, it is preferable to determine the rise time from the course of the speed of the rollers instead of acceleration.

REFERENCES:

1. Biondi, F., Strayer, D. L., Rossi, R., Gastaldi, M., & Mulatti, C. (2017). Advanced driver assistance systems: Using multimodal redundant warnings to enhance road safety. *Applied Ergonomics, 58,* 238-244. doi:10.1016
2. Bojko, A., Fedotov, A. I., Khalezov, W. P., & Młyńczak, M. (2015). Analysis of brake testing methods in vehicle safety. Paper

presented at the *Safety and Reliability: Methodology and Applications - Proceedings of the European Safety and Reliability Conference, ESREL 2014*, 933-937

3. Hecker, F. (2015). Brake-based stability assistance functions for commercial vehicles. *Handbook of driver assistance systems: Basic information, components and systems for active safety and comfort* (pp. 1021-1045) doi:10.1007/978-3-319-12352-3_43
4. Pan, H., Guo, X., Pei, X., & Dong, X. (2017). Modeling, simulation and experimental analysis of brake pedal feel for passenger car. *SAE Technical Papers, 2017-March*(March) doi:10.4271/2017-01-1371
5. PŘEDPIS EHK-OSN č. 13.: Uniform provisions for the approval of category M, N, O vehicles in terms of braking.
6. Statistical data on accidents in the Czech Republic [online], dostupné z: http://www.policie.cz/clanek/statistika-nehodovosti-900835.aspx

Corresponding author:
Ing. Daniel Mader, Department of Quality and Dependability of Machines, Faculty of Engineering, Czech University of Life Sciences, Kamýcká 129, 165 21 Prague-6 Suchdol, Czech Republic, maderd@tf.czu.cz

EVALUATION OF LORA LPWAN TECHNOLOGY FOR DATA TRANSFER TO MEASURING DEVICES

Pavel MATĚJKA

Department of Technological Equipment of Buildings, Faculty of Engineering, Czech University of Life Science Prague

Abstract
The article is focused on evaluation of the low power wide area networks (LPWAN) technologies. It is expected that LPWAN can be part of measuring system inside buildings.Therefore, in this work it is studied the indoor performance of one LPWAN technology, namely LORA. The measurement has been conducted using commercially available equipment in campus of Czech University of Life Science in Prague, which has an area for 400 meters from North to South and over 900 meters from East to West. The measurement was executed by a sensor witch periodically transferring the data to a base station. The obtained results show that when using 14 dB transmit power, the whole campus space can be covered. Measured packet success transferring ratio was 97.3% without retransmission.

Key words: *Internet of the things; LPWAN; packet loss; range.*

INTRODUCTION

The Internet of Things and LPWAN are paradigm that is rapidly gaining ground in the scenario of modern wireless telecommunications. The basic idea of this concept is the pervasive presence around us of a variety of things or objects such as sensors, actuators, mobile phones, etc. which, through unique addressing schemes, are able to interact with each other and cooperate with their neighbors to reach common goals *Bianchi* (2000). Literature classifies the objects and ways of communication conforming to the IoT with a wide range of meaning and understandings including RFID (*Bianchi, 2000*), Wireless Sensor Networks (WSNs) (*Wu, 2011*), Machine-to-Machine (M2M) *(Doherty et al., 2016*), among others.

The PLWAN is typically implement as the basic star topology, where each device communicates to the base station directly. Depending on the environment and application the area covered by a single base station may range from kilometer (e.g.,in city centrer) to dozens of kilometers (e.g. in rural areas). Results of outdoor measurements for Lora technology shows that it can reach 60% reliability for 30 km distance (*Petajajarvi, 2015*). Nonetheless, the author do not know about any attempts of evaluation the performance of LORA indoors.

Aim of this thesis is evaluation of LoRa technology. In general, the results of this study show that PLWAN LoRa is attractive technology for the wireless data transfer between measuring devices placed in indoors environment.

MATERIALS AND METHODS

As the base station was used the Kerlink923Lora IoT station. The station was connected to the local internet network by which saved data to database on external server. Base station was configured to listen to all frequency channels. As an antenna was used Aerial D100-1000. The antenna can transmit or receive the signal in frequency band from 100 MHz to 1 GHz and provides 2 dB gain. Base station and antennafor the base station were placed on Faculty of Economics and Management.

As the end device was used solution based on the Semtech SX1272MB2xAS LoRa™ extension board. To control the LoRa™ extension board used a NUCLEO-L073RZ MCU board based on the ultra-low-power STM32L0 ARM 32-bit microcontroller. Some of tested locations are in the areas which have hard radio signal propagation conditions. Therefore, for the test was end device configured to operate with the largest possible spreading factor. In this case, the sensitivity of the receiver is highest with reaches -137 dBm. It gived the total radio link budget of more than 150 dBm. The drawback of this is very low data transfer speed, which is mere then 293 bps.Messages were sent repeatedly (every 10 seconds). Device was placed on several places of campus (see at Tab. 1).

RESULTS AND DISCUSSION

Tab. 1 list estimated distance between each measurement location and the base station's antenna, with the number of position on the map, as well as respective number of transmitted and received packets with the calculation of packet success ratio for each of the test location.

As can be seen, the total number of packets transmitted during the experiment for the differential locations from 50 to almost 1000. The presented results in Tab. 1 indicate that average 97.3 % of all the data packets were successfully transferred. Unfortunately, the strict duty cycle limitations imposed by the spectrum usage regulations make the measurement very time consuming and hamper. Even this number of packets enabled us to collect the data which reveal important capabilities of the LORA technology.

Tab. 1 Results of measurements in different locations

Location	Distance to BS [m]	No. of Tx packets	No. of Rx packets	Success ratio [%]
Technical faculty	228	1796	1758	97.9
SIC	200	736	717	97.4
Mensa	142	331	329	99.4
Sports centre	512	878	831	94.7

CONCLUSIONS

In current paper was described first attempts of investigation the suitability of LoRa LPWAN technology for data transfer to and from measuring devices. It studied the performance of LoRa communication with indoor location. The measurement was conducted using the LoRa™ extension board as the end device and Kerlink Lora IoT station used as base station placed on roof of the Faculty of Economics and Management.

ACKNOWLEDGMENT

This study was supported by department of Technological Equipment of Buildings, Faculty of Engineering.

REFERENCES

1. Bianchi, G. (2000). Performance Analysis of the IEEE 802.11 Distributed Coordination Function. In*IEEE Journal on Selected Areas in Communications*,535-47.
2. Bianchi, G. (2000). Prototyping Connected Devices for the Internet of Things. In *Computer*, 26-34.
3. Doherty, L., Lindsay, W., Simon, J. (2016). The Internet of Things: A Survey. In *Proceedings - International Conference on Computer Communications and Networks* (pp. 91-98). ICCCN
4. Petajajarvi, J., Pettissalo, M., Mikhaylov, A., Roivainen, A. (2015). On the Outdoor Coverage of Low Power Wide Area Networks: Range Evaluation and Channel Attenuation Model for LoRa Technology. In International Conference on Inteligent Transportatin Systems Telecommunication (pp. 1–6).
5. Wu, G. (2011). M2M: From Mobile to Embedded Internet. In*IEEE Communications Magazine*, 49, 36-43.

Corresponding author:
Ing. Pavel Matějka, Department of Technological Equipment of Buildings, Faculty of Engineering, Czech University of Life Sciences Prague, Kamýcká 129, Praha 6, Prague, 16521, Czech Republic, phone: +420 725 833 560, e-mail: paja.matejka@gmail.com

DEPENDABILITY OF THE INJECTION PRESS

Petra MICHÁLKOVÁ, Václav LEGÁT, Zdeněk ALEŠ

Department for Quality and Dependability of Machines, Faculty of Engineering, Czech University of Life Sciences Prague

Abstract
The aim of this paper is an analysis of dependability of an injection press. Collected data - operating times between failures and times to restoration for a year of the use of the press have been processed using the Weibull distribution. The output includes Weibull distribution parameters and basic functions of reliability and maintainability, i.e. probability of failure and of reliability, density and intensity of failures, then also probability of restoration and restoration probability density. Last but not least, mean time between failures and mean time to restoration including steady-state availability were calculated. The results obtained can be useful for internal benchmarking in an organization with a higher number of presses and for developing a maintenance strategy.

Key words: *Dependability, Weibull distribution, injection press.*

INTRODUCTION

Dependability is a highly significant field not only in technical applications nowadays. During last decades, close attention has been paid above all to production quality, while dependability has often been neglected in practice. Application of dependability tools contributes to ensuring dependability of particular products, machines, systems etc..

Dependability is defined as an ability to perform as and when required. Dependability includes availability, reliability, maintainability and maintenance supportability and in some cases also other characteristics, such as durability, restorability, safety and security. Dependability is used descriptively as a summary term for an object quality characteristics related to time.

In term of operational dependability of machines and manufacturing equipment, following are the most important characteristics: availability, reliability, maintainability and maintenance supportability Fig. 1 (*Legát, 2000; Legát, 2014; Teringl, et al., 2015*).

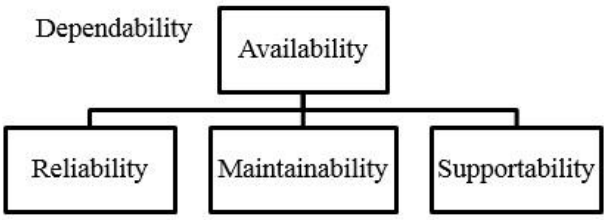

Fig. 1 Relation between dependability characteristics

MATERIALS AND METHODS

The data collection of ES 5550/1300DK injection press was performed for the whole 2016 year. The injection press was manufactured in 1996 with clamping force of 1300 tones – Fig. 2. A programme was implemented to the injection press, recording times of failure occurrence and times of restoration. Operating times between failures and times to restoration were calculated from these data Tab.1. Data concerning the press accessories, such as a printer, a manipulation robot, a conveyor, a video-camera etc., were excluded. The acquired input data converted to times in hours are shown in Tab. 1.

Tab. 1 Input data for a calculation of measures of reliability and maintainability including steady-state availability (time periods are given in a format of hours with rounding to two decimal places)

Failure and restoration no.	1	2	3	4	5	6	7	8	9
Operating time between failures *OTBF* [h]	0,14	0,21	0,47	0,99	1,11	1,11	1,17	1,54	2,01
Time to restoration *TTR* [h]	0,07	0,40	0,57	0,61	0,65	0,73	0,83	0,85	0,99
Failure and restoration no.	10	11	12	13	14	15	16	17	18
Operating time between failures *OTBF* [h]	3,37	4,96	5,11	5,81	8,36	9,60	9,64	11,63	11,66
Time to restoration *TTR* [h]	1,27	1,30	1,31	1,65	1,70	1,77	1,87	1,99	2,00
Failure and restoration no.	19	20	21	22	23	24	25	26	27
Operating time between failures *OTBF* [h]	11,95	12,57	15,30	15,95	18,39	21,28	22,84	29,58	32,09
Time to restoration *TTR* [h]	2,01	2,04	2,14	2,41	2,47	2,85	2,87	2,93	3,08
Failure and restoration no.	28	29	30	31	32	33	34	35	36
Operating time between failures *OTBF* [h]	35,65	36,83	37,59	38,12	41,98	44,57	44,60	46,41	52,31
Time to restoration *TTR* [h]	3,09	3,10	3,15	3,15	3,22	3,37	3,49	3,66	4,22
Failure and restoration no.	37	38	39	40	41	42	43	44	45
Operating time between failures *OTBF* [h]	53,76	54,49	57,57	58,43	62,79	63,64	63,97	64,87	81,06
Time to restoration *TTR* [h]	4,45	4,50	4,80	5,21	5,51	5,72	6,03	6,04	6,08
Failure and restoration no.	46	47	48	49	50	51	52	53	54
Operating time between failures *OTBF* [h]	81,74	91,43	96,42	96,70	97,79	104,53	106,68	108,23	112,52
Time to restoration *TTR* [h]	6,10	6,19	6,41	6,52	7,07	7,19	7,59	7,84	7,85
Failure and restoration no.	55	56	57	58	59	60	61	62	63
Operating time between failures *OTBF* [h]	117,53	121,29	122,53	123,51	130,94	133,56	146,57	149,23	151,44
Time to restoration *TTR* [h]	8,23	9,88	9,88	10,33	10,37	11,43	12,53	13,85	14,42
Failure and restoration no.	64	65	66	67	68	69	70	71	72
Operating time between failures *OTBF* [h]	153,64	155,63	156,05	161,57	163,66	173,29	176,04	177,39	185,35
Time to restoration *TTR* [h]	15,14	15,97	16,73	17,82	18,22	18,86	20,99	21,40	21,83
Failure and restoration no.	73	74	75	76	77	78	79	80	81
Operating time between failures *OTBF* [h]	190,84	221,79	243,70	251,69	271,48	275,76	319,38	326,30	366,65
Time to restoration *TTR* [h]	23,04	24,91	33,83	34,75	39,67	42,83	45,83	55,12	55,94
Failure and restoration no.	82	83	84						
Operating time between failures *OTBF* [h]	372,50	402,59	404,54						
Time to restoration *TTR* [h]	63,21	73,77	--						

The data collected and recomputated to time periods have been processed using the Weibull analysis, for which the following basic steps have been applied in compliance with ČSN EN 61649:2009 standard (*ČSN, 2009*):

- Ascending order of the input data
- Bernard's approximation

- Substitution to a modified distribution function *F (t)*
- Linear regression – a straight line equation
- Calculation of α shape parameter and β scale of the Weibull distribution (*Aleš, 2016; Legát et al., 2017*)

To make the picture complete, basic indicators of reliability and maintainability based on the Weibull distribution of operating times between failures and times to restoration, mean times and availability are given as well:

- The Weibull distribution probability density function of operating time between failures

$$f(OTBF) = \frac{\alpha}{\beta^{\alpha}} \cdot (OTBF)^{\alpha-1} \cdot \exp\left[-\left(\frac{OTBF}{\beta}\right)^{\alpha}\right] \quad (1)$$

Where: α…Shape parameter of Weibull distribution for operating time to failure [-],
β...Scale parameter of Weibull distribution for operating time to failure [-].

- Probability of failure-free operation

$$R(OTBF) = \exp\left[-\left(\frac{OTBF}{\beta}\right)^{\alpha}\right] \quad (2)$$

- Probability of failure

$$F(OTBF) = 1 - \exp\left[-\left(\frac{OTBF}{\beta}\right)^{\alpha}\right] \quad (3)$$

- Failure intensity

$$\lambda(OTBF) = \frac{\alpha}{\beta}\left(\frac{OTBF}{\beta}\right)^{\alpha-1} = \frac{f(OTBF)}{R(OTBF)} \quad (4)$$

- Estimation of mean operating time between failures *MOTBF*

$$\hat{MOTBF} = \frac{1}{m}\sum_{j=1}^{m} OTBF_j \text{ [h]}, \quad (5)$$

Where: m…Number of failures of repaired object [-],
$OTBF_j$…j^{th} operating time between two consecutive failures ($j-1$; j) [h].

- The Weibull distribution probability density function of time to restoration

$$f(TTR) = \frac{\alpha}{\beta^{\alpha}} \cdot (TTR)^{\alpha-1} \cdot \exp\left[-\left(\frac{TTR}{\beta}\right)^{\alpha}\right] \quad (6)$$

Where: α…Shape parameter of Weibull distribution for time to restoration [-],
β…Scale parameter of Weibull distribution for time to restoration [-].

- Probability of performing restoration within a given time

$$R(TTR) = \exp\left[-\left(\frac{TTR}{\beta}\right)^{\alpha}\right] \quad (7)$$

- Probability of not performing restoration within a given time

$$F(TTR) = 1 - \exp\left[-\left(\frac{TTR}{\beta}\right)^{\alpha}\right] \quad (8)$$

- Estimation of mean time to restoration *MTTR*

$$\hat{MTTR} = \frac{1}{m}\sum_{j=1}^{k} TTR_j \text{ [h]}, \quad (9)$$

Where: m…Number of failures (repairs) of repaired object [-],

TTR_j…Time to restoration of j^{th} failure [h].

- Steady-state availability

$$A = \frac{MOTBF}{MOTBF + MTTR} [-], \quad (10)$$

Where: *MOTBF*…Mean operating time between failures,
MTTR…Mean time to restoration (contains mean corrective time + time of undetected failure state and administrative delay).

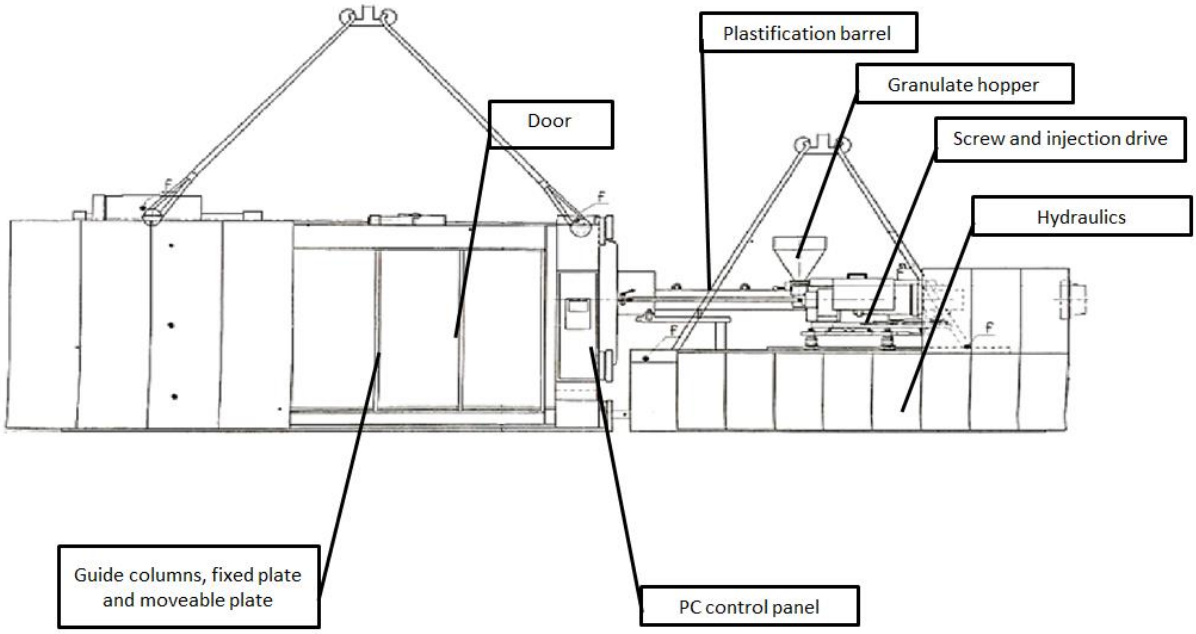

Fig. 2 Scheme of ES 5550/1300DK injection press

RESULTS AND DISCUSSION

No data concerning dependability of similar injection presses have been found in the available literature, therefore one cannot compare the results achieved with other authors dealing with similar issues.

Using formerly derived relations, values of the Weibull distribution parameters for operating time between failures O*TBF* and time to restoration *TTR* can be calculated (Tab. 2)*:*

Reliability indicators and their function values calculated according to equations (1-5) are shown in Fig. 3 and maintainability indicators calculated according to equations (6-10) are shown in Fig. 4.

Tab. 2 Weibull distribution parameters, indicators of reliability, maintainability and availability

Parameter/indicator	α shape parameter	β scale parameter	*MOTBF* [h]	*MTTR* [h]	*A*
reliability	0.674	94.83	100.48	--	0.897
maintainability	0.923	9.90	--	11.39	

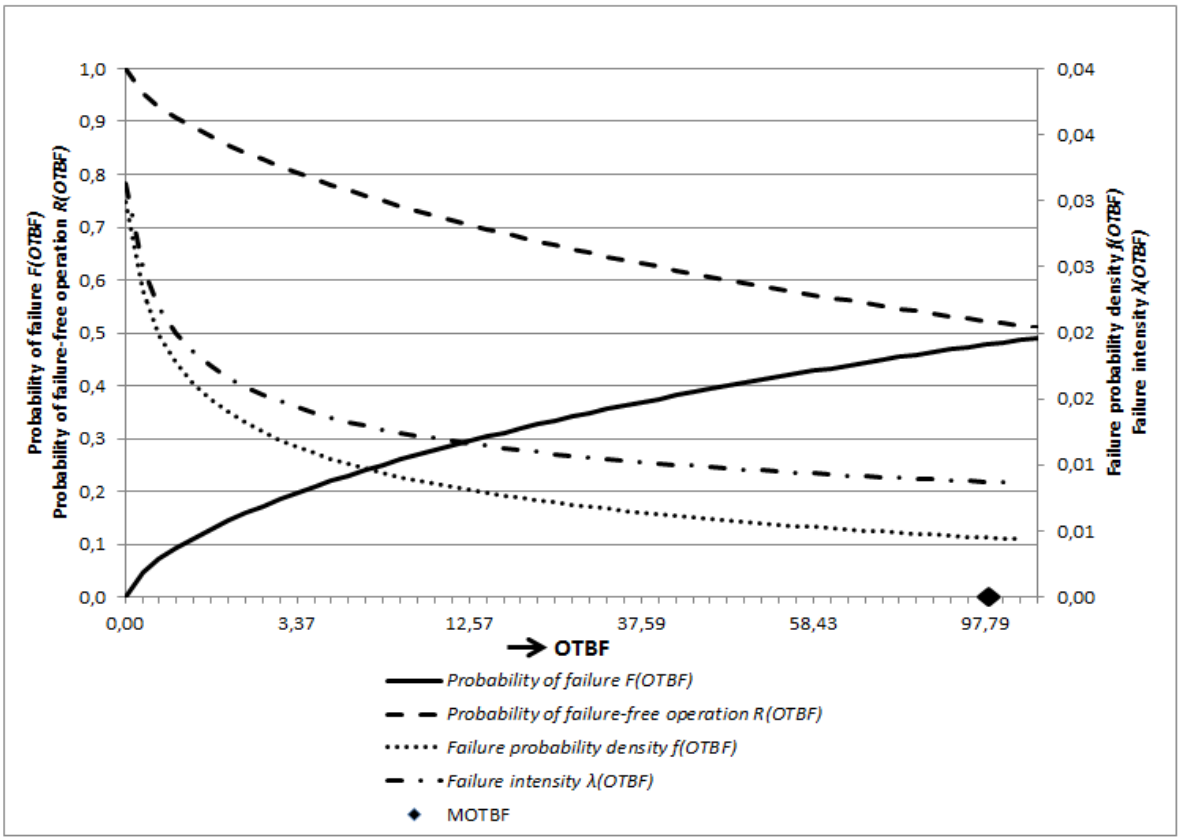

Fig. 3 Dependability indicators depending on operating time between failures

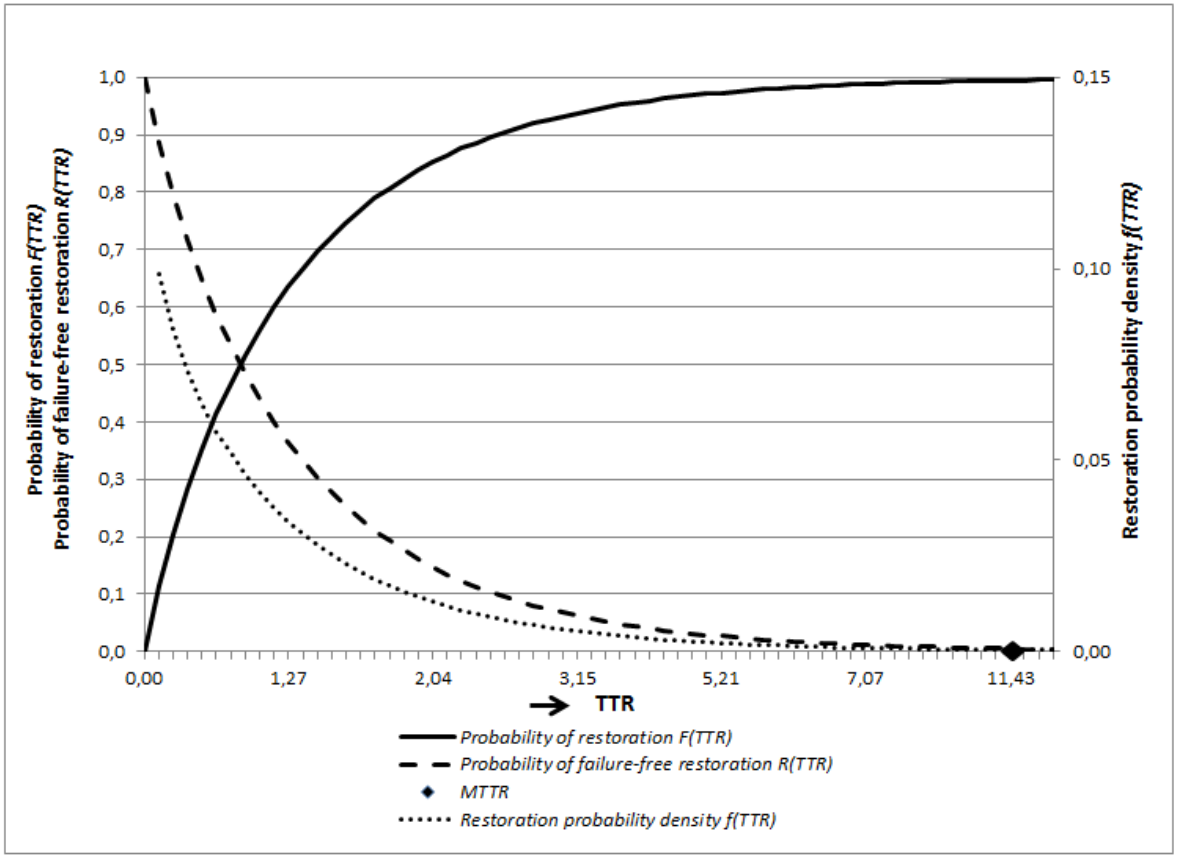

Fig. 4 Maintainability indicators depending on time to restoration

CONCLUSIONS

The acquired reliability and maintainability measures of the injection press can be used for application of restoration theory when deciding on applicability of preventive maintenance or corrective maintenance, creating a maintenance plan (*Legát et al., 2016*), purchasing a new press, looking for ways to increase the machine effectiveness through availability enhancement (*Legát, 2003*).
Long-term monitoring of dependability data can also be used for assessment of production equipment ageing process, for internal objectification of decisions on restoration of a machine as a whole.

ACKNOWLEDGEMENTS

The paper was created with the grant support – CIGA 20173001 - Utilization of butanol in compression ignition engines of generators.

REFERENCES

1. Aleš, Z. (2016). Stanovení parametrů Weibullova rozdělení hustoty pravděpodobnosti poruch v MS Excel. In: *Weibullovo rozdělení náhodných veličin: Materiály z 64. semináře odborné skupiny pro spolehlivost*, Praha, Česká společnost pro jakost, pp. 12-23. IBSN 978-80-02-02696-9.
2. ČSN EN 61649 (010653): 2009 Weibullova analýza.
3. Legát, V. (2003). Management údržby zaměřený na peníze. In: *Sborník druhé mezinárodní konference ÚDRŽBA 2003*, ISSN 80-213-1065-0, 2003, pp. 19 - 26.
4. Legát, V. (2000). Současné problémy v oblasti zabezpečování spolehlivosti strojů. *Mezinárodní konference Provozní spolehlivost strojů 00*, ISSN 80-213-0631-9, 3, pp. 83 – 90.
5. Legát, V. (2014). Úvod do spolehlivosti. *Materiály z 54. setkání odborné skupiny pro spolehlivost*, Praha: Česká společnost pro jakost. ISBN 978-80-02-02514-6.
6. Legát, V. a kol. (2016). Management a inženýrství údržby. *Professional Publishing*, Praha, ISBN978-80-7431-119-2.
7. Legát, V., Mošna, F., Aleš, Z., & Jurča, V. (2017). Preventive maintenance models – higher operational reliability. *Eksploatacja i Niezawodnosc – Maintenance and Reliability*, 19 (1): 134–141,http://dx.doi.org/10.17531/ein.2017.1.19.
8. Legát, V., Stávek, M., & Aleš, Z. (2014). Preventivní údržba - cesta k vyšší výrobě a tržbám. In: *Sborník konference Národné fórum údržby 2014*, Štrbské Pleso, SSÚ Bratislava, ISBN 978-80-554-0880-4
9. Mykiska, A. (2000). Spolehlivost technických systémů. *Skriptum ČVUT Praha, ČVUT*. 177. ISBN 80-01-02079-7.
10. Stávek, M., Aleš, Z., Legát, V., & Teringl, A. (2015). Operational risk management and treatment at technical systems with maintenance support. *Manufacturing Technology*, 15 (3), pp. 429-435. ISSN: 1213-2489.
11. Teringl, A., Aleš, Z., & Legát, V. (2015). Dependability characteristics - indicators for maintenance performance measurement of manufacturing technology. *Manufacturing Technology*, 15 (3), pp. 456-461. ISSN: 1213-2489.

Corresponding author:
Ing. Petra Michálková, Department for Quality and Dependability of Machines, Faculty of Engineering, Czech University of Life Sciences Prague, Kamýcká 129, Praha 6, Prague, 16521, Czech Republic, e-mail: michalkovap@tf.czu.cz

QUALITY OF WORK OF CENTRE PIVOT IRRIGATION MACHINE WITH SPRAYER

Norbert MICHLIAN, František URBAN, Ivan RIGÓ, Henrich BLEHO, Michal SOJKA

Department of Machine and Production Biosystem, Faculty of Engineering, Slovak University of Agriculture in Nitra, Slovak Republic

Abstract
In this paper, we focused on evaluating the quality of work of the already renovated irrigation system Fregat DMU A229. The renovation was carried out by repairing the whole structure and replacing the original rotary sprinklers with sprayers. I-Wob sprayers from Senninger were used as distributors of irrigation water. Practical measurements were carried out on parcels of the agricultural company VPP Kolíňany, s.r.o. We applied the methodology according to the international standard ISO 11545 (2009), where during the measurement the wind speed was less than 1.5 m.s^{-1}. The cultivated and irrigated crop was seed corn in the tested field. The value of the irrigation unity coefficient did not reach the set standard, for the left nozzle spray the value of CuH - 69.15% was achieved (the number of storage rain pots was 64pcs) and on the right nozzle spray the value was 67.81% (the number of storage rain pots was 55pcs). To increase the value of the irrigation uniformity coefficient CuH, we would suggest re-setting of sprayers and changing of nozzles on fields with low quality of irrigation and a subsequent measurement. Waste water, which occurs with movement of each chassis, is recommended to be guided back to the hose of the pivot for irrigation.

Keywords: *irrigation, irrigation uniformity, coefficient CuH.*

ÚVOD

Pod závlahou v poľnohospodárstve rozumieme melioračné opatrenie, ktorým sa uskutočňuje navlaženie pôdy, porastu, alebo prízemnej vrstvy vzduchu, aby sa dosiahla optimalizácia produkčného systému pri získaní vysokých a stálych hektárových úrod v rastlinnej výrobe (*Jobbágy, 2011*). Z dostupných prameňov sa zistilo, že na Slovensko bolo dovezených 450 zavlažovačov Fregat. Z uskutočneného prieskumu vyplynulo, že z nich bolo 120 kusov zošrotovaných. Stav je veľmi nepriaznivý, lebo v priemere bola funkčnosť zavlažovačov Fregat 56,1 %. Následné úpravy a výmena pôvodných distribútorov umožnila využívať následne danú skupinu závlahovej techniky (*Simoník a kol., 2003*). Kvalita zavlažovania sa posudzuje správnou intenzitou a rovnomernosťou zavlažovania. Intenzita vyjadruje množstvo vody v mm dodané zavlažovačom za časovú jednotku *(Jobbágy & Simoník, 2007, 2009*). Zhutnenie pôdy je spôsobené okrem klasicky zaužívanej poľnohospodárskej techniky aj závlahovou technikou, ktorej kvality práce výrazne ovplyvňuje erozívne účinky, vymývanie živín a rovnomernosť úrody (*Jobbágy a kol., 2016a*). Výhodou zavádzania presného zavlažovania je práce preto znižovanie negatívnych účinkov nerovnomernosti závlahovej dávky a na druhej strane je to úspora vody, elektrickej energie (resp. u niektorých zavlažovačov paliva) a nákladov. Uplatnenie rozstrekovačov sa prejavuje ako veľmi výhodné z hľadiska úspory vody a tvorby jemného kvapkového spektra (*Jobbágy, 2013*). Nedochádza pri tom nadmernému utlačeniu pôdy závlahovou vodu ale len závlahovou technikou (*Jobbágy a kol., 2016b*). Cieľom príspevku bolo posúdiť kvalitu práce repasovaného zavlažovača Fregat s modernými rozstrekovačmi.

MATERIÁL A METÓDY

Testovania zavlažovača Fregat sa uskutočnilo na pozemkoch poľnohospodárskeho podniku VPP Kolíňany, s.r.o., časť Oponice, ktorý sa popri pestovaní základných poľnohospodárskych plodín (pšenica, jačmeň, kukurica a slnečnica) venuje aj pestovaniu kukurice na osivo, repky olejky a tekvice. Zameraná lokalita a testovaný repasovaný širokozáberový zavlažovač sú uvedené na obr.1. Testovanie zavlažovača sa vykonalo na základe požiadavky dodávateľa distribútorov a prevádzkovateľa zavlažovača s cieľom dosiahnuť čo najvyššiu kvalitu práce. Niektoré plodiny jednoznačne vyžadujú pre svoju kvalitnú a vysokú úrodu doplnkovú závlahovú dávku aplikovanú práve spomínaným zavlažovačom a to nielen v danom podniku.

Reapasáciou prešla aj čerpacia stanica v Oponiciach, ktorá bola daná do užívania v roku 1974 na zásobovanie zavlažovanej plochy vo výmere 648 ha s celkovým výkonom 270 $l.s^{-1}$ a s dvomi tlakovými pásmami. V rokoch 2011 až 2013 bola realizovaná postupná obnova závlahovej čerpacej stanice vysokoškolského poľnohospodárskeho podniku v Oponiciach zameraná najmä na rekonštrukciu technologických systémov stanice. Cieľom rekonštrukcie bolo obnoviť funkčnosť čerpacej techniky, tlakových systémov, elektroinštalácie, realizovať výmenu potrubí a armatúr a takto zabezpečiť dostatočné množstvo závlahovej vody a požadovaný prevádzkový tlak na jednotlivých hydrantoch závlahovej siete na plánovanej výmere zavlažovanej plochy 300 – 350 ha.

Obr. 1 Lokalita merania a širokozáberový zavlažovač Fregat
Fig. 1 Localized field and centre pivot irrigation machine

Tab. 1 Technické a prevádzkové parametre zavlažovača Fregat
Tab. 1 Technical and operational parameters of Fregat inrrigation machine
1-parameter, 2-Value, 3-Number of Span, 4-Length of irrigation machine, 5-Diameter of pipe, 6-Height of pipe, 7-Required pressure, 8-Width of machine, 9-Height of irrigation machine

Parameter (1)	**Hodnota (2)**
Počet veží, ks (3)	5
Dĺžka zavlažovača, m (4)	154,365
Priemer vodovodného potrubia, mm (5)	177,8 (152,4)
Umiestnenie ramena vo výške, m (6)	2,2
Požadovaný tlak, MPa (7)	0,42
Šírka zavlažovača pracovná, m (8)	5,3 (prepravná 4,5)
Výška zavlažovača, m (9)	6,5

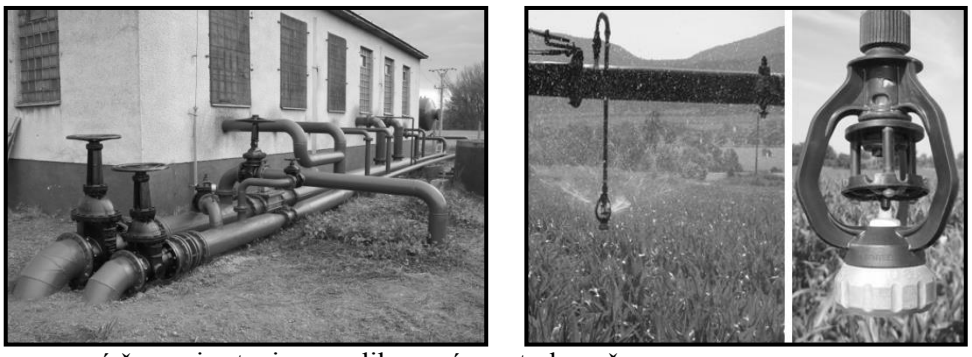

Obr. 2 Repasovaná čerpacia stanica a aplikované rozstrekovače
Fig.2 Repaired water pumping station and Sprayer

Pivotový zavlažovač Fregat konštrukčne, ale aj v princípe činnosti, nadväzuje na úspešné zavlažovače vyrábané firmou Valley. Je určený na zavlažovanie poľnohospodárskych plodín. Zariadenie vykonáva zavlažovanie v pohybe do kruhu okolo pivota, po malej úprave sa môže pohybovať aj v sektore. Technické parametre sú uvedené v tab. 1. Repasácia zavlažovača pozostávala s výmeny distribútorov zá-

vlahovej vody a to klasických otočných postrekovačov za rozstrekovače dodávané firmou B&B Team, Štúrovo. Zavedením rozstrekovačov sa nám podarilo znížiť potrebný prevádzkový tlak z 0,6 na 0,42 MPa (niekedy postačuje aj 0,35 MPa). Zavlažovač Fregat bol teda po repasácii vybavený postrekovačmi značky Senninger radu i-Wob. Tieto postrekovače sa inštalujú na zosilnené flexibilné hadice visiace z horizontálneho ramena zavlažovača minimálne 0,6 metra smerom dole, ako to môžeme vidieť na obr. 2. Postrekovače však musia byť minimálne vo výške 0,91 metrov nad zemou. Regulátor tlaku je umiestnený v hornej časti zosilnenej flexibilnej hadice. Priemer otvoru a tým vlastne typ dýzy umiestnené vo vnútri rozstrekovača boli stanovené dodávateľom distribútorov závlahovej vody.
Praktické merania a overovanie zavlažovača sa vykonalo podľa medzinárodnej normy ISO 11545 (2009), kde bolo treba dodržiavať na jednej strane technologické podmienky a to z hľadiska práce zavlažovača (tlak, prietok), tak na druhej strane to bolo z pohľadu poveternostných podmienok (rýchlosť vetra). Vzťah (1) pre výpočet rovnomernosti postreku podľa Heermanna a Heina je nasledovný:

$$CuH = 100.\left[1 - \frac{\sum_{i=m}^{n} Si.\left|Vi - \overline{Vi}\right|}{\sum_{i=m}^{n} Vi.Si}\right], \quad \% \tag{1}$$

$$\overline{V} = \frac{\sum_{i=m}^{n} Vi.Si}{\sum_{i=m}^{n} Si}, \quad \text{mm} \tag{2}$$

CuH - koeficient rovnomernosti podľa Heermanna a Heina,
n - počet zrážkomerných nádob,
i - číslo určené pre identifikáciu určitej zrážkomernej nádoby so začiatkom i = 1 pre nádobu, ktorá je najbližšie pri pivote a končiace i = n pre zrážkomernú nádobu, umiestnenú najďalej od pivota,
Vi - závlahová dávka v i-tej zrážkomernej nádobe, mm
Si - vzdialenosť i-tej zrážkomernej nádoby od pivota, m
$\overline{V}$ - priemerná závlahová dávka, mm
$\left|Vi - \overline{Vi}\right|$ - absolútna hodnota odchýliek od priemernej dávky.

VÝSLEDKY A DISKUSIA

Merania kvality práce prebehli v júli 2013 bez väčších komplikácii s následným uplatneným návrhov pre zvýšenie hodnoty rovnomernosti postreku zavlažovania. Pestovanou plodinou bola kukurica na osivo, kde výška plodiny neprekážala meraniam, pretože sme použili stojany pre zrážkomerné nádoby. Teplota vzduchu sa pohybovala v intervale 30 – 34 °C. Rýchlosť vetra bola ustálená v rozsahu 1,0 – 1,5 m.s^{-1}. Koncepcia zavlažovača Fregat bola tvorená piatimi podvozkami a krakorcom. Medzi pivotom a jednotlivými podvozkami sa rozstrekovače nachádzali v nasledovnom počte: 3 (Pivot-1 podvozok) – 6 – 6 – 6 – 6. Za posledným, teda piatom podvozkom, bol umiestnený krakorec, na ktorom boli umiestnené tri rozstrekovače. Na konci krakorca bol umiestnený ďalekoprúdový zavlažovač. Repasácia zariadenia popri spomínaných výhodách prešla ešte úpravou hydraulickej ochrany, kde v prípade vyskytnutia poruchy sa zavlažovač zastaví a zablokuje sa aj prívod vody do celého systému prostredníctvom hlavného uzáveru. Rozstup zrážkomerných nádob bol pri meraniach 3 m, čo znamenalo ich celkový počet 64 ks (pre ľavý lúč) a 55 ks (pre pravý lúč). Keďže zavlažovač počas svojej pracovnej činnosti prepúšťal odpadovú vodu cez výpustný ventil, výsledkom závlahovej dávky v nádobách (počet kusov 4 pre ľavý lúč, počet kusov 2 pre pravý lúč) pri podvozkoch boli extrémne hodnoty. Po úprave týchto hodnôt sme dosiahli kvalitu práce určenú koeficientmi rovnomernosti postreku zavlažovača o hodnote 69,15 % (pre ľavý lúč) a 67,81 % (pre pravý lúč).

Tab. 2 Koeficient rovnomernosti postreku CuH, podvozky, zavlažovač
Tab. 2 Coefficient of irrigation uniformity CuH, spans, irrigation machine
1-Span, 2-first measurement, 3-second measurement, 4-overhang, 5- overall, 6-overall without 20 % of cup from pivot

Podvozok (1)	**CuH, %** *Ľavý lúč (2)*	**CuH, %** *Pravý lúč (3)*
1	89,62	81,65
2	88,31	79,85
3	87,47	75,83
4	85,38	81,64
5	85,61	85,44
Krakorec (4)	61,97	44,48
Spolu (5)	69,15	67,81
Spolu, po odstránený prvých 20 % (5)	68,66	61,61

Tab. 3 Popisná štatistika – zavlažovač Fregat DMU A229, ľavý lúč
Tab. 3 Descriptive statistics, FREGAT DMU 229 irrigation machine, first measurement
1-Parameter, 2-Value, 3-Average, 4-Standard error 5-Standard deviation, 6-Variance, 7-Difference max-min, 8-Minimum, 9-Maximum, 10-Sum, 11-Sample size, 12-Coefficient of variation, 13-all cup, 14-without first 20 %

Parameter (1)	**Hodnota (2)** **Všetky nádoby, (13)**	**Hodnota (2)** **Bez prvých 20 % (14)**
Stredná hodnota (3)	9,78	10,10
Chyba strednej hodnoty (4)	0,45	0,55
Smerodajná odchýlka (5)	3,60	3,92
Rozptyl výberu (6)	12,94	15,34
Rozdiel max – min (7)	18,44	18,44
Minimum (8)	5,12	5,12
Maximum (9)	23,56	23,56
Súčet (10)	625,80	515,19
Počet (11)	64,00	51,00
Variačný koeficient, % (12)	36,78	38,77

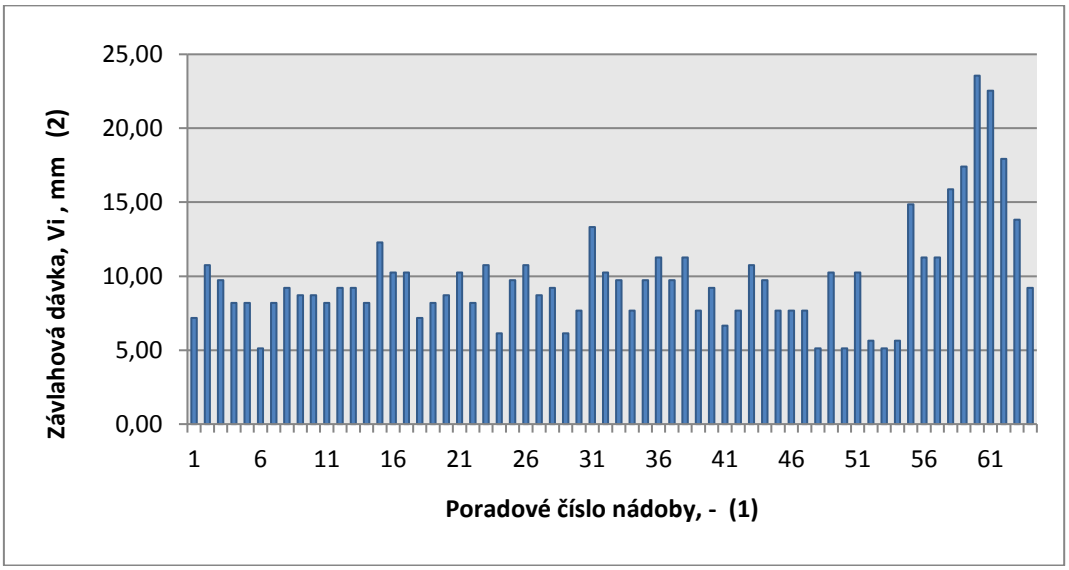

Obr. 3 Rozdelenie množstva vody v zrážkomerných nádobách, ľavý lúč
Fig. 3 Division of the water quantity, first measurement, 1-number of cup, 2-irrigation depth

Výsledky kvality práce jednotlivých podvozkov sú uvedené v tab. 2. Popisná štatistika pre urania ľavého lúča je uvedená v tab. 3 a pre urania pravého leča v tab. 4. Podľa niektorých autorov, ako uvádza aj *Latečka* (*2000*), je možné pri výpočtoch odstrániť prvých 20 % nádob. V našom prípade boli následné výsledky negatívne, rovnomernosť postreku sa v oboch prípadoch znížila, 68,66 % (ľavý lúč) a 61,61 % (pravý lúč) . Bolo to spôsobené tým, že kvalita práce prvých podvozkov bola dosť vysoká a to hlavne pre ľavý lúč s hodnotou až 89,62 %.
Priemerná závlahová dávka dosiahla hodnoty 9,78 mm pre ľavý lúč a 10,10 mm pre pravý lúč. Hodnota variačného koeficienta bola dosť vysoká a to až 35 % čo vyplýva aj výsledkov závlahových dávok, ktoré sa pohybovali v rozpätí od 5,12 do 23,56 mm (pre ľavý lúč) a 1,84 až 22,53 mm (pre pravý lúč).

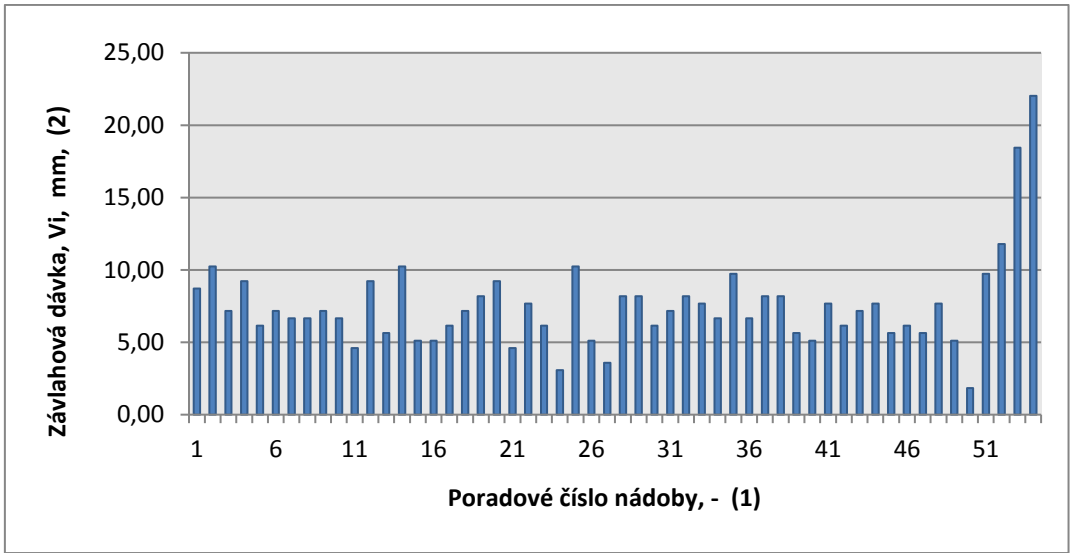

Obr. 4 Rozdelenie množstva vody v zrážkomerných nádobách, pravý lúč
Fig. 4 Division of the water quantity, second measurement, 1-number of cup, 2-irrigation depth

Tab. 4 Popisná štatistika – zavlažovač Fregat DMU A229, pravý lúč
Tab. 4 Descriptive statistics, FREGAT DMU 229 irrigation machine, second measurement
1-Parameter, 2-Value, 3-Average, 4-Standard error 5-Standard deviation, 6-Variance, 7-Difference max-min, 8-Minimum, 9-Maximum, 10-Sum, 11-Sample size, 12-Coefficient of variation, 13-all cup, 14-without first 20 %

Parameter (1)	***Hodnota (2)*** ***Všetky nádoby, (13)***	***Hodnota (2)*** ***Bez prvých 20 % (14)***
Stredná hodnota (3)	7,78	7,90
Chyba strednej hodnoty (4)	0,50	0,62
Smerodajná odchýlka (5)	3,75	4,12
Rozptyl výberu (6)	14,03	16,98
Rozdiel max – min (7)	20,69	20,69
Minimum (8)	1,84	1,84
Maximum (9)	22,53	22,53
Súčet (10)	427,92	347,52
Počet (11)	55,00	44,00
Variačný koeficient, % (12)	48,13	52,17

Pri hodnotení kvality práce závlahovej techniky sa dosiahli uspokojivé výsledky v poraste cukrovej trstiny, v štáte Svazijsko (Afrika). Meraný zavlažovač mal 17 podvozkov a hodnotila sa jeho rovnomernosti postreku podľa Christiansena (Cu). Požiadavkou bolo, aby koeficient rovnomernosti Cu mal hodnoty od 72 % do 92 %. Zo 17 pivotov až 42 % dosiahlo koeficient rovnomernosti nad 90 %. Päť-

desiat tri percent pivotov dosiahlo Cu najmenej 83 %. Iba jeden pivot mal Cu 76% (*Magwenzi & Nkambule, 2003*).
Mnohé experimenty mali cieľ dokumentovať vplyv nerovnomernosti závlahy na úrodu, *Ayars a kol.* (*1991*), *Solomon* (*1984*), *Letey* (*1985*), nezávisle došli k záveru, že s určitou nerovnomernosťou závlahy sa rastliny vyrovnávajú.

ZÁVER

Cieľom predkladaného príspevku bolo posúdiť kvalitu práce pivotového širokozáberového zavlažovača Fregat DMU A229, ktorý mal päť podvozkov. Repasácia zariadenia mala dosiahnuť zvýšenie kvality práce z predpokladaných priemerných 60 % na minimálne 80 % až normou definovaných 90 %. Vzhľadom na dosiahnuté výsledky jednoznačne odporúčame doladiť otvory dýz v jednotlivých rozstrekovačoch, čím dosiahneme zmenu dostreku a prekrytia jednotlivých distribútorov vody. následne je možné dosiahnuť vyššiu kvalitu práce, kde pri dosiahnutí hodnoty 70 % možno hovoriť o uspokojivej kvalite práce.

PODĚKOVANIE

This work was co-funded by European Community under project no 26220220180: Building Research Centre „AgroBioTech".

POUŽITÁ LITERATÚRA

1. Ayars, J. E., Hutmancher, R B., Vail, S. S., & Schoneman, R. A. (1991). Cotton response to nonuniform and varying dophts of irrigation. *Agricultural. Water-Management*, 19 (2), 151-166.
2. ISO 11545 (2009). Poľnohospodárske zavlažovacie zariadenia. Pivotové a čelné zavlažovače s rozstrekovačmi a postrekovačmi. Určenie rovnomernosti zavlažovania. *Norma*.
3. Jobbágy, J. (2011). Hodnotenie závlahovej techniky z hľadiska rovnomernosti závlahy postrekom. *Vedecká monografia*, SPU ES v Nitre, 123 s. ISBN 978-80-552-0617-2
4. Jobbágy, J. (2013). Širokozáberové závlahy v USA. *Roľnícke noviny*. Profi Press, 18.09. 2013, 84 (38), 25-26
5. Jobbágy, J., Beloev, Ch. I., Krištof, K., & Findura, P. (2016a). The benefits and efficiency of precision irrigation. *Mechanization in agriculture*., 62(2), 35-43.
6. Jobbágy, J., Krištof, K., & Findura, P. (2016b). Soil compaction caused by irrigation machinery. *Agronomy Research.*, 14 (3), 790-800 .
7. Jobbágy, J., & Simoník, J. (2007). Hodnotenie kvality práce zavlažovača FREGAT. *Technika v zemědělství a potravinářství ve třetím tisíciletí. Sborník mezinárodní vědecké konference.* .Brno, 24.a 25. 5. 2007.
8. Jobbágy, J., & Simoník, J. (2009). Evaluation of a bauer linestar irrigation machine quality of work. *New Trends in Design and Utilisation of Machines in Agriculture, Landscape Maintenance and Environment Protection : Proceedings of the International Scietific Conference, Prague, 5th - 7th May*. Praha : ČZU. 122-127.
9. Látečka, M. (2000). Rovnomernosť postreku pri závlahe otáčavými postrekovačmi. *Monografia*. Nitra, 58 s. ISBN 80-7137-678
10. Letey, J. 1985. Irrigation uniformity as related to optimum crop production. *Irrigation Science*, 6(4), 253-263. ISSN 0342-7188.
11. Magwenzi, O.E., & Nkambule, S.V. (2003). Suitability of centre pivot irrigation for sugarcane production in Swaziland. Sugar Tech: An International Journal of Sugar Crops and Related Industries. Vol. 77 p. 352–363.
12. Simoník, J., Látečka, M., & Okenka, I. (2003). Obnova parku širokozáberových zavlažovačov. *Acta horticulturae et regiotecturae*. 6(mimoriadne), 63-65. ISSN 1335-2563.
13. Solomon, K. H. (1984). Yield related iterpretation of irrigation uniformity and efficiency measures, *Irrigation Science*, 5, 161-172. ISSN 0342-7188

Corresponding author:
Ing. Norbert Michlian. Katedra strojov a výrobných biosystémov, Slovenská poľnohospodárska univerzita v Nitre, Tr. A. Hlinku 2, 949 76 Nitra, Slovenská republika, e-mail: michlian@bbteamagro.sk

MEASUREMENT OF WOOD DUST CONCENTRATION EMITTED BY RANDOM ORBIT SANDER

Lucia MIKUŠOVÁ, Miroslav DADO

Department of Production Technology and Quality Management, Faculty of Environmental and Manufacturing Technology, Technical University in Zvolen, Slovak Republic

Abstract
Aim of this study was assess the influence of selected factors (type of wood, grain size of the abrasive) on the magnitude of wood dust mass concentration during sanding operation. Sanding of spruce produced statistically higher wood dust mass concentration than sanding of beech. Effect of sanding grid on airborne dust concentration has not been proven.

Key words: *aerosol; sanding; photometer.*

INTRODUCTION

Sanding with hand-held powered tools has been recognized as one of the most significant factor in personal exposure to wood dust in the woodworking industry (*Očkajová et al., 2008; Welling et al, 2009; Ratnasingam et al., 2011; Ojima, 2016; Douwes et al., 2017*). Standard (STN EN 50632-2-4, 2017) defines random orbit sander as sander equipped with a plate positioned eccentrically on the driving spindle which can rotate freely around its axis parallel to the work surface. According to the Machinery Directive 2006/42/EC, random orbit sander have to meet the basic safety requirements related to the health hazards caused by the emission of sanding dust. The dust generated by this tool is mostly controlled by aspirator in combination with a perforated sanding disc. However, the efficiency of the filtration bag is usually insufficient, particularly when sanding wood with finer grain size (*Marková et al., 2016; Douwes et al., 2017*).
Aim of this study was assess the influence of selected factors (type of wood, grain size of the abrasive) on the magnitude of wood dust mass concentration during sanding operation.

MATERIALS AND METHODS

The experimental study was conducted in a test room that fulfils requirements according to standard STN EN 50632-1. Although the temperature and relative humidity inside the test room were not regulated, they remained fairly constant between 20–21°C and 39–40%, respectively, throughout the tests. Average air velocity at sampling point was measured using anemometer (Testo 415, Testo), it ranging from 0,23 $m.s^{-1}$ to 0,27 $m.s^{-1}$. The planning of the experiment determined:

- input factors (wood species - A, abrasive grain size - B),
- output variable (mass concentration of wood dust).

For each factor, the following levels were set:

- factor A (A1 = beech, A2 = spruce);
- factor B (B1 = P80, B2 = P120).

Fig. 1 shows the experimental setup, which consists of a test specimen, aerosol monitor with IOM sampler, and random orbit sander. The input material for the production of the test specimens were cuts of beech (Fagus sylvatica) and spruce (Picea abies), which were cut to the required dimension of 500 mm x 150 mm x 150 mm by longitudinal cutting using the band saw and following by the cross cutting using chain saw. The humidity of the test samples was determined gravimetrically and ranged from 12% to 15%. Sanding was performed using a commercially available handheld random orbit sander (PEX 300 AE, Bosch) without dust box. Sander was adjusted to maximum orbital stroke rate. Abrasive disc with aluminium oxide grain and the paper backing (PS 22 K, Klingspor) was replaced after each measurement. The mass concentration of emitted wood dust was measured using aerosol monitor (DustTrak DRX 8533, TSI Inc.). Before each measurement, zero calibration of the instrument was performed. Sampling period (3 minutes) was estimated from the time required to sand the test specimen. Three repetitions were performed in each trial. To verify adequate cleaning and ventilation after each measurement, the background concentration in test room was monitored using a photometer

(CEL-712 MicroDust Pro, Casella CEL Inc.). Data analysis was performed with statistical software (Statistica v.10, StatSoft). Two-factor analysis of variance was used to determine the influence of type of wood and abrasive grain size on the magnitude of generated wood dust mass concentration. The significance level was set at p=0,05.

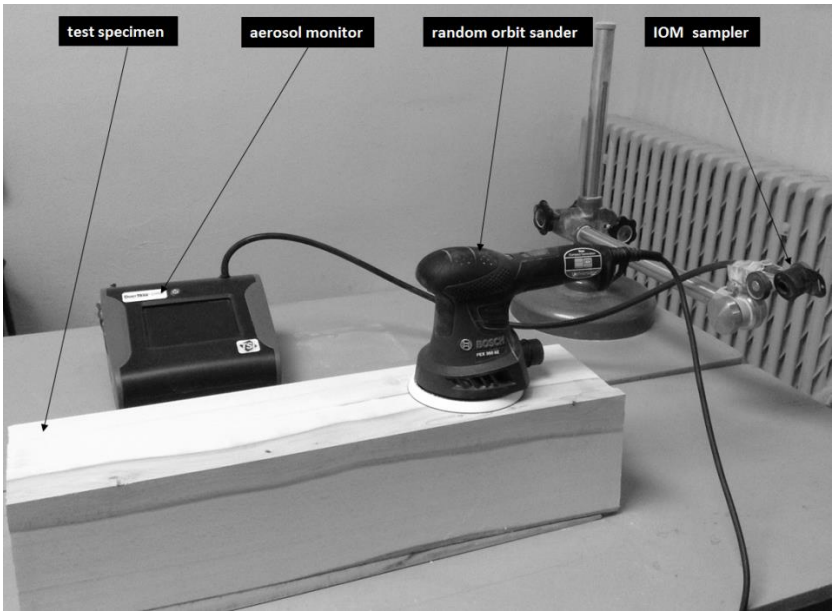

Fig. 1 Experimental set-up

RESULTS

The influence of the type of wood and grain size of the abrasive on the magnitude of the mass concentration of the inhalable fraction of wood dust is shown in Fig. 2. Values of inhalable fraction are arithmetic mean of 3 measurements. The statistical results suggest significant effect of wood species on mass concentration of wood dust (F (1,8) =14,335, p=0,005). On the contrary, grain size of the abrasive and its interaction with type of wood does not significantly influence size of inhalable fraction of wood dust.

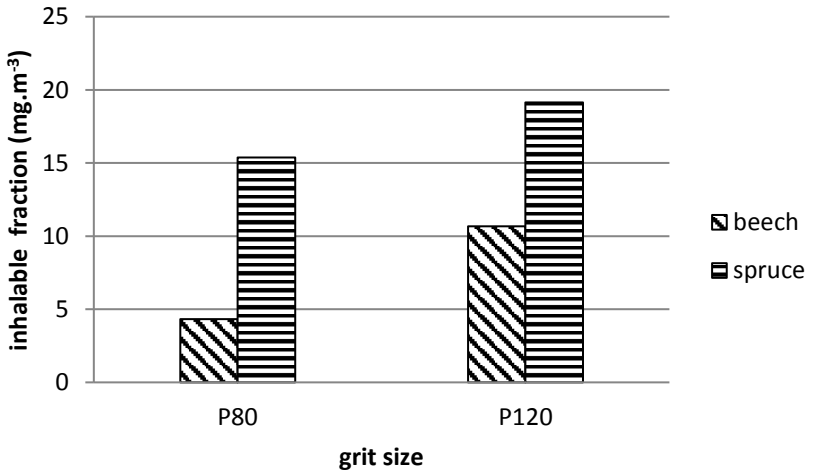

Fig. 2 Effect of wood species and abrasive grain size on inhalable fraction of wood dust mass concentration

The influence of the type of wood and grain size of the abrasive on the magnitude of the mass concentration of the respirable fraction of wood dust is shown in Fig. 3. Values of respirable fraction are

arithmetic mean of 3 measurements. Similarly as in the case of inhalable fraction, only influence of wood species was confirmed (F (1,8) =12,290, p=0,008).

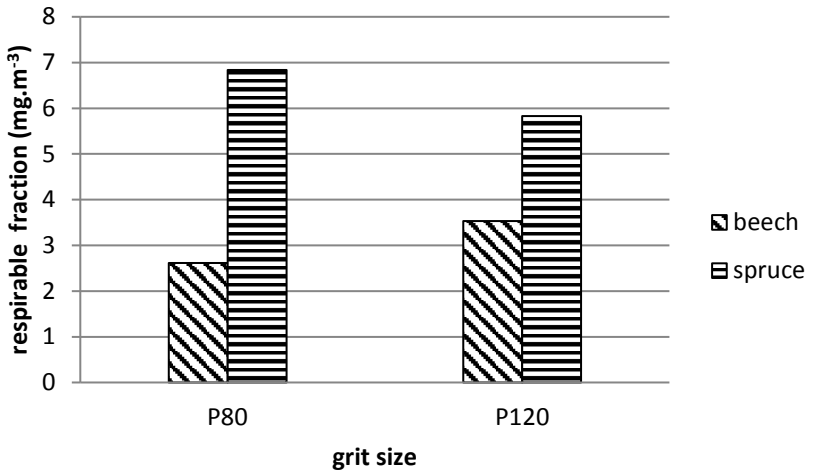

Fig. 3 Effect of wood species and abrasive grain size on respirable fraction of wood dust mass concentration

DISCUSSION AND CONCLUSIONS

The mass concentration of the wood aerosol generated in the wood sanding process is influenced by several factors. These factors, according to Thorp and Brown (1995), can be divided into three groups that characterize the properties of the sanded wood, the properties of the abrasive and the parameters of the sanding process. On the basis of information from available literature on the significance of the effects of individual factors to wood aerosol formation in wood sanding, we identified two factors for the needs of the experiment: the type of wood and the abrasive grain size.

Welling et al. (*2009*) used a pneumatic hand-held belt sanding machine to produce dust from birch plywood sheets, medium density fiberboard (MDF) sheets, and natural pine. They found that higher dust emissions were produced with sanding of MDF sheets than with pine and birch plywood. Further, sanding MDF sheets with coarse sanding paper (grade P100) produced higher emissions than sanding with fine sanding paper (grade P240). *Ratnasingam et al.* (*2011*) found that machine sanding resulted in higher dust concentration compare to hand sanding. Results of their study suggest that minimizing dust-generation during the hardwood sanding process could be achieved by ensuring minimal amount of wood removal as well as the use of the coarset possible abrasive grit in the process. *Ojima* (*2016*) observed by laboratory experiment the generation rate and the particle size distribution of the wood dust produced by handheld sanding operation. He found that soft wood generated more dust than hard wood due to the difference in abrasion durability and further that coarse sand paper produced more dust than a fine sand paper. Comparing results of dust wood concentration evaluation from different experimental setups and field measurements reported in the literature is difficult. Results of our study confirm effect of wood species on wood dust mass concentration. Sanding of spruce produced statistically higher wood dust mass concentration than sanding of beech. Effect of sanding grid on airborne dust concentration has not been proven. We suppose that this could be due to insufficient differences between abrasive grain sizes.

CONCLUSIONS

There are several factors influencing the results of the measurement of mass concentration of solid aerosols in real time and the correct calibration of the measuring instrument is a basic prerequisite for obtaining meaningful data (*Lukáčová et al., 2014, Rasulov & Schwarz, 2016*). Photometers are generally useful for relative assessment of aerosol concentration variations rather than for measuring absolute aerosol concentration (TNI CEN/TR 16013-3, 2013). Due to the fact that for the purpose of the experiment, it was sufficient to know the relative mass concentration values and at the same time we

assuming that the optical properties of beech and spruce wood aerosols is not diametrically different, the corresponding calibration factors were not determined.
The further research will investigate the effect of other factors on the amount of wood dust concentration. Among the observed factors it will be especially the individual technological parameters - type of sander, sanding direction, size of the pressure force, but also the physical and mechanical properties of the sanded wood like density and humidity.

ACKNOWLEDGMENT
The paper is based on work performed under research contract IPA 6/2017 "Investigation of the process of generating a solid aerosol during the sanding of wood" which support is gratefully acknowledged.

REFERENCES

1. Douwe, J., Cheung, K., Prezant, B., Sharp, M., Corbin, M., McLean, D., Mannetje, A., Schlunssen, V., Sigsgaard, T., Kromhout, H., LaMontagne, A., Pearce, N., & McGlothlin, J. (2017). Wood Dust in Joineries and Furniture Manufacturing: An Exposure Determinant and Intervention Study. *Annals of Works Exposures and Health, 61*(4),416-428.
2. Lukáčová, K., Liptai, P., Lumnitzer, E., & Moravec, M. (2014). Possibilities of utilization of equipment usin ir principles for monitoring solid aerosols in real conditions. In *SGEM 2014* (pp. 515-518). STEF92 Technology.
3. Marková, I., Mračková, E., Očkajová A., & Ladomerský, J. (2016). Granulometry of selected wood dust of dust from orbital sanders. *Wood Research, 61*(6), 983-992.
4. Očkajová A., Beljaková, A., & Ľuptáková, J. (2008). Selected properties of spruce dust generated from sanding operations. *Drvna Industrija, 59*(1), 3-10.
5. Ojima, J. (2016). Generation rate and particle size distribution of wood dust by handheld sanding operation. *Journal of Occupational Health, 58*(6), 640-643.
6. Ratnasingam, J., Scholz, F., Natthondan, V., & Graham, M. (2011). Dust-generation characteristics of hardwoods during sanding processes. *European Journal of Wood and Wood Products, 69*(1), 127-131.
7. Rasulov, O., & Schwarz, M. (2016). Monitoring the air pollution and evaluation of the impact of aluminium in Talco. *Journal of environmental management and tourism, 7*(2), 169-174.
8. STN EN 50632-2-4:2013. Electric motor-operated tools. Dust measurement procedure. Part 2-4: Particular requirements for sanders other than disk type.
9. Thorp, A., & Brown, R. (1995). Factors influencing the production of dust during the sanding of wood. *American Industrial Hygiene Association Journal, 56*(3), 236-242.
10. TNI CEN/TR 16013-3:2013. Workplace exposure. Guide for the use of direct-reading instruments for aerosol monitoring. Part 3: Evaluation of airborne particle concentrations using photometers.
11. Welling, I., Lehtimäki, M., Rautio, S., Lähde, T., Enbom, S., Hynynen, P., & Hämeri, K. (2009). Wood Dust Particle and Mass Concentrations and Filtration Efficency in Sanding of Wood Materials. *Journal of Occupational and Environmental Hygiene, 6*(2), 90-98.

Corresponding author:
Ing. Lucia Mikušová, Department of Production Technology and Quality Management, Faculty of Environmental and Manufacturing Technology, Technical University in Zvolen, Studentska 26, Zvolen, 960 53, Slovak Republic, e-mail: lulumikusova@gmail.com

VPLYV AGROTECHNOLÓGIÍ NA ZMENU VLASTNOSTÍ PÔDY

THE IMPACT OF AGRO TECHNOLOGIES ON THE CHANGE OF SOIL PROPERTIES

Miroslav MRÁZ, Pavol FINDURA, Oľga URBANOVIČOVÁ, František URBAN, Ivan RIGO, Peter BAJUS

Department of Machines and Production Biosystems, Faculty of Engineering, SUA in Nitra

Abstract
Thesis deals with the evaluation of the results of research influence preparations for treatment of soil structure adapted cultivation and classical the cultivation of crops to changes structure of soil in agrotechnology in relation to changes in the physical properties of soil chemical properties, soil of resistivity and fertile elements. This selected properties of directly affect the behavior and state land itself. The land has a complex structure of the and its place do not choose. Humidity measurement Kopecky rollers were held in three depth horizons. There is an apparent increase in soil moisture in variants with application of the preparation.The values of infiltration were carried out during the years 2013-2015 from them, there is a difference between the control part of the land and the part to which it was applied preparation.

Key words: *structure of soli; infiltration; humidity.*

ÚVOD

Problematika účinkov strojovej techniky nie je v odborných kruhoch neznáma ani nová. Vplyvom neustálych opakovaných prejazdov po poliach a nadmerného utláčania pôdy ťažkou strojovou technikou dochádza k veľkým stratám na úrodách v rastlinnej výrobe, no keďže sa skúmaniu týchto javov nevenovala dostatočná pozornosť, neprikladal sa ani veľký význam ich vplyvom. Zhutňovanie pôdy, erózia a tvorba prísušku sú faktory, ktoré sa najväčšou mierou pričiňujú a vedú k degradácii pôdy, pričom výrazným spôsobom vplývajú na jej vlastnosti. Spoločenským zdôvodnením riešenia uvedenej problematiky je aktuálna potreba zlepšovania štruktúry pôdy a zvyšovania pôdnej úrodnosti. Postupným využitím získaných poznatkov sa navrhli a vyvinuli ochranné opatrenia, ktoré účinným spôsobom nielenže potláčajú tieto nepriaznivé účinky, ale za určitých podmienok môžu mať aj pozitívny vplyv na pôdnu štruktúru, čím priamo vplývajú na úrodnosť a očakávané výnosy poľnohospodárskych plodín.
Naším cieľom je vytvoriť také podmienky, aby vsiaklo do pôdy čo najväčšie množstvo zrážok potrebných pre rastliny (*Velebný a kol., 2000*). Infiltrácia (vsakovanie) je proces vnikania vody do pôdy, najčastejšie cez jej povrch (*Philip, 1957*).
Okrem klasických prípadov infiltrácie vody zo zrážok, závlah alebo z topiaceho sa snehu, môže voda vsakovať do pôdy z rôznych stojatých vôd ako sú napríklad kaluže, jazerá, nádrže. Z hydrologického hľadiska je najzaujímavejšia infiltrácia zo zrážok. Od intenzity infiltrácie závisí tvorba povrchového odtoku a s ním spojenej erózie pôdy.

MATERIÁL A METÓDY

Na vybranom poľnohospodárskom podniku Agrodružstvo TP, s.r.o. Palárikovo, ktorý pozostáva z 57 pôdnych celkov a štruktúra pôdneho fondu v roku 2010 predstavovala 2 420 ha poľnohospodárskej pôdy, bol vykonaný výskum v priebehu rokov 2013 - 2015 na jednej parcele, rozdelenej na dve časti. Jedna časť bola ošetrená prípravkom na úpravu štruktúry pôdy a druhá časť slúžila ako kontrolná. Aplikácia prípravku na úpravu štruktúry pôdy PRP SOL bola aplikovaná na parcele naširoko. V zmysle stanoveného cieľa práce sa poľné experimenty uskutočnili na tomto vybranom stanovišti a merania boli vykonané v prevádzkových podmienkach.
Pod pojmom prípravok na úpravu štruktúry pôdy, máme na mysli aktivátor vitálnych funkcií pôdy PRP SOL. Pomocné pôdne prípravky neodstraňujú následky, ale vytvárajú priaznivé podmienky pre

biologický život v pôde, čo sa prejavuje aj nižšou spotrebou používanej agrochémie. Preto je PRP SOL vhodný do minimalizácie, ktorá podporuje biologický život v hornej vrstve pôdneho horizontu.
Na danej parcele sa v prvom roku merania (2013) pestovala cukrová repa, v druhom roku merania – jačmeň jarný (2014) a v treťom roku merania – pšenica ozimná (2015). Počas vegetačného obdobia pestovania pšenice a jačmeňa sa vykonávali operácie, ako chemická ochrana a prídavné hnojenie NPK. Pri cukrovej repe sa na rozdiel od predchádzajúcich plodín vykonávala aj medziriadková kultivácia.
Pri poľných meraniach sme sledovali infiltráciu a vlhkosť pôdy. Na meranie infiltrácie sme použili Minidisk infiltrometer (Obr. 1), je veľmi jednoduchý a malý s nízkou náročnosťou na obsluhu. Voda naplnená do spodnej časti sa cez polopriepustnú nerezovú membránu na dne trubky infiltruje do pôdy. Nasávanie vzduchu môžeme nastaviť podľa typu pôdy. Na spodnej časti trubky infiltrometra je stupnica, na ktorej sa po 30 sekundách odpočíta hodnota objemu vody v ml.
Je dôležité vybrať vhodné miesto na meranie. Dôležitým predpokladom je meranie na povrchu pôdy bez puklín, ktoré musíme pripraviť tak, aby bolo rovné a hladké, aby celá plocha membrány bola v styku s povrchom pôdy. Namerané výsledky sa spracujú v počítači.

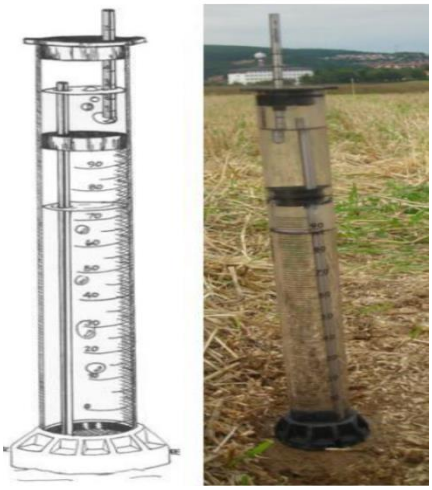

Obr. 1 Infiltromer mini disc

Ako ďalšie sme merali vlhkosť pôdy, ktorú sme robili dvomi metódami. Prvá metóda sa vykonávala elektronickým prístrojom HH2 logger, ku ktorému sme pripojili sondu ML2. Pri meraní vlhkosti pôdy s vlhkomerom sme uskutočnili tri opakovania v každom meracom bode. Pred samotným meraním vlhkosti sa prístroj nakalibroval, aby naše merania boli presné.

Obr. 2 Elektronický prístroj na meranie vlhkosti HH2 logger + ML1 senzor

Druhý spôsob spočíval v stanovení vlhkosti pôdy gravimetrickou metódou s pomocou sady Kopeckého valčekov. Pôdne vzorky sme vždy charakterizovali v hĺbkovom intervale: 5 - 15 cm, 35 - 40 cm, 50 - 60 cm. Pôdnou vlhkosťou rozumieme momentálne množstvo vody v pôde. Vyjadrujeme ju v objemových percentách. Táto metóda spočíva v odobratí vzorky do valčeka, ktorú sme následne hneď odvážili (m1). Vzorka sa vysuší pri 105 °C v časovom intervale 5 - 6 hodín. Po vysušení sa vzorka opäť odvážila (m2).

$$W = \frac{m_1 - m_2}{100}, (100\% objemové)$$

kde:
m1 – hmotnosť vlhkej vzorky, (g)
m2 – hmotnosť suchej vzorky, (g)
W – objem valčeka 100 cm^3

VÝSLEDKY A DISKUSIA

Cieľom práce bolo zhodnotenie výsledkov v oblasti výskumu vplyvu prostriedku pre úpravu štruktúry pôdy v rámci konvenčného a upraveného pestovania vybraných plodín na zmenu štruktúry pôdy v agrotechnológiach vo vzťahu k zmene fyzikálnych vlastností pôdy. Hodnotenie sme vykonali v nasledujúcej postupnosti:

- hodnotenie vlastností pôdy z pohľadu vlhkosti pôdy,
- hodnotenie infiltrácie vody do pôdy.

Parcela sa nachádza v katastrálnom území obce Palárikovo. Jedná sa prevažne o rovinatý pozemok s maximálnym prevýšením 1,5 m v oblasti lokálnych depresií. Historicky bol ovplyvňovaný záplavovou činnosťou rieky Váh.
Pozemok má výraznejšiu pôdnu heterogenitu s vysokým produkčným potenciálom. Väčšia časť výmery pozemku je ťažká až veľmi ťažká pôda, charakteristická problémami so spracovateľnosťou pôdy úzko súvisiacimi s vlhkostným stavom pozemku negatívne ovplyvňovaným nerovnomerným rozložením zrážok počas hospodárskeho roku.

Hodnotenie vlhkosti pôdy

Gravimetricky sme zistili obsah vody v pôde pomocou Kopeckého valčekov a za pomoci vlhkomera na začiatku a na konci vegetácie. Je tu zrejmý nárast vlhkosti pôdy u variant s aplikáciou prípravku. Najvyšší obsah pôdnej vody bol zistený na jeseň v roku 2014, ktorý môžeme vidieť v tab.1, a to s vyšším obsahom prípravku s aplikáciou na široko. Obsah pôdnej vody samozrejme ešte koreluje s množstvom zrážok spadnutých v termíne odberu vzoriek. V tomto roku boli zrážky veľmi nerovnomerné a od júla veľmi nízke. Napriek tomu je zrejmé, že varianty s aplikovaným prípravkom si ponechali vlahu dlhšie obdobie obzvlášť vo vrchnej vrstve pôdy.

Tab. 1 Namerané hodnoty vlhkosti na jeseň 2014

prípravok				kontrola			
č. merania	hĺbka odobratia vzorky (cm)	vlhkosť (hm%)	vlhkosť vlhkomerom (%)	č. merania	hĺbka odobratia vzorky (cm)	vlhkosť (hm%)	vlhkosť vlhkomerom (%)
1	10 – 15	39	39,3	1	10 – 15	37,7	38
2	35 – 40	40,8	41	2	35 – 40	39	39,1
3	50 - 60	42,1	42,5	3	50 - 60	39,2	39
	Ø	40,63	40,93		Ø	38,63	38,7

Hodnotenie infiltrácie

Praktické merania boli vykonané na poľnohospodárskom podniku Agrodruţstvo TP, s.r.o., Palárikovo. Na obrázku 3 je zobrazená mapa zameraného pozemku. Na meranie sa použil Minidisk infiltrometer. Rozloha pozemku bola 21 ha a počet monitorovacích bodov bol 10 (obrázok 3). Podľa manuálu sme nastavili na infiltrometri hodnota *h0*, predpísanú podľa typu pôdy.

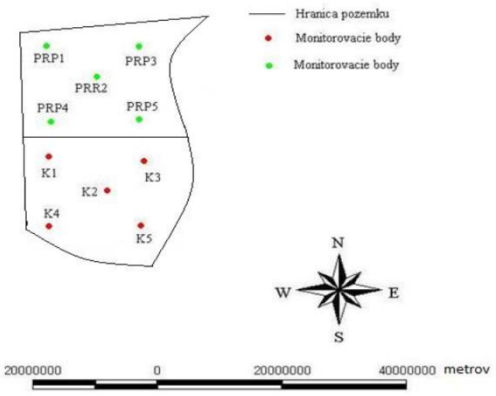

Obr.3 Zameranie pozemku a rozloženie monitorovacích bodov

V našich meraniach môžeme povedať, že po použití infiltromera sme zistili, že rýchlosť infiltrácie je závislá od utuženosti pôdy, kde niektoré vrstvy pôdy vsakujú vodu rýchlejšie a tam kde je utužená vrstva, nastáva vsakovanie pomalšie.
Priemer kumulatívnej infiltrácie na kontrolnej časti bol na jar v roku 2013 0,07 ml. Podobné priemery možno pozorovať na jar v roku 2014 a na jar 2015 na parcele ktorá slúžila ako kontrola. Priemer kumulatívnej infiltrácie je v obdobiach jeseň 2013 až jeseň 2014 vyššia 0,08 ml - 0,11 ml. Mohlo byť spôsobené zrážkovým obdobím ku koncu roka, čo bola exogénna premena ktorú sme my nemohli ovplyvniť.

Tab. 2 Popisná štatistika kumulatívnej infiltrácie pre kontrolu

		kontrola						
		Priemer	Maximum	Medián	Minimum	Percentil 25	Percentil 75	Sm. Odchýlka
V1	2013_jar	0.07	0.13	0.08	0.00	0.06	0.10	0.04
	2013_jeseň	0.08	0.13	0.10	0.00	0.06	0.10	0.05
	2014_jar	0.12	0.19	0.13	0.03	0.06	0.16	0.06
	2014_jeseň	0.11	0.16	0.10	0.06	0.06	0.13	0.04
	2015_jar	0.14	0.23	0.15	0.03	0.10	0.19	0.06

Priemerná hodnota pri použití prípravku je na úrovni 0,19 ml. Najviac je to zreteľné na jeseň v roku 2014, kde štatistická hodnota pohybovala na úrovni 0,27 ml. Tieto rozdiely sú štatisticky významné, v porovnaní s parcelami v ktorých prebiehal výskum. Tieto zmeny boli spôsobené zapracovaním prípravku, ale mohlo to byť aj zrážkovým obdobím ku koncu roka.

Tab. 3 Popisná štatistika kumulatívnej infiltrácie pre prípravok

		prípravok						
		Priemer	Maximum	Medián	Minimum	Percentil 25	Percentil 75	Sm. Odchýlka
V1	2013_jar	0.19	0.29	0.19	0.06	0.13	0.26	0.08
	2013_jeseň	0.26	0.32	0.26	0.13	0.26	0.29	0.05
	2014_jar	0.18	0.23	0.19	0.10	0.16	0.19	0.04
	2014_jeseň	0.27	0.35	0.28	0.13	0.23	0.32	0.07
	2015_jar	0.18	0.26	0.18	0.06	0.13	0.23	0.07

Hodnoty nameraných infiltrácií sa líšia v rokoch 2013 až 2015. Infiltrácia vody do pôdy závisí aj od samotného zloženia pôdneho profilu, od opracovania pôdy, pre nižšie hodnoty infiltrácie môžu byť spôsobené aj použitou technológiu obrábania pôdy. Pôdy obrobené v malej hĺbke budú mať iné hodnoty infiltrácie, ako pôdy ktoré boli hĺbkovo podrývané.

Ako je zrejmé, naše merania poukazujú na pozitívne výsledky použitia prípravku v pôde. Plocha ošetrovaná prípravkom vsakuje zrážkovú vodu rýchlejšie. Rozdiel v rýchlosti infiltrácie do hĺbky na ploche po ošetrovaní prípravkom bol o 2 mm za 1 hodinu!

ZÁVER

Pôda predstavuje hlavnú súčasť prostredia pre mnohé organizmy, najmä však pre vyššie rastliny, ktorým poskytuje potrebné živiny a priestor. K hlavným vlastnostiam pôdy patria jej technické vlastnosti. V práci je podrobne popísaný cieľ a vybraná parcela na ktorej sa vykonávali experimentálne výsledky. Ďalej sa tu nachádza opis meracích zariadení, metódy merania a vyhodnocovanie experimentálnych dát.
Meranie vlhkosti Kopeckého valčekmi prebehli v troch hĺbkových horizontoch, kde namerané hodnoty sme porovnali s hodnotami nameranými pomocou vlhkomera ThetaProbe ML2x s čítacou jednotkou HH 2. Meralo sa v povrchovej zóne 10 – 15 cm, 35 – 40 cm a 50 – 60 cm. Je tu zrejmý nárast vlhkosti pôdy u variant s aplikáciou použitia prípravku. Najvyšší obsah pôdnej vody bol zistený na jeseň v roku 2014 a to s vyšším obsahom prípravku a jeho aplikáciou na široko. Obsah pôdnej vody samozrejme ešte koreluje s množstvom zrážok spadnutých v termíne odberu vzoriek.
Infiltráciu pôdy je možné merať s niekoľkými spôsobmi. Jedna z najrýchlejších a najjednoduchších je meranie s tzv. Minidisk infiltrometrom. Hodnoty nameraných infiltrácií sa líšia v rokoch 2013 až 2015. Infiltrácia vody do pôdy závisí aj od samotného zloženia pôdneho profilu, od opracovania pôdy, pre nižšie hodnoty infiltrácie môžu byť spôsobené aj použitou technológiu obrábania pôdy. Pôdy obrobené v malej hĺbke budú mať iné hodnoty infiltrácie ako pôdy ktoré boli hĺbkovo podrývané. Ako je zrejmé naše merania poukazujú pozitívne výsledky použitia prípravku v pôde. Plocha ošetrovaná prípravkom vsakuje zrážkovú vodu rýchlejšie. Rozdiel v rýchlosti infiltrácie do hĺbky na ploche po ošetrovaní prípravkom bol o 2 mm za 1 hodinu.
Problematika poľnohospodárstva sa skúma už desiatky rokov, či už pri utláčaní pôdy, výnosových parametrov, štruktúry pôdy. Pôda nám jednoznačne umožňuje zjednodušiť si namáhavú prácu a v procese výroby využívať aj benefity ktoré sú v nej ukryté. Výsledkom bude menej námahy s lepším hospodárskym výsledkom.

POUŽITÁ LITERATÚRA

1. DECAGON DEVICES, Inc., 2005. Minidisk infiltrometer, User's manual.
2. Jobbágy, J., Kukan, P., & Jankovič, O. (2006). Vplyv vlhkosti pôdy na penetrometrický odpor. In *VIII. Medzinárodná vedecká konferencia mladých, zborník z medzinárodnej vedeckej konferencie, Zvolen 12. - 14. jún 2006*. ISBN 80-228-1596-9.
3. Kirkham, M., B. (2005), Principles of Soil and Plant Water Relations. Kansas State University. Imprint: Academic Press.. xvii + 500 pages. Hardbound. ISBN: 0-12-409751-0
4. Kováč, K., Nozdrovický, L., & Macák, M. (2010). Minimalizačné a pôd ochranné technológie. NITRA : AGROINŠTITÚT. 2010. 142 s. ISBN 978-80-7139-139-5.
5. Orságová, K., & Nozdrovický, L. (2007). Vplyv rôznych spôsobov obrábania nachemické vlastnosti pôdy. 1. vyd. Nitra: SPU, 2007. 128 s. ISBN 978-80-8069-988-8.
6. Páltik, J., Findura P., & Polc, M. (2003). Stroje pre rastlinnú výrobu. 1. vyd. Nitra: SPU,2003. 241 s. ISBN 80-8069-200-9.
7. Philip, J.R. (1957). The theory of infiltration: 4. Sorptivity and algebraici infiltration equations Soil Science 84, 257-264.
8. Velebný, V., Novák, V., & Skalová, J. (2000). Vodný režim pôdy. Bratislava: STU, 2000. 208 s. ISBN 80-227-1373-2.
9. Zhang, R. (1997). Determination of soil sorptivity and hydraulic conductivity from the disk infiltrometer. *Soil Science Society of America Journal*, 61, 1024-1030.

Korešpondenčná adresa
Ing. Miroslav Mráz, Katedra strojov a výrobných biosystémov, TF SPU v Nitre, Tr. A. Hlinku 2, 949 76 Nitra, tel: +421911 761 128, e-mail: miroslavmraz9@gmail.com

COMPARISON OF PREDICTED AND REAL PARAMETERS OF PV SYSTEMS IN CZECH REPUBLIC AND SPAIN

Tomáš OLŠAN[1], B.Marí SOUCASE[2], Martin LIBRA[1]

[1]*Department of Physics, Czech University of Life Science, Kamycka 129, 16521 Prague, Czech Republic*
[2]*Department of Applied Physics,Universitat Politecnica de Valencia, Camí de Vera, 46022 València, Spain*

Abstract
This article compares predicted performance by a simulation software for a given new constructed PV system of crystalline silicon technology located in Prague with 10 kW peak power and a similar system in Spain. Simulation software used for the sake of this paper was publicly available PVGIS from the website of its creators. Parameters were set to be the same like in the real PV system. The difference between the predicted and the real data was calculated and then discussed in the result section of this paper.

Key words: *PV systems, PVGIS, PV simulation, predicted and real data comparison.*

INTRODUCTION

With some of the advance in PV technology, increased lifespan and especially increased the efficiency of PV cells, solar panels will be an interesting technology to invest in on a big scale as far north as the Czech Republic even without subsidy from the government. Therefore, it is helpful to have a software to predict a performance of a PV system and so return of investment.
There are more PV simulations available online for free, namely PVGIS, RETSCreen, and PVWatts. Though PVGIS design is plain and it can appear difficult for the beginners to use, it provides the best yearly estimate (*Psomopoulos et al., 2015*). These simulations can be used to predict the performance of the PV systems in the long run, one way how to predict weather pattern in a short term is described in (*Rezk et al., 2015*).
Such a prediction can be not only useful to help reach certain environmental goals but it is also important for developing countries who struggle to supply electricity in the remote areas to see if its economically viable to build off grid solar power plants in these areas (*Ajan et al., 2003*). A case study of a PV system in Ivory Coast is done in (Guaita-pradas, MaríSoucase and AKA, 2015). A comparison of PV system cost and payback time in India and Pakistan is in (*Guaita-Pradas, Shafi and Ullah, 2015*). Comparison of return of investment of the PV power plants in Germany, Spain and Morocco is in (*Guaita-Pradas and Soucase, 2014*), due to the subsidy policy in Spain and low cost of electrical energy in Morocco it is actually Spain with the shortest return of investment, also called the internal rate of return.Aim of this article was to compare the predicted performance of a PV system with a real one of the same parameters.

MATERIALS AND METHODS

PVGIS software used for comparison of real and predicted data is available for free on the website: http://re.jrc.ec.europa.eu/pvgis/apps4/pvest.php?lang=en&map=europe. This website provides several options for calculations: PV estimation, monthly radiation, daily radiation and stand-alone estimation. This paper focuses on PV performance estimation given by PVGIS software and its deviation from real PV systems with same parameters. PVGIS software can give the prediction for the area of Europe, Asia, and Africa.
PVGIS software can generate a lot of useful information for potential investor given some necessary information about intended project such as installed peak PV power, used PV technology (the most common one is crystalline silicon), estimated losses, radiation database (there are 2 options, one based on ground measurement and other based on satellite data), inclination and orientation of PV system. This paper deals only with PV estimation option from above-mentioned website. An online interface of PVGIS with parameters set for Prague can be seen on Fig. 1.

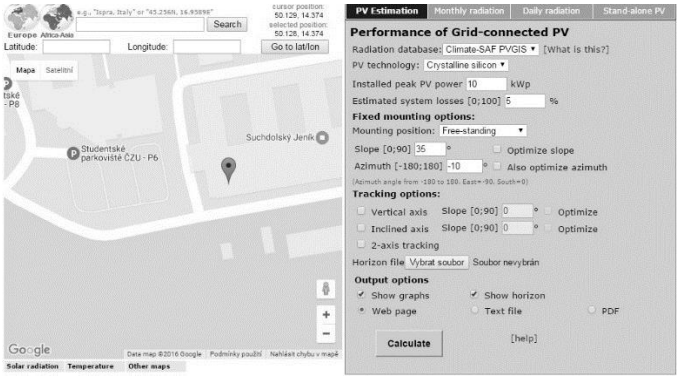

Fig. 1 PVGIS interface on its website

PVGIS software takes into the account losses of the PV system. Estimating losses due to the soiling, aging and degradation of materials are given in (*Thevenard and Pelland, 2011*). Estimating losses thanks to the shading are given in (*Nguyen and Pearce, 2012*). Accuracy of the old and new solar irradiance database available in PV gis software is discussed in (*Huld et al., 2012*).
PV systems from two sites were chosen for comparison, one in Prague in the Czech Republic and one near Valencia in Spain. In both cases we calculate the electricity production by using PVGIS software and then this output is compared with actual production data measured in situ.

RESULTSAND DISCUSSION

The PV installation has a peak power of 10 kWp, the inclination of the panels is 35° and its technology is crystalline silicon. This installation costed around 11 000 euros. The maintenance costs are 2 000 czk per month or (75 €) per month. Losses were set to 0 % because it is a brand new PV installation, total losses were 11 %. The position of this installation is 50°7′42′′ latitude and 14°22′26′′ longitude.
The graph with PV estimation from PVGIS is showed on Fig. 2. The total electricity production per year was estimated to be 10 700 kWh. Currently, the price for 1 kWh generated by renewable resource on the Czech market is same as for any other source, 3.4 czk for 1 kWh, that is around 13 euro cents. According to this estimation, one year would yield the income of 1 445 euro. The cost of the whole PV installation without the cost of the maintenance would be pay off after less than 7 years and 8 months. However, data from the PV installation for the first year actually shows that electricity production was 11 881 kWh, therefore first year yields around 1 533 euro of income and whole installation without the cost of the maintenance will be pay off in 7 years and 3 months. If we consider the cost of the maintenance for 480 euro per year (plus 3 % inflation rate), than the whole PV system in Prague with the maintenance will be pay off in 10 years but that is only if the revenue will be each year the same (plus 3 % of inflation rate).

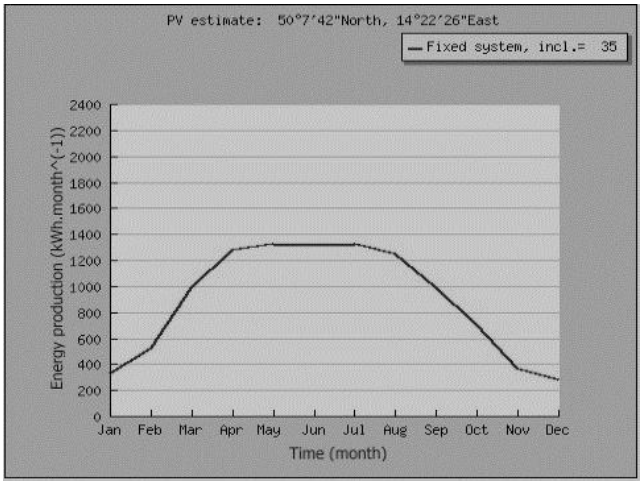

Fig. 2 Estimation of energy production during a year for PV system in Prague on the CULS campus

These calculations are compared with real data from PV installation in the northwest Prague in the Czech University of Life Sciences campus. All calculated values in kWh per month are in Tab. 1 along with the available real data.

Tab. 1 Average electricity in kWh generated in each month

	Prague - estimated Em (kWh)	Prague - real Em (kWh)	Difference (%)
January	293	358	- 18.2
February	472	559	-15.6
March	891	873	+2
April	1 160	1 250	-7.2
May	1 200	1 575	-23.9
June	1 200	1 461	-7.9
July	1 200	1 499	-20
August	1 130	1 493	-24.4
September	893	1 323	-32.6
October	638	542	+17.7
November	328	554	-40.8
December	251	394	-36.3
Average	805	990	-18.7
Sum	9 660	11 881	-18.7

The second PV system is located in Spain in a moderate size city Ontinyent with 100 000 inhabitants located about 80 km south of Valencia. This system was connected to grid in 11/ 2011 when there was a governmental subsidy policy in Spain similar to that one in the Czech Republic where the owner of PV system has a guaranteed price for 1 kWh over a long time. In the case of Spain, the price for energy production was set at 0.28 euro.kWh-1 and this price will remain fixed for next 25 years. The PV system is facing directly towards the south and has the inclination of 35°. This PV system is divided into 4 parts across the whole city with total installed power of 255.3 kW. Because it was built earlier, the price for 1 installed Watt was around 1.8 euro (Standard price in 2011). The cost of this whole PV system was then about 459 540 euro. The estimate for Ontinyent by PVGIS is showed on Fig. 3.

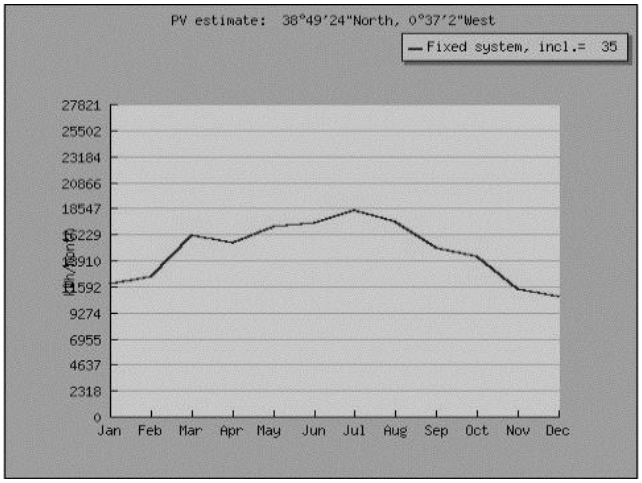

Fig. 3 Estimation of energy production for PV system inOntinyent inSpain

Because the system was connected to the grid at the end of 2011 and the year 2017 is not over yet, all calculations are cumulative for five consecutive years from 2012 till 2016. In Tab. 2 is data from these five years along with estimate from PVGIS, the difference between the two and also losses that were set in PVGIS.

Tab. 2 Yearly yield of PV system in Ontinyent and estimate by PVGIS with losses

	Estimated Energy (kWh)	Real Energy (kWh)	Difference (%)	Losses (%)
2012	392 000	392 542	-0.14	14.5
2013	392 000	392 731	-0.19	14.5
2014	388 000	388 363	-0.09	15.5
2015	381 000	380 902	0.03	17.0
2016	372 000	371 337	0.19	19.0

This PV system was built when the Spanish government was subsiding the renewables and so it has the guaranteed price of 0.28 euro for 1 kWh for 25 years. The policy of Spanish government changed since then and the prefearibility of the investment into PV power plants after the change of the subsidy policy is discussed in (*Guaita-Prada and Soucase, 2014*). In last two months of 2011 when this PV system was operational, the revenue was 8 452 euro. For each year the calculation assumes 3 % inflation rate and also 9 % of revenue will go for the insurance and the maintenance. The cost of the whole PV system was about 459 540 euro and for two months of 2011 and five years between 2012 - 2016 the net revenue of this PV system was 513 357 euro while according to the PVGIS it should be a little smaller at 512 896 euro, the difference is less than 0.05 %. So the PV system is Spain was already payed off in 4 years and 8 months. As can be seen from Tab. 2 PVGIS is quite good for predicting the revenue from a given PV power plant over whole year but not for each month which was the case of Prague. The difference for one month varied widely over the year in the case of Prague, between -40 % to +17 %. But in the case of Ontinyent in Spain, the estimate only varied less than 0.2 %. In Tab. 3 there are some parameters for both PV system in Prague and Ontinyent.

Tab. 3 Production data related to both PV installations in 2016

PV installation	PV peak power (kW_p)	Energy production ($kWh.year^{-1}$)	Energy production/Peak Power ($kWh.kW_p^{-1}$)	Irradiation ($kWh.m^{-2}$)	Income/kWh (€/kwh)	Payback time (months)
Prague	10	11 881	1 188.1	1 250	0.13	120
Ontinyent	255.3	331 337.3	1 297.84	2 010	0.28	56

As can be seen from Tab. 3, the PV system in Ontinyent performs better than the PV system in Prague as well its return of investment is much shorter. This can be due to several factors. Mainly orientation of the panels and the geographical position and thus the irradiation received by the panels of the PV power plant are two main factors for the energy production. Firstly, Ontinyent is in a southern position than Prague, Prague has a latitude of 50°7′ while Valencia has a latitude of 39°28′, the difference is over ten degrees. Prague also has a typical central European climate, in the year 2016 Prague had 590 mm of rainfall which was on 91 % of a longterm average (*Český hydrometeorologický ústav, 2017*). While Ontinyent is less than 50 km away from the Mediterranean Sea and thus it has a weather close to that of a coastal cities. Valencia and Ontinyent also has on average less rainfall during a year, there was 67 rainy days with 518 mm of rainfall in 2016 in Valencia while there was 68 rainy days

with only 404 mm of rainfall in 2015 in Valencia (*AEMET Open Data, 2017*). Less precipitation with a southern position in turn means more average yearly sun irradiation as can be seen from Tab. 3.

CONCLUSIONS

The renewable energies are the main hope in substituting the current fossil based economy and their ecological impact is much lower than that of fossil energies. According to (*Castro et al., 2013*) the global electric power available from the solar energy in the 21st century can be around 2-4 TW while in the year 2013 there was only 0.008 TW of net average solar power production. Especially the countries with a lot of hours of sunshine during a year, like Spain, should be interested the most in the solar energy.

Both countries have a different conditions whenever it's a subsidy policy that supports the investments into the renewable energy sources or amount of irradiation received by a year in that country. However, in both cases, the PV power plant is actually profitable.

The PVGIS can be used to produce estimate accurate enough for the investors who want to invest into PV power plants. It gives pretty accurate estimate of PV production during the whole year but the difference for each month of the year variesgreatly. The difference in the case of Spain was smaller than 0.5 % and so this software can be used by investors for their potential PV projects.

The PVGIS proved to be an accurate and easy to use SW even for the people who are not experts in the solar energy production.

ACKNOWLEDGMENT

This study was made during first author's Erasmus stay in Valencia on UPV university and so it was supported by EU grant for an exchange students.

REFERENCES

1. Psomopoulos, Constantinos S., George Ch. IOANNIDIS, Stavros D. KAMINARIS, Kostas D. MARDIKIS and Nikolaos G. KATSIKAS. A Comparative Evaluation of Photovoltaic Electricity Production Assessment Software (PVGIS, PVWatts and RET-Screen). Environmental Processes. 2015, 2(S1), 175-189. DOI: 10.1007/s40710-015-0092-4. ISSN 2198-7491. Available from: http://link.springer.com/10.1007/s40710-015-0092-4.
2. Rezk, H., Tyukhov, I., &. Raupov, A. (2015). Experimental implementation of meteorological data and photovoltaic solar radiation monitoring system. International Transactions on Electrical Energy Systems, (25), 3573-3585.
3. Ajan, C. W. et al. (2003) On the policy of photovoltaic and diesel generation mix foranoff-gridsite: East Malaysian perspectives. Solar Energy, (74), 453-467.
4. GUAITA-PRADAS, Inmaculada, Bernabé MARÍ SOUCASE and Boko AKA. Energyproduction and financial analysis of photovoltaic energy plants in Ivory coast. Africa science. 2015, 11(2), 24-34.
5. GUAITA-PRADAS, Inmaculada, Shafi ULLAH and Bernabé MARÍ SOUCASE. Sustainable Development withRenewableEnergy in India and Pakistan. International Journal of Renewable Energy Research. 2015, 5(2), 575-580.
6. GUAITA-PRADAS, Inmaculada and Bernabé MARÍ SOUCASE. Energy production in PV plants regarded as economic investments. An assessmentfor PV investments in Germany, Spain and Morroco. Proceedings of Renewable and Sustainable Energy Conference (IRSEC). 2014, 37-41.
7. THEVENARD, Didier and Sophie PELLAND. Estimating the uncertainty in long-term photovoltaic Šeld prediction. Solar Energy. 2013, (91), 432-445.
8. NGUYEN, Ha. T. and Joshua M. PEARCE. In corporatings hading losses in solar photovoltaic potential assessment at the municipal scale. Solar Energy. 2012, (86), 1245-1260.
9. HULD, Thomas, Richard MÜLLER and Attilio GAMBARDELLA. A newsolarradiation database forestimating PV performance in Europe and Africa. Solar Energy. 2012, (86), 1803-1815.
10. CASTRO, Carlos de, Margarita MEDIAVILLA, Luis Javier MIGUEL and Fernando FRECHOSO. Global solar electric potential: A review of their technical and sus-

tainable limits. Renewable and Sustainable Energy Reviews. 2013, (28), 824-835.
11. GUAITA-PRADAS, Inmaculada and Bernabé MARÍ SOUCASE. Endorse of Renewable Energy Plants, Still An Alternative Investment in Spain? SOP Transactions on economic research. 2014, 1(2), 10.
12. Územní srážky v roce 2016. Český hydrometeorologický ústav [online]. Prague, 2017 [cit. 2017-06-07]. Availablefrom: http://portal.chmi.cz/historicka-data/pocasi/uzemni-srazky
13. AEMET OpenData [online]. 2017 [cit. 2017-06-14]. Available from: https://opendata.aemet.es/centrodedescargas/inicio

Corresponding author:
Ing. Tomáš Olšan, Department of Physics, Faculty of Engineering, Czech University of Life Sciences Prague, Kamýcká 129, Praha 6, Prague, 16521, Czech Republic, phone: +420 606 421 962, e-mail: tolsan@email.cz

COMPARISON OF RAW AND USED VEGETABLE OILS THERMAL BEHAVIOR

Ana PETROVIĆ, Daniela KUNECOVÁ, Vlasta VOZÁROVÁ

Department of Physics, Faculty of Engineering, Slovak University of Agriculture in Nitra, Slovak Republic

Abstract
The search for renewable energy is constantly increasing in order to reduce the amount of carbon dioxide emissions. Specifically, waste cooking oils, with their thermal stability and amount of energy, seems to be a promising source for the production of biofuels. This scientific paper is focused on physico-chemical properties of raw and used oils of sunflower and rapeseed. Those oils were evaluated by thermal analysis (thermogravimetric and differential scanning calorimetry). In addition, viscosity, in a range of (25 – 90)°C*, was determined. The aim of this paper is to present energy potential of waste cooking oils.*

Key words: *waste vegetable oils; biofuel; physico-chemical properties.*

INTRODUCTION

Because of the tremendous consumption of fossil fuel sources in present day, the support of renewable energy sources is compulsory to maintain energy security. As the prices of orthodox fuels are increasing and there been some considers about environmental pollution, biofuels have been developed (*Marchetti et al., 2007; Fangrui & Milford, 1999*). As already known, one of the alternative fuels is biodiesel. Biodiesel is defined as short chain alcohol esters of long chain fatty acids supplied from vegetable oil or animal fats (*Canakci & Gerpen, 2001*). Use of biodiesel has the potential to reduce the level of pollutants and of potential or probable carcinogens (*Zhang et al., 2003; Demirbaş, 2002*).
Becide other sources, non-edible bio-residues food processing which are promptly available in large quantities seems to be one of the most promising means for utilizing energy stored in waste biomass. Triacylglycerols (triglycerides), the main component of vegetable oil, consist of three long chain fatty acids esterified to a glycerol backbone. Refined vegetable oils, animal oils, and waste cooking oils can be used biodiesel production. Waste cooking oils are an economical choice for biodiesel production, because of their availability and low costs (*Kulkarni & Dalai, 2006*). According to statistics of Food and Agriculture Organization of United Nations (FAO), production quantities of the selected biomass samples exceed 2 million tones throughout the world (*FAO, 2016*) and a large amount of wastes yielded in after processing. Therefore, used vegetable oils were selected as samples. The most attractive were waste oil of sunflower and rapeseed, because they are abundant and non-edible wastes produced during food processing. The new samples of the same oils were measured for comparison.
The evaluation of the properties of raw materials for biofuel production is indispensable because different raw materials have different physicochemical properties due to their different fatty acid compositions. These differences can affect engine performance and pollutant emissions (*Candeia et al., 2009; Knothe et al., 2005; Ramos et al., 2009*). The monitoring of these aspects includes evaluating the rheological behaviour, specifically viscosity of the raw oil at different temperatures, as well its thermal stability/degradation profile. The methodology proposed in this work is useful for the thermal and rheological characterization of waste cooking oils and therefore it can serve as the useful input information for the quality control of raw materials for biofuel production, enabling their technological use.

MATERIALS AND METHODS

For the research were used the commercial oils as sunflower and rapeseed oils. Samples were selected for their availability and great usability in household kitchen and canteen. Edible oils were purchased in market and they were used for frying about 45 minutes. Sunflower and rapeseed oil were manufactured by the company Palma, Bratislava, their origin is Slovakia. Samples for the measurement of raw oils were removed by pipette from the original bottle of oil. Used oils were collected into boiling cups

and also gathered by pipette. All samples were investigated by the same methods of thermal analysis (TGA and DSC) and in the same temperature range for the measurement of viscosity.
Thermogravimetric analysis (TGA) provides the information regarding the weight loss curve with respect to temperature and time (*Prasad Shadangi & Mohanty, 2004*). For monitoring of thermal stability and entalphy of reaction device METTLER TOLLEDO TGA/DSC was used. Samples were placed in hemispherical alumina crucible (70µl) with the mass between (31–41) mg. Alumina crucible was covered by a perforated lid which helps to escape the formed gases freely. Thermal method was set up from room temperature to 700°C to observe the thermal stability/degradation of oils under nitrogen atmosphere with a flow rate of 20 ml.min^{-1} and speed of heating 10 °C.min^{-1}.
Differential scanning calorimetry (DSC) provides quantitative and qualitative information about physical and chemical changes that involve endothermic or exothermic processes. (*Prasad Shadangi & Mohanty, 2004*). DSC experiment was carried out in a METTLER TOLEDO TGA/DSC 1 STARe system analyzer. Thermal method was the same as with thermogravimetric analysis and experiments were conducted simultaneously using the heating program from 20 °C to 700 °C with nitrogen atmosphere at a rate of heating 10 °C.min^{-1}.
Viscosity as one of the most important rheological parameters is defined as the resistance of a fluid to flow. Viscosity of most of the liquids decreases with increasing temperature according to Arrhenius equation (*Figura & Teixeira, 2007*):

$$\eta = \eta_0 e^{\frac{E_A}{RT}}, \quad (1)$$

where η is, dynamic viscosity (Pa.s), η is reference value of dynamic viscosity (Pa.s), E_A is activation energy (J.mol^{-1}), R is gas constant (J.K^{-1}.mol^{-1}) and T is absolute temperature (K). Present data have been obtained from measurements performed on the laboratory rotating viscometer DV2T fy Brookfield. The experiments have been performed with a use of ULA (0) spindle.

RESULTS AND DISCUSSION

Thermogravimetric analysis (TGA) is one of the most widely applied techniques that are used to study the thermal events. TGA is an instrument that measures the weight changes with respect to temperature. It is used for characterization of polymeric materials. TGA and DSC measurements were performed simultaneously under the same temperature program, in nitrogen atmosphere at a heating rate of 10 °C.min^{-1}.
Samples of vegetable oils showed thermal stability in a nitrogen atmosphere up to 300 °C, where degradation reactions of the oil constituents began. The thermal decomposition profiles for sunflower and rapeseed oils have a similar characteristics, where is observed thermal decomposition from 250 °C to 550 °C. This great drop is composed of three thermal decompositions fatty acid as it can be seen from the Fig. 1 and 2. According to the literature (*Gouveia de Souza et al., 2004*), polyunsaturated fatty acids begin to decompose. In the temperature range of 380 °C to 480 °C it comes to decomposition of monounsaturated fatty acids and up to 550 °C decomposition of saturated fatty acids occurs. These phenomena are less obvious as they follow without a flat section. After 550 °C, the final section of the plate occurs, where all the oil components have been decomposed. To compare the temperature behavior of the raw and used oils, we have chosen normalized TGA curves, which are describing weight loss in percentages as a function of temperature. On the TGA curves is clearly visible similar character of thermal decomposition, where the difference is evident after the polyunsaturated fatty acids first decompose at (250-380) °C for unused vegetable oils. The dashed line describes used oil in all thermograms.

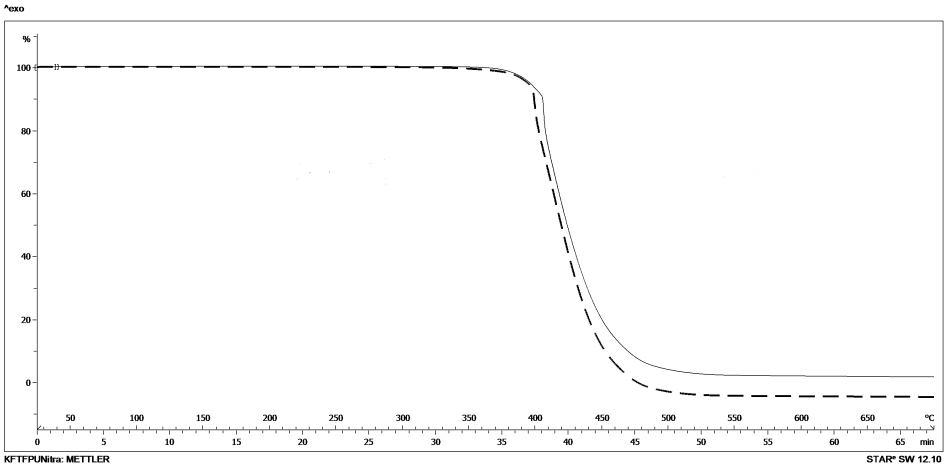

Fig. 1 TGA curves of raw and used sunflower oil (– raw, - - used)

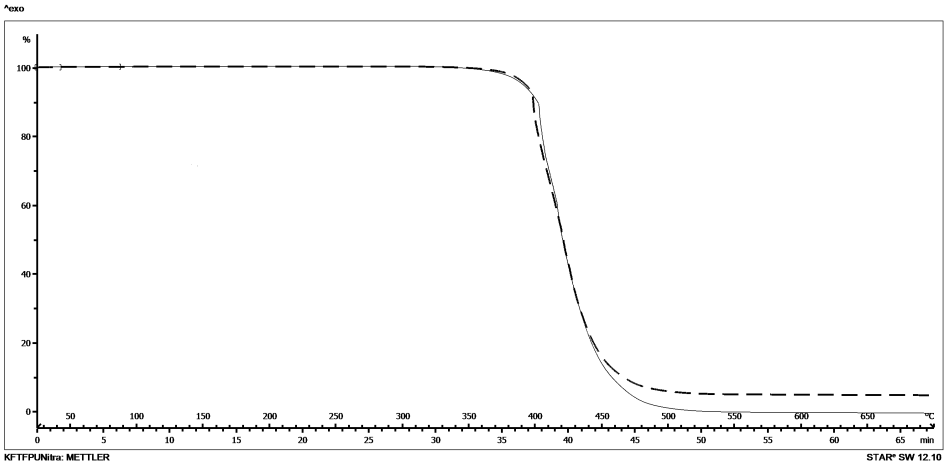

Fig. 2 TGA curves of raw and used rapeseed oils (– raw, - - used)

It can be assumed that this thermal degradation leads to exothermic or endothermic reactions, as seen on the DSC curve of the TGA measurement. To compare the energy character of used and raw vegetable oils, we used the DSC curves. The DSC measurement was performed simultaneously with the TGA measurement for the corresponding energy description of the heat loss of the mass. The dashed line illustrates the used sunflower and rapeseed oil. As we can see from the Fig. 3 and 4, the character of DSC curves is the same for both, sunflower and rapeseed, used and raw oil. In all cases, an exothermic event is visible. It beginning at 400 °C and ending at 480 °C. This exothermic process may correspond to the fatty acid polymerization. Enthalpy of this reaction ranges from 454.32 $J.g^{-1}$ for used sunflower oil to 336.64 $J.g^{-1}$ for raw rapeseed oil. Enthalpy of the process is always higher for used oils, which may be due to the composition and altered nature of the fatty acids.

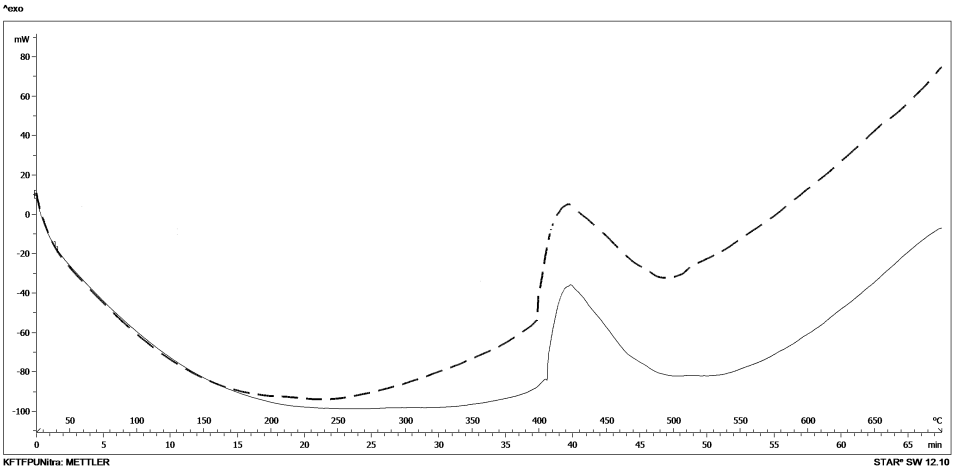

Fig. 3 DSC curves of raw and used sunflower oil (– raw, - - used)

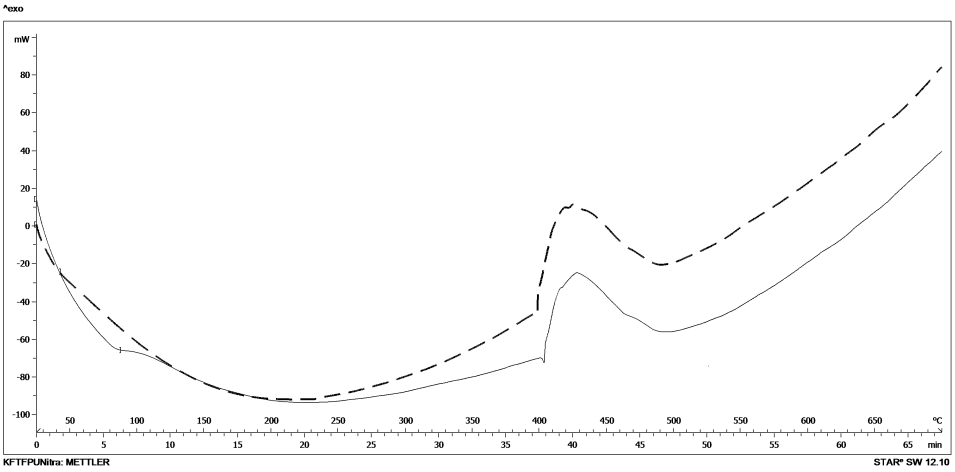

Fig. 4 DSC curves of raw and used sunflower oil (– raw, - - used)

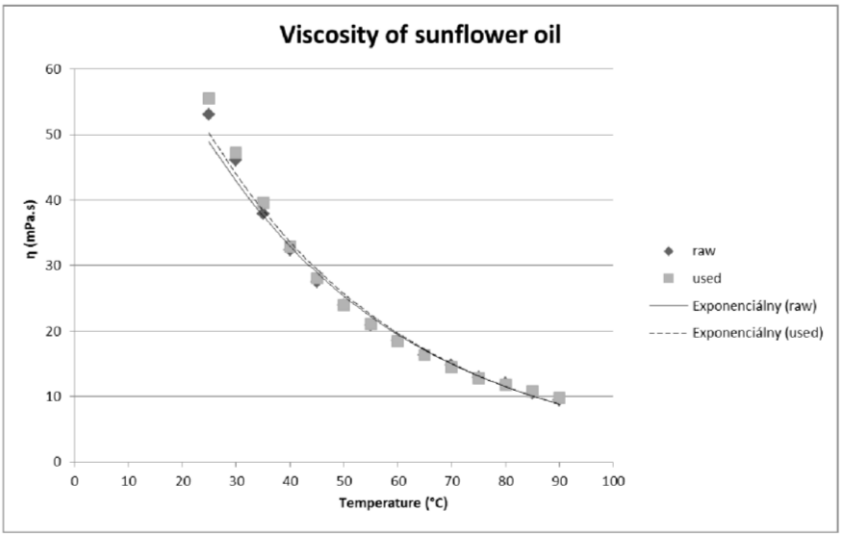

Fig. 5 Viscosity dependence on temperature of raw and used samples of sunflower oil

Dynamic viscosity, as a function of temperature of four different samples of oil has been considered. Results of first two samples, that were raw and used sunflower oil, are presented in Fig.5. The other two, which were raw and used rapeseed oil, are presented in Fig.6. For viscosity measurements the sample preparation corresponded to a typical sampling procedure. The adequate volume - 20 ml of oil

was put into the apparatus cuvette. The viscosity data were obtained in temperature range from 25 °C to 90 °C. All samples were measured in approximately same conditions. More precisely, at about the same speed (7-8) RPM.
It is possible to observe from Fig. 3 and 4 that dynamic viscosity of oils is decreasing exponentially with increasing of temperature, what was expected and corresponds with conclusions reported in literature (*Vozárová et al., 2015; Hlaváč et al., 2014; Hlaváč & Božiková, 2014; Severa et al., 2012*).
In the case of used sunflower oil we observed slight increase in viscosity at lower temperatures, which is explainable with the contamination of oil.

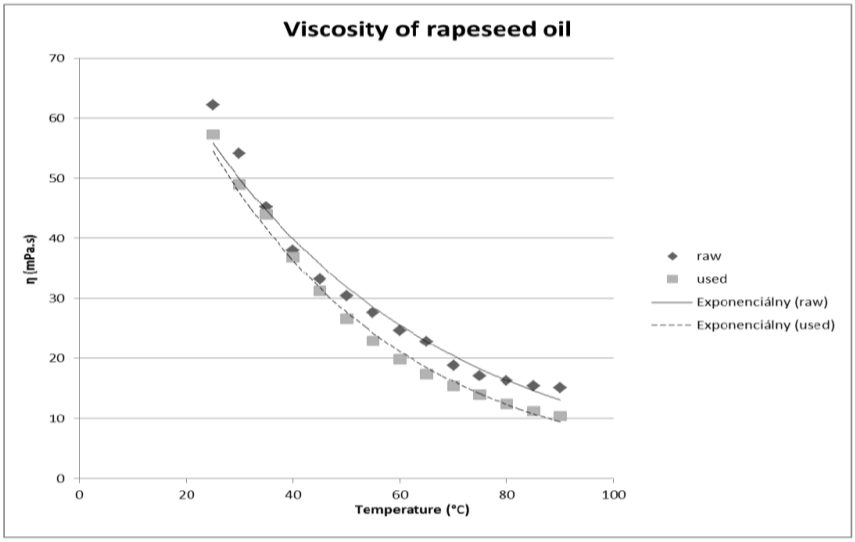

Fig. 6 Viscosity dependence on temperature of raw and used samples of rapeseed oil

Opposite to the used sunflower oil, viscosity of used rapeseed oil is decreasing. The higher temperature is, the viscosity of used sample is lower in comparison to the results of raw sample. The reason of this change can be the water present in oil, which stayed there after frying food. Regression equations and determination coefficients for individual samples are in the Tab. 1. As it can be seen from the results, the determination coefficients for all the samples are very high, which also confirms strong exponentially decreasing dependence.

Tab. 1 Determination coefficients and regression equations

Sample	Regression equation	Determination coefficient R2
Raw sunflower oil	$94.446e^{-0.026x}$	0.9913
Used sunflower oil	$98.118e^{-0.027x}$	0.9869
Raw rapeseed oil	$97.663e^{-0.022x}$	0.9775
Used rapeseed oil	$107.26e^{-0.027x}$	0.992

CONCLUSIONS

The biodiesel production from waste cooking oils has a great potential. It will help in reducing of carbon dioxide emissions and also an easy way to use large quantities of bio waste as a biomass. The analysis of physico – chemical properties of the oil samples revealed characteristic suitable for its conversion to biofuel, such as high thermal stability, big amount of energy and great viscosity behavior. Those properties are encouraging for the future exploration in bioenergy field. All the oils behaved as Newtonian fluids and it can be described by the low model. The data presented here can be used as a basis for further studies evaluating the potential of waste cooking oils as biofuel.

ACKNOWLEDGMENT
This work was co-funded by European Community under project no 26220220180: Building Research Centre „AgroBioTech“.

REFERENCES

1. Canakci, M., Gerpen, J.V. (2001). Biodiesel production from oils and fats with high free fatty acid content. *Transactiones of ASAE*, 44 (6), 1429-1436.
2. Candeia, R.A., Silva, M.C.D., Carvalho Filho, J.R., Brasilino, M.G.A., Bicudo, T.C., Santos, I.M.G., Souza, A.G. (2009). Influence of soybean biodiesel content on basic properties of biodiesel–diesel blends. *Fuel*, 88, 738-743.
3. Demirbaş, A. (2002). Biodiesel from vegetable oils via transesterification in supercritical methanol. *Energy Conversion and Management*, 43, 2349-2356.
4. Fangrui, M., Milford, A.H. (1999). Biodiesel production: a review. *Bioresource Technology*, 70, 1-15.
5. FAO, 2016. Website <http://www.fao.org> (accessed 2016).
6. Figura, L. O., Teixeira, A. A. (2007). Food physics, Physical properties - measurement and applications. USA: Springer. 550 p.
7. Gouveia de Souza, A., Oliveira Santos, J. C., Conceição, M. M., Dantas Silva, M. C., Prasad, S. (2004). A thermoanalytic and kinetic study of sunflower oil. *Brazilian Journal of Chemical Engineering (online)*, 21 (2).
8. Hlaváč, P., Božiková, M. (2014). Effect of Temperature on Dynamic Viscosity and Activation Energy of Milk and Acidophilus Milk. *Advanced Materials Research*, 1059, 53-59.
9. Hlaváč, P., Božiková, M., Presová, R. (2014). Temperature relations of selected engine oils dynamic viscosity. *Acta technologica agriculturae*, 17, 104-107.
10. Knothe, G., Gerpen, J.V., Krahl, J. (2005). The biodiesel handbook. Urbana: AOCS Press.
11. Kulkarni, M.G., Dalai, A.K. (2006). Waste cooking oils an economical source for biodiesel: a review. *Industrial & Engineering Chemistry Research*, 45, 2901-2913.
12. Marchetti, J.M., Miguel, V.U., Errazu, A.F. (2007). Possible methods for biodiesel production. *Journal of Renewable and Sustainable Energy*, 11, 1300-1311.
13. Prasad Shadangi, K., Mohanty, K. (2004). Kinetic study and thermal analysis of the pyrolysis of non-edible oilseed powders by thermogravimetric and differential scanning calorimetric analysis. *Renewable energy*, 63, 337-344.
14. Ramos, M., Fernández, C., Casas, A., Rodríguez, L., Pérez, A. (2009). Influence of fatty acid composition of raw materials on biodiesel properties. *Bioresource Technology*, 100, 261-268.
15. Severa, L., Kumbár, V., Buchar, J., Čorňák, Š., Glos, J., Hlaváč, P., Čupera, J. (2012). On the engineering flow properties of used and new engine oils. *Applications of physical research in engineering: The renewable energy sources and physical properties of selected industrial materials (pp.97-112)*. Nitra : Slovak University of Agriculture.
16. Vozárová, V., Kardjilova, K., Híreš, L., Valach, M., Wollner, A. (2015). Temperature Dependence of Dynamic Viscosity and DSC Analysis of the Plantohyd samples. *Journal of Central European Agriculture*, 16, 221-230.
17. Zhang, Y., Dubè, M.A., McLean, D.D., M. Kates. (2003). Biodiesel production from waste cooking oil: 1. Process design and technological assessment. *Bioresources Technology*, 89, 1-16.

Corresponding author:
Ing. Ana Petrović, Department of Physics, Faculty of Engineering, Slovak University of Agriculture in Nitra, Tr.A.Hlinku 2, Nitra, 949 01, Slovakia, phone: +421 37 641 5785, e-mail: xpetrovica@is.uniag.sk

BASIC CONTROL AND STABILIZATION OF HEXACOPTER USING THE ARDUINO PLATFORM

Lukáš PÍPAL

Department of Electrical Engineering and Automation, Faculty of Engineering, Czech University of Life Science Prague

Abstract
This article is focused on Unmanned Aerial Vehicles (UAV). Specifically, the stabilization and control hexacopter using the Arduino platform with Inertial Measurement Unit (IMU). Basic stabilization of the hexacopter ensures vertical stabilization in the case of manual control by a human, so when the hexacopter remaining in the given position.

Key words: *UAV, Drone, Aircraft, Plane.*

INTRODUCTION

Unmanned Aerial Vehicles (UAV) have gained high popularity over the last decade in civilian, military and engineering applications due to the recent advances in sensing, communication, computing and control technology (*Bodrumlu et al., 2017*). Therefore, nowadays there are already many approaches to solve the UAV stabilization. The study (*Beniak & Gudzenko, 2016*) presents a comparison of three different quadrocopter control models: linear-quadratic controller, inverse dynamics method and full state feedback. UAV control and orientation can be realized by using PID controller and extended Kalman filter, which compensates for delay due to data communication and computations (*Cheng & Liu, 2016*). The Kalman filter is also used in work *(Goslinski et al., 2013*), where an enhanced version of the state estimation based on readings from Inertial Measurement Unit (IMU) and prediction form the model is introduced for stabilization. The aim of this paper is to provide a system for basic control and stabilization of the hexacopter, which will ensure stabilization in the vertical position in human control and in the staying in the given position.

MATERIALS AND METHODS

As a UAV was used hexacopter MikroKopterHexa XL equipped with 6 engines MK3638. It is a fully function UAV. Only the body with motors and their driver was used to our work. Our control unit was created on the Arduino Due programming platform, which has 12 digital I/O, 12 analog inputs and 84MHz internal clock frequency. Because Arduino has I/O logic 3,3V and UAV's system use 5V logic, so Arduino has to be complemented by a Stepdown LM2599 (adjustable converter). Arduino was supplemented whit a galvanic isolation for I^2C bus. In addition, the IMU GY-80, which includes 3 axis accelerometer, 3 axis gyroscope, 3 axis digital compass, pressure and temperature sensor. Rigol MSO 2202A is a two channel digital oscilloscope capable of displaying signals up to 200 MHz and 2GSa/s. This oscilloscope allows recording the measured waveform to external storage, which facilitates later evaluation.
Using a oscilloscope, the communication between the control unit and the engine's driver was intercepted. From the communication record, individual engine addresses were determined. Using Arduino, we imitated the communication between the control unit and the engine driver, and then replaced the original control unit with the control unit created by us. We then added our control unit to the IMU GY-80. The data form the measuring unit oscillated around the idle value for this reason it is necessary to adapt the data accordingly. For data editing, we used the averaging of the least 50 values to achieve a steady value at the output. Next, we programmatically split the data interval to half, to obtain negative values.

RESULTS AND DISCUSSION

The communication record is illustrated in Fig. 1, where the first waveform presents the clock signal and the second waveform represent the data. A block of data for one engine is show in detail in Fig. 1. The first block represents the address and the second data sent to the engine.

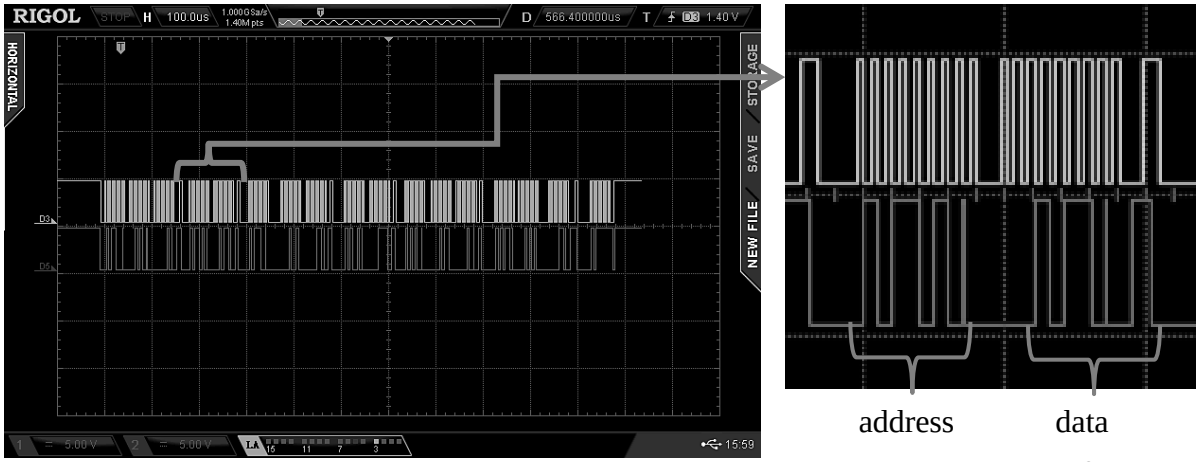

Fig.1: Record of the communication between the control unit and the engine driver via the I^2C bus

From the communication record, individual engine addresses were determined. The individual engine addresses are: 0x29, 0x2A, 0x2B, 0x2C, 0x2D and 0x2E. These addresses have been verified by an address scanner for I^2C bus. Arduino sends data from 0 to 255 to individual engine address. This causes the engine start. The full power that can be set by the operator on the engines is limited to half the maximum power for testing and enabling stabilization. Stabilization of the UAV is solved by adding the modified IMU data to the value sent to the engine. Data from the IMU is modified by dividing it so that it is in line 10 so as not to exceed the possible range of engine power.

CONCLUSIONS

Stabilization of the UAV is solved in the basic way, but it allows the UAV to stay or return to the rest position. However, an unresolved problem is the gradual increase of the drift of gyroscope contained in the IMU, which has been reduced by the set the sensor offset. Solving the problem of sensor drift and thus improving stabilization is the focus of future work, which should also bring about improvements in the control mode. The control is solved by simply setting values and sending messages to individual engines. I consider this work as a preparation of a suitable environment for follow-up work and also served to understand the basic principles of UAV control and stabilization.

ACKNOWLEDGMENT

Acknowledgments belong to my colleagues on the project Ing. Pavel Matějka and Ing. Jan Kadeřábek. In addition, the Department of Technological Equipment of Buildings for borrowing a hexacopter and also the Department of Electrical Engineering and Automation for borrowing an oscilloscope.

REFERENCES

1. Beniak, R., & Gudzenko, O. (2016). Comparing control algorithms of quadrocopters to implement their atypical maneuvers. In *MMAR2016 Conference on Methods and models in Autotation and Robotics* (pp. 1104-1109). IEEE 345 E.
2. Bodrumlu, T., Soylemez, M. T., & Mutlu, I. (2016). Modelling and Control of the Qball X4 Quadrotor System based on Pid and Fuzzy Logic Structure. In *ACD2016 Eurepena Workshop on Advanced Contrlo and Diagnosis*(pp. 34-38). IOP Publisshing.
3. Goslinski, J., Giernacki, W., & Gardecki, S. (2013). Unscented Kalman Filter for an orientation module of a quadrotor mathematical model. In *ASCC2013 Asian Control Conference* (pp. 1–6).IEEE 345 E.
4. Cheng, L. L., & Liu, H. B. (2016). Examples of quadrocopter control on ROS. In*ASID2015 International Conference on Anti-counterfeiting, Security, and Identification* (pp. 92-96). IEEE 345 E.

Corresponding author:
Ing. Lukáč Pípal Department of Electrical Engineering and Automation, Faculty of Engineering, Czech University of Life Sciences Prague, Kamýcká 129, Praha 6, Prague, 16521, Czech Republic, e-mail:pipal@tf.czu.cz

MOŽNOSTI BODOVÉHO HODNOTENIA PROCESOV TECHNICKÝCH SERVISOV VOZIDIEL AKO ŠTATISTICKÉHO UKAZOVATEĽA PRIEBEHU KVALITY OPRÁV
POSSIBILITIES OF POINT EVALUATION OF VEHICLE TECHNICAL SERVICES PROCESSES AS A STATISTICAL INDICATOR OF THE QUALITY OF OPERATIONS

Gabriel POLÓ, Zuzana CSILLAGOVÁ, Martin BALÁŽ, Maroš KORENKO

Department of Physics, Faculty of Engineering, Slovak University of Agriculture in Nitra, Slovak Republic

Key words: PDCA cycle, flowchart,

ABSTRACT
The following article deals with the possibility of point assessments and monitoring the quality of output issues of individual repairs and service services. An important indicator of these issues is the type and brand of the vehicle on which the technical operation was performed together with the delivery speed of the repaired vehicle, given the economic indicator and overall output quality. An important point is to track the progress of repairs at service and to alert the service to the possible lower quality of the overall service. Based on this, a very important indicator is also the connection of different types of quality tools from flowcharts, control sheets to the assembly of the PDCA cycle.

ÚVOD
Odborný článok sa zaoberá prezentáciou možností sledovania vývoja kvality opráv vozidiel z hľadiska kvalitatívnych, ekonomických ako aj časových ukazovateľov, ktoré zásadne ovplyvňujú priebeh a vývoj kvality jednotlivých typov opráv. Samotná údržba a oprava vozidiel a tým aj celkovo základné ukazovatele je možné vyvíjať pomocou nástrojov kvality v súčinnosti s odbornými literatúrami z oblasti systémov kvality ako aj údržieb a opráv. Z tohto hľadiska je významné spomenúť niektoré nástroje systémov kvality ako: vývojové diagramy, kontrolné listy, PDCA cyklus.
Každý z týchto nástrojov kvality môže významnou mierou prispieť k zostaveniu efektívneho bodového hodnotenia, ktorý ilustráciou priebehu môže poukazovať na kvalitatívnu stránku opráv toho ktorého servisu z hľadiska spoľahlivosti výstupných záležitostí akými sú cenová ponuka, rýchlosť dodania, výstupná kvality ako aj celkový technicky výsledok procesných postupností jednotlivých opráv a údržieb.

MATERIÁL A METÓDY
Pri zostavení jednotlivých typov bodových hodnotení je veľkou pomocou určenie vstupných informácií technickej spoľahlivosť jednotlivých komponentov a všetkých súčastí náhradných dielov, ktoré sa v danom servise do vozidiel inštalujú pri dodržiavaní jednotlivých postupností predpísaných pracovných postupov a ich technologickej postupnosti. Na základe toho si ukážeme niektoré typy nástrojov kvality, ktoré nám významnou mierou môžu prispieť k určeniu jednotlivých technických a technologických znakov kvality.

Vývojové diagramy
Vývojový diagram je metódou grafického znázornenia algoritmu, zachytávajúcou jeho štruktúru a nadväznosť operácií . Vývojový diagram je spôsob, ako vyjadriť normovaným formálnym spôsobom zrozumiteľne akúkoľvek úlohu. Pomocou vývojového diagramu môžeme presne a jednoznačne definovať rozhodovanie v zložitejších situáciách a postupnosť vysokoúrovňovej procesnej mapy (mapa zobrazujúca len postavenie procesov a väzieb medzi kontrolu nad zhodou modelu s modelovanou realitou. Preto je vhodný na zobrazenie a zachytenie činností, ktoré sú vykonávané jednotlivými pracovníkmi a môžu nahradiť slovný popis ich pracovnej náplne. Na základe týchto dôležitých znakov je efektívne použiteľný tento nástroj pri zostavovaní vývojového diagramu pre procesy rôzneho charakteru ako napr.: pri niektorých servisných úkonoch jednotlivých servisov.

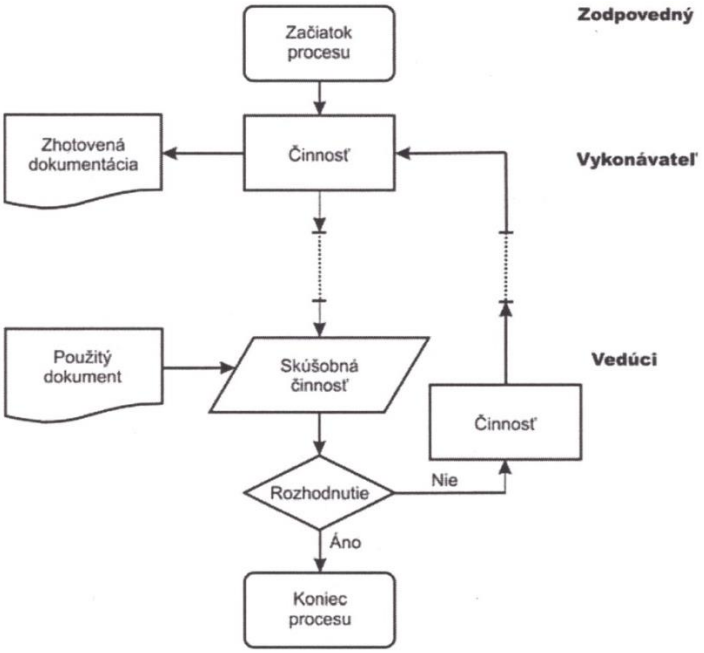

Obr. 1 Vývojový diagram
Fig. 1 Flowchart

Kontrolné hárky

Kontrolný hárok (tabelárny diagram) sa používa pri priebežnej a vstupnej kontrole polotovarov, súčiastok, hotových skupín, atď., pri analýze zariadení a technologického procesu, analýze nezhodných výrobkov a v mnohých iných prípadoch. Kontrolný hárok dáva možnosť určiť v ktoromkoľvek momente tendenciu zmeny nezhodnej výroby/služby a v prípade jej zvyšovania prijať nevyhnutné opatrenia. Súbor údajov s pomocou kontrolných hárkov nepotrebuje veľké množstvo práce a času, ide vlastne len o registráciu výsledkov kontroly, ktorú vykonáva pracovník oddelenia kvality. Na základe týchto záležitostí je veľmi dôležité spomenúť aj dôležitosť jednotlivých splnených cieľov pred vyplneným kontrolného hárku ako aj následné strategické plánovanie splnenia ďalších cieľov, ktoré je možné vyhodnotiť v ďalších kontrolných hárkoch.

PDCA cyklus

Riadiaci cyklus PDCA, označovaný aj ako Demingov kruh v skratke vyjadruje zásadu plánovania a trvalého zlepšovania procesov. PDCA cyklus symbolizuje proces analýzy problémov medzi potrebami odberateľa a súčasnou úrovňou práce. Je to systematický postup založený na korekcii a prevencii pred defektami, pri zdokonaľovaní metód a procedúr. Toto odstraňuje korene príčin problémov a nepretržite zriaďuje a reviduje nové normy. Zásadou riešenia problému je, že regulácia aj v prípade etapovitých činností sa zabezpečuje opakovaným obchádzaním uzavretej slučky alebo cyklu. Tieto kroky vytvárania kvality použitím začiatočných písmen štyroch anglických slov nazývame slučkou PDCA (Plan – Do – Check - Act). Jej význam okrem toho, že sa ľahko zapamätá, je v tom, že na tejto logike stavajú rôzne činnosti odboru logiky. Je to univerzálny model na zlepšovanie kvality, ktorý sa dá vnímať ako nikdy nekončiaci proces, bez začiatku a bez konca. Skladá sa z nasledujúcich fáz:

P – plan – plánovanie, je prvou fázou a môže sa uskutočniť do rôznych hĺbok od výberu oblasti pre rozvoj, prieskumu situácie až po hľadanie príčin nezhôd,

D – do – vykonanie plánovacej časti, je aktívnou časťou realizácie, pričom dochádza k výberu a vyskúšaniu korigujúcich činností,

C – check – kontrola – zaznamenanie a vyhodnotenie údajov, ktoré sú základom pre skúšku. Sem zaraďujeme všetky prehodnotenia, preskúmania a hodnotenia,

A – action – akcia – úlohou je zaviesť a štandardizovať výsledok, prípadne rozhodnúť o opakovaní fáz. Podľa výsledkov kontroly potvrdíme alebo upravíme činnosť v záujme vytýčeného cieľa.

Tab. 1 Hodnotenie splnenia jednotlivých cieľov aj s kontrolným hárkom
Tab. 1 Assessment of the achievement of the individual objectives as well as the checklist

Výkon, rezervy vo výkone, ciele
- Strategické ciele, ktoré chceme dosiahnuť v tomto roku - Ako sme splnili ciele v minulom roku? - Kde vznikli rozdiely? - Prečo?

Spätný pohľad na činnosti minulého roka		
Činnosť	**Hodn**	**Výsledky**
Čo sme mali urobiť v minulom roku?		Čo sa nám podarilo a čo nie, čo sme sa naučili? Čo sme nedosiahli a prečo?

Analýza / Stanovenie činností na tento rok
Čo všetko musíme urobiť, aby sme dosiahli ciele tohto roka?

Ciele	Činnosti	1	2	3	4	5	6	7	8	9	10	11	12

Nedoriešené veci, ktoré treba dotiahnuť do konca
Máme nejaké nedoriešené a nedotiahnuté veci z minulosti? Treba urobiť špeciálne opatrenia na ich dotiahnutie do konca? Aké?

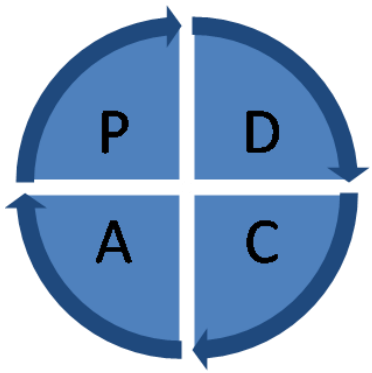

Obr. 2. PDCA cyklus
Fig. 2. PDCA cycle

VÝSLEDKY A DISKUSIA

Nasledujúce záležitosti budú prezentovať možnosti bodového hodnotenia procesov technických servisov vozidiel ako štatistického ukazovateľa priebehu kvality opráv. Prezentujú predovšetkým príklad daného bodového hodnotenia po vykonaní opravy resp. iného technického úkony prijatého od daného servisu. Vzájomná súčinnosť jednotlivých hodnôt po informovaní daného servisu môže významnou mierou napomôcť k neustálemu zvyšovaniu kvality technických úkonov prijatých od servisov.

Bodové hodnotenie kvality opráv a služieb

Dátum	Názov spoločnosti	Vozidlo na ktorom sa mal daný technický úkon vykonať	Servis/údržba	Bodové hodnotenie dodanej služby/opravy/iných technických a prevádzkových činností				Výsledné bodové hodnotenie dodávateľa	Poznámka k výsledku (akcept. / neakcep.)	Pracovník, ktorý kontrolu a hodnotenie vykonal
				Cenová ponuka	Rýchlosť dodania	Výstupná kvalita	Celkový technický výsledok			
15.07.2016	InteCort	KN022CX	výmena oleja	3	3	3	3	12	Akcept	-
27.07.2016	Jancar	KN338BX	výmena drž.motora	4	4	4	4	16	Akcept	-
16.08.2016	Intercort	KN025CX	vým. oleja op.mot	4	3	3	3	13	Akcept	-
16.08.2016	Intercort	KN502DU	olej,poloos,klb	4	4	4	4	16	Akcept	-
06.09.2016	Renault Mag	KN762DP	výmena z.platnič	3	4	3	3	13	Akcept	-
20.09.2016	Téglás sklo	KN502DU	výmena č.skla	4	4	4	4	16	Akcept	-
20.09.2016	Renault Mag	KN300EF	výmena oleja	3	4	3	3	13	Akcept	-
22.09.2016	Intercort	KN502DU	brzdy,lož.kol,dvere	4	3	3	3	13	Akcept	-
21.09.2016	téglás sklo	KN300EF	výmena č.skla	4	4	4	4	16	Akcept	-
23.09.2016	Jancar	KN300EF	STK+EK	4	4	4	4	16	Akcept	-
11.11.2016	Intercort	KN502DU	STK+EK	4	4	4	4	16	Akcept	-

Hodnotenie: 1 – neakceptovateľná kvalita výstupu, 2 – slabá kvalita výstupu, 3 – akceptovateľná kvalita výstupu, 4 – výborná kvalita výstupu.

Grafický priebeh ako kvalitatívny vývoj inherentných znakov práce niektorých servisov ako výstupná informácia akceptovateľnosti.

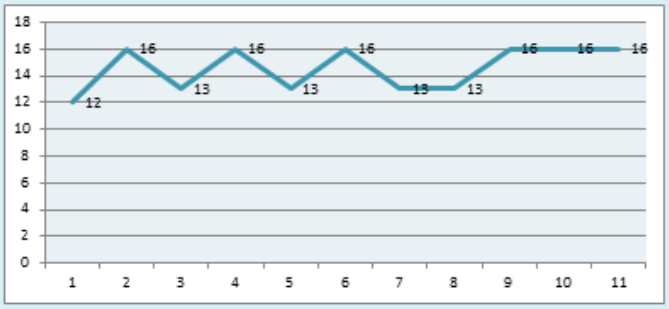

Obr. 3 Príklad bodového hodnotenia kvality opráv a technických úkonov
Fig. 3 An example of a point assessment of the quality of repairs and technical operations

ZÁVER

Na základe týchto technických informácií ako aj prezentovaných výsledkov je možné vidieť významnú dôležitosť pri zavádzaní nástrojov kvality v oblastiach služieb technických úkonov servismi, kde sa táto vysoká dôležitosť prejavuje predovšetkým hĺbkovou kontrolou jednotlivých opravených častí vozidla ako aj celkový kvalitatívny výsledok práce ako výstupnej informácie systémov kvality vykonaných technických úkonov. Cieľom údržby je zabezpečiť použiteľnosť jednotky pre požadovanú funkciu a dbať na požiadavky bezpečnosti spojené s jednotkou tak pre údržbu, ako aj pre obsluhu a v prípade potreby aj pre životné prostredie. Touto významnou informáciou je dôležité riešenie procesných nástrojov kvality v oblastiach služieb technického, technologického ako aj servisného charakteru ako jedného z technických príkladov významného nástroja pre komplexné zabezpečenie systémov manažérstva kvality v danej organizácií.

POUŽITÁ LITERATÚRA

1 Čičo, P. a kol. (2016). Manažérstvo údržby a opráv, Nitra: Slovenská poľnohospodárska univerzita, 2016. 190. ISBN: 978-80-552-1582-2,

2 Hrubec, J., Virčíková, E. a kol. (2009). Integrovaný manažérsky systém, Nitra: Slovenská poľnohospodárska univerzita, 2009. 543 s. ISBN 978-80-552-0231-0,
3 Korenko, M. a kol. (2015). Manažérstvo kvality procesov, Nitra: Slovenská poľnohospodárska univerzita, 2015. 144. ISBN: 978-80-552-1316-3,
4 Interné informácie záchrannej zdravotnej služby ZaMED,
5 Strategické plánovanie (Strategy Deployment) (2012). Základné strategické princípy, zmeny. [online] [cit. 2017-05-31]. Dostupné na internete: http://www.ipaslovakia.sk/sk/ipa-slovnik/strategicke-planovanie-strategy-deployment,
6 Quality for everyone. (2012). Zlepšovanie na štyri písmená? PDCA. [online] [cit. 2017-05-31]. Dostupné na internete: http://q4e1.blogspot.sk/2012/03/zlepsovanie-na-styri-pismena-pdca.html
7 .

Ing. Gabriel Poló, Department of Physics, Faculty of Engineering, Slovak University of Agriculture in Nitra, Tr.A.Hlinku 2, Nitra, 949 01, Slovakia, phone: +421 37 641 5785, e-mail: xpolo@is.uniag.sk, tel.: 0908 401 937

MONITORING OF THE HOUSEHOLDS'ENERGY CONSUMPTON INRURAL MICRO- REGIONS

Petra PROCHÁZKOVÁ

Czech university of Life Sciences Prague, Faculty of Engineering, Department of vehicles and ground transport

Abstract
The aim of paper is to introduce project that will be monitoring households'energy consumption in selected rural micro-regions of the northern and central Bohemia. The public survey will be carried out by a questionnaire method. The attention will be payed to different energy sources to describe a fossil and alternative energy sources proportions. The obtained data will characterise the quality of life in accordance with the selected criteria. The final assessment should serve as influence indicator of energy consumption on the climate system.

Key words: *monitoring energy consumption, alternative source, "post-carbon" future.*

INTRODUCTION

To a certain degree, every human being affects their environment and the whole of humanity with their existence and activity, and in this manner, they also affect the Earth's climate system. The durability of this system is currently under threat, but humanity can extend or shorten it with their actions. One of the possibilities is to slow down the speed of consumption of fossil energy sources and to replace them with other, non-fossil or low-carbon sources. The transfer to a "post-carbon" future is represented by innovation in energy supply from renewable (alternative) sources, for example, to communities in the country. A growing number of such communities is interested in knowing their complete energy demand. Therefore, it is necessary that we concern ourselves with technical possibilities of transferring to alternative energy sources in a complex manner, but also with social and cultural changes that are connected with the origin of a low-carbon society, such that lowers consumption of fossil fuels, overall energy consumption and, based on that, also CO_2 emission production *(Vávra, 2012; Neuvonen et al., 2014; Phillips & Dickie, 2014; Dou et al., 2016; Maier, 2016).*

MATERIALS AND METHODS

A fundamental condition to carry out transformation to a low-carbon society is a clear intervention "from above" in form of regulations and functioning incentives. A change in the system is necessary: it is not possible to rely only on individual changes of behaviour. When we look at the carbon footprint of Czech households, we can make some interesting observations. The greatest share of the footprint falls on emissions from heating and food consumption Since a connection between the expressed pro-environmental opinions of the respondents and their real behaviour is missing, this points out the influence of the infrastructure and the system, that include, for example, heat sources, and also the problematic relation between attitudes and behaviour *(Vávra, 2012; Hulme, 2008; Jones et al., 2012; Dreborg, 1996; Quist & Vergragt, 2006).*

The main cause for concerns about changes is the impact of anthropogenic changes on the climate, that is, the so-called global warming. The methods of research in use thus far are predominantly sociological and they are dedicated to the viewpoint of households and individuals from communities in the country i.e. micro-regions. In each of these micro-regions, it is necessary, using the methodology of qualitative and quantitative solutions, to establish and analyse the true and prospective energy consumption, but also opinions and attitudes of the inhabitants in connection to changes in energy con-

sumption and thereby also in connection to the decrease of emission *production (Curtis & Renne, 2016; Robinson & Bridger, 1982, Urban et al., 1988; Svenfelt et al., 2011).*

A safe, secured, sustainable and affordable energy is a condition of a full-value and quality life of citizens, competitive industry and fully functional society. Already now, an energy infrastructure is being built here, which will become a source of energy for households, industry and services in 2050, the buildings that people are going to use are also designed and constructed. At the same time, a model of energy production and use for the year of 2050 is being set up. The EU has bound itself that until 2050 it will decrease emissions of the greenhouse gasses by 80–90% in comparison to the values from 1990 within the necessary decrease of emissions in the developed countries as a whole. The impacts of this reality have been analysed in the "Roadmap for moving to a competitive low carbon economy in 2050". "Roadmap to a Single European Transport Area" focused on solutions for the transport field and on creation of a singular European transport area. In this energy roadmap drawn for the period until 2050, such tasks are being researched, that are based on fulfilment of the EU decarbonisation goal along with simultaneous provision of energy supplies and preserved competitiveness *(Evropský parlament, 2011; Grunfmann, 2015; Svenfelt et al., 2011; Jenssen, 2010; Urban et al., 1988).*

The prognosis implies, that until 2050, the emissions will be lowered by 40%, however, that is not sufficient to achieve the goal of decarbonisation of the EU. Behind all this, we can imagine the amount of changes and effort, which are going to have to be put forth for the emissions to be lowered and for the competitiveness and security of energetics to be preserved *(Jenssen et al., 2014; Höjer et al., 2000; Svenfelt et al., 2011).*

RESULTS AND DISCUSSION

During July - August 2017 is going to be monitoring energy consumption in selected microregions of the Northern Bohemia using a survey method. In the first case, it will concern a micro-region without an alternative energy source, in the second micro-region, the energy is obtained from an alternative source. Enquiry is make like a questionnaire method. The selected evaluation criteria are presented at the fig. 1. Characteristics of the house units is going to be supported by the thermal camera scanning in autumn 2017.

Structure of household
Household condition
Used of energy sources
Used renewable sources
Usage appliances
Usage of means of transport
Usage of public transport
Characteristics of respondents routs
Supplementary questions about global warming
Supplementary questions about renewable resource support

Fig. 1 Structure of questionnaire

Using the data gathered, the quality of life in accordance with the selected criteria will be assessed along with the influence on the climate system.

CONCLUSIONS

In case of a significant positive influence of the alternative energy source on life of the citizens, the alternative source will be recommended also to the microregion without this source. Further,

an attempt will be made to establish the energy consumption for things such as transport (commuting by private motor vehicle transportation), heating, etc.

ACKNOWLEDGMENT
This paper and obtained results were supported by Internal Grant Agency 2017, project IGA 2017: 31150/1312/3122 "The study of alternative energy resource utilisation under rural conditions"

REFERENCES

1. Vávra, J. (2012). Zrození „post-uhlíkové" společnosti? Kulturní změna očima lokálníkomunity. Praha. Disertace. Univerzita Karlova v Praze, Filozofická fakulta, Katedra teorie kultury (kulturologie). Vedoucí práce PhDr. Miloslav Lapka, CSc.
2. Evropský parlament. COMMUNICATION FROM THE COMMISSION TO THE EUROPEAN PARLIAMENT, THE COUNCIL, THE EUROPEAN ECONOMIC AND SOCIAL COMMI TTEE AND THE COMMITTEE OF THE REGIONS: A Roadmap for moving to a compet itive low carbon economy in 2050. www.europarl.europa.eu [online]. ©2011 [cit. 2016-11-30]. Available from: http://www.europarl.europa.eu/meetdocs/2009_2014/documents/com/com_com %28011%290112_/com_com%282011%290112_en.pdf
3. Neuvonen, A., Kaskinen, T., Leppanen, J., Lahteenoja, S., Mokka, R., & Ritola, M. (2014). Low-carbon Futures and Sustainable Lifestyles: A Backcasting Scenario Approach. *Futures*. 58, 66-76. ISSN:0016-3287.
4. Anderson, B. (2010). Preemption, Precaution, Preparedness: Anticipatory Action and Future Geographies. *Progress in Human Geography*. 34(6), 777-798. ISSN:0309-1325.
5. Phillips, M., & Dickie, J. (2014). Narratives of Transition/non-transition Towards Low Carbon Futures Within English Rural Communities. *Journal of Rural Studies*. 34, 79-95. ISSN:0743-0167.
6. Dou, Y., Luo, X., Dong, L., Wu, C., Liang, H., & Ren, J. (2016). An Empirical Study on Transit-oriented Low-carbon Urban Land Use Planning: Exploratory Spatial Data Analysis (ESDA) on Shanghai, China. *Habitat International*. 53, 379-389. ISSN:0197-3975.
7. Grunfmann, P., & Ehlers, M. H. (2015). Determinants of Courses of Action in Bioenergy Villages Responding to Changes in Renewable Heat UtilizationPolicy. Utilities Policy. 41, 183-192. ISSN:0957-1787.
8. Jenssen, T., König, A., & Eltrop, L. (2014). Bioenergy Villages in Germany: Bringing a Low Carbon Energy Supply for Rural Areasinto Practice. *Renewable Energy*. 61, 74-80. ISSN:0960-1481.
9. Maier, S. (2016). Smart Energy Systems for Smart City Districts: Case Study Reininghaus District. *Energy, Sustainability and Society*. 6(1), 1- 20. ISSN:2192-0567.
10. Curtis, C., & Renne, J. (2016). Transit Oriented Development: Making It Happen.
11. Robinson, J. B. (1982). Energy backcasting A proposed method of policy analysis. Energy Policy [online]. 10(4), 337-344 [cit. 2016-11-30]. DOI: 10.1016/0301-4215(82)90048-9. ISSN 03014215. Available from :http://linkinghub. elsevier.com/retrieve/pii/0301421582900489
12. Hulme, M. (2008). Geographical Work at the Boundaries of Climate Change. *Transactions of the Institute of British Geographers*. 33(1), 5-11. ISSN:0020-2754.
13. Jones, R. D., Robinson, J. & Turner, J. (2012). Introduction. Between Absence and Presence: Geographies of Hiding, Invisibility and Silence. *Space and Polity*. 16(3), 257-263. ISSN:1356-2576.
14. Dreborg, K. H., (1996). Essence of Backcasting. *Futures*. 28(9), 813-828. ISSN:0016-3287.
15. Quist, J., & Vergragt, P. (2006). Past and Future of Backcasting: The Shift to Stakeholder Participation and a Proposal for

a Methodological Framework. *Futures*. 38(9), 1027-1045. ISSN:0016-3287.
16. Svenfelt, Å., Engström, R., & Svane, Ö., (2011). Decreasing Energy Use in Buildings by 50 % by 2050 – a Backcasting Study Using Stakeholder Groups. *Technological Forecasting & Social Change*. 78(5), 785-796. ISSN:0040-1625.
17. Jenssen, T. (2010). The Good, the Bad, and the Ugly: Acceptance and Opposition as Keys to Bioenergy Technologies. *Journal of Urban Technology*. 17(2), 99-115. ISSN:1063-0732.
18. Urban, Glen L., & von Hippel, E. (1988). Lead User Analyses for the Development of New Industrial Products. *Management Science*. (34)5, 569-582. ISSN:0025-1909.
19. Höjer, M., & Mattsson, Lars-Göran (2000). Determinism and Backcasting in Future Studies. *Futures*. 32(7), 613-634. ISSN:0016-3287.
20. Svenfelt, Å., Engström, R., & Svane, Ö. (2011). Decreasing Energy Use in Buildings by 50% by 2050 — a Backcasting Study Using Stakeholder Groups. *Technological Forecasting & Social Change*. 78(5), 785-796. ISSN:0040-1625. 796. ISSN:0040-1625.

Corresponding author:
Ing. Petra Procházková, Department of vehicles and ground transport, Faculty of Engineering, Czech University of Life Sciences Prague, Kamýcká 129, Praha 6, Prague, 16521, Czech Republic, phone: +420224383106, e-mail: prochazkovap@tf.czu.cz

DRYING ASPECTS OF SELECTED AGRICULTURAL CROPS

Ivan RIGÓ, Peter BAJUS, Norbert MICHLIAN, František URBAN, Henrich BLEHO

Department of Machine and Production Biosystem, Faculty of Engineering, Slovak University of Agriculture in Nitra, Slovak Republic

ABSTRACT
From the point of energy efficiency the agricultural waste can be considers as a very important source of energy. Especially the crop residues in form of straw belong into this group. Direct straw combustion can be oriented into the conditions of big power plant or to the agricultural farms with own combustion system. The aim of this article was to evaluate the utilization of cereal straw as a heat source for maize grain drying process in dryer CHIEF on the farm Agrodivizia, ltd., Selice, Slovakia. Monitored straw usage was compared due to economic costs at the drying process utilized the commonly used gas. Obtaining heat from the straw combustion and the next usage for drying appears to be more profitable with regards to final investment due to final costs of energy sources.

Key words: *grain drying, straw, combustion, heat source.*

ÚVOD
Po zbere semenných plodín sa získava semenná zmes zložená z väčšej časti zo semien hlavnej plodiny a z určitého podielu nežiaducich prímesí rôzneho charakteru a pôvodu (*Angelovič a kol., 2015*). Pozberové ošetrovanie zrnín je dnes jedným z kľúčových procesov prebiehajúcich v poľnohospodársky orientovaných podnikoch. Len obilniny zbavené nežiaducich prímesí, nečistôt a prebytočnej vody ide optimálne skladovať a neskôr speňažiť za čo najvyššiu cenu *(Maléř, 1996*). Výroba kvalitných objemových krmovín je dnes nevyhnutnou súčasťou efektívneho podnikania poľnohospodárskych podnikov (*Findura, 2015*), zároveň však táto komodita predstavuje značné rezervy ako energetická prolodina (*Urbanovičová et al., 2017, Križan et al., 2017*). Z tohto dôvodu je dôležité sledovať nielen proces sušenia, ale aj agrofyzilálne vlastnosti poľnohospodárskych plodín (*Angelovič, Findura, 2012*) a ich vplyv na environement (*Šima et al., 2013*). Sušenie je dnes najrozšírenejšou metódou konzervácie zrnín a ostatných poľnohospodárskych produktov. Podstatou sušenia je zníženie obsahu vody v zrne alebo v steble na optimálnu uskladňovaciu vlhkosť (*Frančák a kol., 2012*). Sušenie patrí medzi dôležité aspekty aj pri konverzii biomasy, kde dôležitou vlastnosťou je určitá, a to podľa účelu využitia, výsledná vlhkosť materiálu (*Piszczalka, Jobbágy, 2012*), ktoré sa určujú podobnými metódami ako zvádza *Krištof a kol.* (*2010*) v prípade pôdy a iných biologických materiálov. Cieľom predkladaného príspevku bolo zhodnotiť kvalitu práce sušiarne CHIEF CBS 14-6, pri sušení kukurice na poľnohospodárskom podniku AGRO Divízia s.r.o. Selice.

MATERIÁL A METÓDY
Praktické merania sa vykonali vo vybranom podniku, t. j. AGRO Divízia s.r.o. Selice, ktorá vznikla v roku 2002 s hlavným zameraním na rastlinnú výrobu, spracovanie komodít a poskytovanie služieb v oblasti poľnohospodárstva. Spoločnosť v roku 2015 pestovala na ploche 2800 ha Kukurica na zrno, Pšenicu ozimnú a raž siatu.
Sušiareň CHIEF CBS 14-6 (obr.1) je kontinuálna zásobníková sušiareň zrnín. Linka sa prevažne orientuje na spracovanie kukurice. Účelom vybudovania pozberovej linky na uvedenom poľnohospodárskom podniku bolo a doteraz je zabezpečovať pozberovú úpravu, expedíciu, resp. skladovanie zrnín (obilnín, kukurice). Linka je využívaná takmer celoročne, čo umožňujú aj dostatočné skladovacie priestory s kapacitou nad 10 000 t. Usporiadanie strojnej technológie spočíva v skladbe linky, kde sa nachádza príjem zrnín a predčistenie, čistenie, sušenie, expedícia, resp. skladovanie zrnín.
Sušiareň zrnín CHIEF CBS 14-6 má najväčšiu zásluhu na zachovaní kvality zŕn, preto sme sa experimentálne venovali hodnoteniu kvality práce a exploatačným parametrom tejto sušiarne. Technické parametre sú uvedené v tabuľke 1. Sušiareň je americkej výroby, jej výroba je realizovaná v štáte Nebraska.



Obr.1 Sušička CHIEF CBS 14-6, výmenník tepla, Boiler
Fig. 1 Dryer - CHIEF CBS 14-6, Heat exchanger, Boiler

Tab. 1 Parametre sušičky CHIEF
Tab. 1 Parameter of CHIEF Dryer
1-parameter, 2-Value, 3-Diameter of cylinder (silo), 4-height of the cylinder, 5-Height of centre, 6-performance of the dryer

Parameter (1)	**Hodnota (2)**
Priemer zásobníka, m (3)	12,8
Výška pri obvode, m (4)	4,9
Stredová výška, m (5)	8,91
Výkonnosť sušiarne, $t.h^{-1}$ (6)	15

Tab. 2 Energetické parametre kotla
Tab. 2 Boiler energy parameters
1-parameter, 2-Value, 3-Type of Boiler, 4-Power of Boiler, 5-Water temperature, 6-Water temperature from heat exchanger, 7-maximum performance of Dryer, 8-Input power o Dryer, 9-Input power of Boiler, 10-Storage tank for heat water, 11-Consuption of fytomass

Parameter (1)	**Popis, hodnota (2)**
Typ kotla (3)	BIOLANG TSZB – 45
Výkon kotla (4)	4,5 MW
Teplota vody (5)	75 – 85 °C
Teplota vody za výmenníkom (6)	65 – 75 °C
Maximálna výkonnosť sušiarne (7)	8 – 10 $t.h^{-1}$
Elektrický príkon sušiarne (8)	60 kW
Elektrický príkon kotolne (9)	105 kW
Akumulačný zásobník na teplú vodu (10)	16.500 l
Spotreba fytomasy (slamy) (11)	0,34 – 0,66 $t.h^{-1}$

Rekonštrukcia pozberovej linky (obr.1) spočívala hlavne v zmene zdroja vykurovania z plynu na spaľovanie balíkov slamy a to nainštalovaním kotla (Biolang TSZB 45; 4,5 MW, ohrev vody pre dve sušiarne značky CHIEF) spaľujúceho fytomasu a takisto v nainštalovaní výmenníka tepla (obr.1), keďže kotol nám zohrieva vodu a do sušičky nám ide vzduch. Zohriata voda z kotla je sústavou potrubí rozvádzaná až do výmenníka tepla, ktorý odovzdá teplo zo zohriatej vody vzduchu a ten je ventilátorom vháňaný do sušiarne. Následne je voda vrátená späť do kotla, kde sa opäť zohreje a celý tento cyklus sa opakuje, čo v podobnej forme aplikoval *Jobbágy et al*. (*2017*) v kombinácii so solárnym systémom. Vďaka výmenníku spĺňa sušiareň kritéria HACCP (hazard analysis and critical control points) čo je analýza nebezpečenstiev a metód kritických kontrolných bodov. Je to systém, ktorý bol využívaný na potvrdenie bezpečnosti potravín. Kotol spaľuje slamu a zároveň aj odpad z čistenia zrnín. Balík slamy je narezaný a dopravovaný do spaľovacieho procesu automaticky podľa potreby podobným systémom ako uvádzajú *Krištof et al.* (*2011*). Kotol je vybavený akumulačnou nádržou na teplú vodu o objeme 16500 l. V celej sústave sa nachádza 20 m^3 vody, ktorá je zohrievaná na teplotu 75-85 °C. Tá potom ide do výmenníka, kde sú ventilátory s príkonom 60 kW, ktoré nasávajú chladný atmosférický vzduch, dôsledkom čoho sa voda ochladzuje na 50-55 °C. Tento nám následne vstupuje

do sušiarne. Keďže pri spaľovaní nám vznikajú spaliny, musí byť kotol vybavený filtrom. V našom prípade je to multicyklón s výkonom 20 000 $m^3.h^{-1}$, kde dochádza k oddeleniu tuhých jemných častíc.

Stanovenie vonkajšej a vnútornej kvality zŕn sušenej kukurice
Úlohou laboratórnych meraní je stanovenie vybraných vlastností zrnovej kukurice (*Artim, 1991*).
Experimentálne sme sledovali:
a) Vonkajšiu kvalitu zŕn, podľa STN 46 11 00- 8, podiel prímesí a nečistôt, podľa normy (STN 46 11 00- 8) a čistotu zŕn pred a po vyčistení, podľa normy STN 46 11 00-8.
b) Vnútorná kvalita zŕn (nutričná hodnota, prítomnosť plesní, mikroorganizmov, škodcov a nežiaducich látok). Pre naše možnosti z hľadiska vnútornej kvality zŕn sme sa zamerali na klíčivosť, obsah škrobu, obsah tukov, obsah proteínov a sediment.
Uvedené analýzy boli vykonané v spolupráci s autorizovaným laboratóriom AMYLUM Slovakia s.r.o. Boleráz.

Stanovenie spotreby energie pri sušení
Merania boli zamerané na stanovenie usušeného množstva materiálu, spotreby zemného plynu (celkovo a mernej na 1 t usušeného materiálu), el. energie (celkovo a mernej na 1 t usušeného materiálu), vstupnej vlhkosti zrna kukurice a jednotkových nákladov na 1 tonu usušeného materiálu. Tieto merania sa aplikovali počas 21 rokov (kde výsledky od roku 1995 až po rok 2011 boli získané z archívu podniku).

Zamerali sme sa aj na zhodnotenie a porovnanie nákladov na sušenie zrnín spaľovaním zemného plynu v porovnaní so spaľovaním slamy.

VÝSLEDKY A DISKUSIA
Kukuričné zrno má pri zbere pomerne vysoký obsah vody (okolo 30%) a cukrov, čím sú vytvorené priaznivé podmienky pre mikrobiálnu fermentáciu. Dochádza k rýchlemu zahrievaniu a zhoršovaniu kvalitatívnych parametrov. Preto čím skôr po zbere musíme zrno dosušiť na skladovaciu vlhkosť 14 %, prípadne použiť iné spôsoby konzervácie.

Vonkajšia kvalita zŕn
Vonkajšiu kvalitu zŕn kukurice sme posudzovali podľa STN 46 11 00- 2 na vstupe do sušiarne, t.j. hneď po prečistení a po sušení v skladovacom sile. Hodnotili sme vlhkosť zŕn, - objemovú hmotnosť zŕn, - hmotnosť 1000 zŕn, čistotu zŕn, poškodenie zŕn, nečistoty a prímesi. Experimentálne merania boli vykonané v októbri r. 2015. Z uvedeného rozboru jednoznačne vyplýva nárast poškodených zŕn po sušení. Priemerný nárast poškodených zŕn sa zvýšil zo 4,39 na 7,67 %. Vlhkosť pri zbere bola v rozpätí od 21,5 % až do 25,2 %. Hlavnou príčinou poškodenia zŕn je vysoká vlhkosť pri zbere a nedodržanie pracovných režimov mlátiaceho ústrojenstva mláťačky kombajnu. Čiastočne poškodené zrno s neviditeľnou mikrotrhlinkou pri sušení a pri následnom mechanickom pôsobení miešacích závitoviek v sušiarni sa rozpadne na viacero kúskov, čím sa pri sušení a pri následnej manipulácii zvyšuje podiel poškodených zŕn. Preto pri výmlate kukurice musíme veľmi sledovať vlhkosť zŕn a vykonať tomu zodpovedajúce zriadenie mlátiaceho ústrojenstva. Čistota zŕn po predčistení bola veľmi dobrá, jej percentuálny podiel znižovali poškodené zrná (zlomky zŕn).
Vplyv vlhkosti zŕn kukurice na ich makropoškodenie v procese sušenia a následnej manipulácie do sila je graficky znázornený na obr. 2. Z obrázkov vyplýva jednoznačný trend nárastu makropoškodenia zŕn. Je to súbor rôznych vplyvov pôsobiacich na zrno jednak pri zbere, manipulácii a pri sušení. Pre budúcnosť je žiaduce urobiť experimentálne merania po každom mechanickom pôsobení v technologickom procese zberu, čistenia, sušenia a manipulácie na zrno a presne určiť príčiny ich nadmerného poškodenia a určiť opatrenia na zníženie poškodenia zŕn.

Hodnotenie energetických parametrov a výkonnosti sušiarne
Pre posúdenie a zhodnotenie kvality práce sledovanej sušiarne sme vykonali kontrolné merania prevádzkových parametrov, ktoré sú uvedené v tab.3. Na základe nameraných hodnôt vypočítali:
- spotrebu elektrickej energie na tonu odparenej vody, $kWh.t^{-1}$,

- spotrebu zemného plynu na tonu usušeného materiálu, $m^3.t^{-1}$,
- spotrebu elektrickej energie na tonu usušeného materiálu, $kWh.t^{-1}$,
- spotrebu zemného plynu na tonu odparenej vody, $m^3.t^{-1}$,
- náklady na tonu vysušeného materiálu o 1 % vlhkosti odparenej vody, $€.t^{-1}.vlh^{-1}$.

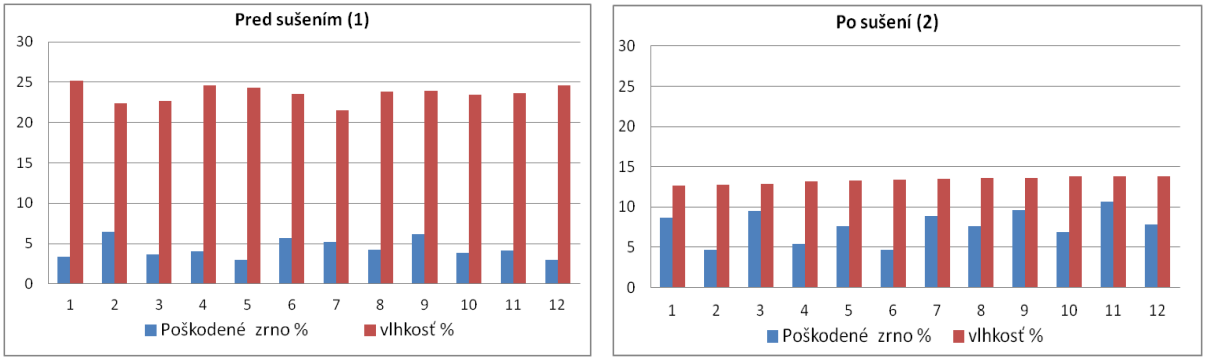

Obr. 2 Poškodenie zrna kukurice pri jednotlivých vlhkostiach pred a po sušení
Fig. 2 Damage of corn grains for individual moisture before and after drying

Slama je najekonomickejším zdrojom tepla pre sušiarne zrnín. Slama ako biomasa je energetická surovina a v súčasnosti predstavuje výhodnú náhradu zemného plynu. Vzhľadom na výhrevnosť nahradí 2,5 kg približne $1m^3$ zemného plynu. Slama má najnižšie výrobné náklady v porovnaní s alternatívnymi zdrojmi energie z odpadovej biomasy (*Prístavka et al., 2017*). Návratnosť investícií do kotlov a prídavnými zariadeniami na biomasu sa pohybuje v rozmedzí 3 až 7 rokov (*Frolo a kol., 2015*).

Tab. 3 Energetické náklady sušičky CHIEF
Tab. 3 Energy costs of CHIEF Dryer
1-Year, 2-Dried quantity, 3, 7-Natural gas, 4, 8- Electric energy, 5-Average humidity, 6-Required humidity, 9-Costs

Rok (1)	**Usušené množstvo,** t (2)	**Zemný plyn,** m^3 (3)	**Elektrická energia,** kwh (4)	**Priemer vlhkosti,** % (5)	**Žiadaná vlhkosť,** % (6)	**Zemný plyn,** $m.t^{-1}$ (7)	**Elektrická energia,** $kWh.t^{-1}$ (8)	**Náklady,** (9) $Sk.t^{-1}.1\%vlh^{-1}$ $€.t^{-1}.1\%vlh^{-1}$
1995	9 271,90	170 870,00	191 670,00	26,08	14	18,42	20,67	8,37
1996	5 647,00	134 007,00	165 784,00	28,58	14	23,73	29,35	9,97
1997	10 181,00	136 962,00	153 371,00	23,00	14	13,45	15,06	9,87
1998	10 010,00	168 904,00	195 239,00	23,00	14	16,87	19,50	12,56
1999	11 000,00	130 987,00	154 140,00	19,85	14	11,91	14,01	13,75
2000	8 580,00	129 708,00	127 926,00	22,57	14	15,12	14,91	11,01
2001	9 638,00	110 705,00	160 000,00	20,08	14	11,48	16,60	16,44
2002	11 880,80	186 934,00	210 408,00	21,52	14	16,17	17,70	17,75
2003	9 933,22	81 401,00	112 200,00	18,88	14	8,19	11,29	19,68
2004	13 767,21	231 793,00	182 549,00	23,22	14	16,83	13,25	16,90
2005	25 013,27	448 726,00	310 700,00	23,68	14	17,94	13,43	21,61
2006	18 145,30	268 567,00	148 649,00	23,05	14	14,80	8,19	25,92
		Slama, t				**t**		
2007	14 111,48	401,83	212 606,00	22,52	14	0,030	15,07	9,87
2008	26364,26	877,00	330 000,00	21,00	14	0,033	12,51	12,49
2009	20 011,00	880,00	342 208,00	22,00	14	0,044	17,10	0,49 €
2010	10 200,00	986,00	325 000,00	25,20	14	0,096	31,86	0,68 €
2011	16 507,00	545,00	260 620,00	21,00	14	0,033	15,78	0,45 €
2012	18 150,00	856,00	310 200,00	21,40	14	0,049	17,09	0,51 €
2013	12 635,80	591,00	124 112,00	23,50	14	0,047	9,82	0,31 €
2014	15030,00	627,5	254 535,00	22,90	14	0,042	16,93	0,40 €
2015	9 287,00	470,00	110 727,00	23,10	14	0,050	11,92	0,35 €

Mareček (2009) hovorí, že optimálna vlhkosť je 14-15 %. My sme sušili zrno kukurice na 14 %, čo je postačujúce na skladovanie. Pri zbere bývajú zrná čiastočne poškodené. *Angelovič* (*1995*) hovorí, že poškodenie zŕn delíme na makropoškodenie, toto poškodenie je viditeľné voľným okom a pohybuje sa v rozmedzí 5-10 % a na mikropoškodenie, ktoré je viditeľné pod mikroskopom a býva v rozmedzí 25-30 %. Naše zrno kukurice malo po zbere poškodenie v rozmedzí 2,95-6,42 %. Po sušení sa nám poškodenie zvýšilo na 4,69-10,68 %, čím môžeme povedať, že sušením nám poškodenie zrna stúpa. Pri správnom technologickom postupe sušenia ale môžeme tiež kvalitu zrna zlepšiť ako napríklad klíčivosť.

Zhodnotenie vplyvu procesu sušenia na vnútornú kvalitu zŕn kukurice

Pri sušení zrnín môže dôjsť k zmene vnútorných vlastností zŕn, vzhľadom k tomu sme dali spraviť rozbor nutričnej hodnoty a klíčivosti v laboratóriu AMYLUS Slovakia s.r.o. v Bolerázi. Klíčivosť je hlavný indikátor kvality a životaschopnosti zŕn po sušení. Rozbor vnútornej kvality zŕn kukurice z úrody r. 2015 v Seliciach je uvedený na obr.3.Klíčivosť sa pohybovala od 88 % do 96 %. Priemerná klíčivosť bola 91,2 %, čo pre potravinársku kukuricu je výsledok výborný. Ostatné parametre ako obsah škrobu, tuku a proteínov sú zrejmé z obr. 3. Obsah uvedených veličín je daný tiež kultivarom.

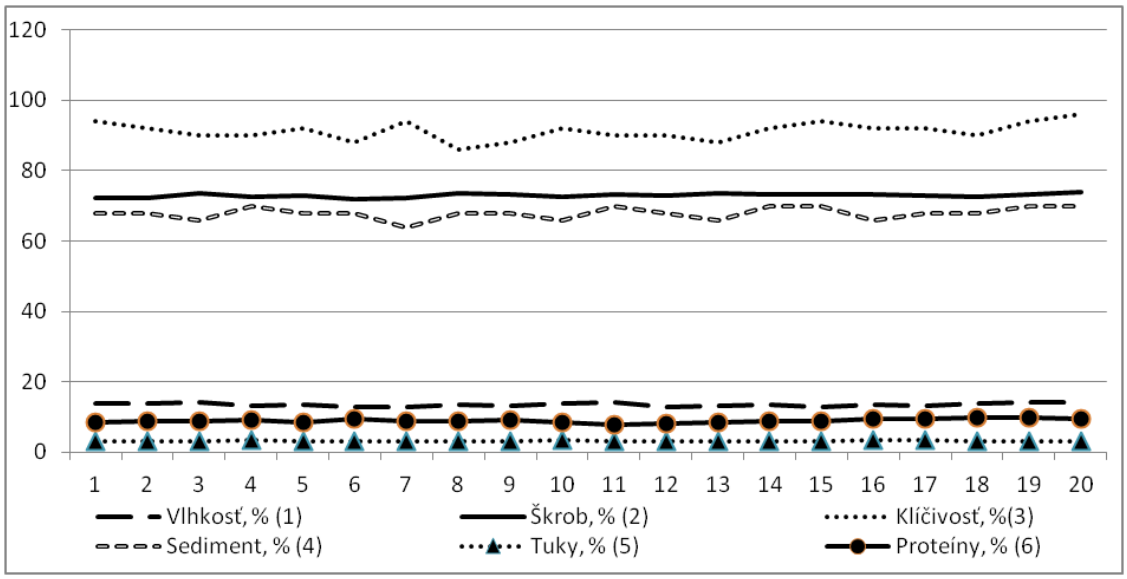

Obr. 3 Vnútorné vlastnosti kukurice
Fig. 3 Inner properties of corn
1-humidity, 2-Starch, 3-Germination, 4-Sediment, 5-Fats, 6-Proteins

ZÁVER

Cieľom predkladaného príspevku bolo zhodnotiť sušenie zŕn kukurice a následne pri tejto pracovnej činnosti porovnať spaľovanie slamy so spaľovaním plynu. Sušenie je energeticky veľmi náročná operácia, kde by sme tohto procesu nemohli skladovať zrná kukurice, ktorých vlhkosť v čase zberu dosahuje až 25-30 %,. Celkovo možno povedať, že pri spaľovaní vlastnej vyprodukovanej slamy, sa nám náklady sa v podstate znížia. Merania prebiehali dlhodobo a to už od roku 2007, kedy bola sušiareň zrekonštruovaná a modernizovaná s kotlom spaľujúcim slamu. Pri sledovaní nákladov na vysušenie 1 % vlhkosti v 1 tone zrna kukurice sme porovnávali roky 2006 a 2015. V roku 2006 bol energetickým zdrojom plyn a jednotkové náklady na sušenie tvorili 0,86 €.t^{-1}. V roku 2015 sa použil kotol spaľujúci slamu (už 9 rok v činnosti), ktorý spaľoval narezané hranaté balíky. Jednotkové náklady v danom prípade činili 0,35 €.t^{-1}, čo znamená, že náklady na energiu boli až o 40 % nižšie ako pri spaľovaní plynu.

PODĚKOVANIE

Príspevok vznikov s finančnou podporou Európskeho spoločenstva v rámci projektu: Vybudovanie výskumného centra „AgroBioTech", projekt číslo 26220220180. This work was co-funded by European Community under project no 26220220180: Building Research Centre „AgroBioTech".

POUŽITÁ LITERATÚRA

1. Angelovič, M. (1995). Vplyv niektorých faktorov na poškodenie zrna osivovej kukurice. *Zemědelská technika* 41 (4), 137-140
2. Angelovič, M., & Findura, P. (2012). Research of agrophysical properties of selected agricultural crops. *Applications of physical research in engineering.* 1st ed. SUA, 184s. Nitra ISBN 978-80-552-0930-2.
3. Angelovič, M., Jobbágy, J., & Findura, P. (2015). Technika v biosystémoch. 1. vyd. Nitra : SPU, 203 s. ISBN 978-80-552-1391-0.
4. Artim, J. (1991). Metódy zisťovania mechanického poškodenia semien. *Acta Technologica Agriculturae,* 3, 62s.
5. Findura, P. (2015). Efektívne využitie strojov pri zbere krmovín.. *Roľnícke noviny*, 86 (15). 13-14.
6. Frančák, J., Mihina, Š., Angelovič, M., Gálik, R., Korenko, M., Simoník, J., Botto, Ľ., Jobbágy, J., & Žitňák, M. (2012). *Technika v agrokomplexe*. 1. preprac. vyd. Nitra : SPU. 195s. ISBN 978-80-552-0777-3.
7. Frolo, T., Maga, J., & Jobbágy, J. (2015). Energetické využitie slamy pri sušení zrnín. *Acta Facultatis Technicae*. 20 (2). 23-31.
8. Maleř, J. (1996). Posklizňové ošetřování zrnin. Vyd. 1. Praha: Institut výchovy a vzdělávání ministerstva zemědělství ČR, 57s. Mechanizace. ISBN 80-710-5112-8.
9. Mareček, J. (2009). Podmienky zachovania kvality zrna pri zbere. [18.08.2009.] http://www.agroporadenstvo.sk
10. Piszczalka, J., & Jobbágy, J. (2012). Bioenergetika:zelená energia. 1. preprac. a dopln. vyd. Nitra:SPU, 149 s. ISBN 978-80-552-0813-8
11. STN 46 1100-8 (2002). Potravinárske obilniny - Časť 8: Zrno potravinárskej kukurice. *Norma.*
12. Urbanovičová, O., Krištof, K., Findura, P., Jobbágy, J., & Angelovič, M. (2017). Physical and mechanical properties of briquettes produced from energy plants. *Acta Universitatis Agriculturae et Silviculturae Mendelianae Brunensis*. 65 (1), 2017, 219-224.
13. Križan, M., Krištof, K., Angelovič, M., & Jobbágy, J. (2017). The use of maize stalks for energy purposes and emissions measurement during their combustion. *Agronomy Research*. 15 (3), 456-467
14. Jobbágy, J., Findura, P., Krištof, K., Urbanovičová, O. & Križan, M. (2017). The utilisation of solar system in combined heating system of water. *Acta Universitatis Agriculturae et Silviculturae Mendelianae Brunensis*. 65 (1), 41-50.
15. Krištof, K., Blaško, M., Angelovič, M., & Chudá, Z. (2011). Využitie kukuričných stebiel na energetické účely a niektoré poznatky pri ich spaľovaní. *Mechanizace zemědělství*. 61, (2011), s. 178-185. ISSN 0373-6776.
16. Prístavka, M., Krištof, K., & Findura, P. (2017). Reliability monitoring of grain harvester. *Agronomy Research*. 15, no. 3, (2017), s. 817-829. ISSN 1406-894X.
17. Šima, T., Nozdrovický, L., Dubeňová, M., Krištof, K., & Krupička, J. (2013). Effect of crop residues on nitrous oxide flux in the controlled traffic farming system during the soil tillage by LEMKEN Rubin 9 disc harrow. *Agronomy Research*. 11 (1), 103-110
18. Krištof, K., Boďo, T., & Misiewicz, P. (2010). Vplyv pracovného náradia na vybrané pôdne vlastnosti. *Technika v technológiách agrosektora 2010,* Nitra:SPU. 86--92. http://www.slpk.sk/eldo/2011/zborniky/04-11/kristof.pdf.

Corresponding author:
Ing. Ivan Rigó, Katedra strojov a výrobných biosystémov, Slovenská poľnohospodárska univerzita v Nitre, Technická fakulta, Tr. A. Hlinku 2, 949 76 Nitra, Slovenská republika, e-mail: ivan.rigo@metsagroup.com

PRINCIPLES OF IMAGE ANALYSIS METHODS USED IN NAVIGATION SYSTEMS OF AUTONOMOUS MOBILE ROBOTIC

Lukáš VACHO, Juraj BALÁŽI, Dušan HRUBÝ, Ondrej LUKÁČ

Department of Electrical Engineering, Faculty of Engineering, SUA in Nitra, Slovak Republic

Abstract
Image analysis plays important role in mobile robots navigation. Robot equipped with camera can retrieve information about environment. Based on the detected objects the robot can perform various operations. Web camera as sensor is a cheap device, yet very advanced and universal for using in mobile robots navigation systems. These systems provide mobile robot autonomy which in many applications from the device requires. Mobile robotic devices are used for performing work activities in various fields. These include various surveys, emergency or maintenance activities, where they can't be used directly by human. Currently, the mobile robots are applied in agricultural conditions. There can be used image analysis to recognition of plant objects and also to navigate the robotic device.
In this paper is presented using computer vision which applied Hough transformation for detect circle in environment. After finding the circle, radius is determined as the number of pixels in a digital image. This information is used to create a general equation for finding the distance between the circular mark and a camera. Such a procedure may be useful if it is known focal length of the camera lens. Importantly, the resulting equation is valid for a particular object used for navigation. Described methods and parts of image analysis, has found application in navigation systems, for mobile robots in agriculture.

Key words: *digital image; navigation system; robot vision.*

INTRODUCTION

Mobile robots are useful in operations that are dangerous for human beings, for example, work with radioactive garbage. Mobile robotics system must fill several key requirements. Capability to move around in environment without fixed on to physical location is base. Next significant attribute is increased autonomy of this device. Autonomous navigation in this environment is most important problem. The robot perceives information about environment through sensors. These sensors typically ultrasonic sensors, laser range finders, 3D lasers sensor and cameras give an estimate of the robot's position in the environment, which has some characteristic marks. In the interior it can be door, table, cabinets, while in the exterior are generally natural objects such as: trees, shrubs or grass. A common features of these objects is that, they are characterized not only shape but also the colour and edges. This knowledge can be used in the design of a navigation system for mobile robot, where are used image processing method for finding important information about environment. Vision-based robot navigation has long been a fundamental goal in both robotics and computer vision research. Cameras have evolved as attractive sensors as they help in the design of economically viable systems with simpler sensor limitations (*Santhos, 2008).* Using the camera to obtained necessary image information that is applied in navigation algorithms. From image information are selected data about environment which are specified colour attribute, brightness or edge. In object recognition can be used principle of learning mechanism. It is based on the principle of autonomy or interacting with operator using the terminal. This process is used in the work (*Greene, 2005*) to find a suitable navigation method for mobile robot with digital camera. Robot moves in known environment and finding geometrical object. They are compared with a set of training data. If is finding unknown object it can be saved to the database or ignored. The colour of object is determined by HSV model, where are extracted H and S component. Using histogram found maximal values of colours. In (*Ushida& Deguchy, 2007*) is used red ball like navigation object for biped mobile robot. In captured camera image is determined shift between frames. Each frame is divided into 4 parts. The movement of the robot, in the image moves the

object and its position is determined in centre of the image frame. Colour information about object can be obtained by HSV model where, is extracted one of colour component. When using H – S component creates mask for compare with threshold value. This process creates a binary image on which after application of the method of central moment are acquired information about object and his position in digital image (*Budiharto, 2014*). This is another way how to apply image processing methods for robots navigation. Next usable method of image processing algorithm for navigation process in autonomous mobile robot is usage Hough transformation. This method allows finding the object by detecting the edges when edges may be incomplete or interrupted. This advantage determines the transformation event in demanding applications in the detection objects. This work presents an approach using computer vision which applied Hough transformation after the image has been processed by based technique of image processing (smooth, erosion, dilation). Environment in front of the camera is looking coloured mark of circular shape. In this study, vision system is applied to extract the information such as the distance of target which can be characterized by shape and colour.

MATERIALS AND METHODS

The design of vision based systems differs depending on the application but they often share some common features. First step is acquired image information for next pre-processing operation, where image is converted to some of colour space for example HSV like as our work. Latest action of image process is edge detection and finding mark in the image. One of possible way of image processing described (*Szeliski, 2011*). In the process of image processing, it is possible to use computational intelligence such as fuzzy logic (*Tóth, 2012*). This typical approach of image processing show figure 1, with base blocks.

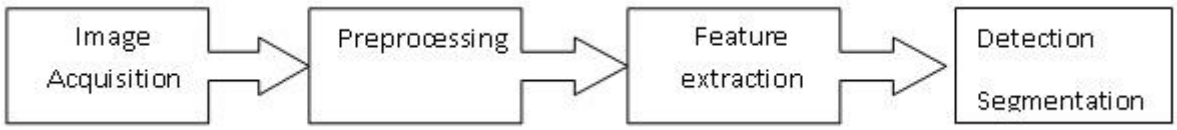

Fig.1 Principle of machine vision and its components

In preprocessing step can be image smoothed by one of image filter for example Gaussian. The Gaussian smoothing operator is a 2-D convolution operator that is used to blur images, remove detail and noise. In this sense it is similar to the mean filter. It uses a different kernel that represents the shape of a Gaussian curve. The effect of Gaussian smoothing is to blur an image, in a similar fashion to the mean filter (*Gonzales& Woods, 2012*). The degree of smoothing is determined by the standard deviation of the Gaussian. This pre-processing is ensured better quality of image for next step in algorithm where can be extract colour like as features with histogram method. Finally process of image analysis is finding some considerable element, line or edge which can be use in navigation method for mobile robots. It is possible to select multiple search methods of geometric shapes. Hough transform described in (Petrou, 2010) is a general method of finding basic geometrical shapes in digital images. In this paper we focus on particular application, how the general concept of Hough transform is used to identify circles in the image acquired from camera. Circle of radius *r* and centre (*a; b*) in Cartesian coordinates is a set of point *f(x; y)* that satisfy the analytical equation (1):

$$(x-a)^2+(y-b)^2=r^2 \tag{1}$$

When we are given radius r and circle centre *(a; b)*, we can use the equation to construct a raster image of that circle.
Each digital camera contains for image sharpening a thin lens. Equation of this lens is (2):

$$\frac{1}{f}=\frac{1}{u}+\frac{1}{v} \tag{2}$$

where *f* is focal length, *u* is mean distance of object, *v* is distance of image. A feature of the lens is breaking optical beam toward the centre of optical axis of the lens in image plane. At this point is miniaturized image. Image size is depending on the distance of the object lens in the object plane.
The magnification *m* of the optical system is determined by the ratio of the distance between the image *v* and the distance of the object *u* from the lens (3):

$$m = \frac{v}{u} \tag{3}$$

By combining equation (3) and (2) we will get a way eq. (4) to determine the focal length at a certain magnification factor and the distance of the object from the lens.

$$f = \frac{m \cdot u}{m+1} \tag{4}$$

If the focal length of the lens used in the digital camera is known and the object size is known, the number of pixels is the size of the image. Common webcams that are used are not familiar with the focal length. Another option to obtain the necessary values is to use an object with known parameters, a known object size.In this case, a circular mark with a diameter of 150 mm is used as the object. Detection of the tag by the proposed image processing algorithm determines the dependence of the marker radius in pixels from the mark distance to the camera. Image analysis is performed on selected (circular mark) object in the laboratory. The circular mark is detected by Hough transformation. The mark is scanned with a digital camera and the image is an input for image processing. For the process of obtaining the necessary marker radius data as well as digital coordinate marker values, conventional devices such as PCs and digital cameras are used. In this case, the iSlim 300x webcam is used to capture the dynamic scene. The resolution is: 640 x 480 pixels with 30 fps. Image capture information: HP Pavilion dv-6, including 4 GB of memory and the Intel Pentium P6100 processor. This application runs an application that processes image data usin g image analysis algorithms. The algorithm is designed in the C ++ programming environment with digital image processing support libraries: OpenCV. Measurement takes place in the laboratory during daylight. The mark is placed on the stand. Motion determined perpendicular to the camera without the ability to shoot the mark and camera. This condition is important for correctly displaying the shape of the circular Hough transformation mark.When measured, the mark is placed at a distance of 165 cm in relation to the camera at a distance of 165 cm, this distance gradually decreasing by 15 cm to a distance of 30 cm between the mark and the camera, where a circular mark can be detected in the digital image. The standard number of measurements for each experiment equals to 100. The mean value is calculating using:

$$\bar{x} = \frac{1}{N}\sum_{i=1}^{N} x_i \tag{5}$$

and standard deviation with:

$$\sigma = \sqrt{\frac{1}{N}\sum_{i=1}^{N}(x_i - \bar{x})^2} \tag{6}$$

The relative error ε are computed using the formula:

$$\varepsilon = 1 - \frac{d_{measured}}{d_{nom}} \tag{7}$$

In the case of experimental measurements of the distance through the system of image analysis to the object, comparative distance measurements are performed by the Hokuyo URG 04LX laser scanner

and the HCSR 04 ultrasonic distance measurement system. The minimum measuring range is 2 cm and the maximum measuring range is 450 cm. The data are the same for both devices and designated by the manufacturers.

RESULTS AND DISCUSSION

The first was to measure the distance between the camera and the circular mark along with the proposed circle detection algorithm. The output of the algorithm was the values of the radius of the circle in pixels. It was based on the assumption of the transverse magnification of the object described in the theoretical part. Practically, this means changing the number of pixels in the radius of the mark when moving the camera to the camera. The result of the measurement is the graphic dependence of the pixel radius in pixels and its distance from the camera to the length. The graphical dependence shows the figure 2.

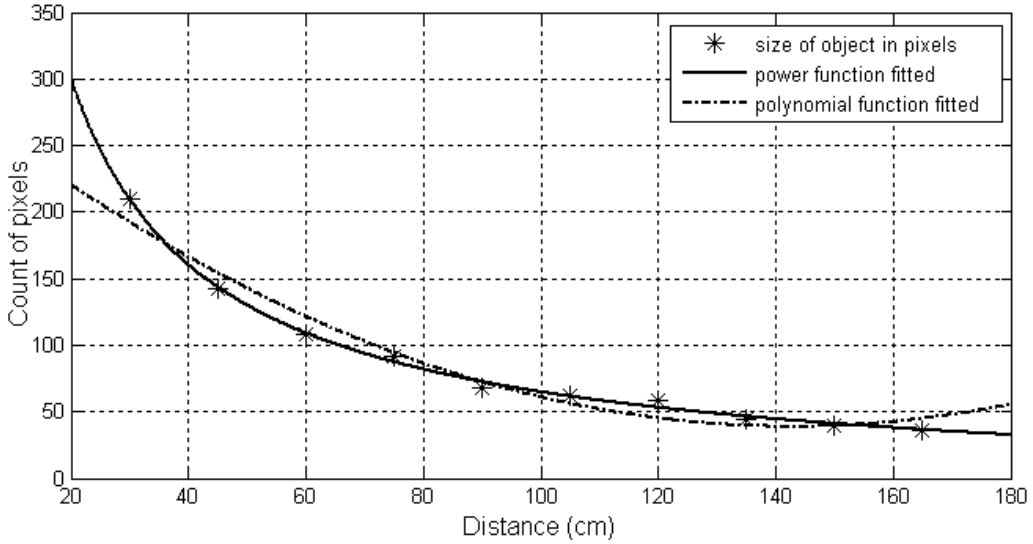

Fig. 2 The size of the tag radius in pixels, depending on the varying distance between: camera - tag.

During the measurement process, a dependence that is approximated by mathematical functions was determined by regression analysis. Values can be approximated by several types of functions. The most appropriate approximation was the power function and the second-order polynomial function, where the regression equations are:

$$dist_{pf} = a \cdot d^{b}{}_{pixels} + c \tag{8}$$

$$dist_{polyf} = p_1 \cdot d^{2}{}_{pixels} + p_2 \cdot d_{pixels} + p_3 \tag{9}$$

where: $dist_{pf}$ is calculated distance from measured pixels d_{pixels} according power function type, a = 3961, b = -0.8404, c = - 17.82 are constant from regression; $dist_{polyf}$ is calculated distance with measured of radius pixels d_{pixels} according polynomial function type, p_1 = 0.01209, p_2 = -3.451, p_3 = 285.1 are constants.

The power function for calculating the camera's distance to the mark appears to be more accurate with the coefficient of determination: R^2 = 0.997152; on the contrary, the coefficient of determination for the polynomial function is: R^2 = 0.964256, which is by 3.299% less compared to the way the curve is transferred by the power function. It follows from the honesty that it is preferable to use the Power function to calculate the distance of the object from the camera. The number of pixels is obtained as an output value of the radius of Hough transformation. Constant values in the equation are used for the calculate diameter of the circular mark. The equations (8) and (9) represent the way in which the distance of the object from the camera can be determined by the image analysis and the known number of pixels at which the constants in the equations are dependent on the ingested object, i.e. its shape or its diameter.

Tab. 1 Comparsion of mean value, standard deviation and relative errors between others form of measure distance

Type of measurement	$\bar{x}$ cm	σ cm	ε %
Image analysis (our approach)	118.676	2.307	1.1
Laser scanner Hokuyo URG 04LX	119.373	3.715	0.5
Ultrasound sensor HCSR 04	115.640	1.702	3.6

Table 1 lists the measured values for the 120 cm distance determined for the test measurement and the determination of the differences between the different methods of distance measurement. Relative errors and standard deviations indicate differences in the measurement principles used, where the most accurate distance measurement is a laser scanner, although the standard deviation is large. This is due to the measuring principle of the devices described in the papers (*Kawata et al., 2005*). The error characteristics of the device are described in the paper (*Ye & Borenstein, 2002*). In the ultrasonic distance measurement method, due to the relative wide angle divergence of ultrasonic waves the field of view becomes larger as the distance between the sensor and target increases reducig the accuracy of the measurements and increasing the possible interference in the signal reception from sensors (*Llorens et al., 2011*). This fact was also found in the experimental measurement of the distance between the tag and the sensor, whereby the relative method of the given method calculates the greatest relative error from among all types of measurement. In our method, factors such as illumination, the object's sensing angle, and, last but not least, the selection of colour model, according to which the proposed algorithm will process image information, influene the measurement results. For these reasons, it can be said that when designing an autonomous mobile robot navigation system, it is appropriate to use higher accuracy of measured data for systems that implement multiple principles of distance measurement to ensure greater relevance of measured data.

CONCLUSIONS

In conclusion, it can be said that there are several methods that are usable in navigation of mobile robots and function is based on image processing. The proposed methods of search objects can be used for several reasons. First, object can be characterized by colour as major of attribute. Second, shape is another most important attribute, which can provide important informatio n about navigation object. Third, when is use edge detection method of image processing, is achieved by quickly find the desired object properties. Finally, previous combination of different attribute we can get the necessary information about environment.

After obtaining the video camera had to be processed before the digital image. This will obtain such an image, for which it is possible to apply Hough transformation. The output value of Hough transformation in terms of the radius was used to obtain the equation for determining the distance from the object known. The proposed method of image processing and the use of selected methods of image analysis find application in mobile robots navigation systems. We assume the connection of multiple systems to create a sophisticated navigation system. Currently in various sectors, without exception agriculture requires the autonomy of robotic devices. To fulfil conditions of autonomy is an absolute need for a navigation system that principles are based on image processing.

REFERENCES

1. Bradski, G., & Kaehler, A. (2008). Learning OpenCV. Sebastopol: O'Reilly.
2. Budiharto, H. (2008). Modern Robotics with OpenCV. UK: Science Publishing Group.
3. Gonzales, R., & Woods, R. (2014). Digital Image Processing. New Jersey: Prentice Hall.
4. Greene, S., Gopalakrishnan, A & Sekman, A. (2005). Vision – based Mobile Learning and Navigation. Robot and Human Interactive Communication, 22, 48-53.
5. Kawata, H., Ohya, A., Yuta, S., Sathos, W., & Mori, T. (2005). Development of ultra-small lightweight optical range sensor system, Edmonton Canada. In Proceedings of the 2005 IEEE/RSJ International Conference

on Intelligent Robots and System (pp. 1078-1083). STEF92 Technology.
6. Llorens, J., Gil, E., Llop, J., & Escolá, A. (2011). Ultrasonic and LIDAR Sensors for Electric Canopy Characterization in Vineyards: Advances to Improve Pesticide Application Methods. Sensors, 11, 2177-2194.
7. Petrou, M., & Petrou, S. (2010). Image processing: The fundamentals. New Jersey: Prentice Hall.
8. Santosh, D., Achar, S & Jawahar, C. (2008). Autonomous Image – based Exploration for Mobile Robot Navigation. Robotics and Automation, 26, 2717-2722.
9. Szelisky, R. (2011). Computer Vision Algorithm and Application. New York: Springer.
10. Tóth, L., Olejár, M., & Cviklovič, V (2012). Fuzzy control algorithm for obstacle avoidance for autonomous mobile robot designed in a graphical programming language labview, Gödöllő. In Tudományos diákköri konferencia. (pp. 160).
11. Ushida, S., Deguchi, K. (2007). Vision – based Motion Control of a Biped Robot Using 2DOF Gaze Control Structure. Humanoid Robots, human like Machines 20, 263-276.
12. Ye, C., & Borenstein, J. (2002). Characterization of 2-D Laser Scanner for Mobile Robot Obstacle Negotiation, Washington DC. In Proceedings of the 2002 IEEE International Conference on Robotics and System (pp. 2512-2518).

Corresponding author:
Ing. Lukáš Vacho, Department of Electrical Engineering, Faculty of Engineering, Slovak University of Agriculture in Nitra, Tr. A. Hlinku 2, Nitra, 949 76, Slovak Republic, phone: +421376414723, e-mail: lukasvacho@centrum.cz

IMPORTS OF CZECH INDUSTRIAL TECHNOLOGIES TO INDONESIA

Michal WASSERBAUER, David HERÁK

Department of Mechanical Engineering, Faculty of Engineering, Czech University of Life Sciences Prague

Abstract
The article is focused on the description of structure of Czech imports of industrial technologies to Indonesia. Primary data of this study were gained from formal documents of governmental, nongovernmental and business offices. Most of used data were also obtained from informal interview and during casual conversations. From conducted study it is evident that they are still big demand for import of Czech technologies into Republic of Indonesia, unfortunately Czech importers didn't reflect actual needs of Republic of Indonesia and they are not able to immediately respond to the dynamically developing market of Indonesia.

Key words: *Asia; business; Czechoslovakia; import; strategy.*

INTRODUCTION

Indonesia is the world's fourth most populous country, with current population of over 255 million people and expected 450 million if current economic and political trend remains (*Kis-Katos & Sparrow, 2015; Lapeyre et al. 2015; Liu & Yamauchi, 2014*). Czech (formerly Czechoslovakia), exporters of investment character goods, have good reputation in Indonesia, and are also supported by references from other Asian countries – India, Pakistan, China, Thailand, Bangladesh, Sri Lanka and Vietnam. Therefore both, current Czech government and non-government scene, are trying to follow up this cooperation established during 1960s with Republic of Indonesia (*Landesmann, 1991*). Until now there are used of industry technologies from Czechoslovakia and also many significant experts and university teachers, businessman, government members and significant artist gained their education in former Czechoslovakia. Unfortunately, due to political reasons, this very strong cooperation was suppressed for almost 30 years and started to improve in 2001. Therefore the goal of this study is to describe options of imports of Czech industrial technologies to Indonesia on which behalf it would be possible to predict its future behavior, and on that account, also impact on Czech import to Indonesia.

MATERIALS AND METHODS

Primary data was collected from Government of Indonesia (Indonesia), United Nations Centre for Regional Development (Indonesia), World Bank (Indonesia), CekIndo (Indonesia) in period from 2010 until 2017. Methods used for the data collection varied according to the target groups, semi structured personal interviews, focus group discussions and analysis of internal documents were the most frequent. Most beginnings and termination parts of the interviews were informal, and many insights were obtained during casual conversations. Secondary data was gained by analysis of published materials of Statistical office of Indonesia (Badan Pusat Statistik Indonesia), analysis of law and regulations of Indonesia (Penelitan Hukum Indonesia) and by analysis of presidential directives (Direktif President RI).

RESULTS AND DISCUSSION

The imports of Czech technologies into Republic of Indonesia in 2016 are presented in Fig. 1 (*World Bank, 2017*). At just time both, current Czech government and non-government scene, are trying to follow up this cooperation established during 1960s with Republic of Indonesia (*Landesmann, 1991*). Unfortunately, due to political reasons, this very strong cooperation was suppressed for almost 30 years and started to improve in 2001. For past 10 years is export from the Czech Republic to this territory based on business realizations of small and medium companies, which shows, that these companies are able to enter on demanding Indonesian market and can be succeed there in long-term horizon (*Wihantoro et al., 2015*). In many cases, they are more active and flexible during their

business activities, compared to have already established big manufacturers and supplier (*Kis-Katos & Sparrow, 2015b; Lehkonen & Heimonen, 2015*).

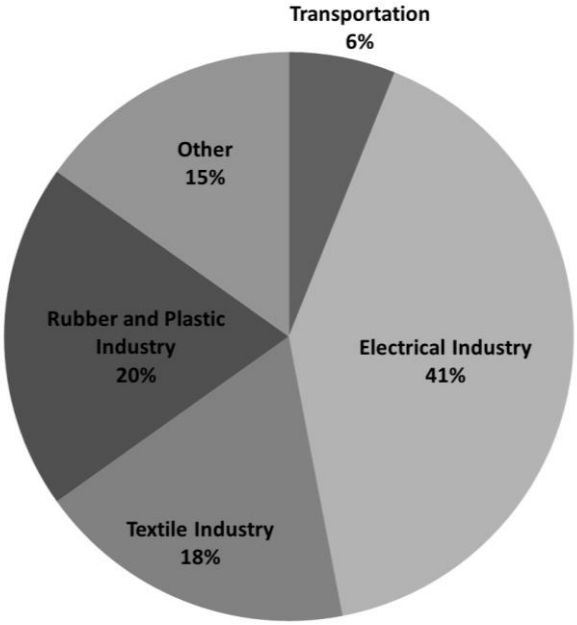

Fig. 1 Imports of Czech technologies into Republic of Indonesia in 2016 (*World Bank, 2017)*

From Tab. 1 and also from Fig. 1 and Fig. 2 it is clear that the structure of Czech import to Indonesia doesn't reflect their actual needs which are describe in Tab. 1 (*World Bank, 2017).*

Tab. 1 Top 10 Indonesia Imports from the World in 2016 (*World Bank, 2017)*

Order	Section	Billion USD
1	Machinery	21.1
2	Mineral fuels including oil	19.3
3	Electronic equipment	15.4
4	Plastic	7
5	Iron and steel	6.2
6	Vehicles	5.3
7	Organic chemicals	4.8
8	Cereal, milk preparations	3.2
9	Iron or steel products	2.9
10	Food waste, animal fooder	2.5

Import of large industrial works to Indonesia is currently supported by the fact that based on the stable economic growth Moody´s Investors Service raised Indonesian investment rating to Baa3 (Naciri, 2015*).* This value represents Indonesia as the best country of investment evaluation from financial crisis during years 1997 and 1998. Another rating company, Standard & Poor´s raised investment rating of Indonesia to BB. This company also raised long-term rating of Indonesian rupiah to BB+ (*Haspolat, 2015*). In accordance with current Indonesian investment rating, some Czech financial institutions - ČRB and EGAP decided to change territorial risk qualification of Indonesia from category 5 to category 4 (*Richter, 2015*).

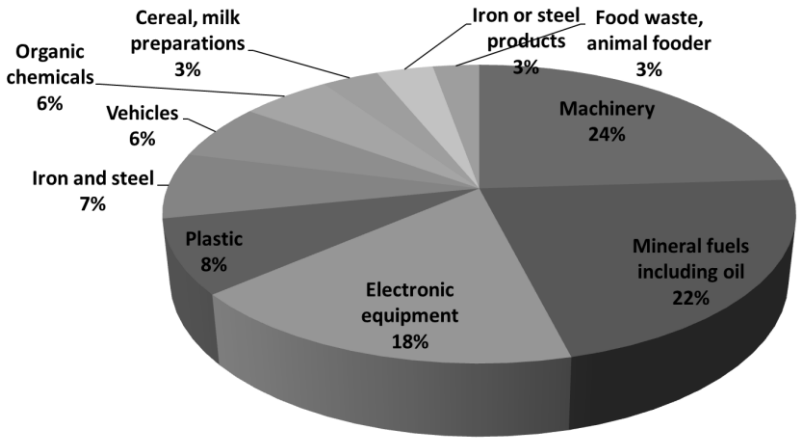

Fig. 2 Top 10 Indonesia Imports from the World in 2016 (*World Bank, 2017)*

Industrial areas with ongoing or possible future participation of Czech exporters are energetics, technology for sugar factory, transportation and infrastructure, environmental technologies, armature pump, radar systems, rotating electrics machines, telecommunication devices, apparatuses and products for paper industry, paper industry goods, food processing apparatuses and technologies, agriculture technologies, specializes medical apparatuses and automotive components. Even more noticeable is long-term commodity alteration of Czech import, where three out of five main import articles are computer technologies or electrical products. Other main import articles are natural rubber, shoes, clothing and lumber (*Kerstens et al., 2015; Kriyantono, 2015; Moeliodihardjo et al, 2012; Nijman, 2015; Rachman et al., 2015; Rudito, 2014; Singh & Setiawan, 2013; Siringoringo et al., 2013; Wiryono et al., 2015*). From conducted study it is evident that they are still big demand for import of Czech technologies into Republic of Indonesia, unfortunately Czech importers didn't reflect actual needs of Republic of Indonesia and they are not able to immediately respond to the dynamically developing market of Indonesia. According to outputs of this study as well as to the mutual discussion and negotiation between governments of Czech Republic and Republic of Indonesia it follows that there is a big huge potential for further cooperation in the field of industrial technologies.

CONCLUSIONS

The structure of Czech imports of industrial technologies to Indonesia was described in this study. It is evident that they are still big demand for import of Czech technologies into Republic of Indonesia, unfortunately Czech importers didn't reflect actual needs of Republic of Indonesia and they are not able to immediately respond to the dynamically developing market of Indonesia. Industrial areas with ongoing or possible future participation of Czech exporters are energetics, technology for sugar factory, transportation and infrastructure, environmental technologies, armature pump, radar systems, rotating electrics machines, telecommunication devices, apparatuses and products for paper industry, paper industry goods, food processing apparatuses and technologies, agriculture technologies, specializes medical apparatuses and automotive components. According to outputs of this study as well as to the mutual discussion and negotiation between governments of Czech Republic and Republic of Indonesia it follows that there is a big huge potential for further cooperation in the field of industrial technologies.

ACKNOWLEDGMENT

This study was supported by CULS FE IGA 2017:31130/1312/3111

REFERENCES

1. Haspolat, F. B. (2015). Analysis of Moody's Sovereign Credit Ratings: Criticisms Towards Rating Agencies Are Still Valid? Procedia Economics and Finance, 30, 283–293.
2. Kerstens, S. M., Leusbrock, I., & Zeeman, G. (2015). Feasibility analysis of wastewater and solid waste systems for application in Indonesia. Science of The Total Environment, 530-531, 53–65.
3. Kis-Katos, K., & Sparrow, R. (2015a). Poverty, labor markets and trade liberalization in Indonesia. Journal of Development Economics, 117, 94–106.
4. Kis-Katos, K., & Sparrow, R. (2015b). Poverty, labor markets and trade liberalization in Indonesia. Journal of Development Economics, 117, 94–106.
5. Kriyantono, R. (2015). Public Relations and Corporate Social Responsibility in Mandatory Approach Era in Indonesia. Procedia - Social and Behavioral Sciences, 211, 320–327.
6. Landesmann, M. (1991). Industrial restructuring and the reorientation of trade in Czechoslovakia. European Economy.
7. Lapeyre, R., Pirard, R., & Leimona, B. (2015). Payments for environmental services in Indonesia: What if economic signals were lost in translation? Land Use Policy, 46, 283–291.
8. Lehkonen, H., & Heimonen, K. (2015). Democracy, political risks and stock market performance. Journal of International Money and Finance, 59, 77–99.
9. Liu, Y., & Yamauchi, F. (2014). Population density, migration, and the returns to human capital and land: Insights from Indonesia. Food Policy, 48, 182–193.
10. Moeliodihardjo, B. Y., Soemardi, B. W., Brodjonegoro, S. S., & Hatakenaka, S. (2012). University, Industry, and Government Partnership: Its Present and Future Challenges in Indonesia. Procedia - Social and Behavioral Sciences, 52, 307–316.
11. Naciri, A. (2015). Credit Rating Governance: Global Credit Gatekeepers.
12. Nijman, V. (2015). CITES-listings, EU eel trade bans and the increase of export of tropical eels out of Indonesia. Marine Policy, 58, 36–41.
13. Rachman, A., Rianse, U., Musaruddin, M., & Pasolon, Y. (2015). The Potential of Delivering Clean Locally Available Limitless Rice Husk Energy in the Celebes Island Indonesia. Energy Procedia, 79, 55–60.
14. Richter, S. (2015). Export Promotion Framework of the Czech Republic. Central European Business Review.
15. Rudito, B. (2014). The Improvement of Community Economy as Impact of Corporate Social Responsibility Program: A Case Study in Pengalengan, Bandung, West Java, Indonesia. Procedia - Social and Behavioral Sciences, 164, 471–476.
16. Singh, R., & Setiawan, A. D. (2013). Biomass energy policies and strategies: Harvesting potential in India and Indonesia. Renewable and Sustainable Energy Reviews, 22, 332–345.
17. Siringoringo, H., Margianti, E. S., Kowanda, A., & Saptariani, T. (2013). Shopping Behavior of Indonesian Consumer Towards Imported Products. Procedia - Social and Behavioral Sciences, 81, 411–415.
18. Wihantoro, Y., Lowe, A., Cooper, S., & Manochin, M. (2015). Bureaucratic reform in post-Asian Crisis Indonesia: The Directorate General of Tax. Critical Perspectives on Accounting, 31, 44–63.
19. Wiryono, S. K., Susatyo, H., Utomo, S., Suryanta, B., Sudrajad, O. Y., Lazuardi, K. M., & Yuanita, H. (2015). Risk Mapping on Dynamics Creative Industry: Case Study at Bandung City, Indonesia. Procedia - Social and Behavioral Sciences, 169, 125–130.
20. World Bank, Czech Indonesia import export in 2016, (2017), retrieved from http://wits.worldbank.org (5 May, 2017)

Corresponding author:
Ing. Michal Wasserbauer, Department of Mechanical Engineering, Faculty of Engineering, Czech University of Life Sciences Prague, Kamýcká 129, Praha 6, Prague, 16521, Czech Republic, phone: +420 22438 3181, e-mail: wasserbauer@tf.czu.cz

Proceeding of 19th International Conference of Young Scientists 2017

September 13th 2017 – September 14th 2017

Publisher:	Czech University of Life Sciences Prague Kamýcká 129, Prague, Czech Republic
Editors:	Rostislav Chotěborský, Stanislav Kovář
Printing house:	CULS Prague
Number of copies:	50
Number of pages:	198
Issue:	First
Year:	2017
ISBN	978-80-213-2771-9